The role of the RNA-binding protein Hfq in the model pathogen *Salmonella* Typhimurium

Dissertation
zur
Erlangung des Doktorgrades
der Naturwissenschaften
(Dr. rer. nat.)

dem Fachbereich
Pharmazeutische Chemie
der Philipps-Universität Marburg
vorgelegt von

Alexandra Sittka
aus Berlin

Berlin 2008

Vom Fachbereich Pharmazeutische Chemie der Philipps-Universität Marburg

als Dissertation am_____angenommen.

Erstgutachter Prof. Dr. Roland K. Hartmann

Zweitgutachter Prof. Dr. Annegret Wilde

Tag der mündlichen Prüfung 19. November 2008

1. Introduction

One fascinating aspect of life is the ability of organisms to act on and to react to their environment. At the most basic level this can be observed in bacteria by the regulation of gene expression. While all information necessary for survival is encoded in the genetic material, i.e. the DNA, life is founded on the appearance of RNA. Protein synthesis is dependent on messenger RNAs (mRNAs) encoding for protein sequences, transfer RNA (tRNA), coupled to amino acids, as building blocks for protein synthesis and ribosomal RNA (rRNA), as part of the translation machinery, the ribosome. RNA very rarely exists in nature on its own, since RNA degrading enzymes (RNases) are ubiquitous. Therefore, RNA is usually found in complex with proteins in so called ribonucleoprotein complexes (RNPs). RNA binding proteins exert various functions in bacteria. For example, they can act as RNA chaperones, changing the folding state of a RNA molecule, or associate permanently with RNA molecules to RNPs such as ribosomes or ribonuclease P (RNase P). One of the RNA chaperones in bacteria is the protein Hfq (host factor for phage Qβ replication; Franze de Fernandez *et al.*, 1968). Hfq belongs to the growing family of Sm and Sm-like (Lsm) proteins known from eukaryotes and archaea.

1.1 Sm and Sm-like proteins

Sm and Lsm proteins constitute a large and ubiquitous family of proteins that are involved in many aspects of RNA metabolism. Sm proteins are part of the small nuclear ribonucleoprotein particles [(snRNPs); reviewed by (Staley and Guthrie, 1998; Will and Luehrmann, 2001)]. The Sm proteins share two conserved motifs, Sm1 and Sm2 (Hermann *et al.*, 1995). The typical Sm fold consists of an N-terminal α-helix, followed by a five-stranded β-sheet. Sm and Lsm proteins form heteroheptameric ring-like structures in eukaryotes and archaea (Kambach *et al.*, 1999; Fromont-Racine *et al.*, 2000). The Sm proteins bind to single stranded regions of the U1, U2, U4, and U5 small nuclear RNAs (snRNAs), components essential for pre-mRNA splicing (Kambach *et al.*, 1999). In eukaryotes 16 different Lsm proteins have been identified by now (Albrecht and Lengauer, 2004). The Lsm2-8 complexes (heteroheptamers of the Lsm proteins 2-8) are localized to the nucleus, while Lsm1-7 complexes (heteroheptamers of the Lsm proteins

1-7) are localized in the cytoplasm in the so called processing bodies (P-bodies), structures involved in mRNA storage. The Lsm2-8 complexes are involved in pre-mRNA splicing, and processing of nuclear RNAs as tRNAs, small nucleolar RNAs (snoRNAs), and rRNAs. In addition they promote decay of nuclear RNAs. Lsm1-7 complexes are involved in decapping of mRNAs after deadenylation (Tharun *et al.*, 2000). Besides adopting their prototypical heteroheptameric structures some Lsm proteins have been shown to form lower molecular weight complexes (Tomasevic and Peculis, 2002).
Lsm proteins are not only present in eukaryotes but also in archaea and bacteria. Archaea usually possess one or two Lsm proteins. In bacteria the Sm-like protein Hfq is present in half of the sequenced Gram-positive and Gram negative organisms.

1.2 The Sm-like protein Hfq

Hfq is one of the most abundant RNA-binding proteins in bacteria (Ali Azam *et al.*, 1999; Kajitani *et al.*, 1994; Franze de Fernandez *et al.*, 1997). Hfq was first identified in *Escherichia coli* as a host factor required for phage Qβ RNA-directed synthesis of complementary minus-strand RNA (Franze de Fernandez *et al.*, 1968). While human Lsm proteins usually form heteroheptameric ring-like structures, the bacterial Hfq protein forms homohexamers *in vivo* (Fig. 1.1). Hfq homologues of bacteria and archaea considerably vary in length. While short Hfq species only comprise the conserved Sm1 and Sm2 motifs and the in between positioned non-conserved so called 'variable region' [these species encompass around 70 amino acids (aa)] other eubacterial Hfq homologues show extended C-termini that differ in amino acid constitution and length (e.g. length of *Escherichia coli* and *Salmonella* Typhimurium Hfq 102 aa, *Pseudomonas aeruginosa* Hfq 82 aa, *Staphylococcus aureus* Hfq 77 aa). The enterobacterial Hfq hexamer is composed of 11.2 kDa monomers.
The resolution of various crystal structures of eubacterial Hfq proteins from *Staphylococcus aureus* (Schumacher *et al.*, 2002), *Escherichia coli* (Sauter *et al.*, 2003), and *Pseudomonas aeruginosa* (Nikulin *et al.*, 2005) revealed the same folding properties (N-terminal α-helix, followed by a five-stranded twisted β-sheet) as had been reported for eukaryotic Sm and Lsm proteins. In Hfq, the Sm1 motif encompasses the first three β strands, the Sm2 motif the β strands four and five.

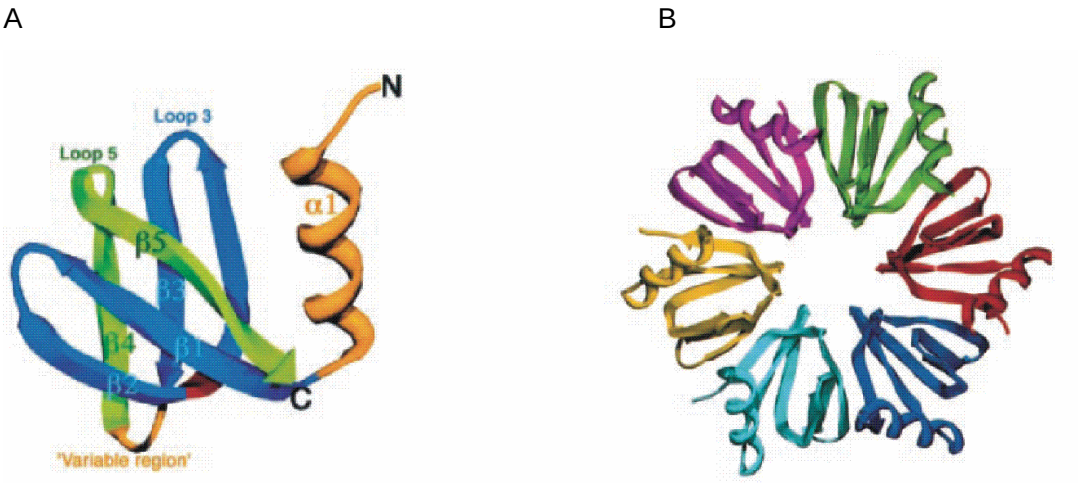

Fig. 1.1: Structure of Hfq. **(A)** Hfq monomer shown as ribbon diagram. Colours highlight the Sm1 and the Sm2 motifs (the Sm1 motif is coloured blue, the Sm2 motif green; α- helix and 'variable region' are coloured yellow, the conserved glycine residue is coloured red). The first (N) and the last (C) residues are indicated. **(B)** Hexameric Hfq structure. Each monomer is indicated by a different colour (from Schumacher *et al.*, 2002)

The Hfq hexamer displays two opposite sites which are distinguished in the proximal and the distal side. While the proximal side contains the positively charged base binding pocket, the distal side varies in between the different Hfq homologues. While the distal side is predominantly positively charged in the Hfq structures of *Escherichia coli* and *Pseudomonas aeruginosa*, the same face is predominantly non-polar in the *Staphylococcus aureus* Hfq and mainly negatively charged in the structure of the archaeal Hfq of *Methanocaldococcus jannaschii* (Nielsen *et al.*, 2008). Oligomerization takes place through interaction of β4 and β5 of two adjacent monomers.

1.3 RNA-binding properties of the Lsm protein, Hfq

When identified ~40 years ago it was shown that Hfq could be purified by binding to homopolymeric RNA columns (Carmichael, 1975), which provided initial evidence that Hfq was a RNA-binding protein. Subsequently, Schumacher and co-workers were able to solve the crystal structure of Hfq from *Staphylococcus aureus* in complex with a 5'-

AUUUUUG-3' ribo-oligonucleotide to elucidate the mechanism of Hfq binding to RNA molecules (Fig. 1.2). The same sequence is known as the canonical sequence recognized by Sm complexes (Kambach *et al.*, 1999; Stark *et al.*, 2001). In the Hfq-RNA structure, the RNA is bound around the pore of the doughnut shaped Hfq hexamer within a basic patch, which is located on the proximal face of the ring.

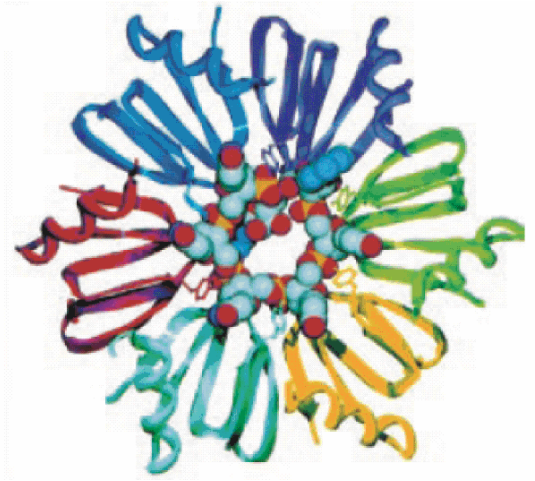

Fig. 1.2: Ribbon diagram of the Hfq-RNA complex. The different Hfq monomers are indicated by different colors. The oxygen, nitrogen, carbon, and phosphorus atoms of the RNA are colored red, blue, turquoise, and yellow, respectively. Also shown as balls and sticks are the tyrosine residues (Tyr42) from each subunit, which stack with the RNA bases (from Schumacher *et al*., 2002).

Residues in the *Staphylococcus aureus* Hfq that confer RNA-interaction and are therefore necessary for RNA-binding properties of Hfq are a glycine residue in the α-helix (note that this is the only conserved residue in the α-helix), a tyrosine residue in loop 3 (within the Sm1 motif, in most species substituted by a phenylalanine residue), and the 'KH' motif located in loop 5 and therefore being part of the Sm2 motif (Fig1.3). These residues are highly conserved among Hfq homologues.

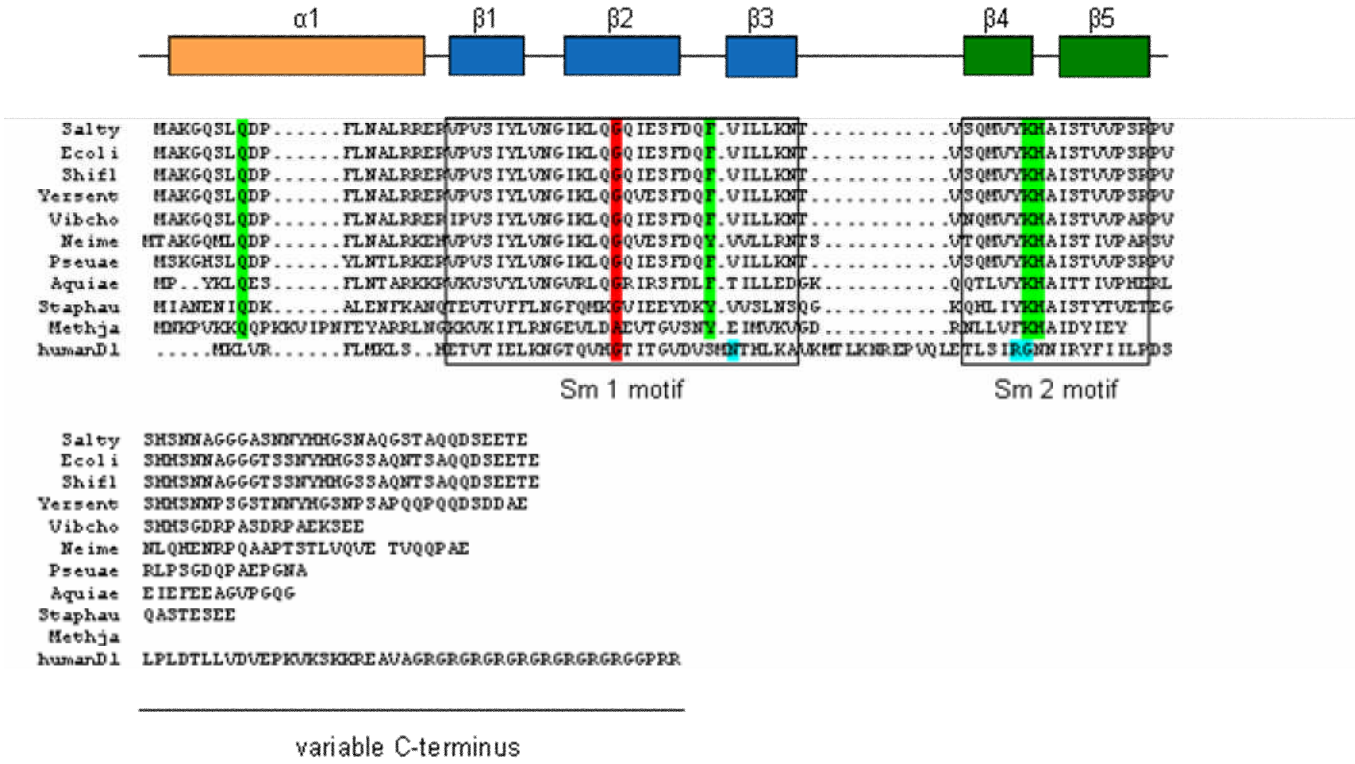

Fig. 1.3: Structure-based alignment of prokaryotic Hfq proteins with an archaeal Hfq and the human Sm protein D1 (Salty = *Salmonella* Typhimurium, E. coli = *Escherichia coli*, Shifl = *Shigella flexneri*, Yersent = *Yersinia enterocolitica*, Vibcho = *Vibrio cholerae*, Neime = *Neisseria meningitidis*, Pseuae = *Pseudomonas aeruginosa*, Aquiae = *Aquifex aeolicus*, Staphau = *Staphylococcus aureus*, Methja = *Methanocaldococcus jannaschii*). The alignment was done in MultAlin (Corpet, 1988) and optimized based on conserved residues. Structural elements are shown above the alignment and are colored as in Fig 1.1A (the α-helix is coloured yellow, the Sm1 motif is coloured blue, and the Sm2 motif green). Both Sm motifs are boxed. The conserved glycine residue in the Sm1 motif (in β2) amongst Hfq and Sm proteins (note that this residue is replaced by an alanine solely in the *Methanocaldococcus* Hfq) is blocked in red. The absolutely conserved glutamine of helix α1 that is important for base recognition and the highly conserved tyrosine (or phenylalanine) residues are blocked in light green in the Hfq proteins, whilst the signature asparagine of the eukaryotic Sm proteins at the start of β3 is blocked in light blue. Within the Sm2 motif, the 'Hfq Sm2 motif KH' is colored light green, whilst the invariant RG dipeptide of the eukaryotic Sm2 motif is colored light blue (adapted from Schumacher *et al.*, 2002).

1.4 Hfq and its pleiotropic binding partners in bacteria

The discovery of small noncoding RNAs (sRNAs) in bacteria has revolutionized our view of gene regulation in bacteria. Those regulators are usually short transcripts that act on their target mRNAs via complementary base pairing. Early biochemical studies on specific sRNAs clearly showed Hfq to interact directly with regulatory RNAs. One of the first sRNAs, shown to interact with Hfq, was the regulator of the oxidative stress response, OxyS (Zhang *et al.*, 1998). Since then an increasing number of sRNAs has been shown to associate with Hfq. Ever since the determination of Hfq as a more general RNA binding protein, global biochemical studies revealed pleiotropic features of this protein. Folichon and co-workers were able to show, that Hfq binds with high affinities to the poly(A) tail of mRNAs, what was exemplarily shown for the *rpsO* mRNA (encoding for ribosomal protein S15), which has been shown to be polyadenylated both, *in vitro* and *in vivo* (Folichon *et al.*, 2003). Aside the fact of Hfq binding to poly(A) tails, present at many mRNAs, for *rpsO* mRNA it has been shown that Hfq also stimulates the polyadenylation and to affect the frequency and length of poly(A) tails (Hajnsdorf and Régnier, 1999; Le Derout et al., 2003), leading to the assumption that this might be a general mechanism. Hfq was shown to bind to an internal site, located between two adjacent stem loops. Upon Hfq binding, the poly(A) tail and the internal binding site become protected from the ribonucleases PNPase, RNase II, and RNase E; these findings lead to the assumption for a role of Hfq in RNA maturation and degradation. Protection by Hfq against RNase E cleavage was also confirmed by Massé *et al.*, 2003 and Moll *et al.*, 2003. Mutational analysis of Hfq by Mikulecky and co-workers first identified specific amino acids on both surfaces (the proximal as well as the distal face) of the hexamer that are involved in binding of mRNAs [shown for poly(A) tails as well as the 5' untranslated region (UTR) of the *rpoS* mRNA, encoding for the stress sigma factor, σS] and sRNAs [shown for DsrA, an sRNA regulating *rpoS* expression (Mikulecky *et al.*, 2004)]. Binding studies of Hfq and different RNA-species as well as the identification of sites protected against RNases upon Hfq binding revealed a canonical binding site for Hfq, consisting of single stranded A/U-rich regions preferentially flanked by stem loop structures. Nevertheless, Hfq has not only been implied in the maturation of mRNAs and the binding of sRNAs. Also a stimulating effect on the CCA-adding enzyme and the interaction of Hfq with tRNAs has recently been reported (Scheibe *et al.*, 2007; Lee and Feig, 2008). One assumes that the complex of Hfq and tRNA

substrate might enhance the product release from the CCA-adding enzyme and that Hfq might be involved in quality control of tRNAs by binding either mature or pre-tRNAs.

Co-immunoprecipitation experiments with RNA polymerase in *E. coli* showed its interaction with the ribosomal protein S1 as well as with Hfq. Trying to determine a functional role of the observed interaction, by using transcription and coupled transcription-translation assays with subsequent analysis of ATPase activity measurements revealed ATPase activity of the RNA-binding protein, Hfq. Fractions containing the ATPase activity in chromatography experiments using cell lysates correlate with the peak of native Hfq and the ATPase activity was absent in lysates of *hfq* null mutants (Sukhodolets and Garges, 2003). Recently, biochemical and genetic analysis by Arluison and co-workers have determined an ATP-binding site in Hfq. It has been suggested that ATP binding by the Hfq-RNA complex results in its significant destabilization (Arluison *et al.*, 2007).

Investigations of the chaperone activity of Hfq revealed that Hfq binding to the sRNA and mRNA partners accelerates their interaction (Kawamoto *et al.*, 2006). While the sRNA SgrS forms a stable duplex with its target mRNA *ptsG* (encoding a major glucose transporter) even in the absence of Hfq, Hfq facilitates markedly the rate of duplex formation. Recently developed fluorescence resonance energy transfer (FRET) studies opened the possibility to look more closely into the effect of Hfq binding to RNA and the facilitation of RNA/RNA duplex formation (Rajkowitsch and Schroeder, 2007). It could be shown that Hfq induces rapid association of DsrA to *rpoS* by premelting a secondary structure of the inhibitory stem loop capturing the Shine-Dalgarno (SD) sequence in the *rpoS* mRNA (Arluison *et al.*, 2007; for further details see below).

Different global studies have proven Hfq to be a riboregulator; co-immunoprecipitation experiments with subsequent analysis of the nucleic acid fraction provided insight in a large pool of regulatory RNAs as well as messenger RNAs bound to Hfq (Wassarman *et al.*, 2001; Zhang *et al.*, 2003; Hu *et al.*, 2006). Finally, it should be mentioned, that Hfq has not only been shown to bind to a variety of RNA species, but also binds to supercoiled as well as linear DNA (Takada *et al.*, 1997) and can be found associated with the nucleoid (Ali Azam *et al.*, 1999). However, this interaction seems to be sequence-unspecific and requires high Hfq concentrations in *in vitro* gel shift experiments.

1.5 Physiological role of Hfq in bacteria

Even though early observed to be an abundant protein in *E. coli* (Carmichael *et al.*, 1975), besides its phage associated function, the importance of Hfq in uninfected bacteria remained unclear for a long time. Ever since, important physiological roles of Hfq have been established in numerous model bacteria (Valentin-Hansen *et al.*, 2004). The first evidence for a general role of Hfq in bacteria came through studies of an *hfq* insertion mutant of *E. coli*, which exhibited broad, pleiotropic phenotypes affecting growth rate, cell morphology and tolerance of stress conditions (Tsui *et al.*, 1994). Subsequent work showed that Hfq was necessary to promote efficient translation of *rpoS* mRNA in *E. coli* and *Salmonella* (Brown and Elliot, 1996; Muffler *et al.*, 1996). *rpoS* encodes for the major alternative stress sigma factor, σS. However, not all *hfq* deletion phenotypes could be assigned to impaired *rpoS* translation.

The requirement of Hfq for efficient expression σS in the enteric bacteria, *E. coli* and *Salmonella* suggested a role for Hfq in bacterial virulence. In *Salmonella*, σS is an important virulence factor as it mediates the expression of the *Salmonella* plasmid virulence (*spv*) genes, which are required for systemic infection, and enables bacteria to cope with diverse stresses (nutrient deprivation, oxidative or acid stress, and DNA damage) relevant to the environments faced in their mammalian hosts (Fang *et al.*, 1992; Bang *et al.*, 2005). A *Salmonella rpoS* mutant exhibits significantly reduced virulence in mice (Fang *et al.*, 1992), and mutated *rpoS* alleles are often found in attenuated *Salmonella* strains (Robbe-Saule *et al.*, 1995; Wilmes-Riesenberg *et al.*, 1997).

Several studies addressed a potential role of Hfq in the virulence of other pathogenic bacteria, e.g. in *Brucella abortus* (Robertson and Roop, 1999), *Vibrio cholerae* (Ding *et al.*, 2004), *Listeria monocytogenes* (Christiansen *et al.*, 2004), *Legionella pneumophila* (McNealy *et al.*, 2005), and *Pseudomonas aeruginosa* (Sonnleitner *et al.*, 2003). In most cases, the virulence defects were accompanied by reduced stress tolerance.

More recent work revealed that Hfq altered the stability of several other mRNAs, indicating that this protein acts to regulate gene expression in general at the post-transcriptional level. Hfq can act alone as a translational repressor of mRNA (Vytvytska *et al.*, 2000; Urban and Vogel, 2008), and can modulate mRNA decay by stimulating polyadenylation (Hajnsdorf and Regnier, 2000; Mohanty *et al.*, 2004).

1.6 Post-transcriptional gene regulation in bacteria

Aside transcriptional regulation exerted by proteins, over the last decade the discovery and study of small noncoding RNAs, a new class of regulators acting post-transcriptionally, expanded. sRNAs in bacteria are typically between 50 and 250 nucleotides (nt) in length and do not contain open reading frames (ORFs). Most of them are transcribed from independent sRNA genes located in intergenic regions (IGRs) which contain Rho-independent transcription terminators. Even though known in bacteria since the early 1970s, recent systematic genome-wide searches have led to an enormous increase in the number of predicted sRNAs in bacteria. While more than 70 sRNAs in *Escherichia coli* have been identified (Vogel and Sharma, 2005), yet only a few have assigned function. Many of the sRNAs found in *E. coli* are conserved in related pathogens, like *Salmonella*.

The first recognized RNA regulators exerted their function by antisense RNA pairing, and were discovered in phages and plasmids (Delihas, 1995; Wagner EG and Brantl S, 1998). These regulators are usually *cis*-encoded and therefore fully complementary to their target mRNA. Another large group of RNA regulators encompasses RNA molecules that are encoded in intergenic regions. By now, the first candidates discovered are classified as so called “housekeeping” RNAs and are present in a large number of bacterial species. These sRNAs are highly abundant, stable transcripts that were identified via direct labelling of RNA and analysis by various fractionation procedures. This category comprises 4.5S RNA (encoded by *ffs*), which is the RNA component of the signal recognition particle (SRP) and part of the secretion machinery (reviewed in Brown S, 1991; Luirink and Dobberstein, 1994); 10Sb RNA, the catalytic part of RNaseP, involved in tRNA maturation (encoded by *rnpB*; Gurevitz *et al.*, 1983), and tmRNA, which serves in translational quality control (encoded by *ssrA*; Oh *et al.*, 1990).

Another class of sRNAs comprises transcripts that confer their action by binding to protein partners. The sRNAs CsrB and CsrC have been shown to act by titration of the global regulatory protein, CsrA [reviewed in (Babitzke and Romeo, 2007)]. CsrA (carbon storage regulator A) is a protein affecting a variety of processes, including glycogen biosynthesis, carbon metabolism, motility, cell size and surface properties. When CsrB and CsrC are absent, CsrA binds to the 5’UTR of messenger RNAs, thereby occupying the ribosome binding site (RBS) and preventing ribosome entry (Baker *et al.*, 2002). In the untranslated stage the mRNAs are then subjected to degradation by RNases.

Additionally, sRNAs have been identified, that are encoded in intergenic regions and act via short, imperfect complementary sequences on their trans-encoded target mRNA. The first identified regulator of this class was the MicF RNA of *E. coli* which is encoded upstream of outer membrane protein C (*ompC*) and regulates another membrane porin, the mRNA of the outer membrane protein F, OmpF (Andersen *et al.*, 1987). Three more sRNAs that have been identified were OxyS, RprA, and DsrA (Altuvia *et al.*, 1997; Majdalani *et al.*, 2001; Sledjeski and Gottesman, 1995). Even though also shown to regulate different target genes, they all influence translation of the *rpoS* mRNA of the alternative stress sigma factor, σS.
Over the last years more and more candidates belonging to the class of trans-encoded sRNAs have been shown to be dependent on Hfq, either only for their own stability or additionally to confer interaction with their targets (see below).

1.6.1 Repression of translation via sRNAs

The most common mechanism of sRNA interaction with target mRNAs is the repression of translation. Here, the sRNA binds to its mRNA target in close proximity to the start codon, overlapping the ribosome binding site. The mostly imperfect double strand hinders ribosome entry and translation of the target. In concerted action with RNase E, this leads to degradation (often including the sRNA) of the mRNA (Massé *et al.*, 2003; Morita *et al*., 2005).
For example the early discovered MicF sRNA translationally represses its target, *ompF* mRNA, by the above described mechanism. It was shown, that MicF inhibits translation of *ompF* by complementary binding to the Shine-Dalgarno sequence and the translational star codon, thereby preventing ribosome entry, resulting in low level of the OmpF porin (Andersen and Delihas, 1990). This mechanism can also be observed for other outer membrane proteins in *E. coli* [MicC and MicA sRNAs target the 5´UTRs of *ompC* and *ompA* mRNAs, respectively (Chen *et al.*, 2004; Udekwu *et al.*, 2005: Fig. 1.4)].

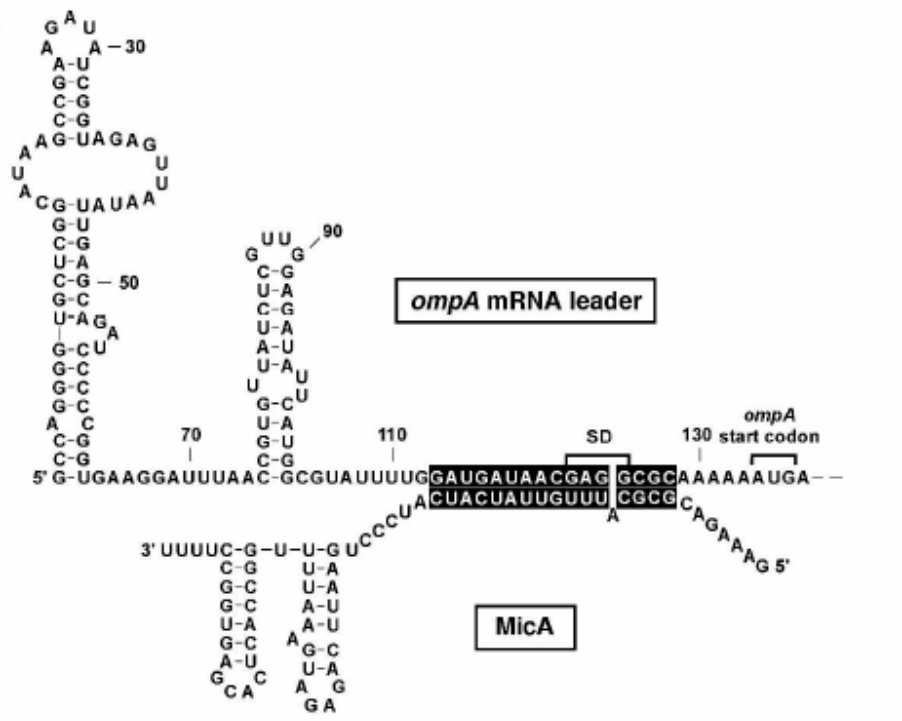

Figure 1.4: sRNA-mediated translation repression. Pairing of MicA sRNA to the 5´UTR of the *ompA* mRNA leads to translation repression by blocking ribosome entry (from Udekwu *et al.*, 2005).

However, recent reports have shown that translational repression not only takes place by direct blocking of the Shine-Dalgarno sequence via sRNAs, but that the same outcome can also be achieved by binding of an sRNA far upstream of the translation initiation site. Sharma and co-workers report, that the sRNA GcvB, which regulates multiple mRNAs of periplasmic substrate-binding proteins of amino acid and peptide transporters in *Salmonella*, binds via a conserved G/U rich region within GcvB to a C/A rich element in its target mRNAs. While for some targets this C/A rich element is located in the close proximity of the ribosomal binding site, the binding sequence for GcvB can also be located upstream of the RBS, outside of the sequence known to be covered by the initiation complex (Sharma *et al.*, 2007).

Another example is the sRNA IstR-1 in *E. coli* (Vogel *et al.*, 2004), which prohibits translation of the SOS-induced toxin TisB by binding to a region ~100 nt upstream of the *tisB* RBS under non-SOS conditions. It was recently shown that *in vitro* the RBS of *tisB* is sequestered by an intrinsic structure, whereas the region to which IstR-1 binds is

single stranded (Darfeuille *et al.*, 2007). Experimental evidence suggests this single stranded region to be a ribosome loading site, which allows translation of *tisB* by standby ribosomes sliding into the transiently open translation initiation region.
sRNA mediated translational repression also takes place within the intergenic regions of polycistronic messenger RNAs. In *E. coli*, the *galETKM* operon (encodes components involved in galactose metabolism) has been shown to be targeted by Spot42 sRNA at internal sequences of the *galETKM* mRNA. Under high nutrition conditions, when Spot42 is highly expressed based on high glucose level, the sRNA occludes the RBS of the *galK* cistron and inhibits its translation without affecting the upstream *galET* cistrons (Møller *et al.*, 2002).

1.6.2 Activation of translation via sRNAs

Another mechanism described for sRNAs is the translational activation of mRNAs upon sRNA binding. The most popular case is the activation of the σS encoding *rpoS* mRNA (Fig. 1.5). The 5'UTR of the *rpoS* mRNA folds back into an inhibitory secondary structure including nucleotides closely upstream of the AUG start codon, which occludes the RBS, rendering the mRNA translationally inactive (Brown and Elliot, 1997). The sRNAs DsrA and RprA are able to overcome this secondary structure of the 5'UTR by binding far upstream of the ribosomal binding site in the 565 nt long leader sequence, thereby activating the *rpoS* mRNA for translation.

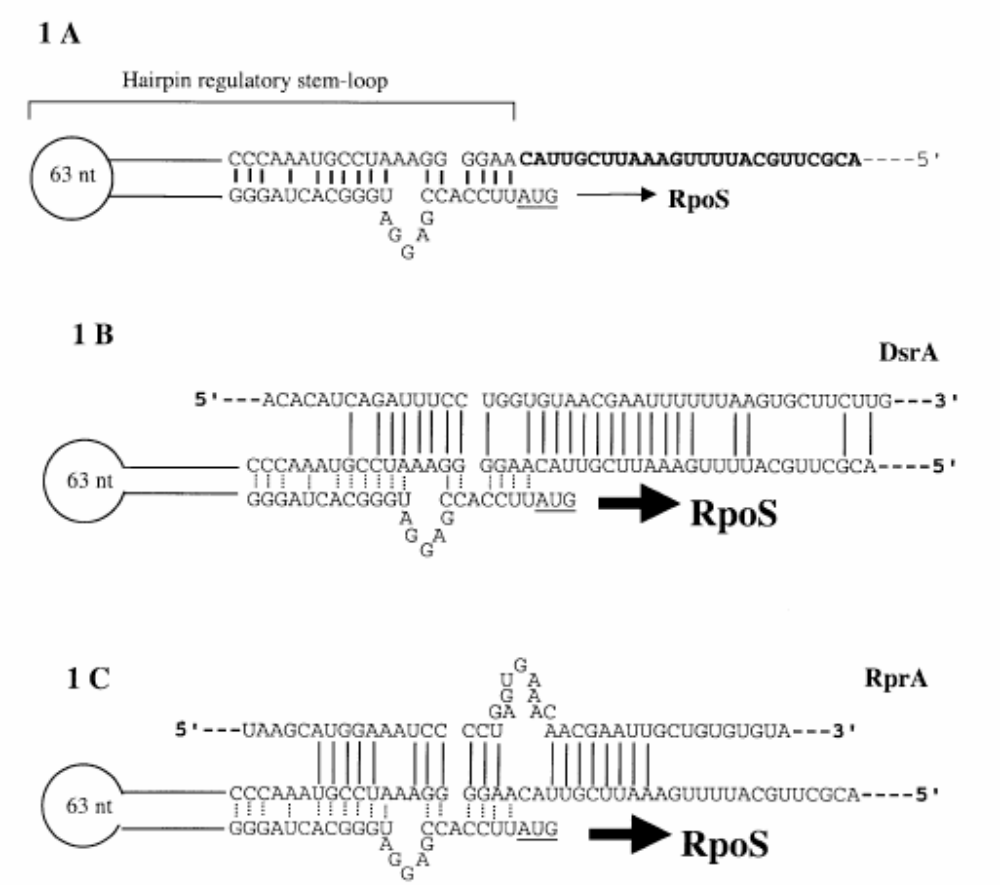

Figure 1.5: sRNA-mediated translation activation. 5´UTR of *rpoS* mRNA **(1A)**. DsrA **(1B)** or RprA **(1C)** pairing, respectively, to the 5´UTR of *rpoS* mRNA activates translation by disrupting an intrinsic inhibitory structure promoting ribosome entry (Repoila *et al*., 2003).

Even though both of them pair with the leader and disrupt hairpin formation (Majdalani *et al.*, 1998; 2001), the two sRNAs act under different conditions on *rpoS* mRNA, based on their different expression profile. While DsrA is induced at low temperatures, RprA expression peaks upon cell surface stress (Repoila and Gottesman, 2001; Majdalani *et al.*, 2002).

GadY represents a sRNA encoded in *cis* to its target mRNA, *gadX*, a transcriptional regulator of the acid response (Opdyke *et al.*, 2004). Since *gadY* is *cis*-encoded and transcribed from the opposite strand of its target, part of it shows perfect complementarity to the *gadX* 3´UTR. Basepairing to this region is suggested to protect the mRNA from exoribonucleases, which in turn leads to stabilization of the mRNA and thereby to accumulation of the GadX protein.

Discoordinate operon expression, as achieved for the *galETKM* by downregulation of *galK* upon Spot42 binding, can also be exerted by activation of a cistron in a polycistronic mRNA. An example is the upregulation of *glmS*, which encodes an essential enzyme in amino-sugar metabolism, glucosamine-6-phosphate (GlcN-6-P). *glmS* is transcribed in conjunction with *glmU* as the dicistronic *glmUS* mRNA. In *E. coli*, direct binding of the sRNA GlmZ in concerted action with Hfq, leads to disruption of an inhibitory mRNA structure, followed by processing of the *glmUS* message by RNase E in the stop codon of *glmU*, thereby rendering the *glmS* message translationally active (Urban *et al.*, 2007; Kalamorz *et al.*, 2007). GlmZ itself is regulated by a second sRNA, GlmY, which controls the processing of GlmZ, thereby preventing the inactivation of this direct regulator of *glmS* (Urban and Vogel, 2008; Reichenbach *et al.*, 2008).

1.7 Influence of Hfq in post-transcriptional gene regulation

Hfq has emerged as a general post-transcriptional regulator through its involvement in mRNA translational control by small non-coding RNAs. Hfq was first observed to be involved in translational repression of *rpoS* mRNA by OxyS (Zhang *et al.*, 1998). Since then, numerous *E. coli* sRNAs have been shown to associate with Hfq *in vivo* (Zhang *et al.*, 2003) and to require this protein for their own stability and/or for interactions with their target mRNAs [reviewed in (Majdalani *et al.*, 2005; Romby *et al.*, 2006; Valentin-Hansen *et al.*, 2004)]. For some sRNAs, it has been established that Hfq binding protects against RNase E digestion, since sites of cleavage of this endoribonuclease share sequence similarity to suggested Hfq binding sites (Moll *et al.*, 2003). Moreover, Hfq acts as an RNA chaperone to induce differential folding within a sRNA or mRNA upon binding. RNase digestion patterns of the OxyS and Spot42 sRNAs have been reported to be different in the presence or absence of Hfq (Zhang *et al.*, 2002; Møller *et al.*, 2002). The group of Hfq-dependent sRNAs also includes the two *E. coli* sRNAs, DsrA and RprA, which activate *rpoS* translation in response to stress conditions [reviewed in (Repoila *et al.*, 2003)]. While sRNAs often require Hfq for intracellular stability, Hfq also exerts its post-transcriptional function by the facilitation of the generally short and imperfect antisense interactions of sRNAs and their targets (Møller *et al.*, 2002; Zhang *et al.*, 2002; Zhang *et al.*, 2003; Mikulecky *et al.*, 2004; Lease and Woodson, 2004; Kawamoto *et al.*, 2006).

Therefore, two different mechanisms seem likely for mediation of sRNA/mRNA interaction and the role of Hfq. Hfq binds two RNA molecules; it has been proposed, that the distal face (the side not containing the RNA binding pocket) can bind to poly(A) tails of mRNAs. The other possible mechanism includes two separate Hfq molecules, bound to one RNA molecule each (one to a sRNA, one to an mRNA), facilitating the interaction between the two RNA species by protein-protein interaction of the two Hfq hexamers.

Once an mRNA is translationally inactivated by binding of a sRNA, often RNases take over the degradation of the RNA-RNA complex. Degradation of most mRNAs is initiated by internal cleavage by RNase E, a 5´ end-dependent endonuclease which cuts RNA in single-stranded A/U-rich regions (Mackie, 1998). While primary transcripts harbouring a 5´ triphosphate have been shown to be poor substrates for RNase E (Carpousis, 2002), the products of RNase E cleaved RNA molecules have 5´ monophosphates that render them highly susceptible to further cleavage events; these in turn lead to rapid degradation, supported by the action of 3´-5´ exonucleases, namely RNase II and polynucleotide phosphorylase, PNPase. RNase E, as part of the bacterial degradosome has been well studied over the last years. The catalytic protein consists of different domains: the N-terminal domain holds the ribonucleolytic activity, the centre part is conferred to as the RNA binding domain, and the C-terminal ´scaffold´ region interacts with other protein components of the degradosome [PNPase, enolase (a glycolytic enzyme) and RhlB (a DEAD-box RNA helicase)]. RhlB is thought to unwind RNA stem-loops in an ATP-dependent manner, thereby facilitating PNPase-mediated degradation of highly structured RNAs. The role of enolase is less clear but it seems to have crucial functions in the degradation of certain mRNA species (Morita *et al.*, 2004).

Studies on degradosome complexes revealed also involvement of Hfq in the process of degradation of the RNA-RNA complexes. The *ptsG* mRNA, encoding a major glucose transporter, is rapidly degraded in an RNase E-dependent manner when its 5´UTR gets targeted by SgrS sRNA, whose expression is induced in response to phosphosugar stress (Morita *et al.*, 2004). When analyzing all components of the ribonucleoprotein complex after pull-down experiments using a FLAG-epitope tagged version of RNase E Morita and co-workers have shown, that Hfq is stably associated with the C-terminal scaffold region of RNase E. Surprisingly, Hfq and other components of the degradosome seem to interact in an exclusive manner with RNase E; Hfq could only be identified in complex with RNase E when neither PNPase or enolase, nor RhlB were present. In turn, Hfq could not be identified in complexes containing all components of the degradosome,

including RNase E (Morita *et al.*, 2005). Since also SgrS could be shown to bind to Hfq the following model is proposed: complexes containing a sRNA, Hfq, and RNase E act on the cognate target mRNAs as specialized RNA decay machines. Herein, the role of the sRNA is to guide RNase E to target mRNAs through Hfq while Hfq acts as an adaptor between RNase E and the sRNA. Upon binding of the sRNA to its target Hfq is likely to leave the complex, freeing the scaffold region of RNase E to interact with other proteins of the degradosome complex.

Another RNase implicated in sRNA mediated gene regulation is the *rnc* encoded RNase III, which cleaves preferentially long double-stranded duplexes. RNase III dependent cleavage of *tisAB* mRNA, along with its cognate sRNA, IstR-1, was observed *in vivo* (Vogel *et al.*, 2004). Moreover, the RyhB sRNA accumulates in *rnc* mutant strains to high levels, and was found to be cleaved by RNase III *in vitro* depending on the presence of its target mRNA, *sodB* (Afonyushkin *et al.*, 2005).

1.8 The model pathogen *Salmonella enterica* Serovar Typhimurium

Pathogenic *Salmonella* species are an important cause of infectious diseases throughout the world. In humans they cause infections ranging from gastroenteritis to typhoid fever. *Salmonella enterica* serovars Enteritidis and Typhimurium cause the majority of human gastroenteritis infections. The development of tissue culture cell infection systems has led to the characterization of many virulence factors necessary for *Salmonella* pathogenesis.

Virulence of *Salmonella* Typhimurium is conferred by a large set of virulence genes. While some are encoded on the plasmid pSLT (*spv* genes) others are encoded in so called *Salmonella* pathogenicity islands (SPIs). SPIs are gene clusters which are acquired via horizontal gene transfer (HGT). The integration of SPI regions into the chromosome is most obvious by the significant difference in AT content of the SPIs when compared to the *Salmonella* core genome. While the overall GC content is on average 52 %, the SPIs are AT-rich regions with a significantly lower GC content. The chromosome of *Salmonella* Typhimurium contains five major pathogenicity islands, SPI1-SPI5.

An early step in non-typhoidal *Salmonella* infections, following ingestion, is the invasion of the bacteria cells into the intestinal epithelium. Epithelial cells, being non-phagocytic, are forced by so called effector proteins, encoded and expressed by the *Salmonella*

cells, to take up the bacteria. Therefore the effector proteins are translocated into the host cells via a type three secretion system (TTSS). *Salmonella* encodes two TTSS, one in SPI1, the other in SPI2. In the intestinal environment, *Salmonella* encounters an environment of high salt and low oxygen conditions. These trigger the expression of SPI1, which encodes the TTSS and several effector proteins necessary for initial invasion (Collazo and Galan, 1996; Galan and Curtiss, 1989; Mills *et al.*, 1995). Gene expression of SPI1 follows a transcription factor cascade; on top of the cascade, the transcription factors HilC and HilD lead to derepression of the downstream transcription factor, HilA (Bajaj *et al.*, 1996; Ellermeier *et al.*, 2005; Lucas and Lee, 2001; Schechter and Lee, 2001). HilA activates the expression of the SPI1 TTSS components and the different effector genes, both directly and indirectly through its activation of InvF (Darwin and Miller, 1999; Eichelberg and Galan, 1999; Lostroh and Lee, 2001). Upon cell-cell contact effector proteins are translocated via a needle into the epithelial cells. Several effector proteins like SipC and SipD lead to membrane rearrangement in the host cells and subsequently to engulfment and uptake of the *Salmonella* cells. Intracellularly, *Salmonella* resides in the *Salmonella* containing vacuole (SCV). Here *Salmonella* replicates and spreads into macrophages, to escape the innate immunity or leads to systemic infections. Once residing in host cells in SCVs the expression of the SPI2 is turned on, encoding for a second TTSS and a set of effector proteins, necessary for survival and replication inside of the host cells (Shea *et al.*, 1996; Cirillo *et al.*, 1998; Hensel *et al.*, 1998). SPI4 encodes a type one secretion system and a large, over 500 kDa, protein to enhance adhesion to epithelial cells (Gerlach *et al.*, 2007). SPI5 encodes additional effector proteins whose expression is coordinated by the SPI1-encoded transcription factor, HilA, and which are translocated by the SPI1 TTSS (e.g. SopB; Ahmer *et al.*, 1999). The biological function of SPI3 in infections remains somewhat elusive. Single effector proteins involved in invasion and establishment of *Salmonella* in the host cell have also been found encoded in the core genome (e.g. SopD).

1.9 References

Afonyushkin T, Vecerek B, Moll I, Bläsi U, Kaberdin VR (2005) Both RNase E and RNase III control the stability of sodB mRNA upon translational inhibition by the small regulatory RNA RyhB. Nucleic Acids Res 33:1678-1689

Ahmer BM, van Reeuwijk J, Watson PR, Wallis TS, Heffron F (1999) Salmonella SirA is a global regulator of genes mediating enteropathogenesis. Mol Microbiol 31: 971-982

Andersen J, Delihas N (1990) micF RNA binds to the 5' end of ompF mRNA and to a protein from Escherichia coli. Biochemistry 29: 9249-9256

Andersen J, Delihas N, Ikenaka K, Green PJ, Pines O, Ilercil O, Inouye M (1987) The isolation and characterization of RNA coded by the micF gene in Escherichia coli. Nucleic Acids Res 15: 2089-2101

Albrecht M, Lengauer T (2004) Novel Sm-like proteins with long C-terminal tails and associated methyltransferases. FEBS Lett 569: 18-26

Ali Azam T, Iwata A, Nishimura A, Ueda S, Ishihama A (1999) Growth phase-dependent variation in protein composition of the Escherichia coli nucleoid. J Bacteriol 181: 6361-6370.

Altuvia S, Weinstein-Fischer D, Zhang A, Postow L, Storz G (1997) A small, stable RNA induced by oxidative stress: role as a pleiotropic regulator and antimutator. Cell 90: 43-53

Arluison V, Hohng S, Roy R, Pellegrini O, Régnier P, Ha T (2007) Spectroscopic observation of RNA chaperone activities of Hfq in post-transcriptional regulation by a small non-coding RNA. Nucleic Acids Res 35: 999-1006

Arluison V, Mutyam SK, Mura C, Marco S, Sukhodolets MV (2007) Sm-like protein Hfq: location of the ATP-binding site and the effect of ATP on Hfq-- RNA complexes. Protein Sci 16:1830-1841

Babitzke P, Romeo T (2007) CsrB sRNA family: sequestration of RNA-binding regulatory proteins. Curr Opin Microbiol 10: 156-163

Bajaj V, Lucas RL, Hwang C, Lee CA (1996) Co-ordinate regulation of Salmonella typhimurium invasion genes by environmental and regulatory factors is mediated by control of hilA expression. Mol Microbiol 22: 703-714.

Baker CS, Morozov I, Suzuki K, Romeo T, Babitzke P (2002) CsrA regulates glycogen biosynthesis by preventing translation of glgC in Escherichia coli. Mol Microbiol 44: 1599-1610

Bang IS, Frye JG, McClelland M, Velayudhan J, Fang FC (2005) Alternative sigma factor interactions in Salmonella: sigma and sigma promote antioxidant defences by enhancing sigma levels. Mol Microbiol 56: 811-823

Brown L, Elliott T (1996) Efficient translation of the RpoS sigma factor in Salmonella typhimurium requires host factor I, an RNA-binding protein encoded by the hfq gene. J Bacteriol 178: 3763-3770.

Brown S (1991) 4.5S RNA: does form predict function? New Biol 3: 430-438

Carmichael GG (1975) Isolation of bacterial and phage proteins by homopolymer RNA-cellulose chromatography. J Biol Chem 250: 6160-6167

Carpousis AJ (2002) The Escherichia coli RNA degradosome: structure, function and relationship in other ribonucleolytic multienzyme complexes. Biochem Soc Trans 30:150-155

Chen S, Zhang A, Blyn LB, Storz G (2004) MicC, a second small-RNA regulator of Omp protein expression in Escherichia coli. J Bacteriol 186: 6689-6697

Christiansen JK, Larsen MH, Ingmer H, Sogaard-Andersen L, Kallipolitis BH (2004) The RNA-binding protein Hfq of Listeria monocytogenes: role in stress tolerance and virulence. J Bacteriol 186: 3355-3362

Cirillo DM, Valdivia RH, Monack DM, Falkow S (1998) Macrophage-dependent induction of the Salmonella pathogenicity island 2 type III secretion system and its role in intracellular survival. Mol Microbiol 30: 175-188

Collazo CM, Galan JE (1996) Requirement for exported proteins in secretion through the invasion-associated type III system of Salmonella typhimurium. Infect Immun 64: 3524-3531

Corpet F (1988) Multiple sequence alignment with hierarchical clustering. Nucleic Acids Res 16:10881-10890

Darfeuille F, Unoson C, Vogel J, Wagner EG (2007) An antisense RNA inhibits translation by competing with standby ribosomes. Mol Cell 26: 381-392

Darwin KH, Miller VL (1999) InvF is required for expression of genes encoding proteins secreted by the SPI1 type III secretion apparatus in Salmonella typhimurium. J Bacteriol 181: 4949-4954

Delihas N (1995) Regulation of gene expression by trans-encoded antisense RNAs. Mol Microbiol 15: 411-414

Ding Y, Davis BM, Waldor MK (2004) Hfq is essential for Vibrio cholerae virulence and downregulates sigma expression. Mol Microbiol 53: 345-354

Eichelberg K, Galan JE (1999) Differential regulation of Salmonella typhimurium type III secreted proteins by pathogenicity island 1 (SPI-1)-encoded transcriptional activators InvF and hilA. Infect Immun 67: 4099-4105

Ellermeier CD, Ellermeier JR, Slauch JM (2005) HilD, HilC and RtsA constitute a feed forward loop that controls expression of the SPI1 type three secretion system

regulator hilA in Salmonella enterica serovar Typhimurium. Mol Microbiol 57: 691-705

Fang FC, Libby SJ, Buchmeier NA, Loewen PC, Switala J, Harwood J, Guiney DG (1992) The alternative sigma factor katF (rpoS) regulates Salmonella virulence. Proc Natl Acad Sci U S A 89: 11978-11982

Folichon M, Arluison V, Pellegrini O, Huntzinger E, Régnier P, Hajnsdorf E (2003) The poly(A) binding protein Hfq protects RNA from Rnase E and exoribonucleolytic degradation. Nucleic Acids Res 31: 7302-7310

Franze de Fernandez MT, Eoyang L, August JT (1968) Factor fraction required for the synthesis of bacteriophage Qbeta-RNA. Nature 219: 588-590.

Franze de Fernandez MT, Hayward WS, August JT (1972) Bacterial proteins required for replication of phage Q ribonucleic acid. Pruification and properties of host factor I, a ribonucleic acid-binding protein. J Biol Chem 247: 824-831.

Fromont-Racine M, Mayes AE, Brunet-Simon A, Rain JC, Colley A, Dix I, Decourty L, Joly N, Ricard F, Beggs JD, Legrain P (2000) Genome-wide protein interaction screens reveal functional networks involving Sm-like proteins. Yeast 17: 95-110

Galan JE, Curtiss R 3rd (1989) Cloning and molecular characterization of genes whose products allow Salmonella typhimurium to penetrate tissue culture cells. Proc Natl Acad Sci U S A 86: 6383-6387

Gerlach RG, Jaeckel D, Stecher B, Wagner C, Lupas A, Hardt WD, Hensel M (2007) Salmonella pathogenicity island 4 encodes a giant non-fimbrial adhesin and the cognate type 1 secretion system. Cell Microbiol 9: 1834-1850

Gurevitz M, Jain SK, Apirion D (1983) Identification of a precursor molecular for the RNA moiety of the processing enzyme RNase P. Proc Natl Acad Sci U S A 80:4450-4454

Hajnsdorf E, Regnier P (2000) Host factor Hfq of Escherichia coli stimulates elongation of poly(A) tails by poly(A) polymerase I. Proc Natl Acad Sci U S A 97: 1501-1505

Hensel M, Shea JE, Waterman SR, Mundy R, Nikolaus T, Banks G, Vazquez-Torres A, Gleeson C, Fang FC, Holden DW (1998) Genes encoding putative effector proteins of the type III secretion system of Salmonella pathogenicity island 2 are required for bacterial virulence and proliferation in macrophages. Mol Microbiol 30: 163-174

Hermann H, Fabrizio P, Raker VA, Hornig H, Brahms H, Lührmann R (1995) snRNP Sm proteins share two evolutionarily conserved sequence motifs which are involved in Sm protein-protein interactions. EMBO J 14: 2076-2088

Hu Z, Zhang A, Storz G, Gottesman S, Leppla SH (2006) An antibody-based microarray assay for small RNA detection. Nucleic Acids Res 34: e52

Kajitani M, Kato A, Wada A, Inokuchi Y, Ishihama A (1994) Regulation of the Escherichia coli hfq gene encoding the host factor for phage Q beta. J Bacteriol 76: 531-534.

Kalamorz F, Reichenbach B, Marz W, Rak B, Goerke B (2007) Feedback control of glucosamine-6-phosphate synthase GlmS expression depends on the small RNA GlmZ and involves the novel protein YhbJ in Escherichia coli. Mol Microbiol 65: 1518-1533

Kambach C, Walke S, Nagai K (1999) Structure and assembly of the spliceosomal small nuclear ribonucleoprotein particles. Curr Opin Struct Biol 9: 222-230

Kambach C, Walke S, Young R, Avis JM, de la Fortelle E, Raker VA, Lührmann R, Li J, Nagai K (1999) Crystal structures of two Sm protein complexes and their implications for the assembly of the spliceosomal snRNPs. Cell 96: 375-387

Kawamoto H, Koide Y, Morita T, Aiba H (2006) Base-pairing requirement for RNA silencing by a bacterial small RNA and acceleration of duplex formation by Hfq. Mol Microbiol 61: 1013-1022

Lease RA, Woodson SA (2004) Cycling of the Sm-like protein Hfq on the DsrA small regulatory RNA. J Mol Biol 344: 1211-1223

Le Derout J, Folichon M, Briani F, Dehò G, Régnier P, Hajnsdorf E (2003) Hfq affects the length and the frequency of short oligo(A) tails at the 3' end of *Escherichia coli rpsO* mRNAs. Nucleic Acids Res 31: 4017-4023

Lee T, Feig AL (2008) The RNA binding protein Hfq interacts specifically with tRNAs. Rna 14: 514-523.

Lostroh CP, Lee CA (2001) The Salmonella pathogenicity island-1 type III secretion system. Microbes Infect 3: 1281-1291.

Lucas RL, Lee CA (2001) Roles of hilC and hilD in regulation of hilA expression in Salmonella enterica serovar Typhimurium. J Bacteriol 183: 2733-2745

Luirink J, Dobberstein B (1994) Mammalian and Escherichia coli signal recognition particles. Mol Microbiol 11: 9-13

Mackie GA (1998) Ribonuclease E is a 5'-end-dependent endonuclease. Nature 395: 720-723

Majdalani N, Cunning C, Sledjeski D, Elliott T, Gottesman S (1998) DsrA RNA regulates translation of RpoS message by an anti-antisense mechanism, independent of its action as an antisilencer of transcription. Proc Natl Acad Sci U S A 95:12462-12467

Majdalani N, Chen S, Murrow J, St John K, Gottesman S (2001) Regulation of RpoS by a novel small RNA: the characterization of RprA. Mol Microbiol 39: 1382-1394

Majdalani N, Hernandez D, Gottesman S (2002) Regulation and mode of action of the second small RNA activator of RpoS translation, RprA. Mol Microbiol. 2002 Nov;46(3):813-26

Majdalani N, Vanderpool CK, Gottesman S (2005) Bacterial small RNA regulators. Crit Rev Biochem Mol Biol 40:93-113

Massé E, Escorcia FE, Gottesman S (2003) Coupled degradation of a small regulatory RNA and its mRNA targets in Escherichia coli. Genes Dev 17: 2374-2383

McNealy TL, Forsbach-Birk V, Shi C, Marre R (2005) The Hfq homolog in Legionella pneumophila demonstrates regulation by LetA and RpoS and interacts with the global regulator CsrA. J Bacteriol 187: 1527-1532

Mikulecky PJ, Kaw MK, Brescia CC, Takach JC, Sledjeski DD, et al. (2004) Escherichia coli Hfq has distinct interaction surfaces for DsrA, rpoS and poly(A) RNAs. Nat Struct Mol Biol 11: 1206-1214

Mills DM, Bajaj V, Lee CA (1995) A 40 kb chromosomal fragment encoding Salmonella typhimurium invasion genes is absent from the corresponding region of the Escherichia coli K-12 chromosome. Mol Microbiol 15: 749-759

Mohanty BK, Maples VF, Kushner SR (2004) The Sm-like protein Hfq regulates polyadenylation dependent mRNA decay in Escherichia coli. Mol Microbiol 54: 905-920.

Moll I, Afonyushkin T, Vytvytska O, Kaberdin VR, Blaesi U (2003) Coincident Hfq binding and RNase E cleavage sites on mRNA and small regulatory RNAs. RNA 9:1308-1314

Møller T, Franch T, Hojrup P, Keene DR, Bachinger HP, et al. (2002) Hfq: a bacterial Sm-like protein that mediates RNA-RNA interaction. Mol Cell 9: 23-30

Morita T, Kawamoto H, Mizota T, Inada T, Aiba H (2005) Enolase in the RNA degradosome plays a crucial role in the rapid decay of glucose transporter mRNA in the response to phosphosugar stress in Escherichia coli. Mol Microbiol 54:1063-1075

Morita T, Maki K, Aiba H (2005) RNase E-based ribonucleoprotein complexes: mechanical basis of mRNA destabilization mediated by bacterial noncoding RNAs. Genes Dev 19: 2176-2186

Muffler A, Fischer D, Hengge-Aronis R (1996) The RNA-binding protein HF-I, known as a host factor for phage Qbeta RNA replication, is essential for rpoS translation in Escherichia coli. Genes Dev 10: 1143-1151.

Nielsen JS, Bøggild A, Andersen CB, Nielsen G, Boysen A, Brodersen DE, Valentin-Hansen P (2008) An Hfq-like protein in archaea: crystal structure and functional characterization of the Sm protein from Methanococcus jannaschii. Rna 13: 2213-2223

Nikulin A, Stolboushkina E, Perederina A, Vassilieva I, Blaesi U, Moll I, Kachalova G, Yokoyama S, Vassylyev D, Garber M, Nikonov S (2005) Structure of Pseudomonas aeruginosa Hfq protein. Acta Crystallogr D Biol Crystallogr 61: 141-146

Oh BK, Chauhan AK, Isono K, Apirion D (1990) Location of a gene (ssrA) for a small, stable RNA (10Sa RNA) in the Escherichia coli chromosome. J Bacteriol 172:4708-4709

Opdyke JA, Kang JG, Storz G (2004) GadY, a small-RNA regulator of acid response genes in Escherichia coli. J Bacteriol 186:6698-6705

Rajkowitsch L, Schroeder R (2007) Dissecting RNA chaperone activity. RNA 13: 2053-2060

Reichenbach B, Maes A, Kalamorz F, Hajnsdorf E, Goerke B (2008) The small RNA GlmY acts upstream of teh sRNA GlmZ in the activation of glmS expression and is subject to regulation by polyadenylation in Escherichia coli. Nucleic Acids Res 36: 2570-2580

Repoila F, Gottesman S (2001) Signal transduction cascade for regulation of RpoS: temperature regulation of DsrA. J Bacteriol 183:4012-4023

Repoila F, Majdalani N, Gottesman S (2003) Small non-coding RNAs, co-ordinators of adaptation processes in Escherichia coli: the RpoS paradigm. Mol Microbiol 48:855-861

Robbe-Saule V, Coynault C, Ibanez-Ruiz M, Hermant D, Norel F (2001) Identification of a non-haem catalase in Salmonella and its regulation by RpoS (sigmaS). Mol Microbiol 39: 1533-1545

Robertson GT, Roop RM Jr (1999) The Brucella abortus host factor I (HF-I) protein contributes to stress resistance during stationary phase and is a major determinant of virulence in mice. Mol Microbiol 34: 690-700

Romby P, Vandenesch F, Wagner EG (2006) The role of RNAs in the regulation of virulence-gene expression. Curr Opin Microbiol 9:229-236

Sauter C, Basquin J, Suck D (2003) Sm-like proteins in Eubacteria : the crystal structure of the Hfq protein from Escherichia coli. Nucleic Acids Res 31: 4091-4098

Scheibe M, Bonin S, Hajnsdorf E, Betat H, Mörl M (2007) Hfq stimulates the activity of the CCA-adding enzyme. BMC Mol Biol 8: 92.

Schechter LM, Lee CA (2001) AraC/XylS family members, HilC and HilD, directly bind and derepress the Salmonella typhimurium hilA promoter. Mol Microbiol 40: 1289-1299

Schumacher MA, Pearson RF, Møller T, Valentin-Hansen P, Brennan RG (2002) Structures of the pleiotropic translational regulator Hfq and an Hfq-RNA complex: a bacterial Sm-like protein. EMBO J 21: 3546-3556

Sharma CM, Darfeuille F, Plantinga TH, Vogel J (2007) A small RNA regulates multiple ABC transporter mRNAs by targeting C/A-rich elements inside and upstream of ribosome-binding sites. Genes Dev 21: 2804-2817

Shea JE, Hensel M, Gleeson C, Holden DW (1996) Identification of a virulence locus encoding a second type III secretion system in Salmonella typhimurium. Proc Natl Acad Sci U S A 93: 2593-2597

Sledjeski D, Gottesman S (1995) A small RNA acts as an antisilencer of the H-NS-silenced rcsA gene of Escherichia coli. Proc Natl Acad Sci U S A 14: 2003-2007

Sonnleitner E, Hagens S, Rosenau F, Wilhelm S, Habel A, Jager KE, Blaesi U (2003) Reduced virulence of a hfq mutant of Pseudomonas aeruginosa O1. Microb Pathog 35: 217-228

Staley JP, Guthrie C (1998) Mechanical devices of the spliceosome: motors, clocks, springs, and things. Cell 92: 315-26

Stark H, Dube P, Lührmann R, Kastner B (2001) Arrangement of RNA and proteins in the spliceosomal U1 small nuclear ribonucleoprotein particle. Nature 409: 539-542

Sukhodolets MV, Garges S (2003) Interaction of Escherichia coli RNA polymerase with the ribosomal protein S1 and the Sm-like ATPase Hfq. Biochemistry 42: 8022-8034

Takada A, Wachi M, Kaidow A, Takamura M, Nagai K (1997) DNA binding properties of the *hfq* gene product of *Escherichia coli*. Biochem Biophys Res Commun 236: 576-579

Tharun S, He W, Mayes AE, Lennertz P, Beggs JD, Parker R (2000) Yeast Sm-like proteins function in mRNA decapping and decay. Nature 404: 515-518

Tomasevic N, Peculis BA (2002) Xenopus LSm proteins bind U8 snoRNA via an internal evolutionarily conserved octamer sequence. Mol Cell Biol 22: 4101-4112

Tsui HC, Leung HC, Winkler ME (1994) Characterization of broadly pleiotropic phenotypes caused by an hfq insertion mutation in Escherichia coli K-12. Mol Micro 13: 35-49

Udekwu KI, Darfeuille F, Vogel J, Reimegård J, Holmqvist E, Wagner EG (2005) Hfq-dependent regulation of OmpA synthesis is mediated by an antisense RNA. Genes Dev 19: 2355-2366

Urban JH, Papenfort K, Thomsen J, Schmitz RA, Vogel J (2007) A conserved small RNA promotes discoordinate expression of the glmUS operon mRNA to activate GlmS synthesis. J Mol Biol 373: 521-528

Urban JH, Vogel J (2008) Two seemingly homologous noncoding RNAs act hierarchically to activate glmS mRNA translation. PLoS Biol 6: e64.

Valentin-Hansen P, Eriksen M, Udesen C (2004) The bacterial Sm-like protein Hfq: a key player in RNA transactions. Mol Microbiol 51: 1525-1533.

Vogel J, Argaman L, Wagner EG, Altuvia S (2004) The small RNA IstR inhibits synthesis of an SOS-induced toxic peptide. Curr Biol 14: 2271-2276

Vogel J, Sharma CM (2005) How to find small non-coding RNAs in bacteria. Biol Chem 386: 1219-1238

Vytvytska O, Moll I, Kaberdin VR, von Gabain A, Bläsi U (2000) Hfq (HF1) stimulates ompA mRNA decay by interfering with ribosome binding. Genes Dev 14: 1109-118

Wagner EG, Brantl S (1998) Kissing and RNA stability in antisense control of plasmid replication. Trends Biochem Sci 23: 451-454

Wassarman KM, Repoila F, Rosenow C, Storz G, Gottesmann S (2001) Identification of novel small RNAs using comparative genomics and microarrays. Genes Dev 15: 1637-1651

Wassarman KM (2002) Small RNAs in bacteria: diverse regulators of gene expression in response to environmental changes. Cell 109: 141-144

Will CL, Lührmann R (2001) Spliceosomal UsnRNP biogenesis, structure and function. Curr Opin Cell Biol 13: 290-301

Wilmes-Riesenberg MR, Foster JW, Curtiss R 3rd (1997) An altered rpoS allele contributes to the avirulence of Salmonella typhimurium LT2. Infect Immun 65: 203-210

Zhang A, Altuvia S, Tiwari A, Argaman L, Hengge-Aronis R, Storz G (1998) The OxyS regulatory RNA represses rpoS translation and binds the Hfq (HF-I) protein. EMBO J 17:6061-6068

Zhang A, Wassarman KM, Ortega J, Steven AC, Storz G (2002) The Sm-like Hfq protein increases OxyS RNA interaction with target mRNAs. Mol Cell 9: 11-22

Zhang A, Wassarman KM, Rosenow C, Tjaden BC, Storz G, et al. (2003) Global analysis of small RNA and mRNA targets of Hfq. Mol Microbiol 50: 1111-1124

2. Goal of the project

Hfq is a bacterial RNA-binding protein that acts as a key player in post-transcriptional gene regulation. With the emergence of small regulatory RNAs in bacteria and their dependence on Hfq, the role of Hfq as a riboregulator became an important focus in research concerning gene regulation in bacteria.

The RNA chaperone Hfq is essential for the virulence of *Salmonella typhimurium*

Hfq has been shown to influence the pathogenicity of a variety of bacterial pathogens. The goal of this study was to characterize an *hfq* deletion mutant of *Salmonella enterica* serovar Typhimurium. One major interest was to analyze the impact of Hfq on virulence of this model pathogen. Therefore, an *hfq* deletion mutant in strain SL1344 was contructed, from here on referred to as Δ*hfq* mutant. Aside from general physiological studies concerning growth and viability of the mutant, we wanted to determine the role of Hfq *in vivo* and performed studies in a mouse model of infection. To gain a more comprehensive view of the *hfq* deletion defect in *Salmonella*, we sought to analyze global changes in protein expression patterns concerning whole cell protein fraction, as well as periplasmic and secreted proteins. *Salmonella* infections of mammalian hosts can be dissected into different stages (e.g. adhesion, invasion, replication, spreading into tissues). To investigate the involvement of Hfq in the infection pathway of *Salmonella* Typhimurium, different types of cell culture infection assays were performed comparing the Δ*hfq* mutant to a control strain, as well as to a complementation strain.

Deep sequencing analysis of small noncoding RNA and mRNA targets of the global post-transcriptional regulator, Hfq

Several studies in *Escherichia coli* based on co-immunoprecipitation experiments have proven Hfq to be a global RNA-binding protein. Most methods used so far were limited in the final step, the determination of the RNA species. Our study on the characterization of a Δ*hfq* mutant of *Salmonella* Typhimurium revealed a broad variety of

phenotypes (reduced virulence, reduced flagellar production, massive differences in membrane constitution). Furthermore, Hfq is known to influence the expression and activity of global transcriptional regulators, like the RNA-polymerase sigma factors, σS and σE. Therefore, it remained unclear what are primary, direct effects of Hfq on mRNA level compared to secondary, indirect effects, based on differences in transcription level, due to altered expression of sigma factors and transcription factors. The major focus of the study was the determination of RNAs directly targeted by Hfq. We aimed for differentiation of directly bound Hfq-targets from downstream effects that appear in the transcriptome. We performed microarrays of the Δ*hfq* mutant and its isogenic wild type strain and compared the transcriptomic data to pyrosequencing data of Hfq co-immunoprecipitation experiments.

The emergence of small regulatory RNAs came with the need to establish a method for verification of predicted sRNAs and to search for so far unknown regulatory small RNAs. Since most detection methods are restricted to reasonable amounts of a certain transcript, we sought to provide a tool for detection of direct Hfq targets based on the method of co-immunoprecipition experiments followed by high-throughput pyrosequencing to search for so far unidentified, new Hfq dependent sRNAs, as well as to verify expression of predicted sRNAs. This provides the possibility in screening hundreds of thousand sequences at a time, so that also transcripts only present in a few copies should be detectable with this method.

3. Methods

3.1 Bacterial cell culture

All materials used throughout this study were autoclaved for 20 minutes (min) at 121°C and 1 bar before use. Where necessary solutions were steril filtered and glassware was sterilized by heating to 180°C for a minimum of three hours (h).

3.1.1 Media

If not stated otherwise bacteria were grown in Lennox-broth (L-broth) or on Lennox agar plates, respectively.

Lennox broth

Tryptone	1 % (w/v)
Yeast extract	0.5 % (w/v)
Sodium chloride	85.6 mM

Lennox agar

as L-broth, but supplemented with 1.2 % (w/v) agar

Growth was carried out at 37°C with an agitation of 220 rotations per minute (rpm) under normal aeration. Cultures were either inoculated from single colony grown overnight (o/n) at 37°C or were diluted 1/100 into fresh medium from o/n cultures that were inoculated from freshly grown single colonies into 3 ml L-broth.
For inducible promoters cultures were supplemented with 0.1 - 0.2 % L-arabinose or 0.5 mM IPTG, were indicated.

The following antibiotica were used throughout the study:

Kanamycin	50 μg / ml
Ampicillin	50 or 100 μg / ml for low- or high-copy plasmids, respectively
Chloramphenicol	20 or 30 μg / ml for low- or high-copy plasmids, respectively

3.1.2 Preparation of electrocompetent *Salmonella* cells

For preparation of electrocompetent *Salmonella*, cells were inoculated either from single colony or 1/100 from o/n cultures in fresh medium. The culture was incubated at 37°C, 220 rpm until the suspension reached an OD_{600} of 0.5. Cells were washed three times in ice-cold steril water. Cells were resuspended in 50 µl ice-cold steril water and subjected to electroporation. Following transformation cells were resuspended in 1 ml SOC medium prior plating. Recovery was carried out for 60 min at 37°C, 220 rpm.

SOC medium

Tryptone	2 % (w/v)
Yeast extract	0.5 % (w/v)
NaCl	85.6 mM
KCl	2.5 mM
$MgCl_2$	10 mM
Glucose	20 mM

3.1.3 Transformation of chemically competent E. coli cells

1 µl of a ligation was mixed with 20 µl of chemically competent E.coli TOP10 or TOP10 F', respectively (Invitrogen). After pre-incubation for 30 min on ice a heat shock was performed for 30 seconds (s) at 42°C. Cells were chilled on ice and resuspended in 100 µl SOC medium. Recovery was carried out for 60 min at 37°C, 220 rpm.

3.1.4 Growth under SPI-1 inducing conditions

For growth under SPI-1 inducing conditions L-broth was supplemented with sodium chloride (NaCl) up to a final concentration of 0.3 M. Bacteria were inoculated from single colony in 5 ml L-broth / 0.3 M NaCl in 15 ml Falcon tubes. Growth was carried out for 12 h at 37°C with agitation of 220 rpm. To maintain oxygen tension lids were kept tightly closed throughout growth.

3.1.5 Growth under SPI-2 inducing conditions

For growth under SPI-2 inducing conditions PCN 1 minimal medium (Lober *et al.*, 2006) was used containing the following stock solutions:

MES	800 mM
Glucose	20 %
NH_4Cl	1.5 M
$MgSO_4$	1 M
$CaCl_2$	10 mM

Phosphate buffer 250 mM, pH5.8

K_2HPO_4	0.7 g
KH_2PO_4	6.26 g

Add H_2O to a final volume of 200 ml.

Micronutrients

Na_2MoO_4	1 µM
$NaSeO_3$	1 µM
H_3BO_3	4 mM
$CoCl_2$	0.3 mM
$CuSO_4$	0.1 mM
$MnCl_2$	0.8 mM
$ZnSO_4$	0.1 mM

PCN 1 medium

MES	50 ml
Phosphate buffer, pH 5.8	2.5 ml
Glucose	10 ml
NH_4Cl	5 ml
Micronutrients	500 µl
$MgSO_4$	500 µl
$CaCl_2$	500 µl

Add H_2O to a final volume of 200 ml.

70 ml SPI-2 medium were inoculated 1/100 from overnight cultures grown in the same medium. Incubation was carried out at 37°C with agitation of 220 rpm until the cultures reached an OD_{600} of 0.3.

3.1.6 Growth curves

For growth curve determination 30 ml L-broth, supplement with the appropriate antibiotic, were inoculated from o/n culture to an OD_{600} of 0.04. Growth was carried out at 37°C, 220 rpm. The OD_{600} was measured in time intervals of 45 min over a time period of 630 min.

3.1.7 Motility assay

1 µl of a culture grown to an OD_{600} of 2 was inoculated in motility agar plates (L-broth / 0.3 % agarose), followed by incubation for 4 h at 37°C. The motility state was measured by the size of the concentric ring around the site of inoculation.

3.2 Mutant construction in *Salmonella* Typhimurium

3.2.1 One-step inactivation of chromosomal genes

Chromosomal mutagenesis of *Salmonella* Typhimurium SL1344 followed the procedure described by (Datsenko and Wanner, 2000) for *E. coli* with few modifications. The wild type *Salmonella* strain carrying plasmid pKD46 (JVS-00008) was grown in L-broth supplemented with ampicillin and 0.2 % L-arabinose at 28°C to an OD_{600} of 0.5 (25 ml culture per transformation). Cells were collected by centrifugation (2 min, 11 000 rpm), washed 3 times with ice-cold water, and dissolved in 50 µl ice-cold water. Polymerase chain reaction (PCR) products of marker genes (50 µl standard reactions) were *Dpn*I-treated for 3 h at 37°C, and purified on agarose gels, followed by purification on Macherey-Nagel spin columns (NucleoSpin Extract II). One-fifth of the 25 µl column eluate (in water) was used for transformation. 50 µl of competent cells were mixed with the purified PCR product in a chilled cuvette (0.1-cm electrode gap) and electroporated

(18 kV / cm). Subsequently, 1 ml of pre-warmed SOC medium was added, and cells were recovered by incubation for 1 h at 37°C before selection on L-broth agar plates with the appropriate antibiotics. All mutations were moved to a fresh SL1344 background by phage P22 transduction.

3.2.2 Chromosomal Flag-tagging

Chromosomal Flag-tagging of *Salmonella* SL1344 followed the procedure described by (Uzzau *et al.*, 2001) for *E. coli*. PCR was performed with primers containing the according flanking sites on plasmid pSUB11, containing the sequence for a 3 x Flag tag followed by a kanamycin resistance cassette. The PCR product of a 50 µl reaction was purified on Macherey-Nagel spin columns (NucleoSpin Extract II) and was eluted in 15 µl water. For transformation 5 µl of the PRC product was used. The following procedure equals the protocol for one-step inactivation of chromosomal genes (see 3.2.1).

3.2.3 Resistance removal following chromosomal one-step inactivation or Flag-tagging

For removal of resistance genes of mutant *Salmonella* the strain was transformed with the FLP recombinase expressing helper plasmid pCP20 (Datsenko and Wanner, 2000) and transformants were selected at 28°C on plates containing ampicillin. Transformants were struck on three fresh plates, one containing no antibiotic, one containing ampicillin (as a control for removal of the pCP20 helper plasmid) and one containing chloramphenicol or kanamycin, respectively (as a control for removal of the chromosomal resitance cassette). Transformants grown o/n exclusively on plate containing no antibiotic were used for further experiments.

3.2.4 P22 transduction

P22 lysates were prepared from soft agar plate lysates of donor strains using P22 phage HT/105-1 by standard procedure (Sternberg and Maurer, 1991). 100 µl of an o/n culture of the donor strain were mixed with 3 ml TOP agar and poured on a pre warmed L-broth plate.

TOP agar	
Tryptone	1 % (w/v)
Agar	1 % (w/v)
$MgSO_4$	10 mM
$CaCl_2$	5 mM
NaCl	86 mM

100 µl of a P22 phage lysate were spread on the TOP agar surface. When plates were dry incubation was carried out o/n at 37°C. TOP agar was collected from the plate and resuspended in 5 ml L-broth containing 10 mM magnesium sulfate and 5 mM calcium chloride. Upon addition of 400 µl Chloroform, the suspension was vigorously vortexed and incubated o/n at 4°C. After centrifugation for 10 min, 4 000 rpm the supernatant was transferred into a glass tube and 400 µl Chloroform were added to the phage lysate. Storage was performed at 4°C

For transduction 100 µl of a culture of the acceptor strain grown to an OD_{600} of 1 were mixed with 1, 10, and 100 µl of the phage lysate, respectively and incubated for 15 min at room temperature. To stop the transduction 100 µl of a 20 mM EGTA solution were added to 100 µl of the mixture. The entire 200 µl aliquot was plated on pre-warmed L-plates containing the appropriate antibiotic. Incubation was carried out for up to 3 days at 37°C. Transformants were verified by PCR.

3.3 Nucleic acids techniques

The concentrations of all nucleic acid solutions (DNA as well as RNA) were determined by measurements using a NanoDrop machine. For purification of PCR products or plasmid mini-preps the NucleoSpin Extract II and the NucleoSpin Plasmid QuickPure kits, respectively, from Macherey-Nagel were used. The standard methods of *in vitro* amplification of DNA by PCR and the ligation of DNA fragments was basically carried out as described in (Sambrook and Russell, 2001).

3.3.1 Nucleic acids gel electrophorese

3.3.1.1 Agarose gel electrophoresis

Agarose gels were used to separate DNA fragments. For gel preparation agarose was dissolved in concentrations of 0.8 to 2% (w/v) in 1x TAE buffer by heating in a microwave.

50x TAE buffer

Tris Base	242 g
Acetic acid	57.1 ml
EDTA (0.5M)	100 ml

Adjust pH to 8.5. Add H_2O to a final volume of 1 l.

At a gel solution temperature of 50-60°C ethidium bromide was added to a final concentration of 40 μg / 100 ml and the solution poured into the prepared chamber. When hardened the gel was covered with 1x TAE buffer and samples were loaded. Prior loading 4 volumes of sample were mixed with 1 volume of 5x sample loading buffer. Gels were run at 100 V for about 30-60 min (according to fragment size).

3.3.1.2 Polyacrylamidde gel electrophoresis (PAGE)

Polyacrylamide (PAA) gels were used to separate RNA fragments of different size. For gel preparation 40% PAA solution was used. Gels were run in the presence of TBE buffer.

10x TBE buffer

Tris Base	0.89 M
Boric acid	0.89 M
EDTA (0.5M, pH8.0)	20 mM

Add H_2O to a final volume of 1 l.

3.3.1.2.1 Denaturing PAGE

For denaturing gels (the native structure of RNA molecules is destroyed) the gels are supplemented with Urea to a final concentration of 8.3 M.

5 % PAA gel solution

PAA solution 40 % (19:1 acrylamide/bisacrylamide)	125 ml
Urea	500 g
10x TBE	100 ml

Add H_2O to a final volume of 1 l.

All gel equipment was cleaned with 70 % ethanol before use (glass plates, spacer, combs etc.). Polymerization was initiated by addition of 1/100 volume of ammonium persulfate (APS) and 1/1000 volume of N,N,N,N,-Tetramethylethylendiamin (TEMED). Prior loading, the RNA samples were denatured for 5 min at 100°C in sample loading buffer.

2x RPA loading buffer

Formamid	98 % (v/v)
EDTA, pH 8.0	2 mM
Xylene cyanole	0.02 % (w/v)
Bromphenol blue	0.02 % (w/v)

Gel run was performed in the presence of 1x TBE (see 3.3.1.2) at 300 V at room temperature for about 2 to 3 h (according to the size of the RNA species to detect).

3.3.1.2.2 Native PAGE

Native polyacrylamide gel electrophoresis was performed in the presence of 0.5x TBE (see 3.3.1.2) at 300 V. Native PAGE was used to analyze preformed RNA-protein complexes. To avoid heating, the gel apparatus was connected to a water cooling system. Complexes were loaded in native sample loading buffer.

5x native sample buffer	
Glycerol	50 %
Bromphenol blue	0.2 % (w/v)
TBE buffer	0.5X

3.4 Protein techniques

3.4.1 Preparation of whole cell protein fraction

After the appropriate incubation bacteria samples were taken (0.5 to 1 OD_{600}, respectively). After centrifugation for 2 min at 13 000 rpm at 4°C the supernatant was discarded and the cell pellet resuspended in 1x sample loading buffer to a final concentration of 0.01 OD / µl buffer. The sample was denatured by heating at 95°C for 5 min and was subsequently chilled on ice.

3.4.2 Preparation of membrane fractions

The total membrane protein fraction was extracted following essentially the protocol by (Matsuyama *et al.*, 1984). At the according OD_{600} culture samples were taken (total of 4 OD_{600}) and spun 20 min at 13 000 rpm at 4°C. Pellets were washed 1x in 2 ml 10 mM phosphate buffer (pH 7.2). Pellets were resuspended in 0.5 ml of the same buffer. Cells were disrupted by sonication on ice (cycle duty 80 %; tip limit 9; 4 cycles of 30 sec with 1 min break on ice). The supernatant was cleared of unbroken cells by centrifugation for 10 min at 4 000 rpm, 4°C. Cell envelopes were recovered by centrifugation of the supernatant for 30 min at 13 000 rpm, 4°C. After resuspending the pellet in 2 ml phosphate buffer containing 2% Triton X-100 the samples were incubated for 30 min at 37°C. The insoluble fraction was recovered by 30 min centrifugation at 13 000 rpm at room temperature. After one wash in 2 ml phosphate buffer followed by 5 min centrifugation at 13 000 rpm the pellet was resuspended in 50 µl phosphate buffer (results in approximately 100 µg in 50 µl). For denaturation 4x sample loding buffer was added and samples were heated for 5 min at 95°C and subsequently transferred on ice.

3.4.3 Preparation of periplasmic fractions

The periplasmic protein fraction was extracted following the cold osmotic shock procedure described by (Neu and Heppel, 1965). At the appropriate OD_{600} cells were harvested by centrifugation for 30 min at 4 000 rpm at 4°C. The pellet was resuspended at room temperature in 'shock buffer'.

Shock buffer

Tris-HCl	30 mM, pH 8.0
Sucrose	20%

EDTA, pH 8.0 was added at a final concentration of 1 mM. Cells were incubated for 10 min at room temperature with occasional shaking. Subsequently, cells were collected by centrifugation for 30 min, at 4 000 rpm at 4°C, and the pellet resuspended in 10 ml ice-cold 5 mM $MgSO_4$. After incubation for 10 min with occasional shaking in an ice-water bath, the suspension was centrifuged as mentioned above. The supernatant is the cold osmotic shock-fluid. For denaturation 4x sample loading buffer was added and samples heated for 5 min at 95°.

3.4.4 Preparation of secreted protein fraction

The protocol for extraction of secreted protein fractions was modified from the protocol described in (Kaniga *et al.*, 1995). After growth to the appropriate OD_{600} culture samples were taken and spun 20 min at 13 000 rpm at 4°C. Proteins from the supernatant were precipitated by adding 25% TCA to a final concentration of 5% followed by 20 min centrifugation at 13 000 rpm, 4°C. The pellet was washed 2x in ice cold acetone and air dried. The pellet was resuspended in 1x sample loading buffer to a final concentration of 0.1 OD / µl. Samples were heated 5 min at 95°C.

3.4.5 One- dimensional SDS PAGE

For denaturing separation of proteins, samples were loaded on 10% to 15% SDS PAGE (according to the size of the proteins to be analyzed). Gel solutions for the separation and the stacking gel were prepared as follows:

PAA gel (%) for separation gel	10	12	15
1 M Tris base pH 8.8	3.75 ml	3.75 ml	3.75 ml
PAA solution 40 % (37.5:1 acrylamide/bisacrylamide)	2.5 ml	3 ml	3.75 ml
H_2O	3.75 ml	3.25 ml	2.5 ml
10% SDS	100 µl	100 µl	100 µl
10% APS	75 µl	75 µl	75 µl
TEMED	7.5 µl	7.5 µl	7.5 µl

PAA gel for stacking gel	
1 M Tris base pH 6.8	1.25 ml
PAA solution 40% (37.5:1 acrylamide/bisacrylamide)	1 ml
H_2O	7.485 ml
10% SDS	100 µl
10% APS	150 µl
TEMED	15 µl

10x running buffer	
Tris	250 mM
Glycine	1.92 M
SDS	1 %

All gel equipment was cleaned with 70 % ethanol before use (glass plates, spacer, combs etc.). Polymerization was initiated by addition of 10 % APS and TEMED (see above) to the separation and stacking gel, respectively. Gels were run for 1 h at 80 V (stacking gel) and for 2-6 h at ~ 150 V (according to gel size and molecular weight of proteins to be detected). Gels were stained using PAGEblue staining solution (Fermentas).

3.4.6 Two-dimensional SDS PAGE

Sample preparation from *Salmonella* cultures, analysis by high-resolution two-dimensional electrophoresis, protein staining, and peptide mass fingerprinting, were performed at the MPI-IB protein analysis core facility (http://info.mpiib-berlin.mpg.de/jungblut/) according to previously published standard protocols (Doherty et al., 1998; Jungblut and Seifert, 1990; Klose and Kobalz, 1995).

3.4.7 Western blot

1x Transfer buffer	
Tris base	25 mM
Glycin	192 mM
Methanol	20 %

$TBST_{20}$ buffer	
Tris base	20 mM
NaCl	150 mM
Tween 20	0.1 %

0.01 to 0.05 OD and 0.1 or 0.2 OD whole cell and secreted protein fractions, respectively were separated via SDS-PAGE. Proteins were blotted for 60 min at 100 V at 4°C in a cable tank blotter or for 2 h at 2 mA / cm^2 membrane in a semi dry blotter (Peqlab), respectively onto PVDF (PerkinElmer) membrane in transfer buffer. Blots were rinsed 1x in $TBST_{20}$ buffer. Membranes were blocked for 1 h in 10 % dry milk in $TBST_{20}$. Hybridization was carried out as follows: appropriate antisera or antibodies were diluted in 3 % BSA, $TBST_{20}$ and blots hybridized for 1 h at room temperature, followed by 5 x 6 min wash in $TBST_{20}$. Subsequently, the blots were hybridized with the second α-rabbit-HRP or α-mouse-HRP (1:5000 in 3 % BSA in $TBST_{20}$) for 1 h at room temperature. The final wash steps were performed 6 x for 10 min in $TBST_{20.}$ Blots were developed using Western Lightning (Perkin Elmer) in a Fuji LAS-3000.

3.4.8 Protein quantification by fluorescent stain

Total protein samples corresponding to ~ 0.1 OD_{600} culture were separated on SDS-PAGE. Gels were stained with Sypro Ruby (Biorad) following the manufacture's protocol. Protein levels were analysed using the fluorescence mode of a phosphorimager (Phosphorimager, FLA-3000 Series, Fuji) using a 473 nm laser and filter O58. Band intensities were quantified with AIDA software (Raytest, Germany).

3.4.9 Fluorescence measurements

GFP fluorescence measurements followed the procedure described in (Urban and Vogel, 2007). Strains carrying the GFP fusion plasmids were inoculated from single colonies in 20 ml L-broth supplemented with 20 µg / ml chloramphenicol and incubated with aeration at 37°C, 220 rpm. At the indicated cell density, 3x 100 µl culture were transferred to a 96-well plate, and fluorescence was measured at 37°C using a VICTOR$^3{}_{TM}$ machine (1420 Multilable Counter, Perkin Elmer). All experiments were done in triplicates. Plasmid pJV859-8, which expresses GFP from a constitutive P_{LtetO} promoter, served as a control. In transcriptional fusion studies, strains carrying plasmid pAS0046 served as background control, while plasmid pJU004 was used in translational fusion studies.

3.4.10 Whole-cell colony plate fluorescence imaging

S. Typhimurium strains expressing plasmid-borne *gfp* fusions (transcriptional or translational, respectively) were streaked on standard L-plates supplemented with the appropriate antibiotics. After overnight growth colonies were photographed in a FUJI LAS-3000 image analyzer using a CCD camera after 2 s excitation at 460 nm with a 510 nm emission filter.

3.4.11 Protein overexpression and purification

Overexpression and purification of *Salmonella* Hfq was carried out as published for *E. coli* Hfq (Møller et al., 2002) using the IMPACT (Intein Mediated Purification with Affinity Chitin-binding Tag)-CN system (New England Biolabs) according to the manufacture's

protocol. Strain ER 2566 carrying plasmid pAS009 was grown to an OD_{600} of 0.5, and Hfq expression was induced by addition of IPTG (final concentration of 0.5 mM). Following growth for 15 h at 15°C, cells were disrupted using a French press (3 passages, 1000 PSI). On-column cleavage of the Hfq moiety was carried out for 24 h at room temperature. The Hfq protein eluate was dialyzed against a buffer containing 25 mM Tris, 150 mM NaCl, and 0.5 mM EDTA (pH 7.6) and concentrated in Vivaspin columns.

3.5 Eukaryotic cell culture

All materials used throughout this study were autoclaved for 20 min at 121°C and 1 bar before use. Where necessary solutions were steril filtered and glassware was sterilized by heating to 180°C for a minimum of three hours.

3.5.1 Media

All cell lines used here were cultured in RPMI medium supplemented with the following substances:

Fetal calf serum (FCS)	10 %
L-glutamine	2 mM
Sodium pyruvate	0.1 mM
β-mercaptoethanol	50 µM

For cultivation the medium was additionally supplemented with 10 µg / ml penicillin and streptomycin. Cells were splitted 1:10 after a 3-4-day growth period.

3.5.2 Gentamicin protection (invasion) assays

The invasion assay was performed as described in (Isberg and Falkow, 1985). HeLa cells (ATCC CCL2) were seeded in RPMI medium (including supplements and antibiotics) in 12-well-plates with a density of 1 x 10^5 / ml per well the day before or 0.5 x 10^5 / ml per well two days before infection, respectively. At the day of infection HeLa cells reached a density of 1-2 x 10^5 / ml per well. When seeded two days before infection

medium was changed the day before the assay was performed. One hour prior to infection medium was changed to RPMI containing no antibiotics.
HeLa cells were infected with an MOI of 10 with 100 µl of bacterial suspension in RPMI medium. The suspension was plated in serial dilutions on L-plates and incubated o/n at 37°C for determination of the input.
Bacterial cells were centrifuged (37°C, 1 100 rpm, 10 min) onto the HeLa cell monolayer, followed by a 50 min incubation step at 37°C in an atmosphere containing 5 % CO_2. For determination of adhesion, after 30 min of incubation cells were washed two times in PBS buffer and collected by scraping HeLa cells from the bottom of each well in PBS / 0.1 % Triton X-100. Dilutions in PBS were plated on L-plates and incubation carried out o/n at 37°C. 1 h after infection media was changed in the remaining wells to RPMI (containing 50 µg / ml gentamicin) to kill non-invasive bacterial cells. Incubation was carried on for additional 60 min. After 2 h of infection medium was changed for the 6 h time point to RPMI containing 10 µg / ml gentamicin and incubation carried on for additional 4 h. For the two h time point cells were washed two times in PBS buffer and collected by scraping HeLa cells from the bottom of each well in PBS / 0.1 % Triton X-100. Dilutions in PBS were plated on L-plates and incubation carried out o/n at 37°C. 6 h after incubation samples for the second time point are treated the same way. Rate of invasion was calculated according to recovered bacterial cells related to the input. Experiments were carried out in duplicates.

3.5.3 Macrophage survival assay

Infection of macrophage cell lines was performed as described in 3.5.2 for HeLa cell infection. The macrophage cell line used was RawB, a derivative of Raw 264.7 (ATCC TIB-71). The number of intracellular bacteria was determined 1, 4 and 24 h after infection. Experiments were carried out in duplicates.

3.5.4 HeLa cell adhesion assay

The adhesion assay was performed as described in (Hara-Kaonga and Pistole, 2004). In brief, Gfp-expressing bacteria were grown for 12 h under SPI-1 inducing conditions. 100 µl HeLa cells (5 x 10^5 per ml in RPMI medium) were incubated with 100 µl of bacterial suspension in RPMI medium for 60 min with an MOI of 50 at 37°C in 96-well plates.

Infections were carried out in triplicates. Non-adherent bacteria were removed by washing cells 4x with 200 µl PBS at 400 x *g*. Each sample was resuspended in 50 µl PBS / 4 % Formaldehyde. Each well was sampled three times, and ten HeLa cells were analyzed per sampling. Cells were counted with 1000x magnification using an Eclipse 50i microscope (Nikon).

3.6 Animal infections

Bacterial cultures for mice infections were grown in L-broth to early stationary phase (OD_{600} of 2-3), harvested by centrifugation, and diluted to the appropriate cfu/ml in sterile PBS for infections. For peroral infections, strains were resuspended to 10^9 cfu/ml, and 0.1 ml of the resuspensions (approx. 10^8 bacteria) used to infect groups of five Balb/c mice per strain. The total infective dose was determined in parallel by plating dilutions to agar plates with or without selection, where appropriate. After 72 h, the mice were sacrificed by euthanization in a CO_2 chamber, and spleens were removed for determination of organ bacterial loads. Isolated spleens were washed once in 70 % ethanol, once in PBS and homogenized in 1 ml of PBS. Cell resuspensions were lysed by addition of 1 ml of 0.2 % Triton X-100 in deionized, distilled water and incubation at room temperature for 15 min. Dilutions of the cell lysates were plated to agar plates with or without antibiotic selection where appropriate for enumeration of total intracellular bacteria. Intraperitoneal infections were performed by injection of 0.1 ml of a 1:1 mixture of bacterial suspensions of 2 x 10^6 cfu/ml of wild type and mutant strains into the peritoneal space, yielding a final infective dose of approximately 10^5 cfu / ml for each strain per animal. 48 h after the infections, mice were sacrificed and spleens isolated and processed as above. The competitive index (CI) was calculated from the ratios of total input and recovered wild-type and chloramphenicol-resistant Δ*hfq* cfu as previously described (Shea *et al.*, 1996).

3.7 RNA techniques

3.7.1 RNA isolation

Throughout the study three different methods for isolation of total RNA from *Salmonella* Typhimurium were used.

3.7.1.1 TRIzol preparation

RNA was prepared by TRIzol extraction, following the protocol in (Vogel and Wagner, 2007). Bacterial culture according to 4 OD_{600} were spun for 2 min at 4°C at 11 000 rpm. After discarding the supernatant the bacterial pellet was dissolved in 1 ml TRIzol. The mixture was transferred to 2 ml Phase lock tubes (heavy) and upon addition of 400 µl chloroform the samples mixed by shaking and centrifuged for 15 min at room temperature at 13 000 rpm. The supernatant was transferred to a fresh reaction tube and the nucleic acids precipitated by addition of 2.5 volumes of a Ethanol:sodium acetate (pH 5.2) mixture (30:1 v/v). Precipitation was carried out either overnight or al least for 2 h at -20°C. Nucleic acids were pelleted by centrifugation for 30 min at 13 000 rpm at 4°C and after a wash step with 350 µl of 75 % ethanol and additional centrifugation for 10 min the supernatant was discarded and the pellets air dried. Following resuspension in H_2O the sample was DNase I treated for 30 min at 37°C in the presence of RNase inhibitor and the RNA isolated by phenol:chloroform:isoamylalcohol (P:C:I) extraction. In brief: one volume dissolved RNA was mixed with one volume P:C:I (25:24:1 v/v) in 2 ml Phase lock (heavy) tubes. Following mixing for 10 s by shaking samples were spun for 15 min at 13 000 rpm at room temperature. The upper phase was mixed with 2.5 volumes of Ethanol:sodium acetate mixture (30:1) and RNA was precipitated overnight at -20°C. After centrifugation for 30 min at 4°C at 13 000 rpm the supernatant was discarded, the pellet washed with 350 µl 75% ethanol and after additional centrifugation for 10 min the supernatant again discarded and the pellets air dried. Finally the RNA pellet was resuspended in H_2O.

3.7.1.2 RNA isolation using the SV40 Total RNA Isolation System (Promega)

The RNA was isolated as described at www.ifr.ac.uk/safety/microarrays/protocols.html.
2 OD_{600} of a bacterial culture are mixed with 1/5 volume of stop-mix (ethanol:phenol 95:5 v/v). After snap-freezing in liquid nitrogen the samples are subsequently thawed on ice. Bacteria are spun for 2 min at 13 000 rpm at 4°C. After resuspension in 100 µl H_2O containing 50 mg/ml lysozyme the samples are incubated for 4 min at room temperature. Upon addition of 75 µl of lysis reagent the samples were mixed and 350 µl RNA dilution buffer were added. The samples were heated for 3 min at 70°C, followed by a 10 min centrifugation step at 13 000 rpm at room temperature. The supernatant was transferred

to a new tube, mixed with 200 µl 95% ethanol and the mixture loaded on a spin column provided with the kit. After centrifugation for 1 min at maximum speed the eluate was discarded and the column washed with 600 µl wash buffer. After additional centrifugation 50 µl of a DNase mix (5 µl 90 mM $MnCl_2$, 40 µl DNase core buffer and 5 µl DNase I; all provided with the kit) were applied to the membrane and incubation carried out for 15 min at room temperature. Upon addition of 200 µl DNase stop mix the columns are centrifuged for 1 min at 13 000 rpm. Following two wash steps with 600 and 250 µl wash buffer, respectively (note that the second centrifugation was carried out for 2 min), the column is transferred to a steril Eppendorf tube and 100 µl RNase-free water were added. After incubation for 1 min at room temperature the RNA was eluted by centrifugation for 2 min at 13 000 rpm.

3.7.1.3 Hot Phenol isolation of total RNA

RNA was prepared by hot phenol extraction, following the protocol in (Mattatall and Sanderson, 1996). 10 OD_{600} of bacterial culture were spun for 30 min at 4 000 rpm at 4°C. The pellet was snap frozen in liquid nitrogen and subsequently thawed on ice. Following resuspension in 12 ml extraction buffer, 10% SDS solution was added to a final concentration of 1%.

Extraction buffer

Sodium acetate, pH 4.8	10 mM
Sucrose	0.15 M

Cells were vigorously vortext in 50 ml Falcon tubes; upon addition of 13 ml preheated (65°C) phenol the samples were transferred to a 65°C water bath and incubated for 5 min with short intervals of vortexing. After 30 min of centrifugation in Corex tubes at 8 000 rpm at 4°C the upper phase was transferred to a new 50 ml Falcon tube and a second phenol extraction (13 ml Phenol, vortexing at room temperature) was carried out. After centrifugation in a Corex tube (see above) the upper phase was transferred to a fresh Corex tube and 12 ml chloroform were added to the sample. After a 30 min centrifugation at 8 000 rpm at 4°C the upper phase was transferred into a fresh Corex tube and RNA precipitated by addition of 2.5 volumes of a Ethanol:sodium acetate mixture (30:1). The nucleic acids were precipitated overnight at -20°C. The samples

were collected by centrifugation for 30 min at 8 000 rpm at 4°C and after aspiration of the supernatant the pellet was washed with 4 ml 75% ethanol. Following subsequent centrifugation for 10 min, 8 000 rpm, 4°C the supernatant was discarded and the pellets air dried. Samples were dissolved in water and following DNase I treatment (30 min incubation at 37°C) the RNA was isolated using phenol:chloroform:isoamylalcohol (P:C:I) extraction, followe by precipitation using 2.5 volumes of Ethanol:sodium acetate mixture (30:1). Finally the RNA was dissolved in water.

3.7.2. *In vitro* transcription and 5' end labelling of RNA

In vitro transcription was performed using the Megascript kit (Ambion), followed by DNase I digestion [1 unit (u)] for 15 min at 37°C. Following extraction with phenol: chloroform:isoamylalcohol (25:24:1 v/v), the RNA was precipitated overnight at -20°C with 1 volume of isopropanol. RNA integrity was checked on a denaturing PAA gel. 20 pmol RNA was dephosphorylated with 10 u of calf intestine alkaline phosphatase (CIP, New England Biolabs) in a 20 μl reaction at 37°C for 1 h. Following phenol extraction, the RNA was precipitated overnight with ethanol:sodium acetate (30:1) and 20 μg glycogen. The dephosphorylated RNA was 5' end-labelled with ^{32}P-γATP (20 μCi), using 1 u of polynucleotide kinase (PNK, New England Biolabs) for 30 min at 37°C in a 20 μl reaction. Unincorporated nucleotides were removed using Microspin^{TM} G-50 Columns (GE Healthcare), followed by purification of the labelled RNA on a denaturing gel (5 % / 8.3 M Urea). Upon visualization of the labelled RNA by exposure on a phosphorimager, the RNA was cut from the gel and eluted with RNA elution buffer at 4°C overnight, followed by phenol extraction and precipitation as before.

RNA elution buffer

Sodium acetate	0.1 M
SDS	0.1 %
EDTA, pH 8.0	10 mM

3.7.3 Generation of radioactive labelled probes for RNA detection

3.7.3.1 DNA oligonucleotides

For labelling of DNA oligos, 1 pmol of the oligo were incubated with 25 μCi of ^{32}P-γATP in the presence of 1 u PNK (New England Biolabs) for 1 h at 37°C in a 10 μl reaction. Unincorporated nucleotides were removed using Microspin™ G-25 Columns (GE Healthcare).

3.7.3.2 DNA PCR probes

25 ng of the PCR product were dissolved in 45 µl TE buffer and random-labelled with [^{32}P] dCTP, using the Rediprime II labeling kit (GE Healthcare).

1x TE buffer

Tris, pH 8.0	10 mM
EDTA, pH 8.0	1 mM

3.7.3.3 Riboprobes

For synthesis of riboprobes PCR products of the genetic region of interest, carrying a T7 promoter were used in *in vitro* transcription by Ambion's T7 polymerase Maxiscript kit. 250 ng of the PCR product were mixed with dNTPs in the presence of [^{32}P]-α-UTP. *In vitro* transcription was performed for 1 h at 37°C. Riboprobes were purified over a Microspin™ G50 column (GE Healthcare).

3.7.4 Northern blot

To detect mRNAs or sRNAs, respectively, 5 to 20 μg RNA were separated on 5 % denaturing (8.3 M Urea) PAA gels. After a 1 h transfer to Hybond-XL membranes (GE Healthcare) in a tankblotter (Peqlab) at 50 V at 4°C in the presence of 1x TBE (see 3.3.1.2), the RNA was cross-linked to the membrane on a UV-table (302 nm). After prehybridization for 1 h in 15 ml Hybri-Quick buffer (GE Healthcare) the radioactive labelled probe was added. After a period of 1 to 12 h of hybridization the membrane was

rinsed with the appropriate 20 x SCC dilution, followed by three 15 min wash steps in SSC (all SSC buffers are supplemented with 0.1% SDS). For hybridization and wash temperatures, as well as SSC concentrations see below.

20x SSC buffer

Sodium chloride	3 M
Sodium citrate	0.3 M

Radioactive Probe	**Pre-/hybridization temperature**	**SSC concentration**	**Wash Temperature**
Oligonucleotides	42°C	5x (rinse and 1st wash step), 1x, 0.5x	all at 42°C
DNA probe	65°C	2x (rinse and 1st wash step), 1x, 0.5x	65°C, 65°C, 42°C
Riboprobe	70°C	2x (rinse and 1st wash step), 1x, 0.5x	all at 65°C

For detection of large transcripts 20 μg RNA were separated on 1.5% MOPS agarose gels.

10x MOPS buffer (pH 7.0)

MOPS	0.2 M
Sodium acetate	20 mM
EDTA, pH 8.0	10 mM

20 μg RNA was lyophilized and dissolved in MOPS buffer in the presence of Glyoxal and DMSO. After a denaturing step for 5 min at 95°C, the sample was chilled on ice and supplemented 2x loading buffer. Gels were run at 70 V and 4°C for ~ 6 h (buffer was changed every 30 min), equilibrated in 10x SSC for 30 min under agitation and RNA transferred to a Hybond-XL membrane by upward capillary transfer in 10x SSC overnight as described in (Sambrook and Russel, 2001). Membranes were rinsed for 5 min in 5x SSC, followed by a 5 min wash step in H_20. The RNA was UV-cross-linked as described for PAA based Northern blots. Hybridization was carried out as described above for Northern blots.

Sample preparation for MOPS agarose gels

RNA (20 µg)	4.8 µl
MOPS buffer (10x)	1.6 µl
Glyoxal (8M)	1.6 µl
DMSO	8 µl

3.7.5 Gel mobility shift assays

Hfq/RNA complexes were formed in the presence of 1x structure buffer in a total reaction volume of 10 µl. 5´ end labelled RNA (~ 4 nM final concentration) and 1 µg yeast RNA (Ambion) were incubated in the presence of increasing Hfq concentrations (final concentrations of 1.25 nM up to 500 nM of the hexamer) at 37°C for 15 min. Hfq dilutions were prepared in 1x dilution buffer. Prior gel loading, the binding reactions were mixed with 3 µl of 5x native loading buffer, and complexes separated on native 6 % polyacrylamide gels (see 3.3.1.2.2). Gels were dried, and analyzed on X-ray films using a phosphorimager.

10x structure buffer

Tris, pH 7.0	100 mM
KCl	1 M
$MgCl_2$	100 mM

1x dilution buffer

structure buffer	1x
glycerol	1 %
Triton-X-100	0.1 %

3.7.6 Stability experiments

To bacterial cultures grown to the appropriate OD_{600}, Rifampicin was added to a final concentration of 500 µg/ml. Incubation was continued at 37°C, 220 rpm, and aliquots (5 ml for OD 0.3; 1.7 ml for OD2 or OD2 + 6h, respectively) were withdrawn prior to or 1, 2, 4, 8, 16, and 32 min after Rifampicin addition, mixed with 0.2 vol of stop solution (5% phenol, 95% ethanol v/v), and snap-frozen in liquid nitrogen. After thawing on ice,

bacteria were pelleted by centrifugation for 2 min at 13 000 rpm at 4°C, and RNA was isolated using the Promega SV40 total RNA purification kit (see 3.7.1.2). RNA was analyzed by Northern blots (see 3.7.4).

3.7.7 Quantitative RT-PCR

The bacterial strains were grown in liquid culture from single colonies to an OD_{600} of 2 or for 12 h under SPI-1 inducing conditions, respectively. Experiments were carried out as described previously (Papenfort *et al.*, 2006). RNA was isolated using the SV40 Total RNA Isolation kit (Promega) (see 3.7.1.2). Gene expression was quantitatively assessed by qRT-PCR in a 7900HT (Applied Biosystems). For each reaction (25 µL final volume) 1 µl of RNA sample (100 ng / reaction) were mixed with 0.25 µl of primer pairs (0.5 µM final) and 12.5 µL of SYBR Green mix (Qiagen). For coupled cDNA synthesis and target gene amplification 0.25 µl of Quantitect RT mix was added. Each sample was assayed in triplicate for each run. Control RNA from wild-type cells was used to construct a standard curve for all inspected genes. Reaction conditions were: 30 min 50°C, 15 min 95°C, and 45 cycles at 94°C for 20 s, 60°C for 40 s, and 72°C for 40 s.

3.8 Transcriptomic experiments

RNA extraction and data generation were carried out as described with SALSA microarrays in (Papenfort *et al.*, 2006). The complete dataset is available at GEO under accession number GSE8985.

3.8.1 Sample preparation for microarray experiments

2 OD_{600} aliquots of a bacterial culture were withdrawn and mixed with 1/5 volume of stop mix (ethanol:phenol 95:5 v/v) and RNA prepared using the SV40 Total RNA Isolation System (see 3.7.1.2).

3.8.2 Microarray data generation

The microarrays used in this study include PCR products of all the genes present in the sequenced *S.* Typhimurium strain LT2. In addition, we added 229 genes specific to *S.*

Typhimurium strain SL1344. Details of all the amplicons can be found at http://www.ifr.ac.uk/Safety/MolMicro/pubs.html. Our experimental design involves the use of *Salmonella enterica* serovar Typhimurium genomic DNA as the co-hybridized control for one channel on all microarrays. This method has the advantage of allowing the direct comparison of multiple samples. Total RNA and chromosomal DNA were labeled by random priming according to the protocols described at http://www.ifr.bbsrc.ac.uk/safety/microarrays/protocols.html. Briefly, 16 µg RNA were reverse transcribed and labelled with Cy3-conjugated dCTP (Pharmacia) using 200 U of Stratascript (Stratagene) and random octamers (Invitrogen). Chromosomal DNA (400 ng) was labeled with Cy5-dCTP using the Kleenow fragment. After labeling, each Cy3-labelled cDNA sample was combined with Cy5-labelled chromosomal DNA and hybridised to a microarray overnight at 65ºC. After hybridisation, slides were washed and scanned using a GenePix 4000A scanner (Axon Instruments, Inc.). Fluorescent spots and the local background intensities were identified and quantified using Bluefuse software (BlueGnome, Oxford). To compensate for unequal dye incorporation, data centring to zero was performed for each block (one block being defined as the group of spots printed by the same pin). We considered genes to be differentially expressed if they displayed ≥ 2-fold changes in all replicates and were statistically significantly different using Significance Analysis of Microarrays (Tusher et al. 2001). Data visualization and data mining was performed using GeneSpring 7.3 (Agilent).

3.9 Co-immunoprecipitation of RNA by Hfq-3xFLAG

Strains were grown in L-broth under normal aeration at 37°C to an OD_{600} of 2. Co-immunoprecipitation was carried out using the protocol published in (Pfeiffer *et al.*, 2007).

3.9.1 Co-immunoprecipitation (coIP)

Cells were cultured to early stationary phase, and collected by centrifugation for 40 min at 4000 rpm at 4°C. The pellet was washed once with 2 ml of lysis buffer, and snap-frozen in liquid nitrogen. Upon re-suspension in 0.8 ml of lysis buffer, 0.8 ml glass beads (Roth, diameter 0.1 mm) were added, and cells broken by vortexing (30 s burst followed by 30 s chill on ice) for 5 min. Lysis buffer (0.4 ml) was added, followed by centrifugation

for 30 min at 4°C at 13 200 rpm. 1/10 of the cleared lysate (0.1 ml) was removed to prepare total RNA. Twenty-five microlitres of FLAG antibody (Sigma) were added to the remaining cleared lysate (0.9 ml), followed by incubation on a rotator at 4°C for 1 h. 50 µl Protein A sepharose beads (Sigma) were added, and incubation continued for 1 h. The suspension was centrifuged for 5 min at 4°C at 13 200 rpm, followed by five washes in 1 ml of lysis buffer. Protein/RNA complexes were recovered from the beads by re-suspension in 0.5 ml of water. Phenol:chloroform extracted RNA was concentrated by ethanol precipitation, followed by DNase I treatment. Efficency of the coIP was determined by Northern blot (3.7.4) detection of sRNAs. Therefore, total RNA and co-immunoprecipitated RNA equivalent to 0.25 or 0.5 and 2.5 or 5 OD_{600}, respectively, of the original culture volume were used.

Lysis buffer

Tris, pH 8.0	20 mM
KCl	150 mM
$MgCl_2$	1 mM
DTT	1 mM

3.9.2 cDNA synthesis and high throughout pyrosequencing (HTPS)

cDNA cloning and pyrosequencing was performed as described for the identification of eukaryotic microRNA (Berezikov *et al.*, 2006) but omitting size-fractionation of RNA prior to cDNA synthesis.

3.9.3 coIP-on-Chip experiments

Microarrays used for the coIP-on-Chip experiments were designed and produced by Oxford Gene Technology (Kidlington, UK). They consist of 21,939 60-mer oligonucleotides tiled throughout the *S.* Typhimurium SL1344 NCTC13347 genome and 636 control oligonucleotides. The SL1344 sequence was obtained from the Sanger Institute (Hinxton, UK) website (http://www.sanger.ac.uk/Projects/Salmonella/). As this genome is not yet fully annotated, the oligonucleotides were associated with corresponding *S*. Typhimurium LT2 genes or intergenic regions, if conserved in both organisms. Full description of the microarray and protocols used for generating and

analyzing the data are associated with the dataset deposited in the GEO data repository (http://www.ncbi.nlm.nih.gov/geo/) under accession number GSE10149.

3.9.4 Analysis of HTPS data using the Integrated Genome Browser Affymetrix)

After 5'end linker and poly(A)-tail clipping from the initial pyrosequencing results, all inserts ≥ 18 nt of the Hfq coIP and control coIP libraries were separately mapped to the *Salmonella* LT2 genome (NC_003197.fna) using WU-BLAST (http://blast.wustl.edu/). From the resulting blast positions one graph for each strand of the *Salmonella* chromosome was calculated, where the number of cDNA hits for each nucleotide position was plotted. To compare the graphs of the Hfq coIP and control coIP, the graphs were normalized to number of blastable reads. Following upload of the *Salmonella* genome sequence and annotation (NC_003197.fna and NC_003197.gff), the two graphs for each library were loaded into the *Integrated Genome Browser (IGB) of Affymetrix (*http://www.affymetrix.com/support/developer/tools/download_igb.aff*, version* IGB-4.56). The ratio of hits per nucleotide of the Hfq coIP to hits from the control coIP was used to calculate the enrichment factor, which can be visualized for every single nucleotide in a stepstair diagram.

3.10 References

Berezikov E, Thuemmler F, van Laake LW, Kondova I, Bontrop R, et al. (2006) Diversity of microRNAs in human and chimpanzee brain. Nat Genet 38: 1375-1377.

Datsenko KA, Wanner BL (2000) One-step inactivation of chromosomal genes in Escherichia coli K-12 using PCR products. Proc Natl Acad Sci U S A 97:6640-645

Doherty, N.S., Littman, B.H., Reilly, K., Swindell, A.C., Buss, J.M., and Anderson, N.L. (1998) Analysis of changes in acute-phase plasma proteins in an acute inflammatory response and in rheumatoid arthritis using two-dimensional gel electrophoresis. Electrophoresis 19: 355-363.

Hara-Kaonga, B., and Pistole, T.G. (2004) OmpD but not OmpC is involved in adherence of Salmonella enterica serovar typhimurium to human cells. Can J Microbiol 50: 719-727.

Isberg, R.R., and Falkow, S. (1985) A single genetic locus encoded by Yersinia pseudotuberculosis permits invasion of cultured animal cells by Escherichia coli K-12. Nature 317: 262-264.

Jungblut, P.R., and Seifert, R. (1990) Analysis by high-resolution two-dimensional electrophoresis of differentiation-dependent alterations in cytosolic protein pattern of HL-60 leukemic cells. J Biochem Biophys Methods 21: 47-58.

Kaniga, K., Trollinger, D., and Galan, J.E. (1995) Identification of two targets of the type III protein secretion system encoded by the inv and spa loci of Salmonella typhimurium that have homology to the Shigella IpaD and IpaA proteins. J Bacteriol 177: 7078-7085.

Klose, J., and Kobalz, U. (1995) Two-dimensional electrophoresis of proteins: an updated protocol and implications for a functional analysis of the genome. Electrophoresis 16: 1034-1059.

Lober S, Jackel D, Kaiser N, Hensel M (2006) Regulation of Salmonella pathogenicity island 2 genes by independent environmental signals. Int J Med Microbiol 296: 435-447

Matsuyama S, Inokuchi K, Mizushima S (1984) Promoter exchange between ompF and ompC, genes for osmoregulated major outer membrane proteins of Escherichia coli K-12. J Bacteriol 158:1041-1047

Mattatall NR, Sanderson KE (1996) Salmonella typhimurium LT2 possesses three distinct 23S rRNA intervening sequences. J Bacteriol 178: 2272-2278

Møller T, Franch T, Højrup P, Keene DR, Bächinger HP, Brennan RG, Valentin-Hansen P (2002) Hfq: a bacterial Sm-like protein that mediates RNA-RNA interaction. Mol Cell 9:23-30.

Neu HC, Heppel LA (1965) The release of enzymes from Escherichia coli by osmotic shock and during the formation of spheroplasts. J Biol Chem 240:3685-3692

Papenfort K, Pfeiffer V, Mika F, Lucchini S, Hinton JC, Vogel J (2006) SigmaE-dependent small RNAs of Salmonella respond to membrane stress by accelerating global omp mRNA decay. Mol Microbiol 62:1674-1688

Pfeiffer V, Sittka A, Tomer R, Tedin K, Brinkmann V, et al. (2007) A small non-coding RNA of the invasion gene island (SPI-1) represses outer membrane protein synthesis from the Salmonella core genome. Mol Microbiol 66: 1174-1191

Sambrook, J., Russell, D.W. (2001) Molecular cloning: A laboratory manual (3rd edition)Cold Spring Harbor Laboratory Press, Cold Spring Harbor, New York, USA.

Shea, J.E., Hensel, M., Gleeson, C., and Holden, D.W. (1996) Identification of a virulence locus encoding a second type III secretion system in Salmonella typhimurium. Proc Natl Acad Sci U S A 93: 2593-2597.

Sternberg NL, Maurer R (1991) Bacteriophage-mediated generalized transduction in Escherichia coli and Salmonella typhimurium. Methods Enzymol 204:18-43

Tusher, V.G., R. Tibshirani, and G. Chu. 2001. Significance analysis of microarrays applied to the ionizing radiation response. *Proc Natl Acad Sci U S A* 98: 5116-21

Urban JH, Vogel J (2007) Translational control and target recognition by Escherichia coli small RNAs in vivo. Nucleic Acids Res 35:1018-1037

Uzzau S, Figueroa-Bossi N, Rubino S, Bossi L (2001) Epitope tagging of chromosomal genes in Salmonella. Proc Natl Acad Sci U S A 98:15264-15269

Vogel J, Wagner EG (2007) Target identification of regulatory sRNAs in bacteria. Curr Opin Microbiol 10: 262-270

4. Results and Discussion

4.1 The RNA chaperone Hfq is essential for the virulence of *Salmonella typhimurium*

Alexandra Sittka, Verena Pfeiffer, Karsten Tedin, and Joerg Vogel

Molecular Microbiology, 2007

Molecular Microbiology (2007) **63**(1), 193–217

doi:10.1111/j.1365-2958.2006.05489.x
First published online 5 December 2006

The RNA chaperone Hfq is essential for the virulence of *Salmonella typhimurium*

Alexandra Sittka,[1] Verena Pfeiffer,[1] Karsten Tedin[2] and Jörg Vogel[1]*

[1]*Max Planck Institute for Infection Biology, RNA Biology Group, Berlin, Germany.*

[2]*Institut für Mikrobiologie und Tierseuchen, Freie Universität Berlin, Berlin, Germany.*

Summary

The RNA chaperone, Hfq, plays a diverse role in bacterial physiology beyond its original role as a host factor required for replication of Qβ RNA bacteriophage. In this study, we show that Hfq is involved in the expression and secretion of virulence factors in the facultative intracellular pathogen, *Salmonella typhimurium*. A *Salmonella hfq* deletion strain is highly attenuated in mice after both oral and intraperitoneal infection, and shows a severe defect in invasion of epithelial cells and a growth defect in both epithelial cells and macrophages *in vitro*. Surprisingly, we find that these phenotypes are largely independent of the previously reported requirement of Hfq for expression of the stationary phase sigma factor, RpoS. Our results implicate Hfq as a key regulator of multiple aspects of virulence including regulation of motility and outer membrane protein (OmpD) expression in addition to invasion and intracellular growth. These pleiotropic effects are suggested to involve a network of regulatory small non-coding RNAs, placing Hfq at the centre of post-transcriptional regulation of virulence gene expression in *Salmonella*. In addition, the *hfq* mutation appears to cause a chronic activation of the RpoE-mediated envelope stress response which is likely due to a misregulation of membrane protein expression.

Introduction

The bacterial Sm-like protein, Hfq, has been increasingly recognized as a post-transcriptional regulator of global gene expression (Valentin-Hansen *et al*., 2004). Hfq was first identified in *Escherichia coli* as a host factor required for replication of Qβ RNA bacteriophage (Franze de Fernandez *et al*., 1968), and shown to be an RNA-binding protein that forms homohexamers of ~12 kDa subunits (Franze de Fernandez *et al*., 1972). Hfq was early observed to be an abundant protein (Carmichael *et al*., 1975), but its importance in uninfected bacteria remained unclear until it was shown that an *hfq* insertion mutant of *E. coli* exhibited broad, pleiotropic phenotypes affecting growth rate, cell morphology and tolerance of stress conditions (Tsui *et al*., 1994). Independently, genetic analysis of *Azorhizobium caulinodans* and *Yersinia enterocolitica* mutants, showing defects in nitrogen fixation or toxin production respectively, found that these phenotypes were due to mutations in *hfq* (Kaminski *et al*., 1994; Nakao *et al*., 1995). Subsequently, Hfq was shown to promote efficient translation of *rpoS* mRNA in *E. coli* and *Salmonella* (Brown and Elliott, 1996; Muffler *et al*., 1996), and to alter the stability of several other mRNAs (e.g. Vytvytska *et al*., 1998; Hajnsdorf and Regnier, 2000), indicating that this protein acts to regulate gene expression at the post-transcriptional level. Hfq has also emerged as a key player in mRNA translational control by small non-coding RNAs (sRNAs). Here, Hfq was first observed to be involved in translational repression of *rpoS* mRNA by OxyS, a small regulatory RNA that is part of the oxidative stress response in *E. coli* (Zhang *et al*., 1998). Since then, numerous *E. coli* sRNAs have been shown to associate with Hfq and to require this protein for their own stability and/or for interactions with their target mRNAs (reviewed in Valentin-Hansen *et al*., 2004; Majdalani *et al*., 2005; Romby *et al*., 2006). These include two *E. coli* sRNAs, DsrA and RprA, which activate *rpoS* translation in response to stress conditions (reviewed in Repoila *et al*., 2003); note, however, that the RpoS regulatory function of these sRNAs may not be conserved in *Salmonella* (Jones *et al*., 2006).

Several recent studies addressed a potential role of Hfq in the virulence of pathogenic bacteria. A *Brucella abortus hfq* mutant displayed significantly reduced survival in cultured murine macrophages, and attenuated virulence in a mouse model (Robertson and Roop, 1999). Similarly, Hfq was reported to be essential for the virulence of *Vibrio cholerae* (Ding *et al*., 2004). An *hfq*

Accepted 19 October, 2006. *For correspondence. E-mail vogel@mpiib-berlin.mpg.de; Tel. (+49) 30 28460 265; Fax (+49) 30 28460 244.

mutant of this bacterium fails to colonize the suckling mouse intestine, a model of cholera pathogenesis. Hfq also contributes to the pathogenesis of *Listeria monocytogenes* in mice (Christiansen *et al*., 2004), and to *Legionella pneumophila* virulence in amoeba and macrophage infection models (McNealy *et al*., 2005). Furthermore, the *hfq* mutation reduces the virulence of the opportunistic human pathogen *Pseudomonas aeruginosa* by affecting both cell-associated (flagellum, adhesion factors) as well as extracellular virulence factors, e.g. elastases and pyocyanin (Sonnleitner *et al*., 2003). In most of these cases, the observed virulence defects were accompanied by reduced stress tolerance, likely reflecting a compromised ability to cope with the harsh environment in the host cell (Robertson and Roop, 1999; Christiansen *et al*., 2004; McNealy *et al*., 2005).

A role for Hfq in bacterial virulence was first indicated by its requirement for efficient expression of the major stress sigma factor, σ^S (also known as RpoS, KatF or σ^{38}) in the enteric bacteria, *E. coli* and *Salmonella*. Here, *hfq* mutants display greatly reduced RpoS levels in stationary phase, due to inefficient translation of the *rpoS* mRNA (Brown and Elliott, 1996; Muffler *et al*., 1996). In *Salmonella*, σ^S is an important virulence factor as it mediates the expression of the *Salmonella* plasmid virulence (*spv*) genes, which are required for systemic infection, and enables bacteria to cope with diverse stresses (nutrient deprivation, oxidative and acid stress, DNA damage) relevant to the environments faced in their mammalian hosts (Fang *et al*., 1992; Bang *et al*., 2005). A *Salmonella rpoS* mutant exhibits significantly reduced virulence in mice (Fang *et al*., 1992), and mutated *rpoS* alleles are often found in attenuated *Salmonella* strains (Robbe-Saule *et al*., 1995; Wilmes-Riesenberg *et al*., 1997).

Based on the importance of Hfq for σ^S expression and the many phenotypes shared by *hfq* and *rpoS* mutants in *E. coli* and *Salmonella* (Fang *et al*. 1992; Muffler *et al*., 1997), it has generally been assumed that Hfq would be important for *Salmonella* virulence. However, experimental evidence for a more general role of Hfq, i.e. beyond promoting *rpoS* mRNA translation, has so far been lacking. To address these questions, we constructed and characterized a set of *hfq* mutants and control strains in *Salmonella enterica* serovar Typhimurium (*S. typhimurium*). We find that loss of Hfq results in drastically reduced virulence *in vitro* and *in vivo*. These phenotypes, which are largely σ^S-independent, are associated with loss of cell motility, altered membrane composition, reduced adhesion and abrogated effector protein secretion. The results indicate that Hfq plays a much more dominant role in *Salmonella* virulence than previously believed.

Results

Construction of Salmonella hfq *mutant and control strains*

The *hfq* gene is located in clockwise orientation at bps 4604575–4604883 in the genome of *S. typhimurium* strain LT2 (McClelland *et al*., 2001). As in *E. coli*, it is located in the *yjeF-yjeE-amiB-mutL-miaA-hfq-hflX-hflK-hflC* cluster of genes (Fig. 1A), part of which may form an operon (Tsui and Winkler, 1994). The *Salmonella* and *E. coli hfq* genes are 93% and 94% identical at the nucleotide and amino acid level respectively, with all amino acid deviations being located in the Hfq C-terminal region (Brown and Elliott, 1996). The sequence of the *hfq* region taken from the unfinished genome of the virulent *Salmonella* strain used in this study, SL1344 (http://www.sanger.ac.uk/Projects/Salmonella), was compared with that of strain LT2 and found to be identical.

Based on the sequence data, three *hfq* mutant or control strains were constructed in SL1344 to study Hfq functions *in vivo* (Fig. 1B). In the Δ*hfq* mutant, the entire *hfq* coding region is replaced by a *cat* (chloramphenicol resistance) marker. As the *cat* gene used here does not carry a transcriptional terminator, transcription of the polycistron should be unaffected. *hfq*-C is a control strain in which the *cat* gene is inserted after the *hfq* stop codon. In control strain *hfq*^{HIS}, the *cat* gene is inserted before the UAA stop codon. In addition, this latter insertion adds six histidine codons to the last *hfq* codon, thus producing a chromosomally encoded His-tagged Hfq protein.

Growth characteristics of the hfq *mutant and control strains*

All three *hfq* strains formed normal colonies when grown on standard Luria–Bertani (LB) plates at 37°C, although the Δ*hfq* strain exhibited slightly slower growth. At room temperature (22°C) however, the Δ*hfq* mutant grew much more slowly than the wild type, seen as a smaller colony size, whereas the *hfq*-C and *hfq*^{HIS} derivatives showed normal growth (data not shown). When we compared the growth of all strains in LB liquid medium with aeration at 37°C, no differences were observed among the wild type, and the two control strains, *hfq*-C and *hfq*^{HIS} (Fig. 1C). The deletion mutant, Δ*hfq*, showed a longer lag phase after inoculation into fresh medium and reached stationary phase at a lower optical density as compared with the other three strains. However, parallel determination of viable counts at three different growth phases showed that cell viability of Δ*hfq* was uncompromised (Fig. 1D).

The observation that the *hfq*-C and *hfq*^{HIS} strains showed growth rates identical to the wild-type strain supported the suggestion that the slightly altered growth of the Δ*hfq* mutant was due to the lack of Hfq protein rather

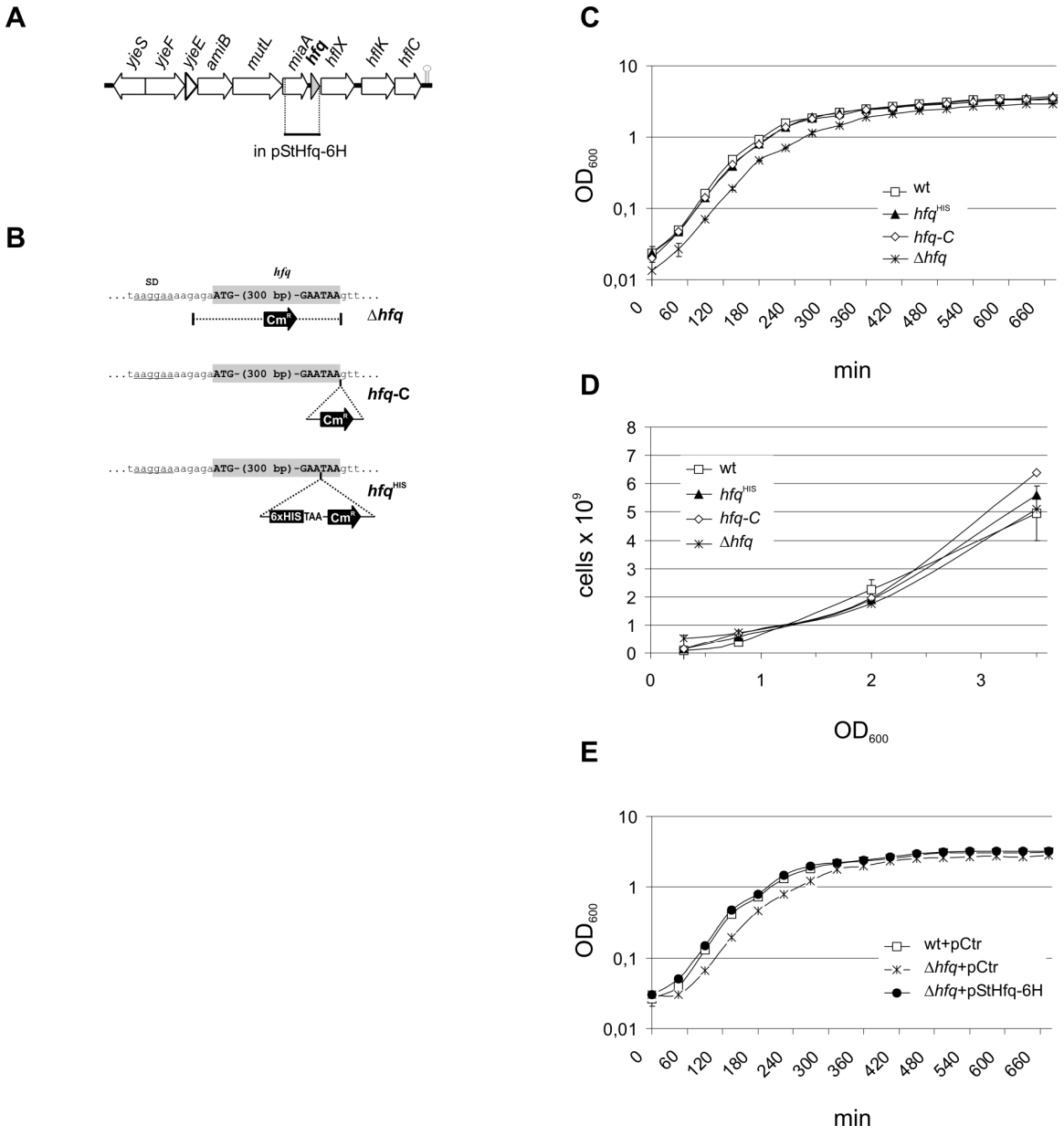

Fig. 1. Details of *Salmonella hfq* mutants and their growth characteristics.
A. Genomic location of *hfq* in SL1344. The region cloned on complementation plasmid, pStHfq-6H, is indicated.
B. Schematic representation of the insertion sites of the *cat* resistance cassette in the deletion mutant Δ*hfq*, the control strain *hfq*-C, and the chromosomally HIS-tagged strain, *hfq*^{HIS}.
C and D. Growth and cell viability of *hfq* mutant strains (open squares: wild-type; filled triangles: *hfq*^{HIS}; open diamonds: *hfq*-C; stars: Δ*hfq*). (C) OD_{600} values of triplicate cultures in LB medium were determined in 45 min intervals. (D) Bacteria were plated to determine viable counts (from triplicate cultures) at an OD of 0.3 and of 2, and 6 h after cultures had reached an OD of 2.
E. Complementation of the slight growth defect of the Δ*hfq* strain by plasmid pStHfq-6H (open squares: wild-type strain carrying control plasmid pVP012; stars: Δ*hfq* carrying a control plasmid; filled circles: Δ*hfq* complemented with pStHfq-6H).

than to polar effects caused by the insertion of the *cat* cassette. To corroborate this, the *hfq*^{HIS} allele including 1014 bp of the upstream *miaA* coding sequence was cloned in a low-copy vector (pSC101* origin), resulting in plasmid pStHfq-6H. This plasmid fully complemented the reduced growth of the Δ*hfq* strain (Fig. 1E), also indicating that the major *hfq* promoter is located within the *miaA* coding region.

Certain growth conditions, e.g. oxygen limitation and high osmolarity, are known to activate *Salmonella* invasion gene expression *in vitro* (e.g. Lee and Falkow, 1990; Song *et al*., 2004). As these so-called *Salmonella* patho-

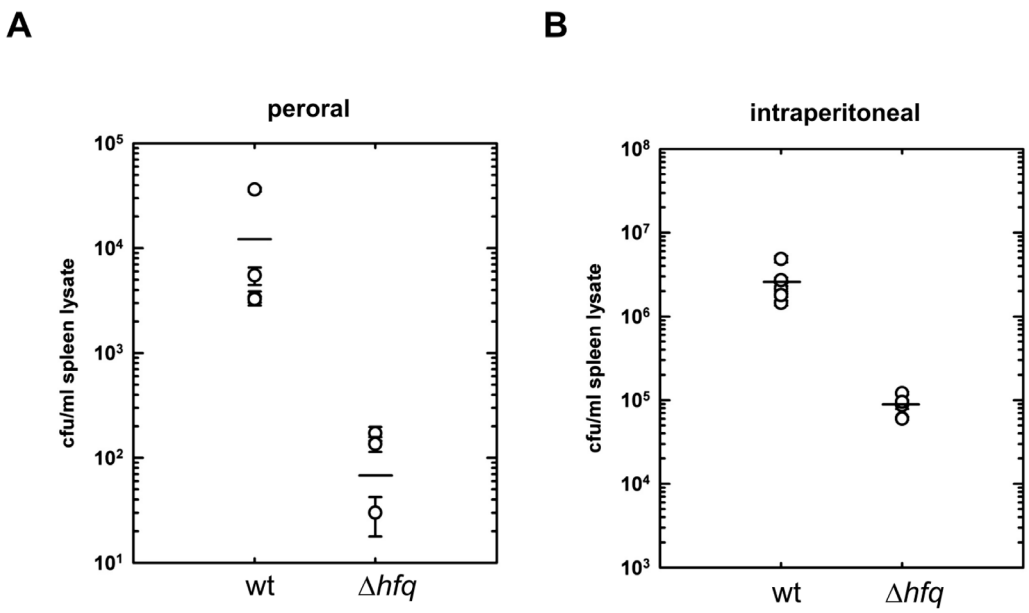

Fig. 2. The *Δhfq* mutant is severely attenuated in mice.
A. Groups of five Balb/c mice were infected perorally with suspensions of ~10^8 bacteria of either the wild-type or Δ*hfq* strains. Bacterial loads in spleen homogenates were determined 72 h post infection. For intraperitoneal infections (B) 1:1 mixtures of both, wild-type and Δ*hfq* strain, each strain at ~10^5 bacteria, were used for infections. Forty-eight hours post infection, spleens were removed and the cfu ml^{-1} for each strain was determined in spleen homogenates by plating to selective plates for calculation of the relative ratios of the two, co-infecting strains (competitive index, CI, see text).

genicity island 1 (SPI1)-inducing conditions were used extensively in this study (see below), we also determined the growth behaviour of all aforementioned strains under these conditions. As seen with aerobic growth, the Δ*hfq* mutant strain exhibited a slightly extended lag phase but reached the same optical density as the wild type while the two control strains *hfq*^{HIS} and *hfq*-C show growth indistinguishable from the wild-type strain (Fig. S1).

The hfq *mutation attenuates virulence in mice*

To address the role of Hfq in *Salmonella* pathogenesis, we first examined the effect of the *hfq* deletion in a typhoid fever mouse model of *Salmonella* infection. Groups of 4- to 5-week-old, female Balb/c mice (five mice per strain) were infected perorally with 10^8 cfu of either the wild-type or Δ*hfq* strains. Mice infected with the wild-type strain showed typical symptoms of infection beginning the following day, whereas mice infected with the Δ*hfq* mutant showed no signs of illness during the course of the experiment. The infected animals were sacrificed 72 h post infection, and organ colonization was determined by plating dilutions of homogenized spleen lysates to agar plates. As shown in Fig. 2A, the *hfq* mutant was recovered at > 100-fold reduced levels relative to the wild-type strain after peroral infection, and for at least two of the mice, no bacteria were recovered. These observations suggested that the *hfq* mutation resulted in defects in either invasion of intestinal epithelial cells, macrophage survival, or both.

To determine whether the virulence defect of the *hfq* mutant extended beyond invasion-related defects, mice were also co-infected intraperitoneally with a mixture of the wild-type and Δ*hfq* strains, where uptake by resident macrophages should circumvent the need for invasion. Two, independent experiments indicated that the *hfq* mutant showed at least a 30- to 100-fold reduced uptake and/or survival in macrophages and subsequent carriage to the spleen compared with the wild-type strain (Fig. 2B), leading to calculated competitive indices (CI; Shea *et al*., 1999) of 0.01–0.03. This is consistent with the idea that both uptake and intracellular survival/proliferation in macrophages were affected. It should be noted that the post-infection time points for determination of bacterial counts shown were chosen to avoid premature death of the infected animals. In preliminary experiments, in animals still surviving 1 week post infection in the mixed infection experiments, the Δ*hfq* strain showed a > 1000-fold reduction in cfu relative to the wild-type strain (CI of 0.0005–0.001; data not shown).

The hfq *mutant is impaired in the invasion of non-phagocytic cells*

Oral infection by *Salmonella* results in active invasion of non-phagocytic epithelial cells of the host intestine. To

determine the effect of the *hfq* mutation on the invasion rate of non-phagocytic cells *in vitro*, cultured HeLa cells were infected with the wild-type and several *hfq* mutant and control strain strains. A *Salmonella* SL1344 Δ*spi1* mutant, which lacks the entire SPI1, served as a negative control in these experiments. SPI1 encodes a type three secretion system (TTSS) and several effector proteins that mediate the uptake of *Salmonella* by non-phagocytic eukaryotic cells (Galan and Curtiss, 1989; Mills *et al.*, 1995; Collazo and Galan, 1996). HeLa cells were infected with a multiplicity of infection (moi) of 10 with bacteria grown aerobically to early stationary phase (OD_{600} of 2). Following gentamicin treatment to kill remaining extracellular bacteria, the number of intracellular bacteria was determined 2 and 6 h post infection (Table 1).

The *hfq* deletion mutant showed a 100-fold reduced initial rate of invasion at 2 h post infection compared with the wild-type strain. We also compared the number of intracellular bacteria present after an additional 4 h. Within these 4 h, the number of wild-type bacteria doubled, whereas the number of *hfq* mutant bacteria remained unchanged, suggesting an intracellular growth defect in addition to an invasion defect. Despite its drastic invasion defect, the invasion rate of the *hfq* mutant remains above that of a non-invasive Δ*spi1* mutant for which only single cells could be recovered (Table 1 and Fig. S2A).

To determine whether the *hfq* mutant was still impaired in invasion when grown under SPI1-inducing conditions, the invasion assays were repeated with bacterial cultures grown for 12 h under high-salt, oxygen-limiting conditions (Table 1 and Fig. S2B). These growth conditions increased the invasion rate of both the wild type and the Δ*hfq* strain to 30% and 3% respectively (as calculated for the 2 h time point). However, the Δ*hfq* strain remained 10-fold less invasive than the wild type, and intermediate with respect to the non-invasive Δ*spi1* mutant. While the wild-type strain showed more than one replication in additional 4 h, the Δ*hfq* strain only doubled in the 4 h period.

Three other strains included as controls in all of these experiments, Δ*rpoS*, *hfq*-C and *hfq*^{HIS}, all displayed only slightly reduced invasion rates in the range of 1.3- to threefold in comparison with the wild type, and none of these strains were affected in intracellular growth (Table 1 and Fig. S2A and B). To corroborate that the lack of Hfq protein was the main cause of the invasion defect of the Δ*hfq* mutant, we tested whether it could be complemented by a plasmid-borne *hfq* allele. Providing Hfq *in trans* with plasmid pStHfq-6H not only fully restored invasion to the *hfq* deletion strain, but enhanced invasion relative to the wild type (Table 1 and Fig. S2B). Taken together, these data suggest that Hfq is required for efficient invasion of non-phagocytic cells, which is likely to underlie the strong attenuation of virulence seen in oral mouse infections.

Table 1. Invasion and intracellular replication (% of the bacterial input).

	Aerobic growth to early stationary phase (OD_{600} of 2), gentamicin protection assay (HeLa cells)		SPI1-inducing growth conditions, gentamicin protection assay (HeLa cells)		Aerobic growth to early stationary phase (OD_{600} of 2), macrophage survival assay (RawB)		
Strain/infection time	2 h	6 h	2 h	6 h	1 h	4 h	24 h
wt	14.16	30.38	29.4	82.11	16.53	29.79	47.48
hfq^{HIS}	7.92	14.53	13.59	41.58	5.54	10.31	18.08
hfq-C	4.76	19.66	15.74	38.59	4.90	12.37	15.74
Δ*hfq*	0.13	0.13	3.25	6.58	0.39	0.40	3.25
Δ*spi1*	0.00	0.01	0.05	0.07	ND	ND	ND
Δ*rpoS*	8.79	22.61	22.88	65.89	ND	ND	ND
wt + pCtr	ND	ND	22.19	70.74	9.98	26.55	28.63
Δ*hfq* + pCtr	ND	ND	2.35	6.29	0.54	0.57	0.67
Δ*hfq* + pStHfq-6H	ND	ND	40.87	118.38	15.16	41.21	42.24

We also examined both the invasion and long-term intracellular growth phenotypes of the Δ*hfq* mutant in an intestinal epithelial cell line (Fig. S3A). Consistent with the results using the HeLa cell line, the initial invasion rate of LoVo cells was 10- to 100-fold reduced at either a 10-fold higher or equivalent infective dose as the wild-type strain respectively. In addition, whereas the wild-type strain showed an approximately 10- to 20-fold increase in intracellular cfu over a 24 h period, the Δ*hfq* strain showed either no change or a slight reduction in viable bacteria over the same period. These results were consistent with a requirement for Hfq for both invasion as well as intracellular replication in non-phagocytic cells.

The hfq *strain survives but shows an intracellular growth defect in macrophages*

Salmonella survival in the host is also dependent on the ability to survive and replicate in macrophages. To test a possible role for Hfq in macrophage survival, we infected *in vitro* cultured murine macrophages (RawB) with equal numbers of wild-type and *hfq* mutant bacteria (Table 1 and Fig. S2C). At 1 h post infection, we noted 30-fold fewer intracellular bacteria in macrophages infected with the *hfq* mutant, likely reflecting the reduced invasion rate of this strain. However, complementation with plasmid pStHfq-6H fully restored macrophage invasion, comparable to levels observed with wild-type bacteria. Intracellular replication as determined 4 and 24 h after infection also revealed drastic differences between the wild-type strain and the *hfq* deletion mutant. While the wild-type and the *hfq*-C and *hfq*^{HIS} control strains at least doubled within the 4 h post infection, the *hfq* deletion mutant showed no significant increase in intracellular bacteria per macrophage. At 24 h post infection the number of intracellular bacteria had increased to > threefold as compared with the 1 h time point for the wild-type, the control strains and the complemented deletion mutant (Table 1).

In other experiments, infection of the J774A.1 murine macrophage cell line showed a similar reduction in initial uptake, but no significant increase in intracellular cfu for up to 24 h (Fig. S3B). Thus, Hfq appeared to have little or no effect on the expression of genes required for macrophage survival, although the lack of significant intracellular growth in both epithelial and macrophage cell lines suggested an effect on expression of the second, major pathogenicity island, SPI2, which is required for intracellular proliferation (Shea *et al*., 1996; Cirillo *et al*., 1998; Hensel *et al*., 1998).

Lack of Hfq results in global changes of protein expression and loss of protein secretion

Considering the pleiotropic effect of Hfq on mRNA stability and translational regulation in other bacteria, we sought to determine Hfq-dependent changes in protein expression. We first compared the whole-cell protein patterns in one-dimensional gels of wild-type and Δ*hfq* cells from cultures grown aerobically in L-broth in three different growth phases: exponential growth, early and late stationary phase. As shown in Fig. 3A, Δ*hfq* cells exhibit no significant difference to the wild type in exponential phase. In contrast, in stationary phase the Δ*hfq* mutation showed a markedly different protein pattern, with the most prominent and reproducible changes being two abundant protein bands of ~40 and ~55 kDa (Fig. 3A). Mass spectrometry (MALDI-TOF) identified the 40 kDa band as the major outer membrane protein (OMP), OmpD. Analysis of the 55 kDa band proved more complex, because MALDI-TOF analysis indicated the presence of two proteins, GlpK (glycerol kinase) and FliC (major phase-1 flagellin). This band was further resolved with longer gel runs (Fig. 3B, left panel) and revealed that in the Δ*hfq* mutant, FliC levels were strongly reduced whereas GlpK accumulated to higher levels. Parallel analysis of the protein profile of an *rpoS* deletion strain showed that the Hfq-dependent regulation of OmpD, FliC and GlpK, was not related to lower σ^S levels in Δ*hfq* cells. Additional analyses revealed an increase in the levels of HtrA, YbfM, OmpF, CyoA and Tsf, and a decrease of the ribosomal proteins RpsD and RplC in the Δ*hfq* strain. To obtain a preliminary picture of global changes in the expression profiles of less abundant proteins, we also analysed early stationary phase samples of wild-type and Δ*hfq* cells resolved on two-dimensional gels (Fig. S4). Of the 69 protein candidates analysed by MALDI-TOF, 32 were upregulated in Δ*hfq* cells, whereas 37 showed downregulation. These results are summarized in Table 2 (further details are given in Table S1).

Loss of Hfq also affected the composition of the periplasmic protein population (Fig. 3B, right panel). While some of the changes in protein expression seen in Δ*hfq* cells are shared with the *rpoS* deletion strain (e.g. OppA and GltI), loss of Hfq leads to a specific increase in DppA, a decrease in TufB levels, and higher levels of OppA, MglB, GltI and GlnH as compared with the Δ*rpoS* strain (Table 2).

The most drastic effects of the *hfq* deletion, however, were observed with the secreted protein fraction (Fig. 3C). FliC, the most prominent protein found in *Salmonella* supernatants (Komoriya *et al*., 1999) and other secreted proteins typically seen in SL1344 supernatants, e.g. effector proteins that are translocated by the SPI1 TTSS (Ehrbar *et al*., 2002), were either strongly reduced or undetectable. The loss of secreted SPI1 effectors was consistent with the reduced invasion phenotype of the Δ*hfq* strain. None of these reductions were observed with the Δ*rpoS* strain (Fig. 5A).

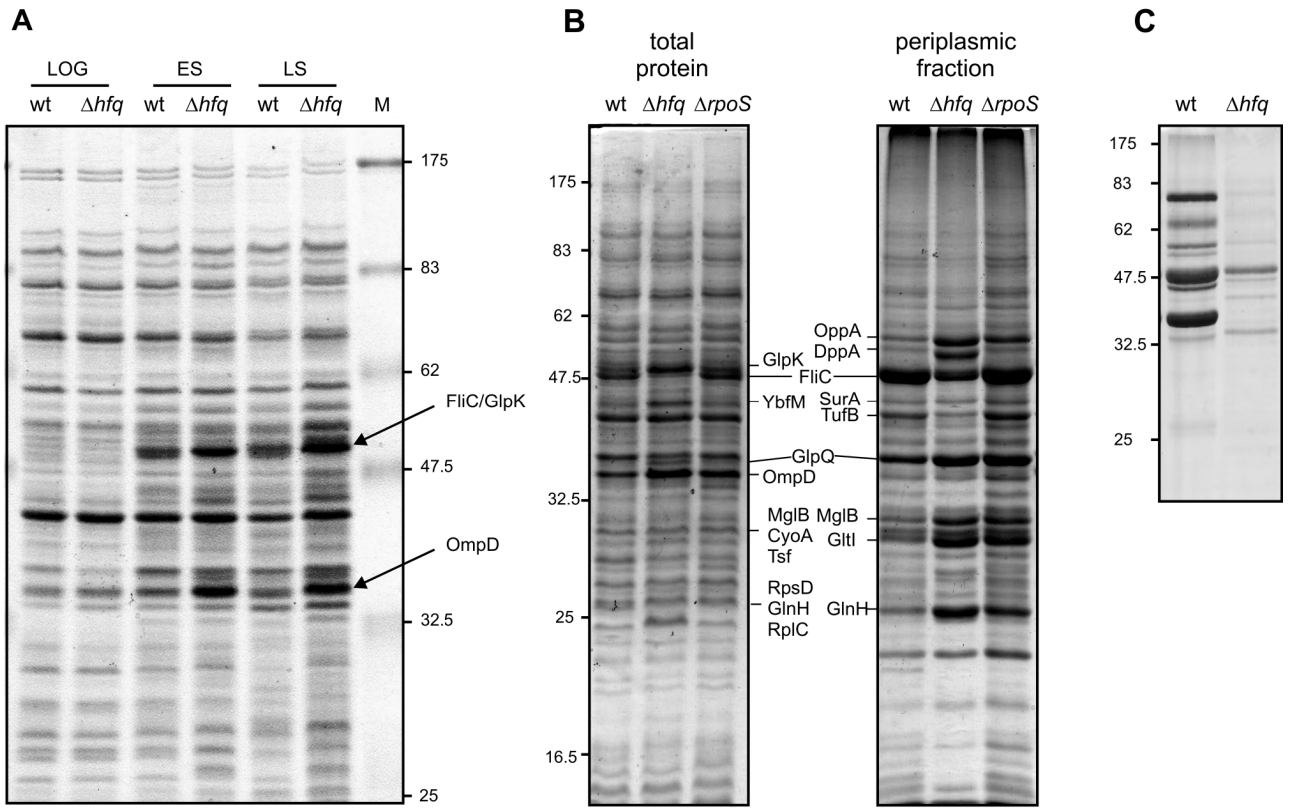

Fig. 3. Altered protein expression in *Salmonella Δhfq*. SDS-PAGE (10–12% gels) of protein samples of SL1344 wild-type and Δ*hfq* prepared from different growth phases (LOG: logarithmic phase, OD_{600} of 0.3; ES: early stationary phase, OD_{600} of 2; LS: late stationary phase, 6 h after cells had reached an OD_{600} of 2).
A. Total protein samples.
B. Total protein and periplasmic fractions; samples of a Δ*rpoS* strain were included as an additional control.
C. Secreted protein fractions of early stationary phase bacteria.

Overexpression of HilA in Δhfq *rescues SPI1 effector protein expression but not secretion*

Consequently, we sought to determine if the Hfq-dependent loss of secreted SPI1 effectors was due to a more general defect on SPI1 gene expression. The activation of SPI1 genes is mediated by a transcription factor cascade. On top of this cascade, the transcription factors, HilC and HilD, along with RtsA (encoded outside SPI1) cooperate to transmit environmental signals that lead to derepression of *hilA* (Bajaj *et al*., 1996; Lucas and Lee, 2001; Schechter and Lee, 2001; Ellermeier *et al*., 2005). HilA is the SPI1 major transcriptional activator responsible for most of the SPI1 TTSS and effector gene expression, both directly and indirectly through its activation of InvF (Darwin and Miller, 1999; Eichelberg and Galan, 1999; Lostroh and Lee, 2001). In addition, HilA also activates expression of secreted effector proteins encoded outside SPI1, e.g. SopB encoded within SPI5 (Ahmer *et al*., 1999).

To quantify the amount of HilA protein, we constructed a chromosomal FLAG epitope-tagged derivative of the *hilA* gene. Quantification of Western blot signals obtained for $HilA^{FLAG}$ revealed a > sixfold reduction of the protein in the Δ*hfq* mutant as compared with the wild type (Fig. 4A, left panel). In addition, Northern blot quantification showed that in Δ*hfq* cells *hilA* mRNA was reduced to ~8% of wild-type levels (Fig. 4B). Several transcriptional reporter fusions were also used to determine if the changes in *hilA* expression resulted from a reduced *hilA* promoter activity (Fig. 4B). Depending on the fusion used, *hilA* transcription in Δ*hfq* was found to be reduced to between 30% and 70% of wild-type levels. Collectively, this suggested that Hfq regulates HilA synthesis at both the transcriptional and the post-transcriptional level.

To verify that the lower HilA levels in the Δ*hfq* strain cause a reduction of SPI1 effector protein synthesis, we first determined the intracellular levels of SipC, SipD, SopB and SopE on Western blots, all of which were readily detected in wild-type cells (Fig. 4C, lanes 1 and 3). In stark contrast, no (SipC, SopB, SopE) or drastically reduced (SipD) signals were obtained in the Δ*hfq* background (lane 5). To determine whether HilA overexpres-

Table 2. Results of 1D and 2D gel analysis of protein patterns of SL1344 wild-type and Δ*hfq* cultures grown to early stationary phase (OD_{600} = 2).

Candidate protein[a]	Regulation[b]	Localization[c]	Function[d]	Analysis[e]
CarA	–	CP	Carbamoyl-phosphate synthetase, glutamine-hydrolysing small subunit	2D
SurA	+	CP	Peptidyl-prolyl *cis-trans* isomerase, survival protein	1D, 2D
HtrA	+	PP	Periplasmic serine protease Do, heat shock protein	1D, 2D
PyrH	–	CP	Uridine 5′-monophosphate kinase	2D
Upp	–	CP	uracil phosphoribosyltransferase	2D
YaeT	+	(OM)	Putative outer membrane antigen	2D
GltI	+	PP	ABC transporter periplasmic binding protein; ABC superfamily, glutamate/aspartate transporter	1D, 2D
SucD	–	CP	Succinyl-CoA synthetase, alpha subunit	2D
Pal	+	PP	Tol protein required for outer membrane integrity, uptake of group A colicins, and translocation of phage DNA to cytoplasm	2D
YbgF	–	(PP)	Putative periplasmic protein	2D
Dps	–	CP	Stress response DNA-binding protein; starvation induced resistance to H_2O_2; DNA protection during starvation protein	2D
CspD	+	CP	Cold shock-like protein CspD; similar to CspA but not cold shock induced	2D
TrxB	–	CP	Thioredoxin reductase; thioredoxin reductase	2D
FabF	–	CP	3-oxoacyl-[acyl-carrier-protein] synthase II	2D
IcdA	+	CP	Isocitrate dehydrogenase in e14 prophage, specific for NADP+	2D
PagC	+	OM	PhoP regulated: reduced macrophage survival; virulence membrane protein PagC precursor	2D
STM1254	–	(OM)	Putative outer membrane lipoprotein	2D
STM1328	–	(OM)	Putative OMP	2D
AroD	–	CP	3-Dehydroquinate dehydratase	2D
LppB	–	OM	Putative methyl-accepting chemotaxis protein; major outer membrane lipoprotein	2D
LppA	–	OM	Murein lipoprotein, links outer and inner membranes; major outer membrane lipoprotein	2D
YnaF	–	CP	Putative universal stress protein	2D
Tpx	+	CP	Thiol peroxidase	2D
TrpB	–	CP	Tryptophan synthase beta chain	2D
OppA	+	PP	ABC superfamily, oligopeptide transport protein with chaperone properties	1D, 2D
KdsA	–	CP	3-deoxy-D-manno-octulosonic acid 8-P synthetase	2D
PrsA	–	CP	Phosphoribosylpyrophosphate synthetase	2D
FliC	–	OM/SUP	Flagellin, filament structural protein	2D
Gnd	–	CP	Gluconate 6-phosphate dehydrogenase, decarboxylating	2D
GlpQ	+	PP	Glycerophosphodiester phosphodiesterase, periplasmic	1D, 2D
AckA	–	CP	Acetate kinase A (propionate kinase 2)	2D
HisJ	–	PP	ABC superfamily, histidine-binding periplasmic protein	2D
CysP	+	PP	ABC superfamily, thiosulphate transport protein	2D
MaeB	+	CP	Paral putative transferase; phosphate acetyltransferase	2D
NlpB	+	OM	Lipoprotein-34	2D
STM2494	+	(IM)	Putative inner membrane or exported	2D
NifU	–	CP	NifU homologue involved in Fe-S cluster formation	2D
YfiA	–	CP	ribosome associated factor, stabilizes ribosomes against dissociation; putative sigma(54) modulation protein	2D
LuxS	–	CP	Quorum sensing protein, produces autoinducer – acyl-homoserine lactone-signalling molecules	2D
SipA	–	SUP	Cell invasion protein	2D
SipC	–	SUP	Cell invasion protein	2D
GudD	–	CP	D-Glucarate dehydratase	2D
Ptr	+	PP	Protease III	2D
OmpX	–/+	OM	Ail and ompX homologue; outer membrane protein X precursor	2D
YraP	+	(PP)	Paral putative periplasmic protein; possible lipoprotein	2D
RbfA	–	CP	Ribosome-binding factor, role in processing of 10S rRNA	2D
GreA	+	CP	Transcription elongation factor, cleaves 3′ nucleotide of paused mRNA	2D
Mdh	–/+	CP	Malate dehydrogenase	2D
AccB	+	CP	acetyl-CoA carboxylase, BCCP subunit, biotin carboxyl carrier protein	2D
FkpA	+	CP	FKBP-type peptidyl-prolyl *cis-trans* isomerase (rotamase)	2D
DppA	+	PP	ABC superfamily, dipeptide transport protein	1D, 2D
YiaD	+	(OM)	Putative outer membrane lipoprotein	2D
Kbl	–	CP	2-amino-3-ketobutyrate CoA ligase (glycine acetyltransferase)	2D
PstS	+	PP	ABC superfamily, high-affinity phosphate transporter	2D
RbsB	+	PP	ABC superfamily, D-ribose transport protein; D-ribose-binding periplasmic protein	2D
FadA	–	CP	3-ketoacyl-CoA thiolase (thiolase I, acetyl-CoA transferase), small (beta) subunit of the fatty acid-oxidizing multienzyme complex	2D
RplL	–	CP	50S ribosomal subunit protein L7/L12	2D

Table 2. *cont.*

Candidate protein[a]	Regulation[b]	Localization[c]	Function[d]	Analysis[e]
MalE	–	PP	ABC superfamily maltose transport protein, substrate recognition for transport and chemotaxis	2D
AphA	+	PP	Non-specific acid phosphatase/phosphotransferase, class B	2D
OsmY	–	PP	Hyperosmotically inducible periplasmic protein, RpoS-dependent stationary phase gene	2D
Tsf	+	CP	Protein chain elongation factor EF-Ts	1D
CyoA	+	IM	Cytochrome o ubiquinol oxidase subunit II	1D
YbfM	+	(OM)	Putative OMP	1D
GlnH	+	PP	ABC superfamily (bind_prot), glutamine high-affinity transporter	1D
OmpF	+	OM	OMP 1a (ia; b; f), porin	1D
MglB	+	PP	ABC superfamily (peri_perm), galactose transport protein	1D
STM2786	+	PP	Tricarboxylic transport	1D
RpsD	–	CP	30S ribosomal subunit protein S4	1D
RplC	–	CP	50S ribosomal subunit protein L3	1D
GlpK	+	CP	Glycerol kinase	1D
TufB	–	CP	Protein chain elongation factor EF-Tu (duplicate of tufA)	1D

a. Nomenclature according to coliBASE (http://colibase.bham.ac.uk/; Chaudhuri *et al*., 2004).
b. Up- or downregulation in *hfq* strain as compared with SL1344.
c. Predicted subcellular protein localization: CP, cytoplasmic; PP, periplasmic; OM, outer membrane; IM, inner membrane; SUP, secreted.
d. Functional classification according to KEGG (http://www.genome.jp/kegg/; Goto *et al*., 1997).
e. Protein identified on one-dimensional (1D) or two-dimensional (2D) gel.
See Table S1 for further details.

sion could restore effector protein expression in the absence of Hfq, the wild-type and the Δ*hfq* strains were transformed with plasmid pBAD-HilA (Lostroh *et al*., 2000), which carries a *myc*-tagged *hilA* gene under control of an arabinose-inducible P_{BAD} promoter. Arabinose induction yielded comparable $HilA^{myc}$ protein levels in both genetic backgrounds (Fig. 4A, right panel), and fully restored the intracellular levels of effector proteins in Δ*hfq* cells to wild-type amounts (Fig. 4C, compare lanes 3 and 6). We next examined whether HilA overexpression could also restore effector protein secretion. Supernatants of the same cultures used for whole-protein determinations in Fig. 4C were examined for extracellular levels of the aforementioned effector proteins. In stark contrast to the full restoration of intracellular effector protein levels, HilA expression failed to significantly increase the extracellular amounts of these proteins in the Δ*hfq* strain (lanes 11 and 12). HilA overexpression in the Δ*hfq* background was therefore able to overcome the loss of expression of these effector proteins but not of their secretion.

One possible explanation for this secretion defect was that the *hfq* mutation does not permit assembly of a functional SPI1 secretion apparatus. The secreted PrgI protein, the main component of the needle of the SPI1-encoded TTSS, provides a testable marker for a functional secretion apparatus (Kimbrough and Miller, 2000; Kubori *et al*., 2000). We determined both the intra- and extracellular PrgI levels in all of the strains, and found that this protein was absent in the Δ*hfq* mutant (Fig. 4C, lower panel, lanes 1 and 3 versus 5, lanes 7 and 9 versus 11). In contrast, HilA overexpression led to elevated intracellular and secreted PrgI levels in the wild-type but not *hfq* strains (lanes 4 and 6 versus 10 and 12). These results indicated that under aerobic growth conditions, Hfq affected SPI1 expression at multiple levels, and was required for the expression of the TTSS structural genes independent of HilA expression.

Effector protein secretion independent of hfq *under SPI1-inducing conditions*

As we had observed that the invasion defect of the Δ*hfq* strain was less pronounced when grown under SPI1-inducing conditions, we considered whether this was the result of improved effector protein secretion. Indeed, supernatants of Δ*hfq* cells cultured under SPI1-inducing conditions displayed a protein pattern close to the wild type (Fig. 5A, compare lanes 5 and 6), except for the flagellar protein, FliC. When these samples were probed on Western blots for the effectors SipC, SipD, SopB and SopE, a similar level of secretion as for the wild-type strain was evident for the *hfq* mutant (Fig. 5B). Furthermore, under these growth conditions, the Δ*hfq* strain accumulated the needle protein, PrgI, to wild-type levels both intracellularly and in the supernatant, arguing that under this growth condition, Δ*hfq* bacteria also possess a fully active SPI1 TTSS.

Impaired adhesion contributes to the non-invasive phenotype of Δhfq

Although the Δ*hfq* strain appeared to show wild-type levels of expression in terms of SPI1 function when grown

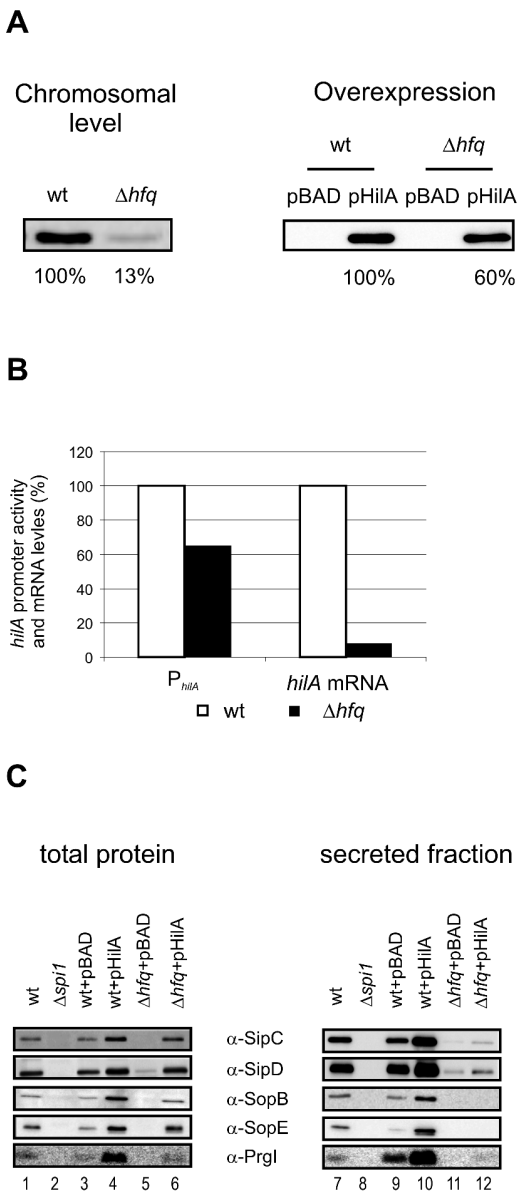

Fig. 4. The *hfq* deletion mutant is impaired in HilA expression and shows reduced effector levels.
A. HilA levels in wild-type and Δ*hfq Salmonella* grown to early stationary phase. Shown are Western blots probed for chromosomally encoded $HilA^{FLAG}$ protein (left panel), or $HilA^{myc}$ protein as expressed from pBAD-HilA expression plasmid (right panel). Bacteria carrying the empty pBAD vector were included as control.
B. *hilA* promoter activity determined with a transcriptional *hilA-gfp* fusion in early stationary phase (P_{hilA}), and *hilA* mRNA levels as determined by Northern analysis. Given are relative values obtained for Δ*hfq*, with the levels determined for the wild-type strain set to 100%.
C. Western blot detection of effector and needle proteins in total protein samples and secreted fractions of bacteria grown to early stationary phase. Bacterial strains from left to right: wild-type, Δ*spi1*, wild-type strain carrying a pBAD control vector, wild-type strain carrying a pBAD-HilA expression plasmid, Δ*hfq* carrying a pBAD control vector, Δ*hfq* with pBAD-HilA expression plasmid. All strains were grown in LB medium complemented with 0.05% L-arabinose to facilitate HilA expression from plasmid pBAD-HilA.

under SPI1-inducing conditions, it was puzzling that the mutant remained much less invasive. One important factor that contributes to *Salmonella* invasion of host cells in addition to SPI1 function is successful adhesion to epithelial cells, mediated by fimbrial adhesins. We therefore performed assays to compare the adhesion phenotypes of the wild-type and Δ*hfq* strains. To better visualize bacteria, both strains were transformed with a low-copy plasmid that constitutively expresses green fluorescent protein (GFP). Transformants were grown under SPI1-inducing conditions, and used for infection of HeLa cells at a moi of 50. Following incubation at 37°C for 1 h, bacteria that had not attached to the HeLa cells were removed by extensive washing of the cells. The remaining bacteria and cells were fixed, and the number of bacteria per HeLa cell determined by fluorescence microscopy (Fig. S5A). For the wild-type strain, an average of ~30 bacteria per HeLa cell were found to be adherent. In contrast, the average number observed with the Δ*hfq* strain was significantly lower, i.e. ~10 bacteria per HeLa cell. For both strains, we observed that a significant proportion of bacteria became internalized during the 1 h incubation step prior to counting. As the assay does not allow us to clearly distinguish extra- from intracellular bacteria, our calculation includes all bacteria associated with HeLa cells, based on the assumption that every internalization event was preceded by successful adhesion.

To better separate adhesion from invasion rates, bacterial adherence was also determined in HeLa cell infection assays without gentamicin treatment. To this end, serial dilutions of HeLa cells and adhered bacteria were plated on LB agar 30 min upon infection, and cfu determined (Fig. S5B). These experiments revealed a > twofold reduction in adhesion of the *hfq* deletion mutant as compared with wild-type *Salmonella* (25% adherence of wild-type compared with 11% of the *hfq* strain related to the input). In contrast, adherence of the two control strains, hfq^{HIS} and *hfq*-C, did not significantly differ from the wild type (21% and 24% respectively). Collectively, the data suggest that a lower adhesion rate may contribute to the non-invasive phenotype of the *hfq* strain.

Δhfq *is impaired in motility*

The strong Hfq dependence for expression of the phase 2 flagellin protein, FliC, suggested that Hfq would be required for *Salmonella* motility. To verify reduced FliC expression, we first analysed *fliC* mRNA levels in wild type and Δ*hfq Salmonella* at different growth phases (Table 3 and Fig. 6A). Interestingly, loss of Hfq caused a mere 1.6-fold reduction of *fliC* mRNA levels in exponential phase, however, a sixfold reduction at early stationary phase (Table 3). We also compared *fliC* mRNA stability in wild-type strain and Δ*hfq* cells, and found it largely unaf-

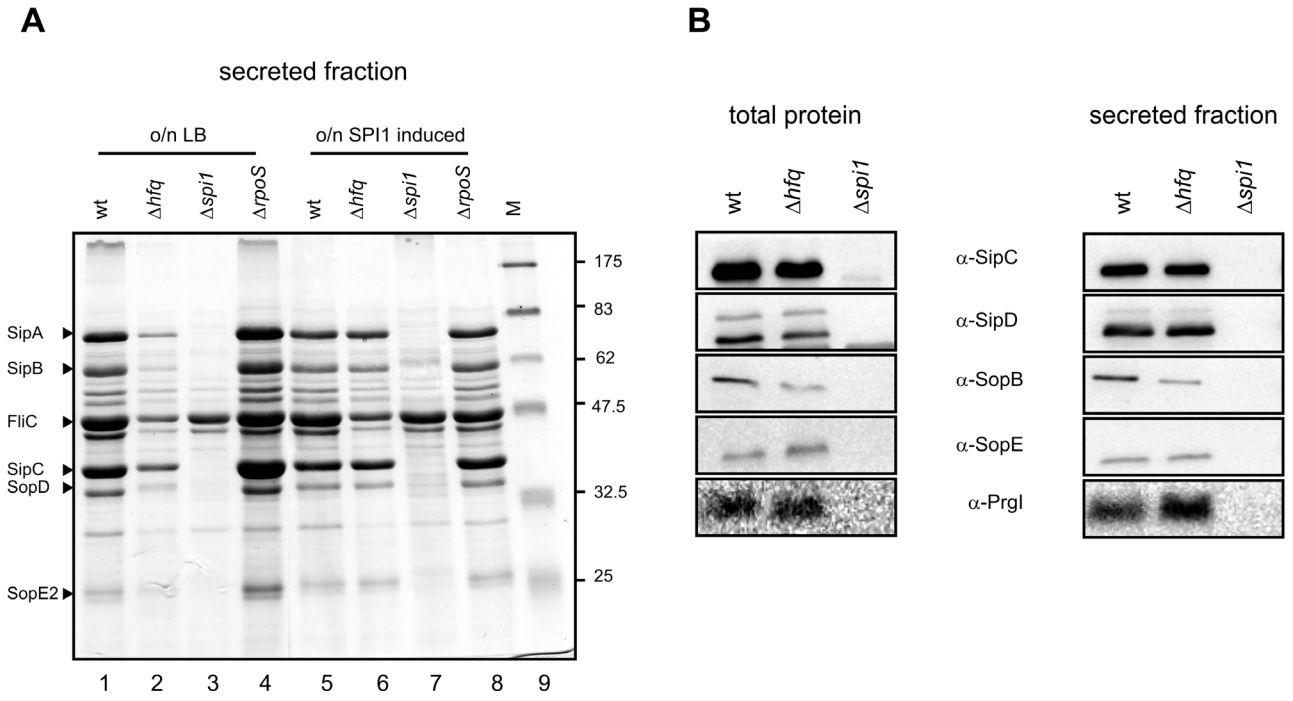

Fig. 5. SPI1-inducing conditions restore effector levels and their secretion in the Δ*hfq* strain.
A. Comparison of secreted proteins of wild-type, Δ*hfq*, Δ*spi1* and Δ*rpoS* grown for 12 h under standard conditions (lanes 1–4) or SPI1-inducing conditions (lanes 5–8) by SDS-PAGE analysis.
B. Western blot detection of effector and needle proteins in total protein samples and secreted fractions of bacteria grown for 12 h under SPI1-inducing conditions. Bacterial strains from left to right: wild-type, Δ*hfq*, Δ*spi1*.

fected by the *hfq* mutation at either growth phase (Fig. 6A). In contrast to *fliC* mRNA, we failed to detect *fljB* mRNA on any of these Northern blots (data not shown). Taken together, the reduced FliC expression of Δ*hfq* is unlikely to result from phase variation of the invertible flagellar switch (*fljB/fljA* promoter), but rather from reduced *fliC* transcription.

Next, we compared the motility of the wild-type and the Δ*hfq* strains, harbouring either a control or complementation plasmid pStHfq-6H, on motility agar plates. Wild-type cells were motile and formed concentric motility rings around the point of inoculation (Fig. 6B). In contrast, the Δ*hfq* mutant displayed impaired motility, as judged by the much smaller motility ring formed. The strongly reduced motility of Δ*hfq* could also be seen by light microscopy of samples from liquid culture (data not shown). Complementation with plasmid pStHfq-6H fully restored motility. Two control strains, *hfq*-C and *hfq*^{HIS}, were found to be as motile as the wild type (data not shown), further supporting that loss of motility was a direct consequence of the lack of Hfq.

Table 3. Quantification of Hfq-dependent gene expression.

	Relative mRNA levels[a]		Relative transcriptional/ translational fusion activity[b]
Gene/OD_{600}	0.3	2	2
fliC	–1.6	–6	ND
ompC	1.7	1.6	0.84/1.1
ompD	1.7	1.4	0.82/2.5
P_{LtetO}-*gfp*	ND	ND	1.0

a. Fold change of mRNA levels in *hfq* strain as compared with SL1344 as determined by Northern hybridization.
b. Fold change of GFP reporter fusion activity in *hfq* strain as compared with SL1344.

Growth rate-dependent repression of OmpD

In addition to the positive regulation of secreted effector protein expression, the protein patterns obtained from different growth phases showed that Hfq was also involved in the repression of OmpD synthesis as cells progress into stationary phase (Fig. 3A). To confirm a negative regulatory role for Hfq in OmpD regulation, protein samples of wild-type, Δ*hfq*, Δ*ompD* and Δ*hfq*/Δ*ompD* strains grown to early stationary phase were compared (Fig. 7A). MALDI-TOF analysis of the 40 kDa protein band which showed higher levels of accumulation in the Δ*hfq* strain unequivocally identified it as OmpD, consistent with the complete loss of this protein band in Δ*ompD* and Δ*hfq*/Δ*ompD* cells. Using fluorescent dye staining, we also quantified the relative OmpD accumulation, and found approximately twofold elevated levels of this protein in whole cell lysates (Fig. 7A).

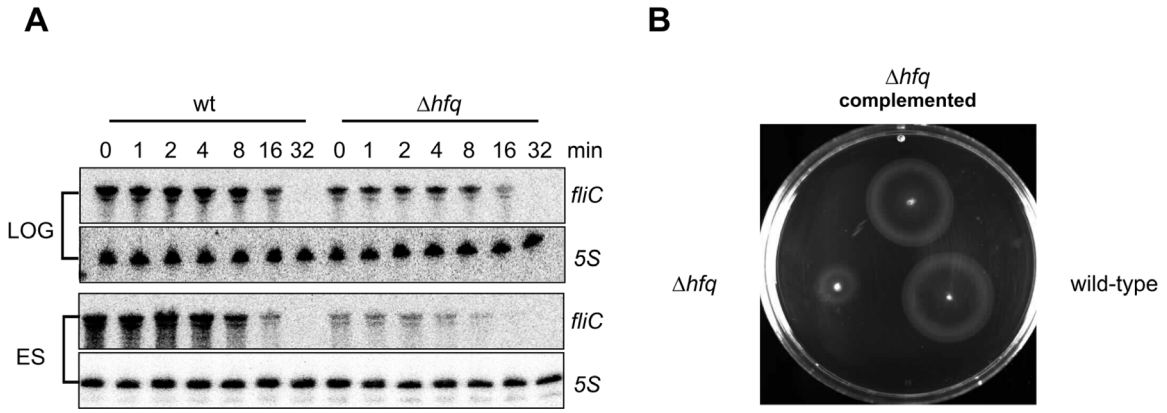

Fig. 6. The Δ*hfq* strain is non-motile.
A. Northern blot detection of *fliC* mRNA levels in wild-type and Δ*hfq* cells at logarithmic and early stationary phase before and within 32 min after rifampicin treatment. Densitometry of the Northern blot signals showed that the *fliC* mRNA decays with the same half-life in both genetic backgrounds (~9 min or ~7 min in logarithmic or early stationary phase cultures respectively). 5S signals are shown as loading control.
B. To measure motility, equal numbers of bacteria from each strain were inoculated onto a motility agar-plate. The image was obtained following 4 h of incubation at 37°C.

To learn more about the underlying mechanism of Hfq-dependent *ompD* regulation, we first determined the relative changes in *ompC* and *ompD* mRNA abundance at three different points during the growth phase (Table 3). We found that the Δ*hfq* strain exhibited elevated *ompC/D* mRNA levels throughout growth. We also followed the decay of both mRNAs after rifampicin treatment (transcription block, Fig. 7B). Figure 7C shows that absence of Hfq slowed *ompD* mRNA decay twofold (half-lives: ~9 min versus ~16 min in wild-type and Δ*hfq* strains), whereas *ompC* decay was not affected.

Next, we constructed transcriptional and translational reporter (GFP) plasmids for both mRNAs. Quantification of GFP reporter activity showed a slightly decreased *ompD* promoter activity (0.82-fold) at early stationary phase, whereas *ompD* translation was upregulated > 2.5-fold (Table 3). As the enhanced activity of the translational *ompD* fusion was consistent with elevated OmpD protein levels (Fig. 7A), we reasoned that Hfq may bind to the 5′ region of the *ompD* mRNA to interfere with its translation. To test this hypothesis, we synthesized a 5′ fragment of the *ompD* mRNA, encompassing its 5′ UTR and 118 nucleotides of the coding region, and performed *in vitro* mobility shift assays with purified Hfq protein. Figure 7D shows that Hfq binds this fragment with high affinity. Up to four different Hfq/*ompD* complexes are observed with increasing Hfq concentration, indicating that there are several Hfq binding sites in the *ompD* 5′ UTR. In contrast, no significant shift was observed with an Hfq-independent RNA (5′ UTR of *metK*) within a 250 nM range of Hfq (Fig. 7D). Taken together, these data suggests a direct role for Hfq in translational repression of the *ompD* mRNA.

Discussion

The RNA chaperone, Hfq, has recently been recognized as a major post-transcriptional regulator of bacterial gene expression which participates in numerous regulatory pathways (Valentin-Hansen *et al*., 2004). First identified as a host factor for replication of RNA phage Qβ in *E. coli*, Hfq has been shown to have a broad impact on physiology in several bacteria. The role of Hfq beyond phage replicative functions was first shown with an *E. coli hfq*::Ω mutation, which resulted in pleiotropic phenotypes related mainly to reduced survival of stress conditions (Tsui *et al*., 1994). Later, Hfq was found to be required in *E. coli* and *Salmonella* for efficient translation of *rpoS* mRNA, encoding the general stress sigma factor, σ^S (Brown and Elliott, 1996; Muffler *et al*., 1996). As RpoS is required for *Salmonella* proliferation in mice (Fang *et al*., 1992; Nickerson and Curtiss, 1997; Humphreys *et al*., 1999), it has been assumed that Hfq plays an important role in *Salmonella* virulence (e.g. Ding *et al*., 2004). However, the mechanisms by which Hfq affects the pathogenicity of *Salmonella* remained undefined. Previous work in *E. coli* established that Hfq also has regulatory functions independent of its effects on σ^S expression (Muffler *et al*., 1997). Likewise, *B. abortus* does not possess an RpoS-like σ factor (Roop *et al*., 2003), yet an *hfq* mutant of *B. abortus* has a pronounced virulence defect (Robertson and Roop, 1999). Similarly, the virulence defect of a *V. cholerae hfq* mutant was not accompanied by reduced σ^S levels (Ding *et al*., 2004).

Peroral infection of the *Salmonella hfq* mutant revealed about the same degree of attenuation (Fig. 2A) as reported for a *Salmonella* Δ*rpoS* mutant, i.e. approximately a three-

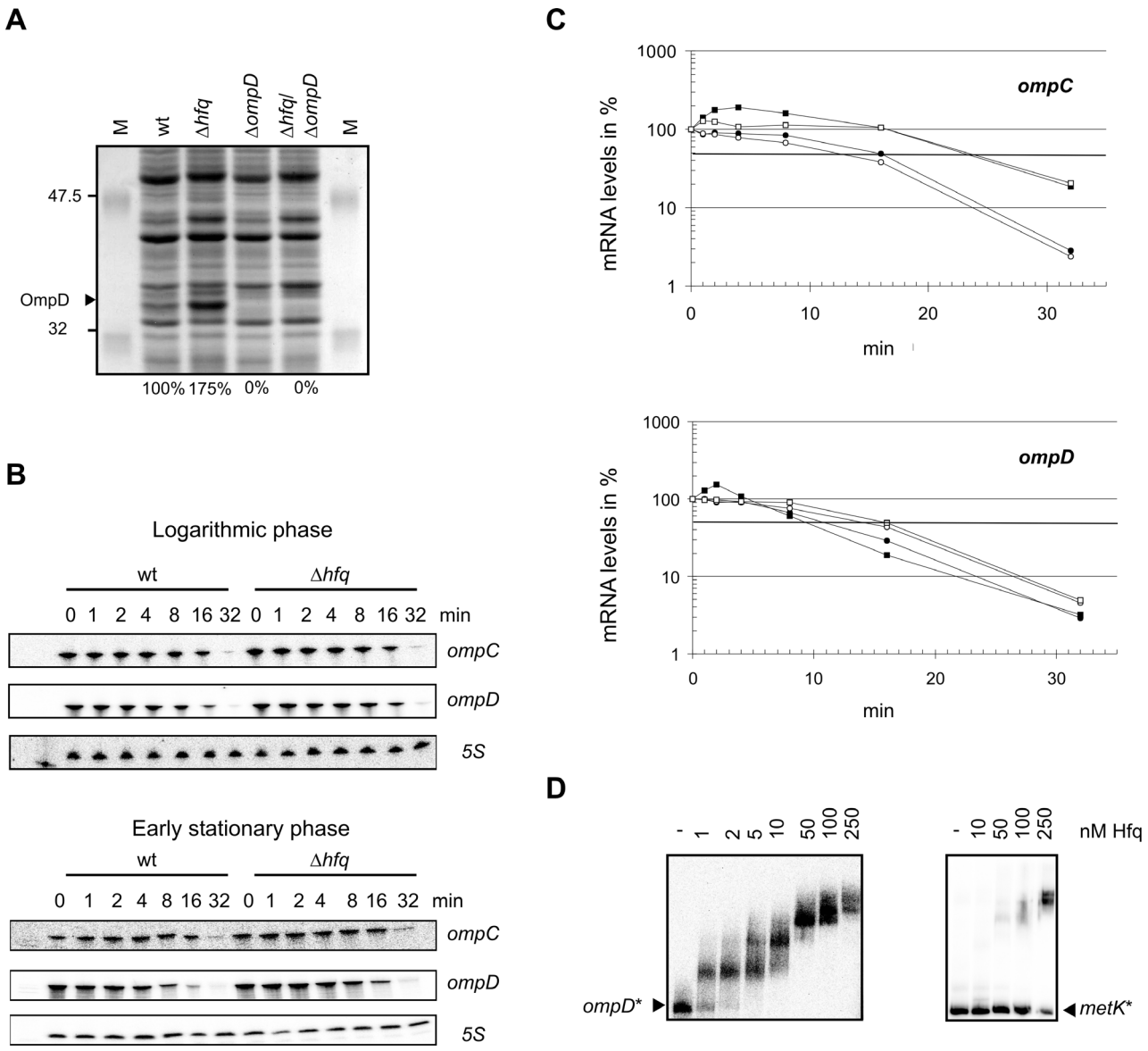

Fig. 7. Hfq is essential for growth rate-dependent repression of OmpD.
A. SDS-PAGE analysis of total protein prepared from wild-type, Δ*hfq*, Δ*ompD* and Δ*hfq*/Δ*ompD* bacteria grown to early stationary phase. OmpD protein levels as quantified by fluorescent staining (not shown) are given below each lane.
B. Northern blot detection of *ompC* and *ompD* mRNA levels of wild-type and Δ*hfq* bacteria grown to either logarithmic or early stationary phase prior to (0 min) and within 32 min of rifampicin treatment. 5S sRNA probing (loading control) is shown below each panel.
C. Decay of *ompC* and *ompD* mRNA upon rifampicin treatment as derived from quantification of the Northern blot signals shown in (B). Logarithmic phase, wild-type (filled circles) or Δ*hfq* (open circles); early stationary phase, wild-type (filled squares) or Δ*hfq* (open squares).
D. Hfq binds to *ompD* 5′ UTR RNA *in vitro* (gel mobility shift assay). Left panel: 1 nM of ^{32}P-labelled *ompD* was incubated with increasing concentrations of Hfq protein (given above the lanes). Following a 15 min incubation at 37°C samples were run on a native 6% gel. Shown is an autoradiograph of the gel. A control gel shift assay with an Hfq-independent RNA derived from the *metK* 5′ UTR is shown in the right panel.

log difference in cfu recovered from the spleen 3 days post infection using a 10-fold higher infective dose (Nickerson and Curtiss, 1997). Generally, *hfq* mutants of several *Salmonella* strains exhibit four- to sevenfold reduced RpoS levels (Fig. S6; Brown and Elliott, 1996; Bang *et al.*, 2005). This is about the degree of RpoS reduction observed in the mouse-avirulent strain, LT2, which has an altered *rpoS* start codon. At first glance, these observations appear to support a model in which reduced σ^S production would fully account for the attenuation of Δ*hfq*. However, using a set of newly constructed SL1344 *hfq* mutant and control strains, we defined *hfq* phenotypes that relate to virulence and global gene expression (see Fig. 8 for a summary), and which are largely independent of σ^S.

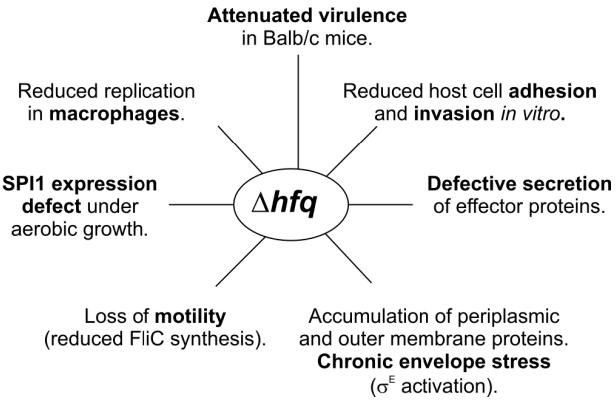

Fig. 8. Summary of phenotypes of the *Salmonella hfq* mutation determined in this study.

The most prominent virulence-associated phenotype we observed is the drastically reduced invasiveness of the Δ*hfq* mutant (Table 1). The ability of *Salmonellae* to invade cultured non-phagocytic cells is dependent on the expression of SPI1-encoded genes (Lee *et al*., 1992), and is strongly dependent on growth rate and media. Two growth conditions showing maximal invasiveness have been defined: growth in LB with aeration to early stationary phase, and growth in low-oxygen, high-salt media (SPI1-inducing). We found that although the *hfq* mutant is defective for invasion under both conditions, the underlying mechanisms are different. When grown to early stationary phase, the Δ*hfq* strain fails to activate the SPI1 transcription factor cascade, characterized by reduced HilA levels and the lack of SPI1 effector protein expression. Our observation that HilA overexpression resulted in the re-appearance of secreted protein expression indicated that the major target of Hfq regulation is HilA activation. This conclusion is also supported by the appearance of normal intracellular levels of SopB and SopE (Fig. 4C), both of which are encoded outside of SPI1 and whose expression requires the concerted function of InvF and SicA. The latter, SPI1-encoded genes are also highly dependent on HilA for expression (Darwin and Miller, 2000, and references therein).

The regulation of *hilA* promoter activity is complex, involving the coactivators HilC, HilD and RtsA, as well as other factors which act upstream of these proteins (Lostroh and Lee, 2001; Ellermeier *et al*., 2005; and references therein). A global transcriptome microarray analysis indicated that Δ*hfq* cells have several-fold reduced levels of *hilC/D* and *rtsA* mRNAs (A. Sittka *et al*., unpubl. results), suggesting that Hfq affects signal transmission further upstream in the SPI1-activating cascade. Strikingly, complementation with the HilA plasmid restored intracellular levels of several effector proteins encoded within SPI1, yet not their secretion. The latter observation may result from a failure to assemble a functional SPI1 TTSS, because only traces of the needle protein, PrgI, were detected in supernatants of HilA-complemented Δ*hfq* cells. The *prgI* gene is encoded within the SPI1 *prgHIJKorgABC* operon (Klein *et al*., 2000), and is directly controlled by HilA. These observations suggest that the role of Hfq as a novel factor of SPI1 gene activation may not be confined to promoting HilA expression. It remains possible that Hfq either is also involved in the mRNA stability of the *prgHIJKorgABC* operon transcript, or affects the translation of the encoded gene products. Further work is required to clarify the effects of Hfq on this subset of HilA-dependent genes.

In contrast to aerobic growth, under SPI1-inducing conditions the Δ*hfq* mutant shows normal SPI1 gene expression, TTSS assembly (as judged by PrgI levels in the supernatant) and effector protein secretion (Fig. 5B). Under these growth conditions, the Δ*hfq* mutant should have been capable of invasion of non-phagocytic cells, yet invasion was strongly reduced compared with the wild-type strain (Table 1). Our results from adhesion and motility assays as well as proteome analysis indicate several other factors may contribute to this impairment. The *hfq* mutant shows a significantly reduced ability to adhere to HeLa cells (Fig. S5), which is likely to affect the rate of invasion. The *hfq* mutant is non-motile (Fig. 6), due most likely to the loss of the flagellar subunit protein, FliC (Figs 3A–C and 6A). However, while flagella-mediated bacterial motility accelerates the invasion of *Salmonella*, motility *per se* is not required for invasion (van Asten *et al*., 2004). Finally, a preliminary proteome analysis (Table 2) showed differential regulation of numerous lipoproteins and OMPs, suggesting that Hfq is also involved in regulation of genes related to the bacterial envelope composition. Importantly, Δ*hfq* cells exhibit strongly elevated levels of HtrA, also known as DegP. HtrA/DegP has recently been shown in *Salmonella* and *E. coli* to be part of the σ^E regulon that mediates the response to envelope stress (Rhodius *et al*., 2006; Skovierova *et al*., 2006), and activation of the σ^E pathway (by RpoE overexpression) results in a strong induction of *htrA* mRNA (Rhodius *et al*., 2006). Three additional proteins that promote OMP assembly, FkpA, YraP and YaeT, and whose genes are members of the σ^E core regulon (Rhodius *et al*., 2006; Skovierova *et al*., 2006), also showed elevated levels in the *hfq* mutant. In addition, two strictly σ^E-dependent small RNAs, MicA and RybB, showed promoter activation in the *hfq* mutant under the same conditions used in this study (Papenfort *et al*., 2006, and unpublished results). Interestingly, strong induction of the σ^E response was also observed in a *V. cholerae hfq* mutant (Ding *et al*., 2004). Based on the activation of multiple σ^E-dependent genes, the Δ*hfq* strain appears to experience chronic envelope stress which

would ultimately change outer membrane properties. In summary, we suggest that the multiple phenotypes of the *hfq* mutant on motility and adherence, and an apparent chronic cell envelope stress in *Salmonella* all contribute to the observed reduced invasiveness of the *hfq* mutant.

A comparison of the *hfq* phenotypes that relate to virulence of *Salmonella* and other previously studied pathogenic bacteria reveals interesting similarities yet also major differences. Hfq mutants of the rather closely related species, *V. cholerae* and *P. aeruginosa*, are severely attenuated for virulence in mice (Sonnleitner *et al*., 2003; Ding *et al*., 2004). In contrast, *hfq* mutants of *L. monocytogenes* and *L. pneumophila* show only mild virulence defects in Balb/c mice and an amoeba infection model respectively (Christiansen *et al*., 2004; McNealy *et al*., 2005). A mouse virulence defect was also described for the *B. abortus hfq* mutant, although Hfq did not appear to affect spleen colonization *per se*, but rather the survival and/or persistence in this organ (Robertson and Roop, 1999). Survival in macrophages was investigated for *L. pneumophila*, *L. monocytogenes* and *B. abortus*, and the effects of the respective *hfq* mutations were comparable to those described here for *Salmonella*, although the *B. abortus hfq* was affected in long-term macrophage survival (Robertson and Roop, 1999; Christiansen *et al*., 2004; McNealy *et al*., 2005). Thus far, *L. monocytogenes* is the only other species for which an *hfq* mutant has been studied with respect to non-phagocytic cell invasion, and unlike *Salmonella*, the *L. monocytogenes hfq* mutant was found to be fully invasive (Christiansen *et al*., 2004). Also in contrast to the *Salmonella hfq* mutant, the assembly of functional pili and secretion of cholera toxin was not affected in the *hfq* mutant of *V. cholerae* (Ding *et al*., 2004). In light of the variability and diversity of Hfq function(s) in virulence among these pathogens, the clear loss of SPI1 expression and the secretion phenotype shown here for *Salmonella* provide an excellent basis to dissect the mechanisms of Hfq functions in a well-characterized model pathogen.

Analyses of protein patterns on one- and two-dimensional gels showed that the expression of a large number of *Salmonella* genes is affected by Hfq. Classification of these genes according to the genome annotation of *Salmonella* LT2 (McClelland *et al*., 2001) shows that the encoded proteins belong to diverse functional categories (Table 2). The increase of GlpK and GlpQ in the *hfq* mutant is currently unexplained, but might indicate changes in glycerophospholipid metabolism (note that the *glpK* and *glpQ* genes are not linked). Other pronounced changes include OMPs such as OmpD, the flagellin FliC, and numerous periplasmic proteins. Given that Hfq has recently been in the spotlight as a small RNA-binding protein (Valentin-Hansen *et al*., 2004), the altered periplasm of Δ*hfq* cells is of particular interest. Specifically, the ~200 nt GcvB RNA of *E. coli* as well as its *Yersinia pestis* homologue was shown to negatively regulate the periplasmic proteins, OppA, DppA and GltI (Urbanowski *et al*., 2000; McArthur *et al*., 2006), which all accumulate to higher levels in the Δ*hfq* strain (Fig. 3B). The molecular mechanism of GcvB action in these two species remains unknown, but OppA was found to strongly accumulate in an *E. coli* Δ*hfq* mutant (Ziolkowska *et al*., 2006). Moreover, GcvB co-immunoprecipitates with *E. coli* Hfq (Zhang *et al*., 2003), suggesting that this protein mediates GcvB binding to *trans*-encoded target mRNAs. As the *gcvB* gene is conserved and expressed in *Salmonella* (Urbanowski *et al*., 2000; C.M. Sharma and J. Vogel, unpublished), it is tempting to speculate that the high levels of OppA, DppA and GltI observed here results from a loss of GcvB-mediated mRNA repression in the absence of Hfq.

Of the 71 proteins with altered levels in the *hfq* mutant (Table 2), five have no known homologues in *E. coli* (SipA, SipC, STM1254, STM1328 and STM2494). Of the remaining 66, seven overlap with previously published Hfq-associated *E. coli* mRNAs, i.e. CspD, Dps, LppA, LppB, OmpX, RplL and YfiA (Zhang *et al*., 2003). Notably, the majority of these are proteins whose expression was reduced, suggesting Hfq might function to stabilize their mRNAs, either directly or indirectly by promoting efficient translation.

One of the most drastic changes we observed in the absence of Hfq is the increase in OmpD levels (Fig. 7A). OmpD is a *Salmonella*-specific porin, and is the most abundant protein in the outer membrane under standard growth conditions. Together with the other major porins, OmpC and OmpF, it accounts for ~$1–2 \times 10^5$ porins per cell (Santiviago *et al*., 2003). Expression of this porin is regulated primarily at the level of transcription, is subject to catabolite repression, and the *ompD* promoter is repressed by low pH. However, post-transcriptional activation of OmpD expression under anaerobiosis has also been reported, and shown to depend on the global transcription regulator, FNR (Santiviago *et al*., 2003), whereas bile appears to repress *ompD* post-transcriptionally (Prouty *et al*., 2004). Despite its abundance, the physiological roles of OmpD remain unclear. Unlike the other two major porins, OmpC and OmpF, OmpD is not regulated by osmolarity (Santiviago *et al*., 2003). The only physiological role of OmpD elucidated thus far is its requirement for the efficient efflux of the toxic compound, methyl viologen (Santiviago *et al*., 2002). In contrast, possible contributions of OmpD to *Salmonella* pathogenicity remain a matter of debate. Two LD_{50} studies of *Salmonella* wild-type and *ompD* mutant strains in mice yielded inconsistent results (Dorman *et al*., 1989; Meyer *et al*., 1998). Other studies postulated a requirement of OmpD for adherence to human macrophages and intestinal epithelial cell lines (Negm and Pistole, 1998; Hara-

Kaonga and Pistole, 2004). Intriguingly, the presence of *ompD* correlates with the ability of *Salmonella* serovars to grow in alternative, non-human hosts. Santiviago *et al*. (2003) identified *ompD* in all *Salmonella* serovars that have multiple mammalian hosts, e.g. *S. typhimurium* and *Salmonella enteritidis*, but its absence in *Salmonella typhi*, which is restricted to humans.

In any case, the conservation of *ompD* argues for an important function, and the data obtained here implicate Hfq as a novel factor of *ompD* mRNA regulation at the post-transcriptional level. Hfq binds with high affinity and presumably at multiple sites to the *ompD* 5′ UTR *in vitro*, and its absence stabilizes the *ompD* mRNA *in vivo*. Interestingly, both these observations bear striking similarity to the previously reported Hfq-dependent control of OmpA, the major OMP of *E. coli*, i.e. increased *ompA* mRNA stability in *E. coli hfq* mutants, and Hfq binding of this messenger (Vytvytska *et al*., 1998; Udekwu *et al*., 2005). Importantly, it has recently become clear that one role of Hfq in this regulation may be the promotion of MicA function, an Hfq-dependent sRNA that represses *ompA* mRNA translation in stationary phase (Rasmussen *et al*., 2005; Udekwu *et al*., 2005). There is ample evidence of fine tuning of *E. coli* OMP expression by Hfq-dependent sRNAs. In addition to MicA, six *E. coli* sRNAs, namely MicC, MicF, OmrA/B, RseX and RybB, were shown to mediate repression of single or multiple OMP-encoding mRNAs (reviewed in Guillier *et al*., 2006; Vogel and Papenfort, 2006). Similarly, unpublished results from our laboratory show that *ompD* mRNA is acted upon by the *Salmonella* homologues of the *E. coli* sRNAs, MicC and RybB. In addition, the SPI1-endoded 80 nt InvR RNA negatively regulates *ompD* expression. As all these sRNAs are Hfq-dependent, we hypothesize that the post-transcriptional effect of Hfq on *ompD* expression reported here is mediated by Hfq-dependent regulatory sRNAs.

In summary, this study implicates Hfq as a major post-transcriptional regulator of *Salmonella* gene expression. Unlike other abundant global regulatory proteins, e.g. Fis, IHF, H-NS and HU (Harrison *et al*., 1994; Wilson *et al*., 2001; Schechter *et al*., 2003; Mangan *et al*., 2006), Hfq is primarily known to act at the RNA level. Interestingly, similar to H-NS that recognizes AT-rich sequences in DNA, Hfq binds to AU-rich RNA species. It has recently been proposed that H-NS repression serves to silence newly acquired genomic loci with different GC-content, thus avoiding detrimental consequences from unregulated expression of these genes following their uptake by *Salmonella* (Lucchini *et al*., 2006; Navarre *et al*., 2006). Experiments are currently underway to determine if Hfq plays a similar role by specifically acting on AU-rich mRNAs of newly acquired genes. If so, Hfq may again turn out to be the 'host factor' as which it was originally described 40 years ago (Franze de Fernandez *et al*., 1968).

Experimental procedures

Oligonucleotides

The complete list of DNA oligonucleotides used for cloning and as probes in hybridization is provided as supplementary material (Table S2).

Bacterial strains, media and growth conditions

Growth in LB broth or on LB plates at 37°C was used throughout this study unless stated otherwise. SOC medium was used to recover transformants after heat shock or electroporation and prior to plating. Green plates for screening against lysogens in P22 transductions were prepared as described (Sternberg and Maurer, 1991). For SPI1 induction, cultures were inoculated in 5 ml LB containing 0.3 M NaCl in 15 ml Falcon tubes with a tightly closed lid. Cultures were incubated for 12 h at 37°C with shaking. To determine growth rates of strains, the inoculated culture was split in 12 aliquots and each aliquot was opened only once to measure OD_{600}. Antibiotics (where appropriate) were applied at the following concentrations: 100 μg ml^{-1} ampicillin, 50 μg ml^{-1} kanamycin, 20 μg ml^{-1} chloramphenicol. For HilA expression from plasmid pCH112, cultures were grown to an OD_{600} of 1 and induced with L-arabinose in a final concentration of 0.05% until cells reached an OD_{600} of 2.

The bacterial strains used in this study are listed in Table 4. Chromosomal mutagenesis of *Salmonella* SL1344 followed the protocol described by Datsenko and Wanner (2000) with few modifications. Strain JVS-00008, which carries plasmid pKD46, was grown in LB at 28°C complemented with ampicillin and 0.2% L-arabinose to an OD_{600} of 0.5. Cells were collected by centrifugation (2 min, 11 000 *g*), washed three times with ice-cold H_2O, and dissolved in 1/100 of the original culture volume. PCR products of marker genes (50 μl standard reactions) were DpnI-treated for 30 min at 37°C, and purified on Macherey-Nagel spin columns (NucleoSpin Extract II). One-fifth of the 25 μl column eluate (in water) was used for transformation. Forty microlitres of competent cells was mixed with the purified PCR product in a chilled cuvette (0.1 cm electrode gap) and electroporated (18 kV cm^{-1}). Subsequently, 1 ml of pre-warmed SOC medium was added, and cells were recovered by incubation for 1 h at 37°C before selection on LB agar plates with the appropriate antibiotics. All mutations were moved to a fresh SL1344 background by phage P22 transduction.

To construct the *hfq* deletion strain, the *cat* chloramphenicol-resistance gene was amplified from plasmid pKD3 with oligonucleotides JVO-0252 and JVO-0318. Strains *hfq*-C and *hfq*^{HIS} were constructed in the same way, using primer pairs JVO-0252/JVO-0253 and JVO-0252/JVO-0319 respectively. Mutants were verified by colony PCR using primers JVO-0076/JVO-0077. For removal of the *cat* gene the Δ*hfq* strain was transformed with the FLP helper plasmid pCP20 (for detailed procedure, see Datsenko and Wanner, 2000). The *ompD* deletion strain was constructed by replacing the gene with a kanamycin marker gene amplified from pKD4 with primers JVO-0817/JVO-0818. The deletion mutant was verified using oligonucleotides JVO-0818/0819. Chromosomal FLAG-tagging (3xFLAG) of *hilA* was carried out as described in Uzzau *et al*. (2001), using primers JVO-

Table 4. Strains and plasmids used in this study.

Strain	Relevant markers/genotype	Reference/source
S. typhimurium		
SL1344	Str^R *hisG rpsL xyl*	Hoiseth and Stocker (1981), provided by D. Bumann, MPI-IB Berlin
JVS-00255	SL1344 Δ*hfq*::Cm^R	This study
JVS-00177	SL1344 *hfq*-6HIS-Cm^R	This study
JVS-00179	SL1344 *hfq*-Cm^R	This study
JVS-00756	SL1344 *hilA*-3xFLAG-Km^R	This study
JVS-00405	SL1344 Δ*spi1* (Km^R cassette removed)	S. Pätzold, MPI-IB Berlin (unpublished)
JVS-00748	SL1344 Δ*rpoS*::Km^R	Kowarz *et al.* (1994)
JVS-00584	SL1344 Δ*hfq* (Cm^R cassette removed)	This study
JVS-00735	SL1344 Δ*ompD*::Km^R	This study
JVS-00822	SL1344 Δ*hfq*::Cm^R/Δ*ompD*::Km^R	This study
E. coli		
TOP10	*mcr*A Δ(*mrr-hsd*RMS-*mcr*BC) Φ80*lacZ*ΔM15 Δ*lac*X74 *deo*R *rec*A1 *ara*D139 Δ(*ara-leu*)7697*gal*U *gal*K *rps*L *end*A1 *nup*G	Invitrogen
TOP10F′	F′{*lac*I^q Tn*10* (Tet^R)} *mcr*A Δ(*mrr-hsd*RMS-*mcr*BC) Φ80*lacZ*ΔM15 Δ*lac*X74 *deo*R *rec*A1 *ara*D139 Δ(*ara-leu*)7697*gal*U *gal*K *rps*L *end*A1 *nup*G	Invitrogen
ER 2566	F$^-$ λ$^-$ *fhuA*2 [*lon*] *ompT lacZ::T7 gene*1 *gal sulA*11 Δ(*mcrC-mrr*) 114::*IS10 R*(*mcr*-73:: *miniTn*10)2 *R*(*zgb*-210::*Tn*10) (*Tet^S*) *end*A1 [*dcm*]	New England Biolabs

0837/0838 on template pSUB11. The chromosomal tagging was verified by PCR with oligonucleotides JVO-839/840, and sequencing of the PCR product.

Plasmids

Plasmids used, and details of their construction are described in Table 5. Maps of selected plasmids are provided in the supplementary material (Fig. S7). *E. coli* TOP10 and TOP10F′ strains were used for cloning. All plasmids were purified using the Machery-Nagel Plasmid QuickPure Kit. To transform *Salmonella* strains, these were rendered competent using the same protocol as described above, except that cells were cultured at 37°C without arabinose.

Control plasmids based on pZE12-luc were constructed as follows: to lower the copy number of plasmid pZE12-luc, the ColE1 origin was swapped to pSC101* by inserting the AvrII-SacI fragment of plasmid pZS*24-MCS1, resulting in pVP003. To obtain plasmid designated pVP012, a low-copy version of control plasmid pJV968-1, the 1.5 kb '*lacZ*' XbaI/XhoI fragment of the latter was introduced into pVP003 by the same enzymes. Note that these plasmids lack the P_{LlacO} promoter region of pZE12-luc, hence the insert is not transcribed.

To express Hfq-6HIS under control of its own promoter, low-copy vector pVP003 was digested with XhoI/XbaI and ligated to a PCR product obtained with the primer pair JVO-0370/0182 (JVO-0370 binds 1014 bp upstream of the *hfq* open reading frame (ORF) in *miaA* while JVO-182 adds a 6HIS-tag sequence followed by a stop codon to the last codon of *hfq*). For clarity, the obtained plasmid, pVP004-1, is designated in figures as pStHfq-6H.

Control plasmid pJV300 was obtained by ligation of a pZE12-luc derived PCR product. The −1 site of promoter P_{LlacO} is fused to the second position of the XbaI site (which is destroyed upon cloning). Transcription from the P_{LlacO} promoter now yields a ~50 nt nonsense transcript derived from the *rrnB* terminator on pJV300. To obtain a low-copy version of this plasmid, the origin was changed to pSC101* as described above, yielding pVP009.

To clone transcriptional GFP fusions, a PCR fragment was amplified from plasmid pJV859-8 (GFP expression plasmid) using oligonucleotides JVO-0888/pZE-XbaI. JVO-0888 introduces stop codons after a XhoI and NheI site in all three ORFs, a ribosome binding site, a 7 bp spacer, and the sequence of the first six amino acids (aa) of the GFP coding region with a silent mutation at position 6 (T(r)C) to destroy the GFP internal NheI site. Plasmid pJV859-8 was cut XhoI (removing the promoter region, the ribosome binding site and the sequence for the first 142 aa of GFP), gel-purified, and the vector backbone ligated to the PCR fragment digested with the same enzyme. Due to the internal XhoI site in the GFP coding region (cuts in the sequence after aa 142) this leads to a promoterless transcriptional fusion plasmid (used as a negative control plasmid in transcriptional fusion experiments). The resulting plasmid was designated pAS0046. For construction of the *ompC-gfp* transcriptional fusion plasmid pAS0057-1 and the *ompD-gfp* transcriptional fusion plasmid pAS0058-1, pAS0046 was digested with AatII/NheI and ligated to PCR products amplified with primer pairs JVO-0801/0805 and JVO-0806/0807 respectively, cut with the same enzymes.

For translational *ompD::gfp* and *ompC::gfp* fusions, PCR fragments of oligonucleotides JVO-0726/0802 and JVO-0717/0801 respectively, were inserted into plasmid pJV859-8 by AatII/NheI cloning, yielding plasmids pVP019 (GFP fusion to 15th aa of OmpD) and pVP020 (GFP fusion to 12th aa of OmpC) respectively.

To overexpress and purify *Salmonella* Hfq protein, the *hfq* coding region was amplified with primer pair JVO-0078/0084. The PCR product was SapI digested and ligated to the N-terminal fusion vector pTYB11 cut with enzymes SapI/SmaI, yielding plasmid pAS009.

P22 transduction

P22 lysates were prepared from soft agar plate lysates of donor strains using P22 phage HT/105-1 by standard procedures. Transductions were performed as described by Sternberg and Maurer (1991) using P22 phage HT/105-1 and

Table 5. Plasmids used in this study.

Name	Fragment	Comment	Origin/marker	Reference
pJV300		ColE1 control plasmid, based on pZE12-luc, P_{LlacO} promoter transcribes a ~50 nt nonsense transcript (*rrnB* terminator)	ColE1/Amp^R	This study
pJV859-8	P_{LtetO}-*gfp*	GFP control plasmid (constitutive GFP expression)	pSC101*/Cm^R	Urban and Vogel (2006)
pJV968-1	'*lacZ*'	ColE control plasmid, carries 1.5 kb internal *lacZ* fragment	ColE1/Amp^R	Vogel *et al.* (2004)
pVP003	*luc*	Control plasmid; low-copy version of pZE12-luc	pSC101*/Amp^R	This study
pVP004-1	*Hfq*-6HIS	pStHfq-6H, expresses a HIS-tagged Hfq under control of its own promoter; includes 1014 bp upstream of *hfq* reading frame	pSC101*/Amp^R	This study
pVP009		Low-copy version of control plasmid pJV300	pSC101*/Amp^R	This study
pVP012	'*lacZ*'	Low-copy version of control plasmid pJV968-1	pSC101*/Amp^R	This study
pVP019	*ompD::gfp*	*ompD* translational GFP fusion plasmid		This study
pVP020	*ompC::gfp*	*ompC* translational GFP fusion plasmid		This study
pAS009	*hfq*	Overexpression plasmid of *Salmonella hfq* (cloned in N-terminal fusion vector pTYB 11)	M13/AmpR	This study
pAS0046	*gfp*	Transcriptional fusions plasmid, based on pJV859-8	pSC101*/Cm^R	This study
pAS0047-2	P_{hilA} -*gfp*	*hilA* transcriptional GFP fusion plasmid	pSC101*/Cm^R	This study
pAS0057-1	P_{ompC} -*gfp*	*ompC* transcriptional GFP fusion plasmid	pSC101*/Cm^R	This study
pAS0058-1	P_{ompD} -*gfp*	*ompD* transcriptional GFP fusion plasmid	pSC101*/Cm^R	This study
pJU004		GFP control plasmid	pSC101*/Cm^R	Urban and Vogel (2006)
pBAD/*Myc*-His A		pBAD control plasmid	pBR322/Amp^R	Invitrogen
pZS*24-MCS1	*luc*	General expression vector	pSC101*/Km^R	Lutz and Bujard (1997)
pBAD 18-Kn		pBAD control plasmid	pBR322/Km^R	Guzman *et al.* (1995)
pCH112	P_{BAD}-*hilA*-*Myc-His*	pHilA; *hilA* ORF in pBAD/*Myc*-His	pBR322/Amp^R	Lostroh *et al.* (2000)
pKD3		Template for mutant construction; carries chloramphenicol cassette	oriRγ/Amp^R	Datsenko and Wanner (2000)
pKD4		Template for mutant construction; carries kanamycin cassette	oriRγ/Amp^R	Datsenko and Wanner (2000)
pKD46	P_{araB}-γ -β-*exo*	Temperature sensitive *red* recombinase expression plasmid	oriR101/Amp^R	Datsenko and Wanner (2000)
pCP20		Temperature sensitive FLP recombinase expression plasmid	oriR101/Amp^R, Cm^R	Datsenko and Wanner (2000)
pSUB11		Template for mutant construction; 3xFLAG linked to a Km^R cassette	R6KoriV, Amp^R	Uzzau *et al.* (2001)
pZA31-luc	*luc*	General expression plasmid	p15A/Cm^R	Lutz and Bujard (1997)
pZE12-luc	*luc*	General expression plasmid	ColE1/Amp^R	Lutz and Bujard (1997)
pTYB-11		Protein overexpression plasmid (IMPACT-CN system)	M13/AmpR	NEB

further purified on Green plates. For unknown reasons, we were not able to prepare lysates of the *hfq* deletion mutant, hence Δ*hfq*/P22 lysates were prepared from this strain upon complementation with plasmid pVP004. Transformants were verified by PCR.

Gentamicin protection (invasion) assays

The invasion assay was performed as described in Isberg and Falkow (1985). HeLa cells (ATCC CCL2) were seeded in RPMI medium (Gibco), supplemented with 10% FCS, 2 mM L-glutamine, 1 mM sodium pyruvate, 50 μM β-mercaptoethanol, and containing 10 μg ml^{-1} penicillin and streptomycin in 12 well plates with a density of 1×10^5 per well the day before or 0.5×10^5 per well 2 days before infection respectively. At the day of infection HeLa cells reached a density of $1–2 \times 10^5$. When seeded 2 days before infection medium was changed the day before the assay was performed. One hour prior to infection medium was changed to RPMI containing no antibiotics.

Bacterial cultures were inoculated 1/100 from overnight cultures into fresh medium. For experiments with cultures in early stationary phase cultures were grown in LB (with 50 μg ml^{-1} ampicillin if indicated) at 37°C, 220 rpm, with normal aeration. For experiments with SPI1-induced bacteria, cultures were grown for 12 h in 15 ml Falcon tubes containing 5 ml LB/0.3 M NaCl (with 50 μg ml^{-1} ampicillin if indicated) at 37°C, 220 rpm, under limited oxygen conditions.

HeLa cells were infected with a moi of 10 with 100 μl of bacterial suspension in RPMI medium. The suspension was plated in serial dilutions on LB plates and incubated o/n at 37°C for determination of the input.

Bacterial cells were centrifuged (37°C, 250 *g*, 10 min) onto the HeLa cell monolayer, followed by a 50 min incubation step at 37°C in an atmosphere containing 5% CO_2. One hour after infection medium was changed to RPMI (containing 50 μg ml^{-1} gentamicin) to kill non-invasive bacterial cells. Incubation was carried on for additional 60 min. After 2 h of infection medium was changed for the 6 h time point to RPMI containing 10 μg ml^{-1} gentamicin and incubation carried on for additional 4 h. For the 2 h time point cells were washed two times in PBS buffer and collected by scraping HeLa cells from the bottom of each well in PBS/0.1% Triton X-100. Dilutions in PBS were plated on LB plates and incubation carried out o/n at 37°C. Six hours after incubation samples for the second time point are treated the same way. Rate of invasion was calculated according to recovered bacterial cells related to the input. Experiments were carried out in duplicates.

Macrophage survival assay

Infection of macrophage cell lines was performed as described in Thompson *et al.* (2006). The macrophage cell line used was RawB, a derivative of Raw 264.7 (ATCC TIB-71). Macrophages were seeded in 12 well plates 1 day prior to infection at 1×10^5 cells per well. Next day bacteria were harvested for infection at early stationary growth phase (OD_{600} ~2–3). Macrophages were infected with a moi of 1. Bacterial cells were centrifuged (37°C, 250 *g*, 10 min) onto the macrophages, followed by a 20 min incubation step at 37°C in an atmosphere containing 5% CO_2. Thirty minutes in total after infection medium was changed to RPMI (containing 50 μg ml^{-1} gentamicin) to kill non-invasive bacterial cells. Incubation was carried on for additional 30 min. Medium was changed for the 4 and 24 h time points to RPMI containing 10 μg ml^{-1} gentamicin and incubation carried on for additional 3 or 23 h respectively. The number of intracellular bacteria was determined 1, 4 and 24 h after infection and given in per cent related to the input. Experiments were carried out in triplicates and data are representative of two independent experiments.

HeLa cell adhesion assay

The adhesion assay was performed as described in Hara-Kaonga and Pistole (2004). In brief, bacteria were grown for 12 h under SPI1-inducing conditions. One hundred microlitres of HeLa cells (5×10^5 per ml in RPMI medium) was incubated with 100 μl of bacterial suspension in RPMI medium for 60 min with a moi of 50 at 37°C in 96 well plates. Infections were carried out in triplicates. Non-adherent bacteria were removed by washing cells 4× with 200 μl PBS at 400 *g*. Each sample was resuspended in 50 μl PBS/4% formaldehyde. Each well was sampled three times, and 10 HeLa cells were analysed per sampling. Cells were counted with 1000× magnification using an Eclipse 50i microscope (Nikon).

In a further adhesion assay similar to the macrophage assay by Buchmeier and Heffron (1989), 1×10^5 HeLa cells per well ml^{-1} were infected with a moi of 10 for 30 min with bacteria grown to early stationary phase (bacteria were spun for 10 min on the HeLa cell monolayer followed by 20 min incubation at 37°C). Each well was washed three times with 1 ml PBS and cells were collected by scraping HeLa cells from the bottom of each well in PBS/0.1% Triton X-100. Dilutions in PBS were plated on LB agar and incubation carried out o/n at 37°C. Rate of adhesion and invasion (determined in parallel as above) was calculated according to recovered bacterial cells related to the input. Experiments were carried out in triplicates.

Animal infections

Bacterial cultures for mice infections were grown in L-broth to early stationary phase (OD_{600} of 2–3), harvested by centrifugation, and diluted to the appropriate cfu ml^{-1} in sterile PBS for infections. For peroral infections, strains were resuspended at 10^9 cfu ml^{-1}, and 0.1 ml of the resuspensions (~10^8 bacteria) used to infect groups of five Balb/c mice per strain. The total infective dose was determined in parallel by plating dilutions to agar plates with or without selection, where appropriate. After 72 h, the mice were sacrificed by euthanization in a CO_2 chamber, and spleens were removed for determination of organ bacterial loads. Isolated spleens were washed once in 70% ethanol, once in PBS and homogenized in 1 ml of PBS. Cell resuspensions were lysed by addition of 1 ml of 0.2% Triton X-100 in deionized, distilled water and incubation at room temperature for 15 min. Dilutions of the cell lysates were plated to agar plates with or without antibi-

otic selection where appropriate for enumeration of total intracellular bacteria. Intraperitoneal infections were performed by injection of 0.1 ml of a 1:1 mixture of bacterial suspensions of 2×10^6 cfu ml^{-1} of wild-type and mutant strains into the peritoneal space, yielding a final infective dose of approximately 10^5 cfu ml^{-1} for each strain per animal. Forty-eight hours after the infections, mice were sacrificed and spleens isolated and processed as above. The CI was calculated from the ratios of total input and recovered wild-type and chloramphenicol-resistant Δ*hfq* cfu as previously described (Shea *et al*., 1996).

Motility assay

Cultures were diluted 1/100 into fresh media and incubated at 37°C/220 rpm to an OD_{600} of 2. One microlitre of culture was inoculated in motility agar plates (LB/0.3% agarose), followed by incubation for 4 h at 37°C.

Whole cell protein fractions

Culture samples were taken according to 1 OD_{600}. Samples were spun 2 min at 16 100 *g* at 4°C. The cell pellet was resuspended in 1× sample loading buffer (1× SLB; Fermentas) to a final concentration of 0.01 OD μl^{-1}. Samples were heated 5 min at 95°C. For small and large SDS-PAGE 0.1 OD and 0.2 OD, respectively, were loaded per lane.

Secreted protein fractions

The protocol for extraction of secreted protein fractions was modified from the protocol described in Kaniga *et al*. (1995). Culture samples were taken either from regular LB cultures at OD 2 or after 12 h of growth or after 12 h of growth in SPI1-induction media, and spun 20 min at 16 100 *g* at 4°C. Proteins from the supernatant were precipitated by adding 25% TCA to a final concentration of 5% followed by 20 min centrifugation at 16 100 *g*, 4°C. The pellet was washed 2× in ice-cold acetone and air dried. The pellet was resuspended in 1× SLB to a final concentration of 1 OD/10 µl. Samples were heated 5 min at 95°C. For small and large SDS-PAGE 1 OD and 2 OD, respectively, were loaded per sample.

Periplasmic protein fractions

Periplasmic proteins were extracted following the cold osmotic shock procedure described by Neu and Heppel (1965). Overnight cultures were inoculated 1/100 in fresh media and grown to an OD_{600} of 2. Cells were harvested (30 min, 4000 *g*, 4°C) and the pellet was resuspended at room temperature in 'shock buffer' (30 mM Tris-HCl, pH 8.0, 20% sucrose). EDTA, pH 8.0 was added at a final concentration of 1 mM. Cells were incubated for 10 min at room temperature with occasional shaking. Cells were collected by centrifugation (30 min, 4000 *g*, 4°C) and the pellet resuspended in 10 ml ice-cold 5 mM $MgSO_4$. After incubation for 10 min with occasional shaking in an ice-water bath, the suspension was centrifuged as mentioned above. The supernatant is the cold osmotic shock-fluid.

Membrane fractions

The total membrane protein fraction was extracted essentially as described (Matsuyama *et al*., 1984). Culture samples were taken at OD_{600} of 2 (4 OD total) and spun 20 min at 16 100 *g* at 4°C. Pellets were washed 1× in 2 ml 10 mM phosphate buffer (pH 7.2). Pellets were resuspended in 0.5 ml of the same buffer. Cells were disrupted by sonication on ice (cycle duty 80%, tip limit 9, four cycles of 30 s with 1 min break on ice). The supernatant was cleared of unbroken cells by centrifugation for 10 min at 1400 *g*, 4°C. Cell envelopes were recovered by centrifugation of the supernatant for 30 min at 16 100 *g*, 4°C. After resuspending the pellet in 2 ml phosphate buffer containing 2% Triton X-100 the samples were incubated for 30 min at 37°C. The insoluble fraction was recovered by 30 min centrifugation at 16 100 *g* at room temperature. After one wash in 2 ml phosphate buffer followed by 5 min centrifugation at 16 100 *g* the pellet was resuspended in 50 µl phosphate buffer (results in approximately 100 µg in 50 µl). Five microlitres per sample was separated on 10% SDS-PAGE.

Western blot

Commercially available antibodies and antisera used in this study are listed in Table S3. 0.01 or 0.02 OD and 0.1 or 0.2 OD whole cell and secreted protein fractions, respectively, were separated via SDS-PAGE. Proteins were blotted for 60 min at 100 V at 4°C in a cable tank blotter (Peqlab) onto PVDF (Perkin Elmer) membrane in transfer buffer (25 mM Tris base, 190 mM Glycin, 20% Methanol). Blots were rinsed 1× in $TBST_{20}$ buffer (20 mM Tris base, 150 mM NaCl, 0.1% Tween 20). Membranes were blocked for 1 h in 10% dry milk in $TBST_{20}$. Hybridization as follows: appropriate antisera or antibodies (in 3% BSA, $TBST_{20}$; see Table S3 for dilutions) for 1 h at room temperature, 5 × 6 min wash in $TBST_{20}$, α-Rabbit-HRP or α-mouse-HRP (1:5000 in 3% BSA in $TBST_{20}$) for 1 h at room temperature, 6 × 10 min wash in $TBST_{20}$. Blots were developed using Western Lightning (Perkin Elmer) in a Fuji LAS-3000.

Two-dimensional gel analysis and protein identification

Sample preparation from *Salmonella* cultures at the growth phases given in the respective figure legends, analysis by high-resolution two-dimensional electrophoresis, protein staining, and peptide mass fingerprinting, were performed at the MPI-IB protein analysis core facility (http://info.mpiib-berlin.mpg.de/jungblut/) according to previously published standard protocols (Jungblut and Seifert, 1990; Klose and Kobalz, 1995; Doherty *et al*., 1998; Jungblut *et al*., 2000).

Protein quantification by fluorescent stain

Cultures of the wild-type, the *hfq* mutant, the *ompD* mutant, and the *hfq/ompD* double mutant strain were grown with aeration at 37°C, 220 rpm to OD 2. Total protein samples corresponding to 0.1 OD culture were separated on SDS-PAGE (15% gel). Gels were stained with Sypro Ruby (Bio-Rad) following the manufacture's protocol. Protein levels

were analysed using the fluorescence mode of a phosphorimager (Phosphorimager, FLA-3000 Series, Fuji) using a 473 nm laser and filter O58. Band intensities were quantified with AIDA software (Raytest, Germany).

Protein overexpression and purification

Overexpression and purification of *Salmonella* Hfq was carried out as published for *E. coli* Hfq (Møller *et al*., 2002) using the IMPACT (Intein Mediated Purification with Affinity Chitin-binding Tag)-CN system (New England Biolabs) according to the manufacture's protocol. Strain ER 2566 carrying plasmid pAS009 was grown to OD of 0.5, and Hfq expression was induced by addition of IPTG (final concentration of 0.5 mM). Following growth for 15 h at 15°C, cells were disrupted using a French press (three passages, 1000 PSI). On-column cleavage of the Hfq moiety was carried out for 24 h at room temperature. The Hfq protein eluate was dialysed against a buffer containing 125 mM NaCl, 12 mM Tris/HCl pH 7.6, 0.5 mM EDTA and concentrated in Vivaspin columns.

Stability experiments, RNA isolation and Northern detection

Overnight cultures were diluted 1/100 in fresh medium and grown to exponential (OD 0.3) and early stationary phase (OD 2). Rifampicin was added to a final concentration of 500 μg ml^{-1}. Incubation was continued at 37°C, 220 rpm, and aliquots (5 ml for OD 0.3; 1.7 ml for stationary phase) were withdrawn prior to or 1, 2, 4, 8, 16 and 32 min after rifampicin addition, mixed with 0.2 vol. of stop solution (5% water-saturated phenol, 95% ethanol), and snap-frozen in liquid nitrogen. After thawing on ice, bacteria were pelleted by centrifugation (2 min, 16 100 *g*, 4°C), and RNA was isolated using the Promega SV total RNA purification kit as described (Kelly *et al*., 2004). The purified RNA was quantified on a Nanodrop machine (NanoDrop Technologies).

RNA samples (~5 μg) were denatured for 5 min at 95°C in loading buffer containing 95% formamide, separated on 8.3 M urea – 5% polyacrylamide gels (PAGE), and transferred to Hybond-XL membranes (GE Healthcare) by electro-blotting (1 h, 50 V, 4°C) in a tank blotter (Peqlab). Membranes were hybridized at 42°C with gene-specific [^{32}P] end-labelled oligodeoxyribonucleotides, random-labelled PCR fragments, or at 70°C with riboprobes, in Rapid-hyb Buffer (GE Healthcare).

ompC transcripts were detected with a random-labelled ([^{32}P] dCTP; Rediprime II labelling kit, GE Healthcare) PCR fragment generated with primer pair JVO-0717/0719. To detect the *ompD* and *hilA* mRNAs, PCR fragments generated with primer pairs JVO-0751/0934 and JVO-1298/1299, respectively, were *in vitro* transcribed from the T7 promoter (added by primers JVO-0934 and JVO-1299) in the presence of [^{32}P]-α-UTP using Ambion's T7 polymerase Maxiscript kit. Riboprobes were purified over a G50 column. *fliC* and *fljB* transcripts were probed using end-labelled oligodeoxyribonucleotides JVO-1592 and JVO-1595. For normalization of RNA amounts 5S signals were detected using end-labelled oligodeoxyribonucleotide JVO-0322. Following hybridization for 2 h, membranes hybridized with riboprobes were washed at 65°C in three subsequent 15 min steps in SSC (2×, 1× or 0.5×)/0.1% SDS solutions, after rinsing the membrane first in 2× SSC/0.1% SDS. Membranes hybridized with PCR fragments were rinsed in 2× SSC/0.1% SDS, followed by 15 min washes in 2× (65°C), 1× and 0.5× (42°C) SSC/0.1% SDS. For end-labelled oligodeoxyribonucleotides hybridization membranes were rinsed in 5× SSC followed by three wash steps at 42°C in SSC (5×, 1× and 0.5× respectively). Signals were visualized on a phosphorimager (Phosphorimager, FLA-3000 Series, Fuji), and band intensities quantified with AIDA software (Raytest, Germany).

Gel mobility shift assay

The ompD DNA template for *in vitro* transcription with T7 RNA polymerase was generated with the primers JVO-1186/-1058. It starts with a T7 promoter fused to the +1 transcriptional start site of OmpD (mapped with 5′RACE; V. Pfeiffer *et al*., in preparation) at position –69 relative to the *ompD* AUG start codon, and ends with the 39th codon of the *ompD* coding sequence. *In vitro* transcription was performed using the Megascript kit (Ambion, #1333), followed by DNase I digestion (1 unit, 15 min, 37°C). Following extraction with phenol : chloroform : isopropanol (25:24:1 v/v), the RNA was precipitated overnight at –20°C with 1 vol. of isopropanol. RNA integrity was checked on a denaturing polyacrylamide gel. 20 pmol RNA was dephosphorylated with 10 units of calf intestine alkaline phosphatase (New England Biolabs) in a 20 μl reaction at 37°C for 1 h. Following phenol extraction, the RNA was precipitated overnight with ethanol/sodium acetate and 20 μg glycogen. The dephosphorylated RNA was 5′ end-labelled with ^{32}P-γATP (20 μCi), using 1 unit of polynucleotide kinase (New England Biolabs) for 30 min at 37°C in a 20 μl reaction. Unincorporated nucleotides were removed using Microspin™ G-50 Colums (GE Healthcare), followed by purification of the labelled RNA on a denaturing polyacrylamide gel (6%/7 M urea). Upon visualization of the labelled RNA by exposure on a phosphorimager, the RNA was cut from the gel and eluted with RNA elution buffer (0.1 M sodium acetate, 0.1% SDS, 10 mM EDTA) at 4°C overnight, followed by phenol extraction and precipitation as before.

Binding assays were performed in 1× structure buffer (100 mM Tris pH 7, 1 M KCl, 100 mM $MgCl_2$, provided along with RNase T1 from Ambion #2283) as follows: 5′-labelled RNA (0.01 pmol of *ompD* mRNA; final concentration in binding reaction: ~1 nM) and 1 μg of yeast RNA (final concentration: 4.3 μM) were incubated with increasing concentrations of Hfq in 10 μl reactions at 37°C for 15 min. The Hfq dilutions (1, 2, 3.9, 7.8, 15.6, 31.3, 62.5, 125, 250, 500 or 1000 nM; calculated for the Hfq hexamer) were prepared in 1× dilution buffer (1× structure buffer with 1% glycerol, 0.1% Triton X-100). Prior to gel run, the binding reactions were mixed with 3 μl of loading buffer (50% glycerol, 0.5× TBE, 0.2% bromphenolblue), and electrophoresed on native 6% polyacrylamide gels in 0.5× TBE buffer at 300 V at 4°C for 3 h. Gels were dried, and analysed using a phosphorimager (see above).

To synthesize the Hfq-independent *metK* control RNA, a DNA template for T7 RNA polymerase *in vitro* transcription was amplified with primers JVO-1701/1702. The resulting RNA spans the entire 5′ UTR (129 nt) according to the +1 transcriptional start site mapped in Wei and Newman (2002) and 80 bp

of the *metK* coding region. *In vitro* transcription and the labelling reaction were performed as described for *ompD* RNA.

Fluorescence measurements

Strains carrying the GFP fusion plasmids were inoculated from single colonies in 20 ml LB medium supplemented with 20 μg ml^{-1} chloramphenicol and incubated with aeration at 37°C/220 rpm. At the indicated cell density, 3 × 100 μl culture were transferred to a 96 well plate, and fluorescence was measured at 37°C using a VICTOR$^{TM}_3$ machine (1420 Multilable Counter, Perkin Elmer). All experiments were done in triplicates. Plasmid pJV859-8, which expresses GFP from a constitutive P_{LtetO} promoter, served as a control. In transcriptional fusion studies, strains carrying plasmid pAS0046 served as background control, while plasmid pJU004 was used in translational fusion studies. A detailed protocol of fluorescence measurement will be described elsewhere (Urban and Vogel, 2006).

Acknowledgements

We thank Monica Schmid, Ursula Zimny-Arndt and Peter Jungblut (MPI-IB Berlin protein analysis core facility) for 2D gel analysis and peptide identification, and Robert Hurwitz and Ralf Winter (MPI-IB Berlin protein purification core facility) for help with Hfq purification. We are indebted to Michael Kolbe and Vivien Wolter (MPI-IB Berlin), WD Hardt (ETH Zurich) and Regine Hengge (Free University Berlin), for their generous gifts of antisera. We thank Peter Schwerk for help with animal experiments. K.T. was supported by operating funds from the Institut für Mikrobiologie und Tierseuchen, Freie Universität Berlin. Work in the Vogel lab is supported by the Max Planck Society, Germany.

References

Ahmer, B.M., van Reeuwijk, J., Watson, P.R., Wallis, T.S., and Heffron, F. (1999) *Salmonella* SirA is a global regulator of genes mediating enteropathogenesis. *Mol Microbiol* **31:** 971–982.

van Asten, F.J., Hendriks, H.G., Koninkx, J.F., and van Dijk, J.E. (2004) Flagella-mediated bacterial motility accelerates but is not required for *Salmonella* serotype Enteritidis invasion of differentiated Caco-2 cells. *Int J Med Microbiol* **294:** 395–399.

Bajaj, V., Lucas, R.L., Hwang, C., and Lee, C.A. (1996) Co-ordinate regulation of *Salmonella typhimurium* invasion genes by environmental and regulatory factors is mediated by control of *hilA* expression. *Mol Microbiol* **22:** 703–714.

Bang, I.S., Frye, J.G., McClelland, M., Velayudhan, J., and Fang, F.C. (2005) Alternative sigma factor interactions in *Salmonella*: sigma and sigma promote antioxidant defences by enhancing sigma levels. *Mol Microbiol* **56:** 811–823.

Brown, L., and Elliott, T. (1996) Efficient translation of the RpoS sigma factor in *Salmonella typhimurium* requires host factor I, an RNA-binding protein encoded by the *hfq* gene. *J Bacteriol* **178:** 3763–3770.

Buchmeier, N.A., and Heffron, F. (1989) Intracellular survival of wild-type *Salmonella typhimurium* and macrophage-sensitive mutants in diverse populations of macrophages. *Infect Immun* **57:** 1–7.

Carmichael, G.G., Weber, K., Niveleau, A., and Wahba, A.J. (1975) The host factor required for RNA phage Qbeta RNA replication in vitro. Intracellular location, quantitation, and purification by polyadenylate-cellulose chromatography. *J Biol Chem* **250:** 3607–3612.

Chaudhuri, R.R., Khan, A.M., and Pallen, M.J. (2004) coliBASE: an online database for *Escherichia coli*, *Shigella* and *Salmonella* comparative genomics. *Nucleic Acids Res* **32:** D296–D299.

Christiansen, J.K., Larsen, M.H., Ingmer, H., Sogaard-Andersen, L., and Kallipolitis, B.H. (2004) The RNA-binding protein Hfq of *Listeria monocytogenes*: role in stress tolerance and virulence. *J Bacteriol* **186:** 3355–3362.

Cirillo, D.M., Valdivia, R.H., Monack, D.M., and Falkow, S. (1998) Macrophage-dependent induction of the *Salmonella* pathogenicity island 2 type III secretion system and its role in intracellular survival. *Mol Microbiol* **30:** 175–188.

Collazo, C.M., and Galan, J.E. (1996) Requirement for exported proteins in secretion through the invasion-associated type III system of *Salmonella typhimurium*. *Infect Immun* **64:** 3524–3531.

Darwin, K.H., and Miller, V.L. (1999) InvF is required for expression of genes encoding proteins secreted by the SPI1 type III secretion apparatus in *Salmonella typhimurium*. *J Bacteriol* **181:** 4949–4954.

Darwin, K.H., and Miller, V.L. (2000) The putative invasion protein chaperone SicA acts together with InvF to activate the expression of *Salmonella typhimurium* virulence genes. *Mol Microbiol* **35:** 949–960.

Datsenko, K.A., and Wanner, B.L. (2000) One-step inactivation of chromosomal genes in *Escherichia coli* K-12 using PCR products. *Proc Natl Acad Sci USA* **97:** 6640–6645.

Ding, Y., Davis, B.M., and Waldor, M.K. (2004) Hfq is essential for *Vibrio cholerae* virulence and downregulates sigma expression. *Mol Microbiol* **53:** 345–354.

Doherty, N.S., Littman, B.H., Reilly, K., Swindell, A.C., Buss, J.M., and Anderson, N.L. (1998) Analysis of changes in acute-phase plasma proteins in an acute inflammatory response and in rheumatoid arthritis using two-dimensional gel electrophoresis. *Electrophoresis* **19:** 355–363.

Dorman, C.J., Chatfield, S., Higgins, C.F., Hayward, C., and Dougan, G. (1989) Characterization of porin and *ompR* mutants of a virulent strain of *Salmonella typhimurium*: *ompR* mutants are attenuated *in vivo*. *Infect Immun* **57:** 2136–2140.

Ehrbar, K., Mirold, S., Friebel, A., Stender, S., and Hardt, W.D. (2002) Characterization of effector proteins translocated via the SPI1 type III secretion system of *Salmonella typhimurium*. *Int J Med Microbiol* **291:** 479–485.

Eichelberg, K., and Galan, J.E. (1999) Differential regulation of *Salmonella typhimurium* type III secreted proteins by pathogenicity island 1 (SPI-1)-encoded transcriptional activators InvF and *hilA*. *Infect Immun* **67:** 4099–4105.

Ellermeier, C.D., Ellermeier, J.R., and Slauch, J.M. (2005) HilD, HilC and RtsA constitute a feed forward loop that controls expression of the SPI1 type three secretion system regulator *hilA* in *Salmonella enterica* serovar Typhimurium. *Mol Microbiol* **57:** 691–705.

Fang, F.C., Libby, S.J., Buchmeier, N.A., Loewen, P.C., Switala, J., Harwood, J., and Guiney, D.G. (1992) The alternative sigma factor katF (*rpoS*) regulates *Salmonella* virulence. *Proc Natl Acad Sci USA* **89:** 11978–11982.

Franze de Fernandez, M.T., Eoyang, L., and August, J.T. (1968) Factor fraction required for the synthesis of bacteriophage Qbeta-RNA. *Nature* **219:** 588–590.

Franze de Fernandez, M.T., Hayward, W.S., and August, J.T. (1972) Bacterial proteins required for replication of phage Q ribonucleic acid. Purification and properties of host factor I, a ribonucleic acid-binding protein. *J Biol Chem* **247:** 824–831.

Galan, J.E., and Curtiss, R., 3rd (1989) Cloning and molecular characterization of genes whose products allow *Salmonella typhimurium* to penetrate tissue culture cells. *Proc Natl Acad Sci USA* **86:** 6383–6387.

Goto, S., Bono, H., Ogata, H., Fujibuchi, W., Nishioka, T., Sato, K., and Kanehisa, M. (1997) Organizing and computing metabolic pathway data in terms of binary relations. *Pac Symp Biocomput* **00:** 175–186.

Guillier, M., Gottesman, S., and Storz, G. (2006) Modulating the outer membrane with small RNAs. *Genes Dev* **20:** 2338–2348.

Guzman, L.M., Belin, D., Carson, M.J., and Beckwith, J. (1995) Tight regulation, modulation, and high-level expression by vectors containing the arabinose PBAD promoter. *J Bacteriol* **177:** 4121–4130.

Hajnsdorf, E., and Regnier, P. (2000) Host factor Hfq of *Escherichia coli* stimulates elongation of poly(A) tails by poly(A) polymerase I. *Proc Natl Acad Sci USA* **97:** 1501–1505.

Hara-Kaonga, B., and Pistole, T.G. (2004) OmpD but not OmpC is involved in adherence of *Salmonella enterica* serovar typhimurium to human cells. *Can J Microbiol* **50:** 719–727.

Harrison, J.A., Pickard, D., Higgins, C.F., Khan, A., Chatfield, S.N., Ali, T., *et al.* (1994) Role of hns in the virulence phenotype of pathogenic salmonellae. *Mol Microbiol* **13:** 133–140.

Hensel, M., Shea, J.E., Waterman, S.R., Mundy, R., Nikolaus, T., Banks, G., *et al.* (1998) Genes encoding putative effector proteins of the type III secretion system of *Salmonella* pathogenicity island 2 are required for bacterial virulence and proliferation in macrophages. *Mol Microbiol* **30:** 163–174.

Hoiseth, S.K., and Stocker, B.A. (1981) Aromatic-dependent *Salmonella typhimurium* are non-virulent and effective as live vaccines. *Nature* **291:** 238–239.

Humphreys, S., Stevenson, A., Bacon, A., Weinhardt, A.B., and Roberts, M. (1999) The alternative sigma factor, sigmaE, is critically important for the virulence of *Salmonella typhimurium*. *Infect Immun* **67:** 1560–1568.

Isberg, R.R., and Falkow, S. (1985) A single genetic locus encoded by *Yersinia pseudotuberculosis* permits invasion of cultured animal cells by *Escherichia coli* K-12. *Nature* **317:** 262–264.

Jones, A.M., Goodwill, A., and Elliott, T. (2006) Limited role for the DsrA and RprA regulatory RNAs in *rpoS* regulation in *Salmonella enterica*. *J Bacteriol* **188:** 5077–5088.

Jungblut, P.R., and Seifert, R. (1990) Analysis by high-resolution two-dimensional electrophoresis of differentiation-dependent alterations in cytosolic protein pattern of HL-60 leukemic cells. *J Biochem Biophys Methods* **21:** 47–58.

Jungblut, P.R., Bumann, D., Haas, G., Zimny-Arndt, U., Holland, P., Lamer, S., *et al.* (2000) Comparative proteome analysis of *Helicobacter pylori*. *Mol Microbiol* **36:** 710–725.

Kaminski, P.A., Desnoues, N., and Elmerich, C. (1994) The expression of nifA in *Azorhizobium caulinodans* requires a gene product homologous to *Escherichia coli* HF-I, an RNA-binding protein involved in the replication of phage Q beta RNA. *Proc Natl Acad Sci USA* **91:** 4663–4667.

Kaniga, K., Trollinger, D., and Galan, J.E. (1995) Identification of two targets of the type III protein secretion system encoded by the inv and spa loci of *Salmonella typhimurium* that have homology to the *Shigella* IpaD and IpaA proteins. *J Bacteriol* **177:** 7078–7085.

Kelly, A., Goldberg, M.D., Carroll, R.K., Danino, V., Hinton, J.C., and Dorman, C.J. (2004) A global role for Fis in the transcriptional control of metabolism and type III secretion in *Salmonella enterica* serovar Typhimurium. *Microbiology* **150:** 2037–2053.

Kimbrough, T.G., and Miller, S.I. (2000) Contribution of *Salmonella typhimurium* type III secretion components to needle complex formation. *Proc Natl Acad Sci USA* **97:** 11008–11013.

Klein, J.R., Fahlen, T.F., and Jones, B.D. (2000) Transcriptional organization and function of invasion genes within *Salmonella enterica* serovar Typhimurium pathogenicity island 1, including the *prgH*, *prgI*, *prgJ*, *prgK*, *orgA*, *orgB*, and *orgC* genes. *Infect Immun* **68:** 3368–3376.

Klose, J., and Kobalz, U. (1995) Two-dimensional electrophoresis of proteins: an updated protocol and implications for a functional analysis of the genome. *Electrophoresis* **16:** 1034–1059.

Komoriya, K., Shibano, N., Higano, T., Azuma, N., Yamaguchi, S., and Aizawa, S.I. (1999) Flagellar proteins and type III-exported virulence factors are the predominant proteins secreted into the culture media of *Salmonella typhimurium*. *Mol Microbiol* **34:** 767–779.

Kowarz, L., Coynault, C., Robbe-Saule, V., and Norel, F. (1994) The *Salmonella typhimurium* katF (*rpoS*) gene: cloning, nucleotide sequence, and regulation of spvR and spvABCD virulence plasmid genes. *J Bacteriol* **176:** 6852–6860.

Kubori, T., Sukhan, A., Aizawa, S.I., and Galan, J.E. (2000) Molecular characterization and assembly of the needle complex of the *Salmonella typhimurium* type III protein secretion system. *Proc Natl Acad Sci USA* **97:** 10225–10230.

Lee, C.A., and Falkow, S. (1990) The ability of *Salmonella* to enter mammalian cells is affected by bacterial growth state. *Proc Natl Acad Sci USA* **87:** 4304–4308.

Lee, C.A., Jones, B.D., and Falkow, S. (1992) Identification of a *Salmonella typhimurium* invasion locus by selection for hyperinvasive mutants. *Proc Natl Acad Sci USA* **89:** 1847–1851.

Lostroh, C.P., and Lee, C.A. (2001) The *Salmonella* pathogenicity island-1 type III secretion system. *Microbes Infect* **3:** 1281–1291.

Lostroh, C.P., Bajaj, V., and Lee, C.A. (2000) The *cis* requirements for transcriptional activation by HilA, a viru-

lence determinant encoded on SPI-1. *Mol Microbiol* **37:** 300–315.

Lucas, R.L., and Lee, C.A. (2001) Roles of *hilC* and *hilD* in regulation of *hilA* expression in *Salmonella enterica* serovar Typhimurium. *J Bacteriol* **183:** 2733–2745.

Lucchini, S., Rowley, G., Goldberg, M.D., Hurd, D., Harrison, M., and Hinton, J.C. (2006) H-NS mediates the silencing of laterally acquired genes in bacteria. *PLoS Pathog* **2:** 746–752.

Lutz, R., and Bujard, H. (1997) Independent and tight regulation of transcriptional units in *Escherichia coli* via the LacR/O, the TetR/O and AraC/I1-I2 regulatory elements. *Nucleic Acids Res* **25:** 1203–1210.

McArthur, S.D., Pulvermacher, S.C., and Stauffer, G.V. (2006) The *Yersinia pestis gcvB* gene encodes two small regulatory RNA molecules. *BMC Microbiol* **6:** 52.

McClelland, M., Sanderson, K.E., Spieth, J., Clifton, S.W., Latreille, P., Courtney, L., *et al.* (2001) Complete genome sequence of *Salmonella enterica* serovar Typhimurium LT2. *Nature* **413:** 852–856.

McNealy, T.L., Forsbach-Birk, V., Shi, C., and Marre, R. (2005) The Hfq homolog in *Legionella pneumophila* demonstrates regulation by LetA and RpoS and interacts with the global regulator CsrA. *J Bacteriol* **187:** 1527–1532.

Majdalani, N., Vanderpool, C.K., and Gottesman, S. (2005) Bacterial small RNA regulators. *Crit Rev Biochem Mol Biol* **40:** 93–113.

Mangan, M.W., Lucchini, S., Danino, V., Croinin, T.O., Hinton, J.C., and Dorman, C.J. (2006) The integration host factor (IHF) integrates stationary-phase and virulence gene expression in *Salmonella enterica* serovar Typhimurium. *Mol Microbiol* **59:** 1831–1847.

Matsuyama, S., Inokuchi, K., and Mizushima, S. (1984) Promoter exchange between *ompF* and *ompC*, genes for osmoregulated major outer membrane proteins of *Escherichia coli* K-12. *J Bacteriol* **158:** 1041–1047.

Meyer, P.N., Wilmes-Riesenberg, M.R., Stathopoulos, C., and Curtiss, R., 3rd (1998) Virulence of a *Salmonella typhimurium* OmpD mutant. *Infect Immun* **66:** 387–390.

Mills, D.M., Bajaj, V., and Lee, C.A. (1995) A 40 kb chromosomal fragment encoding *Salmonella typhimurium* invasion genes is absent from the corresponding region of the *Escherichia coli* K-12 chromosome. *Mol Microbiol* **15:** 749–759.

Møller, T., Franch, T., Hojrup, P., Keene, D.R., Bachinger, H.P., Brennan, R.G., and Valentin-Hansen, P. (2002) Hfq: a bacterial Sm-like protein that mediates RNA–RNA interaction. *Mol Cell* **9:** 23–30.

Muffler, A., Fischer, D., and Hengge-Aronis, R. (1996) The RNA-binding protein HF-I, known as a host factor for phage Qbeta RNA replication, is essential for *rpoS* translation in *Escherichia coli*. *Genes Dev* **10:** 1143–1151.

Muffler, A., Traulsen, D.D., Fischer, D., Lange, R., and Hengge-Aronis, R. (1997) The RNA-binding protein HF-I plays a global regulatory role which is largely, but not exclusively, due to its role in expression of the sigmaS subunit of RNA polymerase in *Escherichia coli*. *J Bacteriol* **179:** 297–300.

Nakao, H., Watanabe, H., Nakayama, S., and Takeda, T. (1995) *yst* gene expression in *Yersinia enterocolitica* is positively regulated by a chromosomal region that is highly homologous to *Escherichia coli* host factor 1 gene (*hfq*). *Mol Microbiol* **18:** 859–865.

Navarre, W.W., Porwollik, S., Wang, Y., McClelland, M., Rosen, H., Libby, S.J., and Fang, F.C. (2006) Selective silencing of foreign DNA with low GC content by the H-NS protein in *Salmonella*. *Science* **313:** 236–238.

Negm, R.S., and Pistole, T.G. (1998) Macrophages recognize and adhere to an OmpD-like protein of *Salmonella typhimurium*. *FEMS Immunol Med Microbiol* **20:** 191–199.

Neu, H.C., and Heppel, L.A. (1965) The release of enzymes from *Escherichia coli* by osmotic shock and during the formation of spheroplasts. *J Biol Chem* **240:** 3685–3692.

Nickerson, C.A., and Curtiss, R., 3rd (1997) Role of sigma factor RpoS in initial stages of *Salmonella typhimurium* infection. *Infect Immun* **65:** 1814–1823.

Papenfort, K., Pfeiffer, V., Mika, F., Lucchini, S., Hinton, J.C., and Vogel, J. (2006) σ^E-dependent sRNAs of *Salmonella* respond to membrane stress by accelerating global *omp* mRNA decay. *Mol Microbiol* **62:** 1674–1688.

Prouty, A.M., Brodsky, I.E., Manos, J., Belas, R., Falkow, S., and Gunn, J.S. (2004) Transcriptional regulation of *Salmonella enterica* serovar Typhimurium genes by bile. *FEMS Immunol Med Microbiol* **41:** 177–185.

Rasmussen, A.A., Eriksen, M., Gilany, K., Udesen, C., Franch, T., Petersen, C., and Valentin-Hansen, P. (2005) Regulation of *ompA* mRNA stability: the role of a small regulatory RNA in growth phase-dependent control. *Mol Microbiol* **58:** 1421–1429.

Repoila, F., Majdalani, N., and Gottesman, S. (2003) Small non-coding RNAs, co-ordinators of adaptation processes in *Escherichia coli*: the RpoS paradigm. *Mol Microbiol* **48:** 855–861.

Rhodius, V.A., Suh, W.C., Nonaka, G., West, J., and Gross, C.A. (2006) Conserved and variable functions of the sigmaE stress response in related genomes. *PLoS Biol* **4:** e2.

Robbe-Saule, V., Coynault, C., and Norel, F. (1995) The live oral typhoid vaccine Ty21a is a *rpoS* mutant and is susceptible to various environmental stresses. *FEMS Microbiol Lett* **126:** 171–176.

Robertson, G.T., and Roop, R.M., Jr (1999) The *Brucella abortus* host factor I (HF-I) protein contributes to stress resistance during stationary phase and is a major determinant of virulence in mice. *Mol Microbiol* **34:** 690–700.

Romby, P., Vandenesch, F., and Wagner, E.G. (2006) The role of RNAs in the regulation of virulence-gene expression. *Curr Opin Microbiol* **9:** 229–236.

Roop, R.M., 2nd, Gee, J.M., Robertson, G.T., Richardson, J.M., Ng, W.L., and Winkler, M.E. (2003) *Brucella* stationary-phase gene expression and virulence. *Annu Rev Microbiol* **57:** 57–76.

Santiviago, C.A., Fuentes, J.A., Bueno, S.M., Trombert, A.N., Hildago, A.A., Socias, L.T., *et al.* (2002) The *Salmonella enterica* sv. Typhimurium *smvA*, *yddG* and *ompD* (porin) genes are required for the efficient efflux of methyl viologen. *Mol Microbiol* **46:** 687–698.

Santiviago, C.A., Toro, C.S., Hidalgo, A.A., Youderian, P., and Mora, G.C. (2003) Global regulation of the *Salmonella enterica* serovar typhimurium major porin, OmpD. *J Bacteriol* **185:** 5901–5905.

Schechter, L.M., and Lee, C.A. (2001) AraC/XylS family members, HilC and HilD, directly bind and derepress the *Salmonella typhimurium hilA* promoter. *Mol Microbiol* **40:** 1289–1299.

Schechter, L.M., Jain, S., Akbar, S., and Lee, C.A. (2003) The small nucleoid-binding proteins H-NS, HU, and Fis affect *hilA* expression in *Salmonella enterica* serovar Typhimurium. *Infect Immun* **71:** 5432–5435.

Shea, J.E., Hensel, M., Gleeson, C., and Holden, D.W. (1996) Identification of a virulence locus encoding a second type III secretion system in *Salmonella typhimurium*. *Proc Natl Acad Sci USA* **93:** 2593–2597.

Shea, J.E., Beuzon, C.R., Gleeson, C., Mundy, R., and Holden, D.W. (1999) Influence of the *Salmonella typhimurium* pathogenicity island 2 type III secretion system on bacterial growth in the mouse. *Infect Immun* **67:** 213–219.

Skovierova, H., Rowley, G., Rezuchova, B., Homerova, D., Lewis, C., Roberts, M., and Kormanec, J. (2006) Identification of the sigmaE regulon of *Salmonella enterica* serovar Typhimurium. *Microbiology* **152:** 1347–1359.

Song, M., Kim, H.J., Kim, E.Y., Shin, M., Lee, H.C., Hong, Y., *et al.* (2004) ppGpp-dependent stationary phase induction of genes on *Salmonella* pathogenicity island 1. *J Biol Chem* **279:** 34183–34190.

Sonnleitner, E., Hagens, S., Rosenau, F., Wilhelm, S., Habel, A., Jager, K.E., and Blasi, U. (2003) Reduced virulence of a *hfq* mutant of *Pseudomonas aeruginosa* O1. *Microb Pathog* **35:** 217–228.

Sternberg, N.L., and Maurer, R. (1991) Bacteriophage-mediated generalized transduction in *Escherichia coli* and *Salmonella typhimurium*. *Methods Enzymol* **204:** 18–43.

Thompson, A., Rolfe, M.D., Lucchini, S., Schwerk, P., Hinton, J.C., and Tedin, K. (2006) The bacterial signal molecule, ppGpp, mediates the environmental regulation of both the invasion and intracellular virulence gene programs of *Salmonella*. *J Biol Chem* **281:** 30112–30121.

Tsui, H.C., and Winkler, M.E. (1994) Transcriptional patterns of the mutL-miaA superoperon of *Escherichia coli* K-12 suggest a model for posttranscriptional regulation. *Biochimie* **76:** 1168–1177.

Tsui, H.C., Leung, H.C., and Winkler, M.E. (1994) Characterization of broadly pleiotropic phenotypes caused by an *hfq* insertion mutation in *Escherichia coli* K-12. *Mol Microbiol* **13:** 35–49.

Udekwu, K.I., Darfeuille, F., Vogel, J., Reimegard, J., Holmqvist, E., and Wagner, E.G. (2005) Hfq-dependent regulation of OmpA synthesis is mediated by an antisense RNA. *Genes Dev* **19:** 2355–2366.

Urban, J.H., and Vogel, J. (2006) Translational control and target recognition by *Escherichia coli* small RNAs *in vivo*. *Nucleic Acids Res* (in press).

Urbanowski, M.L., Stauffer, L.T., and Stauffer, G.V. (2000) The *gcvB* gene encodes a small untranslated RNA involved in expression of the dipeptide and oligopeptide transport systems in *Escherichia coli*. *Mol Microbiol* **37:** 856–868.

Uzzau, S., Figueroa-Bossi, N., Rubino, S., and Bossi, L. (2001) Epitope tagging of chromosomal genes in *Salmonella*. *Proc Natl Acad Sci USA* **98:** 15264–15269.

Valentin-Hansen, P., Eriksen, M., and Udesen, C. (2004) The bacterial Sm-like protein Hfq: a key player in RNA transactions. *Mol Microbiol* **51:** 1525–1533.

Vogel, J., and Papenfort, K. (2006) Small non-coding RNAs and the bacterial outer membrane. *Curr Opin Microbiol* **9:** 605–611.

Vogel, J., Argaman, L., Wagner, E.G., and Altuvia, S. (2004) The small RNA IstR inhibits synthesis of an SOS-induced toxic peptide. *Curr Biol* **14:** 2271–2276.

Vytvytska, O., Jakobsen, J.S., Balcunaite, G., Andersen, J.S., Baccarini, M., and von Gabain, A. (1998) Host factor I, Hfq, binds to *Escherichia coli* ompA mRNA in a growth rate-dependent fashion and regulates its stability. *Proc Natl Acad Sci USA* **95:** 14118–14123.

Wei, Y., and Newman, E.B. (2002) Studies on the role of the metK gene product of *Escherichia coli* K-12. *Mol Microbiol* **43:** 1651–1656.

Wilmes-Riesenberg, M.R., Foster, J.W., and Curtiss, R., 3rd (1997) An altered *rpoS* allele contributes to the avirulence of *Salmonella typhimurium* LT2. *Infect Immun* **65:** 203–210.

Wilson, R.L., Libby, S.J., Freet, A.M., Boddicker, J.D., Fahlen, T.F., and Jones, B.D. (2001) Fis, a DNA nucleoid-associated protein, is involved in *Salmonella typhimurium* SPI-1 invasion gene expression. *Mol Microbiol* **39:** 79–88.

Zhang, A., Altuvia, S., Tiwari, A., Argaman, L., Hengge-Aronis, R., and Storz, G. (1998) The OxyS regulatory RNA represses *rpoS* translation and binds the Hfq (HF-I) protein. *EMBO J* **17:** 6061–6068.

Zhang, A., Wassarman, K.M., Rosenow, C., Tjaden, B.C., Storz, G., and Gottesman, S. (2003) Global analysis of small RNA and mRNA targets of Hfq. *Mol Microbiol* **50:** 1111–1124.

Ziolkowska, K., Derreumaux, P., Folichon, M., Pellegrini, O., Regnier, P., Boni, I.V., and Hajnsdorf, E. (2006) Hfq variant with altered RNA binding functions. *Nucleic Acids Res* **34:** 709–720.

Supplementary material

The following supplementary material is available for this article online:

Table S1. Summary of Hfq-dependent changes of protein expression.

Table S2. Oligonucleotides used in this study.

Table S3. Commercially available antibodies and antisera used in this study.

Fig. S1. Growth characteristics of *Salmonella* strains under SPI1-inducing conditions.

Fig. S2. The Δ*hfq* mutant is defective for invasion and intracellular replication.

Fig. S3. The Δ*hfq* strain shows an invasion and intracellular growth defect in intestinal epithelial cells and J774A murine macrophage.

Fig. S4. The *hfq* mutation leads to various differences in protein levels.

Fig. S5. The *hfq* mutant shows reduced adhesion.

Fig. S6. RpoS expression is Hfq-dependent in SL1344.

Fig. S7. Physical maps of plasmids.

This material is available as part of the online article from http://www.blackwell-synergy.com

4.1.1 Supplementary information

to the paper

The RNA chaperone Hfq is essential for the virulence of *Salmonella typhimurium*

Alexandra Sittka, Verena Pfeiffer, Karsten Tedin, and Joerg Vogel

Supplementary material

The RNA chaperone Hfq is essential for the virulence of *Salmonella typhimurium*

Alexandra Sittka[1], **Verena Pfeiffer**[1], **Karsten Tedin**[2] **and Jörg Vogel**[1]

[1]Max Planck Institute for Infection Biology, RNA Biology Group, Berlin, Germany;

[2] Institut für Mikrobiologie und Tierseuchen, Freie Universität Berlin, Berlin, Germany

Table S1: Summary of Hfq-dependent changes of protein expression.

Name[a]	Reg[b]	Loc[c]	Function[d]	Functional class[e]	mRNA[f]	location[g]	spot[h]	MW[i]
CarA	-	CP	carbamoyl-phosphate synthetase, glutamine-hydrolysing small subunit	AMINO ACID TRANSPORT & METABOLISM / NUCLEOTIDE TRANSPORT & METABOLISM		75880..77028	**44 c+d**	41625
SurA	+	CP	peptidyl-prolyl cis-trans isomerase, survival protein	POSTTRANSLATIONAL MODIFICATION, PROTEIN TURNOVER, CHAPERONES		(104470..105756)	**50 and Fig4B**	47221
HtrA	+	PP	periplasmic serine protease Do, heat shock protein	POSTTRANSLATIONAL MODIFICATION, PROTEIN TURNOVER, CHAPERONES		244492..245919	**51 and Fig. 4B**	49284
PyrH	-	CP	uridine 5'-monophosphate kinase	NUCLEOTIDE TRANSPORT & METABOLISM		256276..257001	**22**	25939
Upp	-	CP	undecaprenyl pyrophosphate synthetase (di-trans,poly-cis-decaprenylcistransferase); uracil phosphoribosyltransferase	NUCLEOTIDE TRANSPORT & METABOLISM		259355..260113	**21**	22519
YaeT	+	(OM)	putative outer membrane antigen	CELL WALL/MEMBRANE BIOGENESIS		262379..264793	**39+58**	89471
GltI	+	PP	ABC transporter periplasmic binding protein; ABC superfamily, glutamate/aspartate transporter	AMINO ACID TRANSPORT & METABOLISM / SIGNAL TRANSDUCTION MECHANISMS		(728909..729835)	**26+27 and Fig. 4B**	34111
SucD	-	CP	succinyl-CoA synthetase, alpha subunit	ENERGY PRODUCTION & CONVERSION		807077..807946	**31**	29757
Pal	+	PP	tol protein required for outer membrane integrity, uptake of group A colicins, & translocation of phage DNA to cytoplasm; peptidoglycan-associated lipoprotein precursor	CELL WALL/MEMBRANE BIOGENESIS		817291..817815	**10**	18853
YbgF	-	(PP)	putative periplasmic protein	FUNCTION UNKNOWN		817825..818613	**29**	28230
Dps	-	CP	stress response DNA-binding protein; starvation induced resistance to H2O2; DNA protection during starvation protein	INORGANIC ION TRANSPORT & METABOLISM	+	(897487..897990)	**14**	18706
CspD	+	CP	cold shock-like protein CspD; similar to CspA but not cold shock induced	no COG	+	(1021802..1022023)	**2**	7880
TrxB	-	CP	thioredoxin reductase; thioredoxin reductase	POSTTRANSLATIONAL MODIFICATION, PROTEIN TURNOVER, CHAPERONES		(1035228..1036196)	**33**	34662
FabF	-	CP	3-oxoacyl-[acyl-carrier-protein] synthase II	LIPID TRANSPORT & METABOLISM / SECONDARY METABOLITES BIOSYNTHESIS, TRANSPORT & CATABOLISM		1280435..1281676	**48**	42926
IcdA	+	CP	isocitrate dehydrogenase in e14 prophage, specific for NADP+	ENERGY PRODUCTION & CONVERSION		1324385..1325635	**46**	45759
PagC	+	OM	PhoP regulated: reduced macrophage survival; virulence membrane protein PagC precursor	CELL WALL/MEMBRANE BIOGENESIS	not in *E. coli*	1332251..1332808	**12**	20171
STM1254	-	(OM)	putative outer membrane lipoprotein	no COG	not in *E. coli*	(1338127..1338441)	**55**	10626
STM1328	-	(OM)	putative outer membrane protein	FUNCTION UNKNOWN	not in *E. coli*	(1407118..1408077)	**29**	33818
AroD	-	CP	3-dehydroquinate dehydratase	no COG		(1439617..1440375)	**24**	27308
LppB	-	OM	putative methyl-accepting chemotaxis protein; major outer membrane lipoprotein	no COG	+	(1459057..1459296)	**5**	8472
LppA	-	OM	murein lipoprotein, links outer & inner membranes; major outer membrane lipoprotein	no COG	+	(1459379..1459615)	**1**	8386
YnaF	-	CP	putative universal stress protein	SIGNAL TRANSDUCTION MECHANISMS		1746131..1746565	**7**	15704

Tpx	**+**	CP	thiol peroxidase	POSTTRANSLATIONAL MODIFICATION, PROTEIN TURNOVER, CHAPERONES		1775584..1776090	**25**	18014
TrpB	**-**	CP	Tryptophan synthase beta chain	AMINO ACID TRANSPORT & METABOLISM		1823079..1824272	**44 a**	
OppA	**+**	PP	ABC superfamily, oligopeptide transport protein with chaperone properties	AMINO ACID TRANSPORT & METABOLISM		(1839608..1841356)	**54 and Fig. 4B**	65526
KdsA	**-**	CP	3-deoxy-D-manno-octulosonic acid 8-P synthetase	CELL WALL/MEMBRANE BIOGENESIS		(1870407..1871261)	**30**	30776
PrsA	**-**	CP	phosphoribosylpyrophosphate synthetase	NUCLEOTIDE TRANSPORT & METABOLISM / AMINO ACID TRANSPORT & METABOLISM		1877761..1878708	**33**	34195
FliC	**-**	OM / SUP	flagellin, filament structural protein	CELL MOTILITY		(2047658..2049145)	**45**	51581
Gnd	**-**	CP	gluconate-6-phosphate dehydrogenase, decarboxylating	CARBOHYDRATE TRANSPORT & METABOLISM		(2159361..2160767)	**47**	51363
GlpQ	**+**	PP	glycerophosphodiester phosphodiesterase, periplasmic	ENERGY PRODUCTION & CONVERSION		(2387530..2388600)	**37+38 and Fig. 4B**	40399
AckA	**-**	CP	acetate kinase A (propionate kinase 2)	ENERGY PRODUCTION & CONVERSION		2447939..2449141	**44 c**	43230
HisJ	**-**	PP	ABC superfamily, histidine-binding periplasmic protein	AMINO ACID TRANSPORT & METABOLISM / SIGNAL TRANSDUCTION MECHANISMS		(2464491..2465273)	**24**	28362
CysP	**+**	PP	ABC superfamily, thiosulfate transport protein	INORGANIC ION TRANSPORT & METABOLISM		(2555425..2556441)	**32**	37559
MaeB	**+**	CP	paral putative transferase; phosphate acetyltransferase	ENERGY PRODUCTION & CONVERSION		(2579979..2582258)	**56**	82270
NlpB	**+**	OM	lipoprotein-34	CELL WALL/MEMBRANE BIOGENESIS		(2602992..2604026)	**36**	36915
STM2494	**+**	(IM)	putative inner membrane or exported	GENERAL FUNCTION PREDICTION ONLY	not in *E. coli*	2607971..2609434	**52**	53707
NifU	**-**	CP	NifU homolog involved in Fe-S cluster formation	ENERGY PRODUCTION & CONVERSION		(2681123..2681509)	**6**	13812
YfiA	**-**	CP	ribosome associated factor, stabilizes ribosomes against dissociation; putative sigma(54) modulation protein	TRANSLATION	+	2807668..2808006	**4**	12645
LuxS	**-**	CP	quorum sensing protein, produces autoinducer - acyl-homoserine lactone-signaling molecules	no COG		(2966270..2966785)	**19**	19296
SipA	**-**	SUP	cell invasion protein	no COG	not in *E. coli*	(3024679..3026736)	**57**	73897
SipC	**-**	SUP	cell invasion protein	no COG	not in *E. coli*	(3027857..3029086)	**43**	42957
GudD	**-**	CP	D-glucarate dehydratase	CELL WALL/MEMBRANE BIOGENESIS / GENERAL FUNCTION PREDICTION ONLY		(3110539..3111879)	**49**	49143
Ptr	**+**	PP	protease III	POSTTRANSLATIONAL MODIFICATION, PROTEIN TURNOVER, CHAPERONES		(3149646..3152534)	**59**	107419
OmpX	**-/+**	OM	ail & ompX Homolog; outer membrane protein x precursor	no COG	+	(3193102..3193638)	**8/9**	18483
YraP	**+**	(PP)	paral putative periplasmic protein; possible lipoprotein	GENERAL FUNCTION PREDICTION ONLY		3436344..3436919	**11**	20085
RbfA	**-**	CP	ribosome-binding factor, role in processing of 10S rRNA	TRANSLATION		(3452988..3453389)	**7**	15156
GreA	**+**	CP	transcription elongation factor, cleaves 3' nucleotide of paused mRNA	TRANSCRIPTION		(3467930..3468406)	**13**	17645
Mdh	**-/+**	CP	malate dehydrogenase	ENERGY PRODUCTION & CONVERSION		(3526676..3527614)	**35/34**	32455

AccB	+	CP	acetylCoA carboxylase, BCCP subunit, biotin carboxyl carrier protein	LIPID TRANSPORT & METABOLISM		3550095..3550565	**16+20**	16676
FkpA	+	CP	FKBP-type peptidyl-prolyl cis-trans isomerase (rotamase)	POSTTRANSLATIONAL MODIFICATION, PROTEIN TURNOVER, CHAPERONES		(3604871..3605689)	**28**	28927
DppA	+	PP	ABC superfamily, dipeptide transport protein	AMINO ACID TRANSPORT & METABOLISM		(3814422..3816029)	**53 a+b and Fig. 4B**	60181
YiaD	+	(OM)	putative outer membrane lipoprotein	CELL WALL/MEMBRANE BIOGENESIS		3832806..3833468	**17**	22291
Kbl	-	CP	2-amino-3-ketobutyrate CoA ligase (glycine acetyltransferase)	COENZYME TRANSPORT & METABOLISM		(3903917..3905113)	**44 a+b**	43004
PstS	+	PP	ABC superfamily, high-affinity phosphate transporter	INORGANIC ION TRANSPORT & METABOLISM		(4063585..4064625)	**40**	36794
RbsB	+	PP	ABC superfamily, D-ribose transport protein; D-ribose-binding periplasmic protein	CARBOHYDRATE TRANSPORT & METABOLISM		4094587..4095477	**23**	30943
FadA	-	CP	3-ketoacyl-CoA thiolase; (thiolase I, acetyl-CoA transferase), small (beta) subunit of the fatty acid-oxidizing multienzyme complex	LIPID TRANSPORT & METABOLISM		(4188137..4189300)	**42**	40978
RplL	-	CP	50S ribosomal subunit protein L7/L12	TRANSLATION	+	4365225..4365590	**3**	10805
MalE	-	PP	ABC superfamily maltose transport protein, substrate recognition for transport & chemotaxis	CARBOHYDRATE TRANSPORT & METABOLISM		(4449329..4450528)	**41**	43456
AphA	+	PP	non-specific acid phosphatase/phosphotransferase, class B	GENERAL FUNCTION PREDICTION ONLY		4470683..4471396	**60**	26298
OsmY	-	PP	hyperosmotically inducible periplasmic protein, RpoS-dependent stationary phase gene	GENERAL FUNCTION PREDICTION ONLY		4815879..4816496	**18**	21436
Tsf	+	CP	protein chain elongation factor EF-Ts	no COG		255280..256131	**Fig.4B**	30339
CyoA	+	M	cytochrome o ubiquinol oxidase subunit II	ENERGY PRODUCTION & CONVERSION		(497191..498147)	**Fig.4B**	35270
YbfM	+	(OM)	putative outer membrane protein	no COG		749534..750940	**Fig.4B**	52631
GlnH	+	PP	ABC superfamily (bind_prot), glutamine high-affinity transporter	AMINO ACID TRANSPORT & METABOLISM / SIGNAL TRANSDUCTION MECHANISMS		(896264..897010)	**Fig.4B**	27245
OmpF	+	OM	outer membrane protein 1a (ia;b;f), porin	CELL WALL/MEMBRANE BIOGENESIS		(1089781..1090872)	**Fig.4B**	40266
MglB	+	PP	ABC superfamily (peri_perm), galactose transport protein	CARBOHYDRATE TRANSPORT & METABOLISM		(2286618..2287616)	**Fig.4B**	35791
STM2786	+	PP	tricarboxylic transport	FUNCTION UNKNOWN	not in E. coli	2934590..2935567	**Fig.4B**	35457
RpsD	-	CP	30S ribosomal subunit protein S4	TRANSLATION		(3584316..3584936)	**Fig.4B**	23471
RplC	-	CP	50S ribosomal subunit protein L3	TRANSLATION	+	(3595557..3596186)	**Fig.4B**	22234
GlpK	+	CP	glycerol kinase	ENERGY PRODUCTION & CONVERSION		(4294342..4295850)	**Fig.4B**	56016
TufB	-	CP	protein chain elongation factor EF-Tu (duplicate of tufA)	TRANSLATION		4360603..4361787	**Fig.4B**	47221

[a] Candidate protein name according to coliBASE (http://colibase.bham.ac.uk/index.cgi?help=searchbox&frame=genome; (Chaudhuri *et al.*, 2004)).

[b] Up- or down-regulation in *hfq* strain as compared to SL1344.

[c] Predicted cellular protein localization, CP (cytoplasm), PP (periplasm), OM (outer membrane), IM (inner membrane), SUP (secreted into supernatant).

[d] Protein function according to KEGG (http://www.genome.jp/kegg/; (Goto *et al.*, 1997)).

[e] Functional classification according to (McClelland *et al.*, 2001)

[f] + indicates Hfq co-immunoprecipitation of the mRNA in E. coli (Zhang *et al.*, 2003)

[g] Genomic localization according to (McClelland *et al.*, 2001). Numbers in parentheses indicate counter-clockwise orientation of the gene.

[h] Spot number according to Figure S2 or the bands labeled in Fig. 4.

[i] Protein molecular weight according to (Chaudhuri *et al.*, 2004).

Table S2: Oligonucleotides used in this study.

Name	Sequence[a]
JVO-0076	GAAGTATTACAGGTTGTTGGTG
JVO-0077	GCATCATAACGGTCAAACA
JVO-0078	GGTGGTTGCTCTTCCAACATGGCTAAGGGGCAATCTTT
JVO-0084	TTATTCAGTCTCTTCGCTGTCCT
JVO-0182	GTTTTTTCTAGATTAATGATGATGATGATGATGTTCAGTCTCTTCGCTGTCC
JVO-0252	GCGATTATCCGACGCCCCCGACATGGATAAACAGCGCGTGAAGTGTAGGCTGGAGCTGCTTC
JVO-0253	ACGCGCAGGGGTCTACTGCGCAACAGGACAGCGAAGAGACTGAATAAGGTCCATATGAATATCCTCCTTAG
JVO-0318	CAGAATCGAAAGGTTCAAAGTACAAATAAGCATATAAGGAAAAGAGGTCCATATGAATATCCTCCTTAG
JVO-0319	ACGCGCAGGGGTCTACTGCGCAACAGGACAGCGAAGAGACTGAACATCATCATCATCATCATTAAGGTCCAT ATGAATATCCTCCTTAG
JVO-0322	CTACGGCGTTTCACTTCTGAGTTC
JVO-0370	GTTTTTCTCGAGCCTGCCTAAGGC
JVO-0397	CGGTAGAGTAACTATTGAGCAGAT
JVO-0398	GTTTTTTTTTTAATACGACTCACTATAGGGAGGCCTAACCAGTCGTAGC
JVO-0717	GTTTTTGCTAGCTGGTACCAGGAGGG
JVO-0719	GTTTTATGCATGCCGACTGGTTAATGAG
JVO-0726	GTTTTTGCTAGCCAACAGGGAAGTCAC
JVO-0751	GTTTTATGCATAGTCTGCCATTGACAAAC
JVO-0801	GTTTTGACGTCTATTTGTGCTTATTTTTACTTG
JVO-0802	GTTTTGACGTCAAATCAATATTGAAACGG
JVO-0805	GTTTTGCTAGCATGCCTTTATTGCTTTTTTATG
JVO-0806	GTTTTGACGTCTCGACCCGCTGTACCT
JVO-0807	GTTTTGCTAGCGCGTGTTTCCTCAACCA
JVO-0811	GGAGATCTCGATCACACAAATTAAAATAATTTGTAATCGTGTAGGCTGGAGCTGCTTC
JVO-0812	CCAGCCCTGAAAGGACTGGCTTTGTATTCAGACTACAACAAAAGGTCCATATGAATATCCTCCTTAG
JVO-0817	GTTTTTCTCGAGCCAATAGTCCCCTCCGA
JVO-0818	GTTTTTTCTAGACTGCACGGCATACTCCT
JVO-0837	CAAAAGATGGAAACAGGATCCCCGCTTGATTAAATTACGGGACTACAAAGACCATGACGG
JVO-0838	ATGATAAAAAAATAATGCATATCTCCTCTCTCAGATTTTACCATATGAATATCCTCCTTAG
JVO-0839	CCACGGCGAAGCTATT
JVO-0840	GCCCATGCCGTATTTAT
JVO-0888	GTTTTCTCGAGGCTAGCTAAGTAGTACTTAGATTTAAGAAGGAGATATACATATGGCCAGCAAAGGAGAA
JVO-0889	GTTTTTGACGTCAGCGTAAGAATTCGTCC
JVO-0890	GTTTTTGCTAGCTATCTTACTGCATTTTTTT
JVO-0934	GTTTTTTTTTTAATACGACTCACTATAGGGAGGTTAACTGATCGTTGATCTG
JVO-1058	CGTGAACTTTACCGTACA
JVO-1186	TTTTCTCGAGTTAATACGACTCACTATAGGCCATTGACAAACG
JVO-1298	CGAGCCCGTAGAATATGA
JVO-1299	GTTTTTTTTTTAATACGACTCACTATAGGGAGGCTTCGAGCAGGATG
JVO-1592	GCGTATCCAGACCCAGGGTCTGAGAG
JVO-1595	GCGCCAGCCGCAAGGGT
JVO-1701	GTTTTTTTTAATACGACTCACTATAGGATCCATCCATACTGATTAACACT
JVO-1702	GCAGGATAGCGTCCAAC
pZE-Xba	TCGTTTTATTTGATGCCTCTAGA

[a] Oligonucleotides used for cloning, and Northern hybridization. Sequences are given in 5'->3' direction.

Table S3: Commercially available antibodies and anti sera used in this study

Epitope	Antibody/anti sera	Working dilution	Source	Provided by
Myc	α-Myc antibody	1:1000	mouse	Santa Cruz Biotechnology, Inc.
3xFLAG	α-FLAG antibody	1:1000	mouse	Sigma
IgG	α–rabbit IgG antibody HRP-linked	1:5000	donkey	Amersham
IgG	α–mouse IgG antibody HRP-linked	1:5000	sheep	Amersham
SipC	α-SipC antiserum	1:3000	rabbit	MPI-IB Berlin, Michael Kolbe
SipD	α-SipD antiserum	1:3000	rabbit	MPI-IB Berlin, Michael Kolbe
SopB	α-SopB antiserum	1:3000	rabbit	MPI-IB Berlin, Michael Kolbe
SopE	α-SopE antiserum	1:15000	rabbit	ETH Zurich, Wolf-Dietrich Hardt
PrgI	α-PrgI antiserum	1:3000	rabbit	MPI-IB Berlin, Michael Kolbe
RpoS	α-RpoS antiserum	1:5000	rabbit	FU Berlin, Regine Hengge

Figure legends

Figure S1. Growth characteristics of *Salmonella* strains under SPI1-inducing conditions.
(A) OD_{600} values of triplicate cultures in LB medium containing 0.3M sodium chloride and grown under oxygen limitation were determined in 60 minute intervals (open squares: wild-type, filled triangles: *hfq*^{HIS}, open diamonds: *hfq*-C, stars: Δ*hfq*). (B) Complementation of the slight growth defect of the Δ*hfq* strain by plasmid pStHfq-6H when grown under SPI1-inducing conditions (open squares: wild-type strain carrying a control plasmid; stars: Δ*hfq* carrying a control plasmid; filled circles: Δ*hfq* complemented with pStHfq-6H).

Figure S2. The Δ*hfq* mutant is defective for invasion and intracellular replication.
(A and B) Invasion properties of the Δ*hfq* strain and several control strains. HeLa cells were infected with an MOI of 10, and intracellular bacteria were enumerated 2 hr and 6 hours post infection. (A) Bacteria were grown to early stationary phase in standard LB medium (strains: wild-type, *hfq*^{HIS}, *hfq*-C, Δ*hfq*, Δ*spi1*, Δ*rpoS*). (B) Bacteria were grown to late stationary phase under SPI1-inducing conditions (strains: wild-type, *hfq*^{HIS}, *hfq*-C, Δ*hfq*, Δ*spi1*, Δ*rpoS*, wild-type strain carrying a control plasmid, Δ*hfq* carrying a control plasmid, Δ*hfq* complemented with pStHfq-6H). (C) RawB macrophages were infected with a MOI of 1 with bacteria grown to early stationary phase (OD of 2), and intracellular bacteria were enumerated 1 hour, 4 hours, and 24 hours post infection. The number of intracellular bacteria is given as percentage of the number of input bacteria. The bacterial strains included were wild-type, *hfq*^{HIS}, *hfq*-C, Δ*hfq*,, wild-type strain carrying a control plasmid, Δ*hfq* carrying a control plasmid, Δ*hfq* complemented with pStHfq-6H).

Figure S3. The Δ*hfq* strain shows an invasion and intracellular growth defect in intestinal epithelial cells and J774A murine macrophage. (A) Monolayers of LoVo intestinal epithelial cells

were infected at a multiplicity of infection (MOI) of 1 or 10 with the wild-type (open circles) and Δ*hfq* strains (filled circles), respectively. One hour post-infection, extracellular bacteria were killed by addition of 50 μg/ml gentamicin and further incubation for one hour. Two hours post-infection, the medium was changed to one containing gentamicin at 10 μg/ml, and infected cells were washed twice with PBS and lysed by addition of 0.1% Triton X-100. Dilutions were plated to agar plates for determination of total intracellular bacteria. Remaining wells were washed and lysed at 4 or 24 hours post-infection. (B) J774A murine macrophages were infected at a MOI of 1 with either the wild-type or Δ*hfq* strains for 30 min, followed by a change of medium containing 50 μg/ml gentamicin for an additional 30 min. The medium was replaced to contain gentamicin at 10 μg/ml, and the first time points (one hour post-infection) were washed and lysed for determination of intracellular bacteria. Remaining samples were taken at 4 and 24 hours post-infection. The results shown are the averages of duplicate wells for each time point, and are representative of at least two, independent experiments.

Figure S4. The *hfq* mutation leads to various differences in protein levels

(A) Two dimensional gel electrophoresis of total protein (300 μg) of wt SL1344 and its *hfq* deletion mutant. Protein spots (listed in Table S1) differing in intensity between the two strains were analyzed by MALDI TOF.

Figure S5. The *hfq* mutant shows reduced adhesion.

Adherence of *Salmonella* serovar Typhimurium SL1344 and *hfq* mutant strains to HeLa cells. (A) HeLa cells were infected with an MOI of 50. Given is the number of bacteria per HeLa cell one hour post infection, as determined by fluorescence microscopy. (B) Adhesion/invasion assay with bacteria grown to early stationary phase in standard LB medium. Cells were infected for 30 minutes with an MOI of 10 and bacteria enumerated immediately after (no Gentamycin-treatment) as well as 2 and 6 hours after infection (with Gentamycin-treatment). Open squares: wild-type, filled triangles: hfq^{HIS}, open diamonds: *hfq*-C, and stars: Δ*hfq*.

Figure S6. RpoS expression is Hfq-dependent in SL1344.

(A) Western blot analysis of whole cell protein samples from SL1344 wild-type, Δ*hfq*, and Δ*rpoS* strains. Samples were taken from cultures grown in LB at 37°C at early stationary phase (OD 2). Hybridization was carried out using an *E. coli* RpoS-specific antiserum (Table S2). The quantified RpoS levels are given in relative values of wild-type levels below the lanes.

Figure S7. Physical maps of plasmids.

(A) pJV300

(B) pVP003

(C) pVP009 control plasmid

(D) pVP012 control plasmid

(E) pVP004 complementation plasmid

(F) pAS0046 *gfp* transcriptional fusion plasmid

(G) pAS0047 *hilA-gfp* transcriptional fusion plasmid

(H) pAS0048 *hilA*-5'UTR-*gfp* transcriptional fusion plasmid

(I) pAS0057 *ompC-gfp* transcriptional fusion plasmid

(J) pAS0058 *ompD-gfp* transcriptional fusion plasmid

(K) pVP019 *ompD-gfp* translational fusion plasmid

(L) pVP020 *ompC-gfp* translational fusion plasmid

References

Chaudhuri, R.R., Khan, A.M., and Pallen, M.J. (2004) coliBASE: an online database for Escherichia coli, Shigella and Salmonella comparative genomics. *Nucleic Acids Res* **32**: D296-299.

Goto, S., Bono, H., Ogata, H., Fujibuchi, W., Nishioka, T., Sato, K., and Kanehisa, M. (1997) Organizing and computing metabolic pathway data in terms of binary relations. *Pac Symp Biocomput*: 175-186.

McClelland, M., Sanderson, K.E., Spieth, J., Clifton, S.W., Latreille, P., Courtney, L., Porwollik, S., Ali, J., Dante, M., Du, F., Hou, S., Layman, D., Leonard, S., Nguyen, C., Scott, K., Holmes, A., Grewal, N., Mulvaney, E., Ryan, E., Sun, H., Florea, L., Miller, W., Stoneking, T., Nhan, M., Waterston, R., and Wilson, R.K. (2001) Complete genome sequence of Salmonella enterica serovar Typhimurium LT2. *Nature* **413**: 852-856.

Zhang, A., Wassarman, K.M., Rosenow, C., Tjaden, B.C., Storz, G., and Gottesman, S. (2003) Global analysis of small RNA and mRNA targets of Hfq. *Mol Microbiol* **50**: 1111-1124.

Figure S1

Sittka *et al.*, 2006

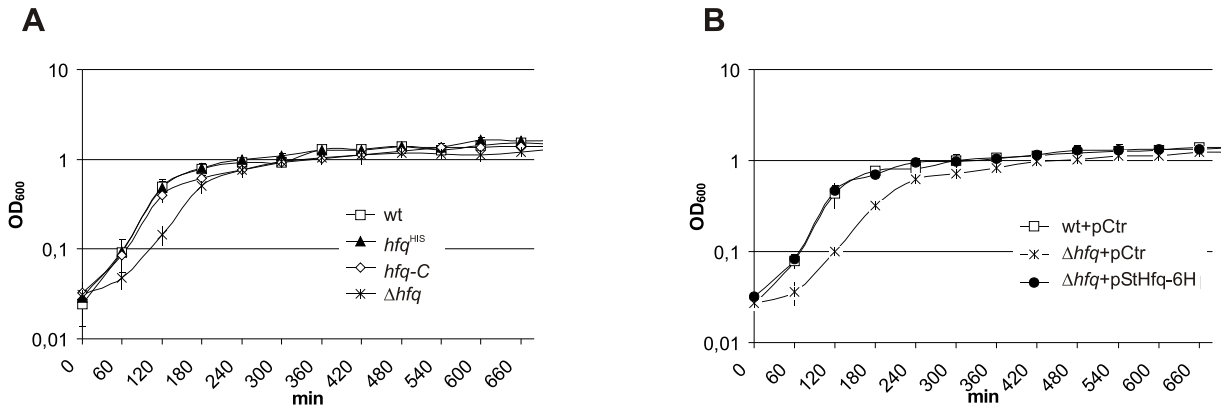

Figure S2

Sittka *et al.*, 2006

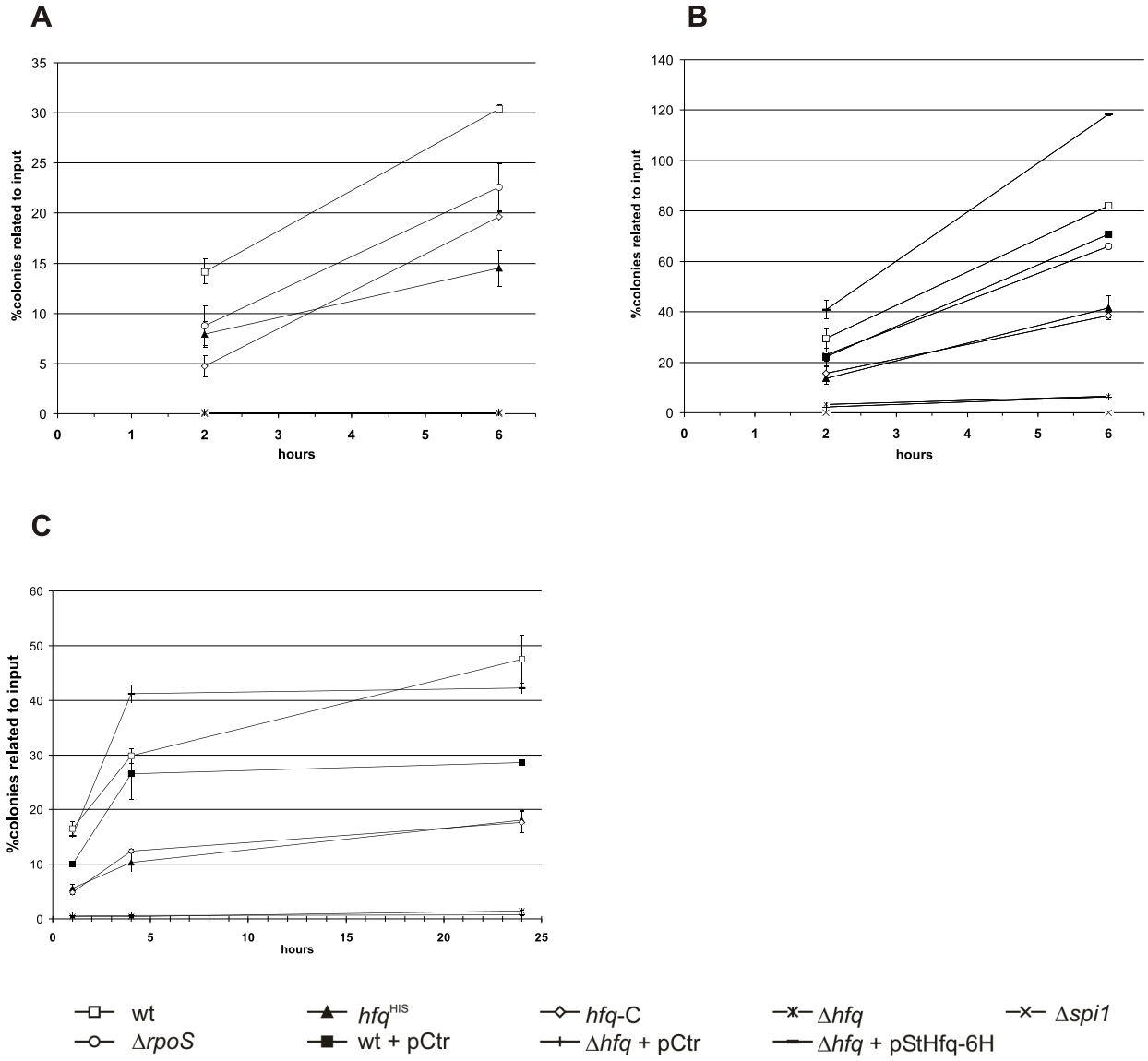

Figure S3

Sittka *et al.*, 2006

A

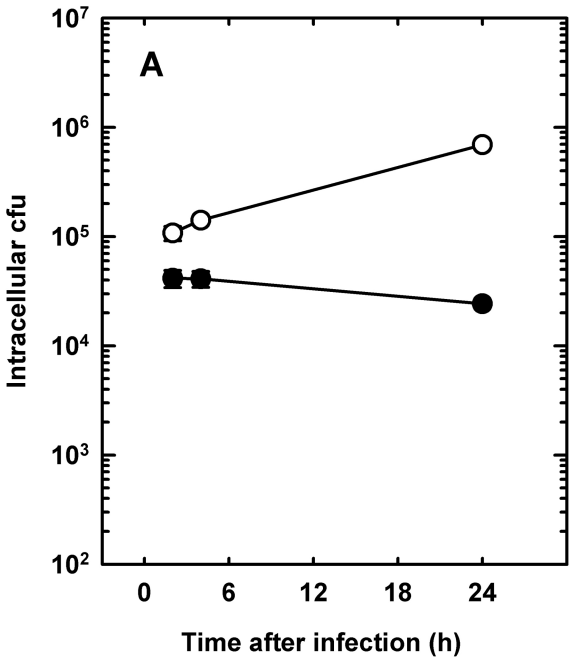

B

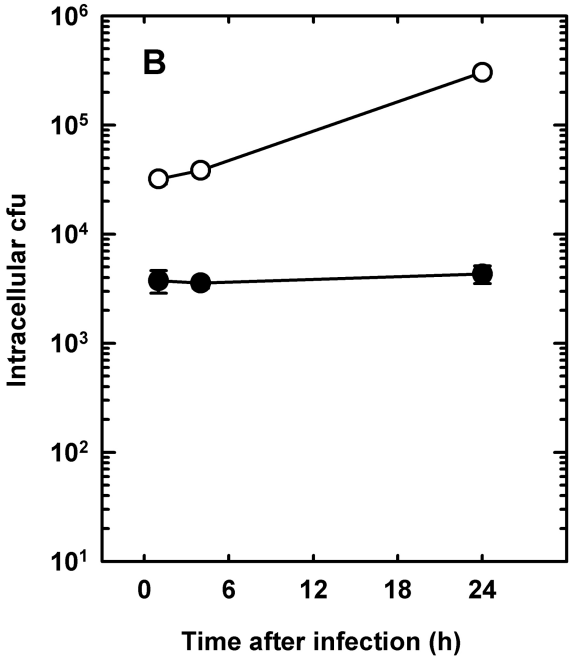

Figure S4

Sittka *et al.*, 2006

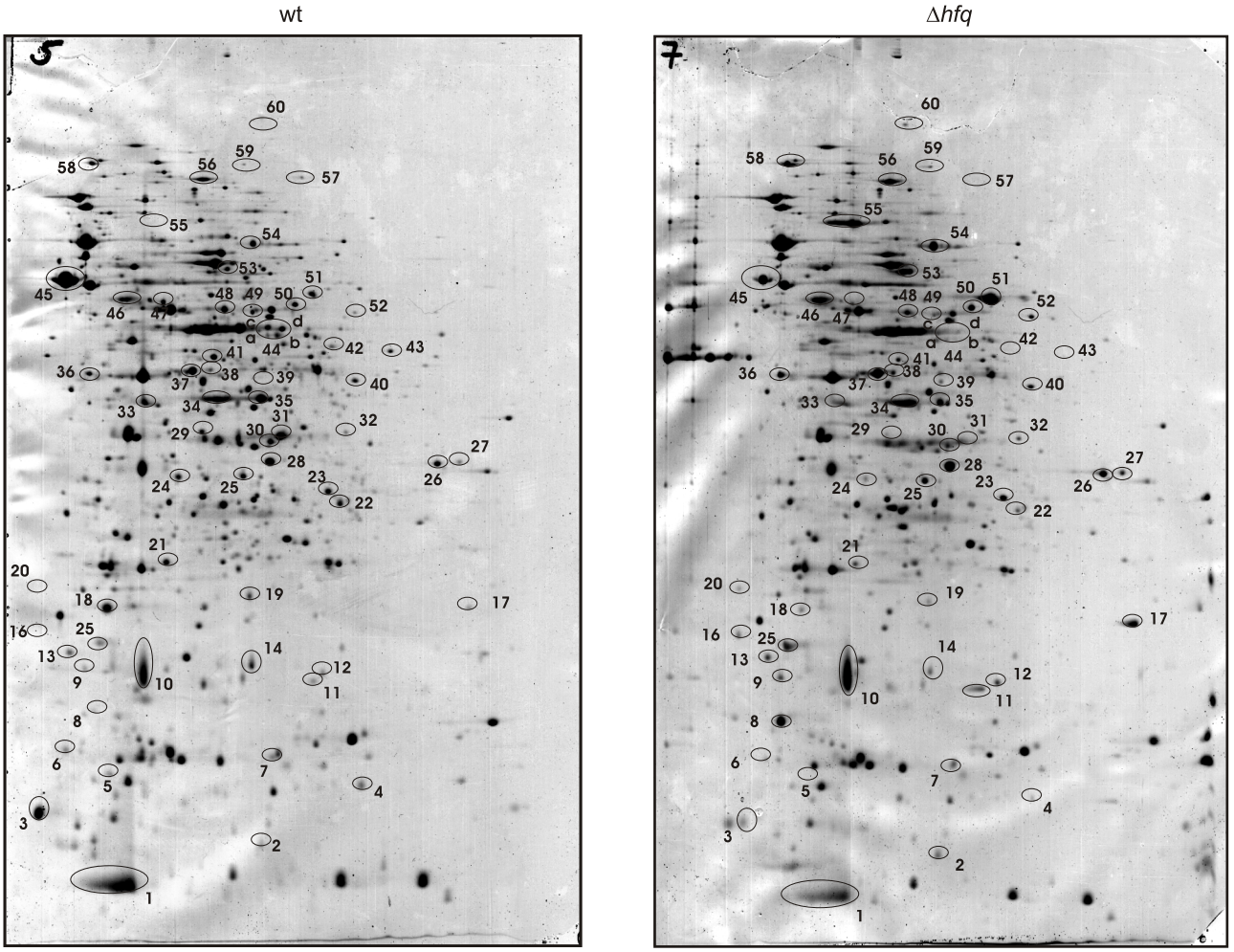

Figure S5

Sittka *et al.*, 2006

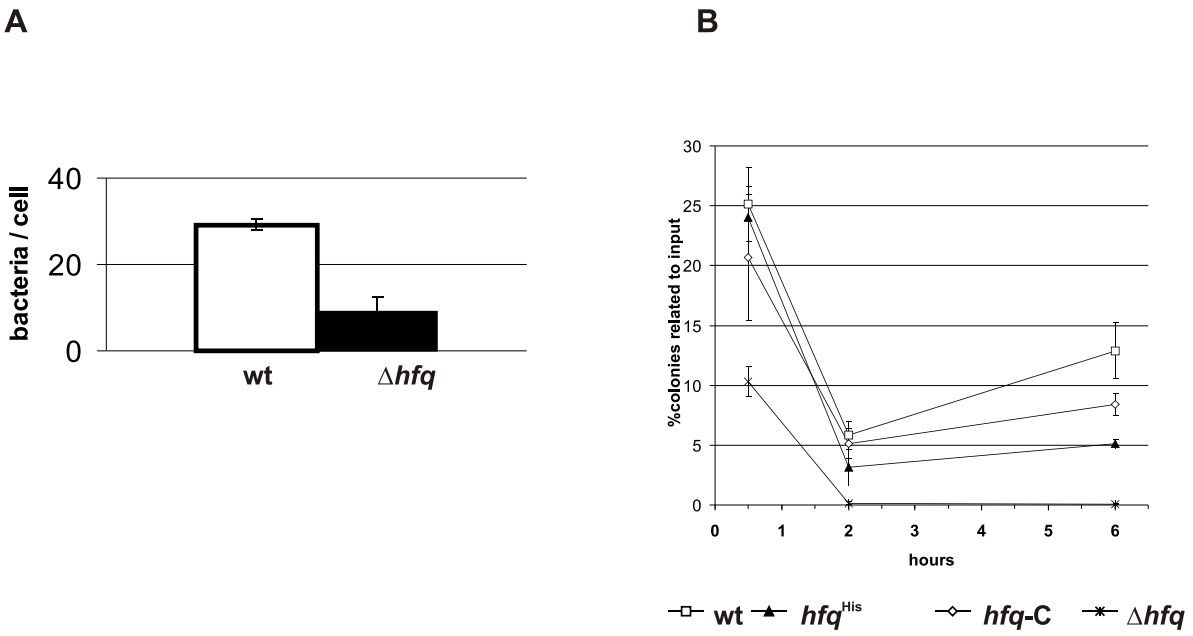

Figure S6

Sittka *et al.*, 2006

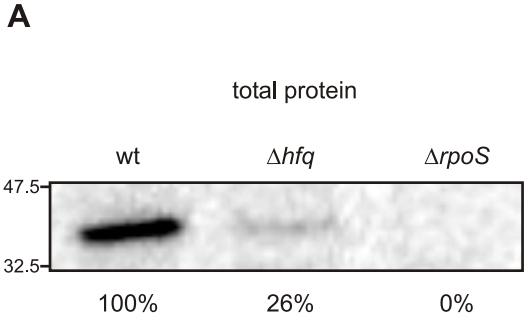

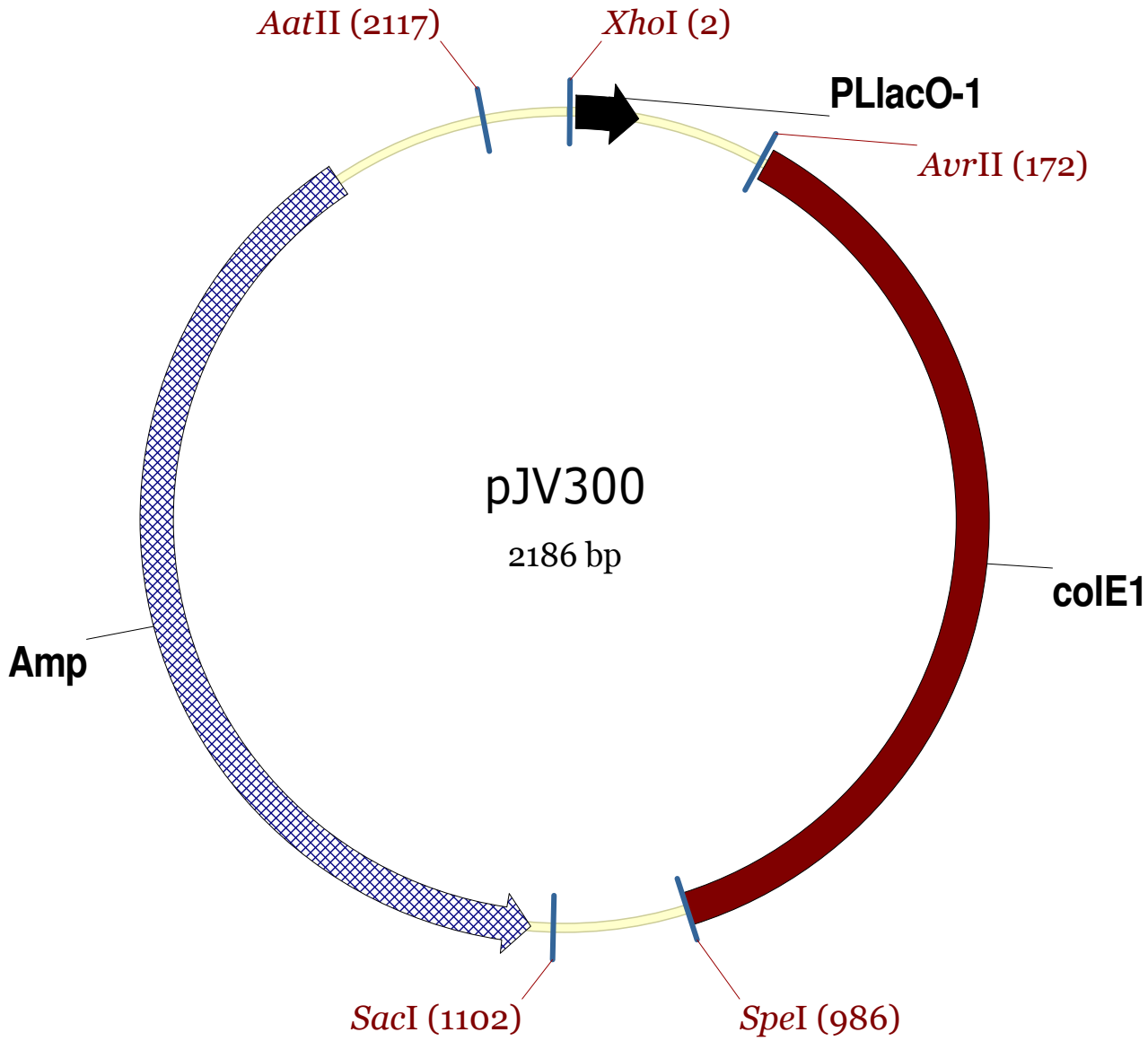
AatII (2117)
XhoI (2)
PLlacO-1
AvrII (172)
pJV300
2186 bp
colE1
Amp
SacI (1102)
SpeI (986)

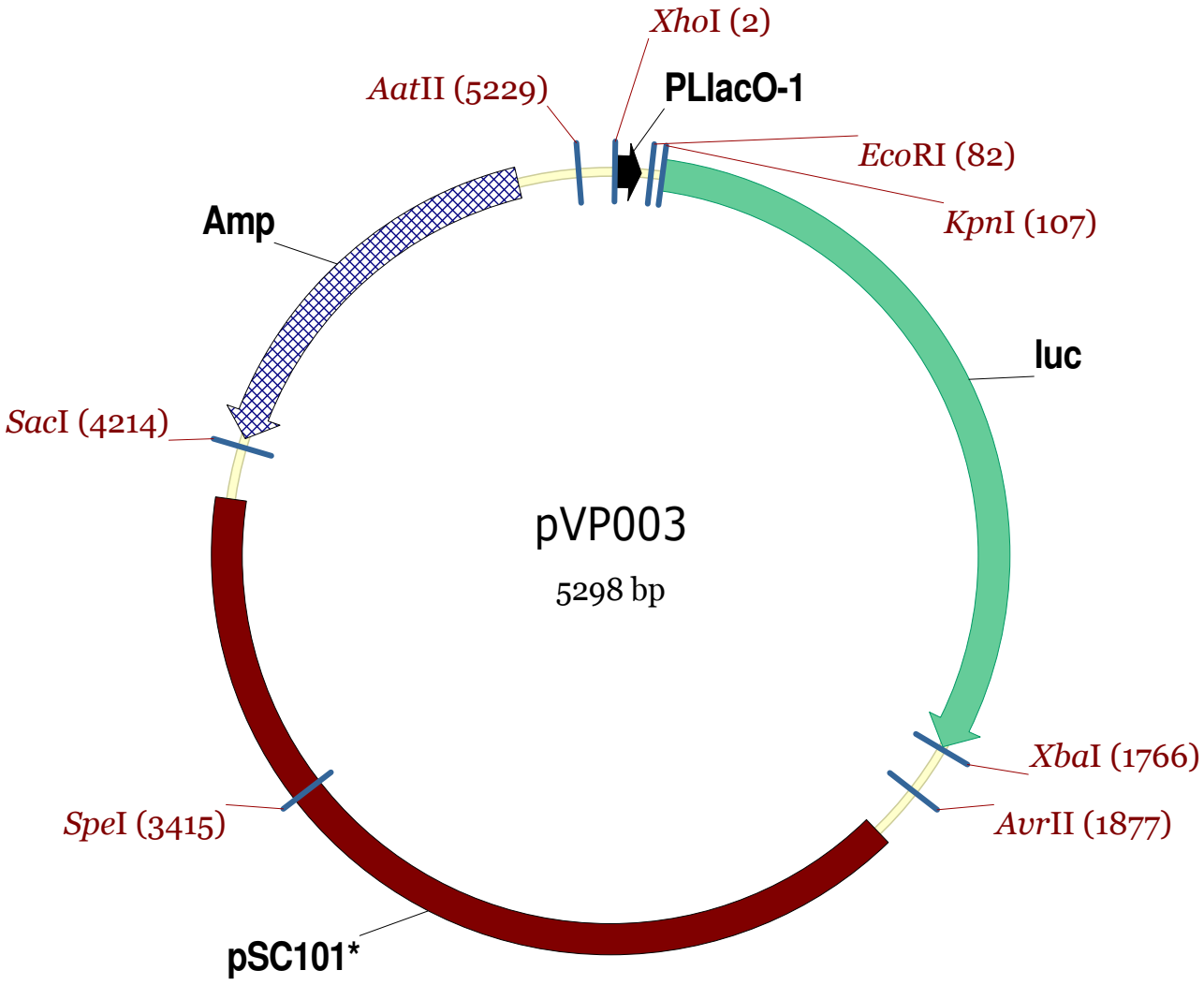
XhoI (2)
AatII (5229)
PLlacO-1
EcoRI (82)
KpnI (107)
Amp
luc
SacI (4214)
pVP003
5298 bp
XbaI (1766)
SpeI (3415)
AvrII (1877)
pSC101*

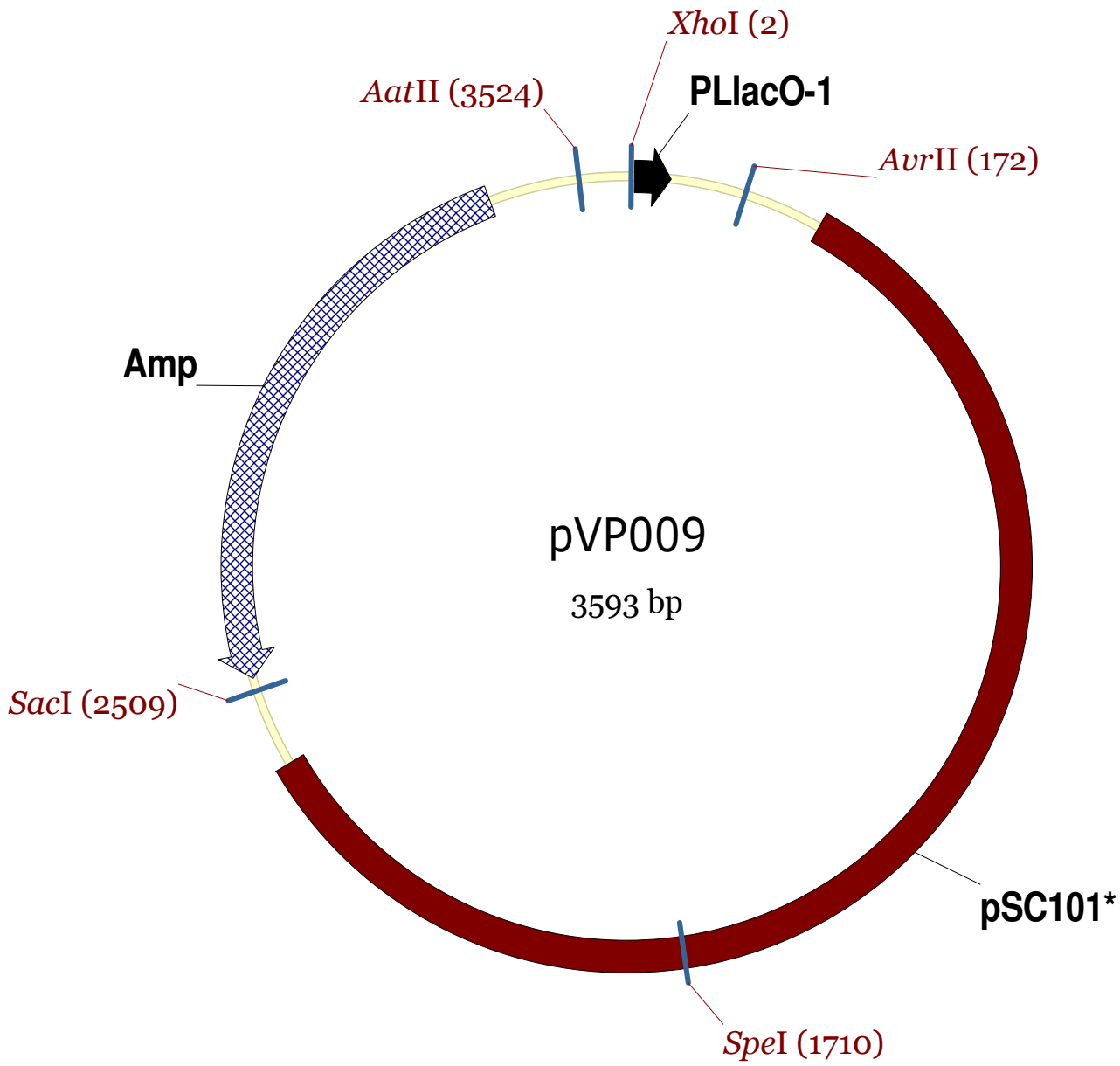
XhoI (2)
AatII (3524)
PLlacO-1
AvrII (172)
Amp
pVP009
3593 bp
SacI (2509)
pSC101*
SpeI (1710)

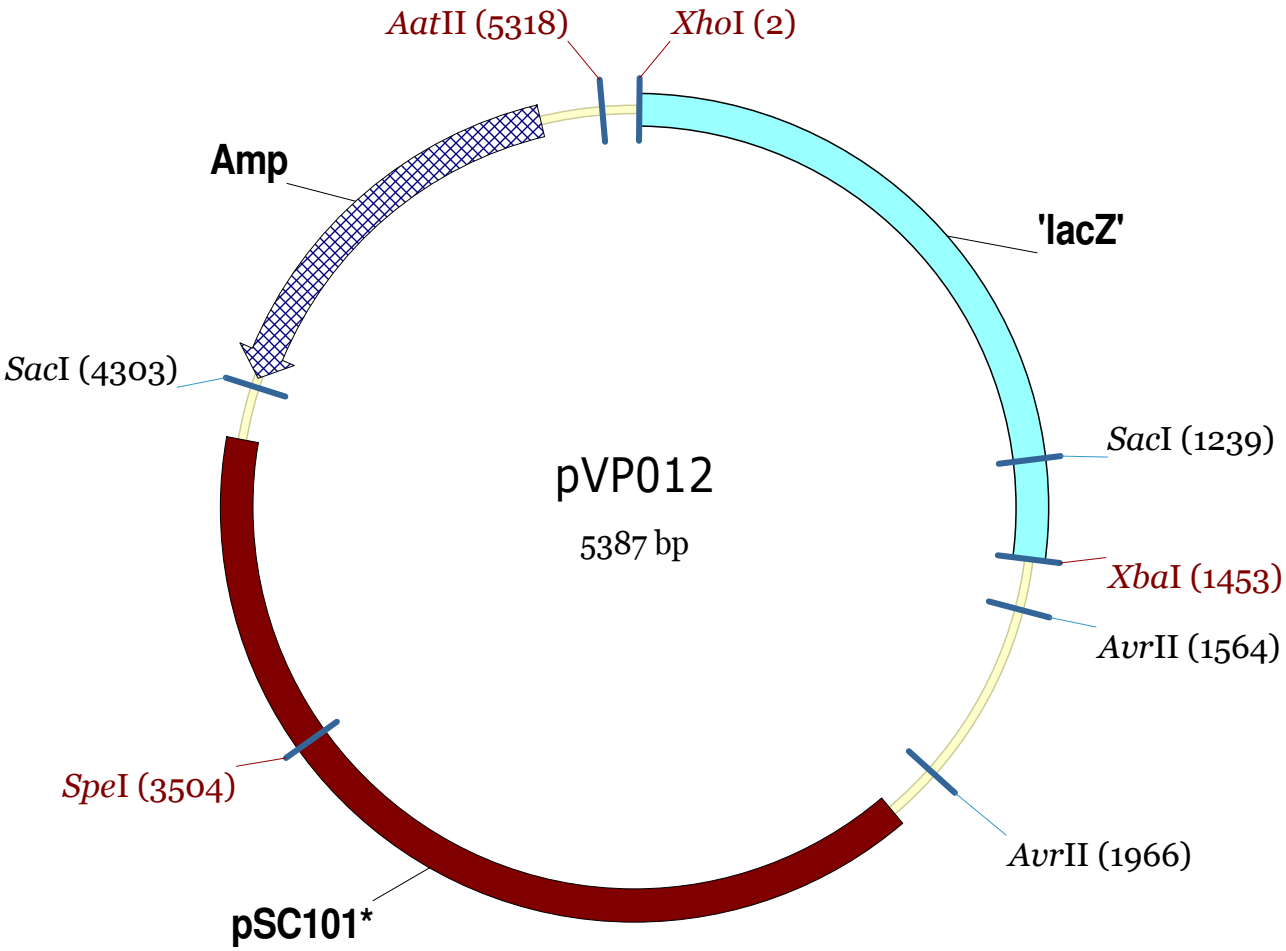
AatII (5318)
XhoI (2)
Amp
'lacZ'
SacI (4303)
SacI (1239)
pVP012
5387 bp
XbaI (1453)
AvrII (1564)
SpeI (3504)
AvrII (1966)
pSC101*

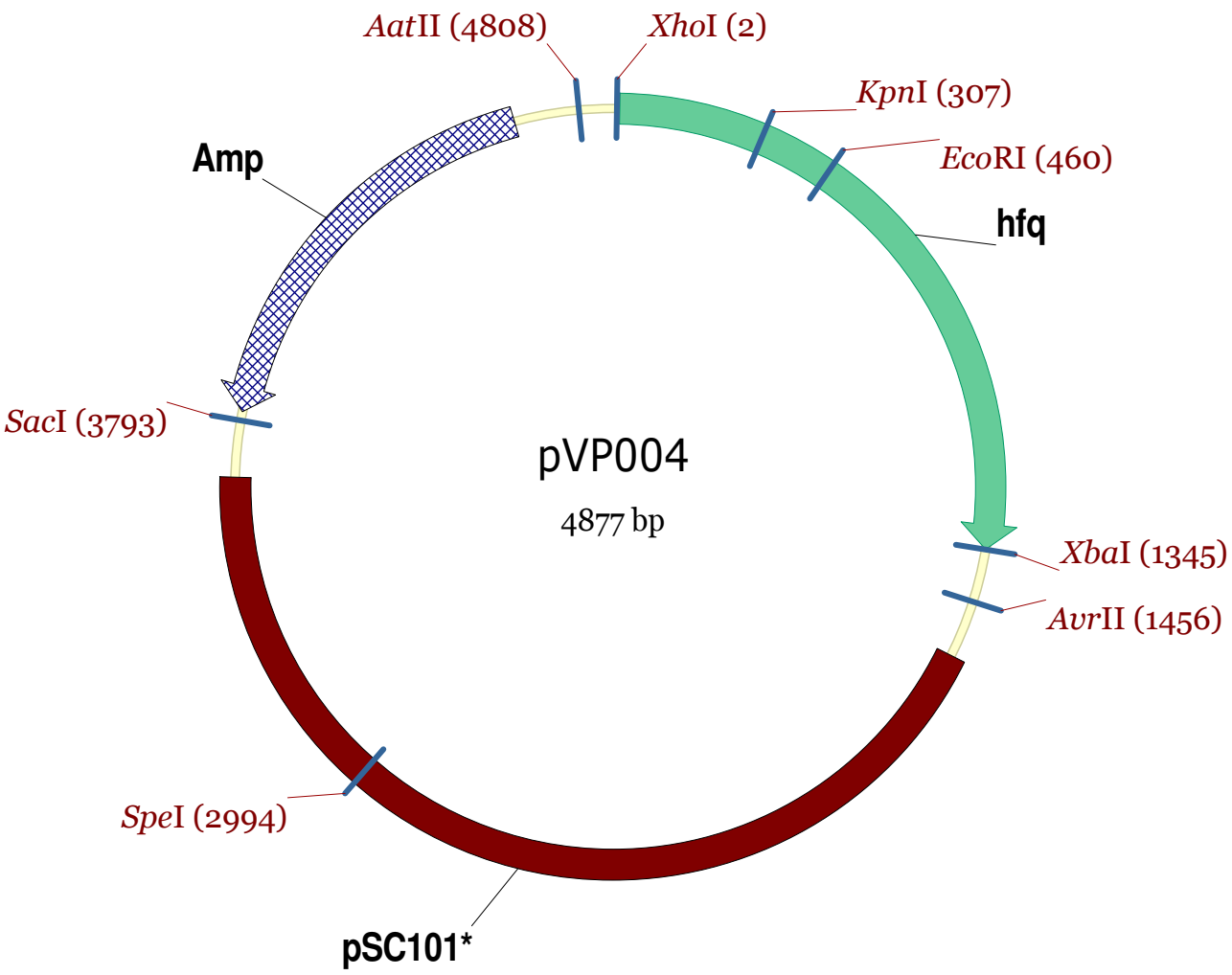
AatII (4808)
XhoI (2)
KpnI (307)
EcoRI (460)
hfq
Amp
SacI (3793)
pVP004
4877 bp
XbaI (1345)
AvrII (1456)
SpeI (2994)
pSC101*

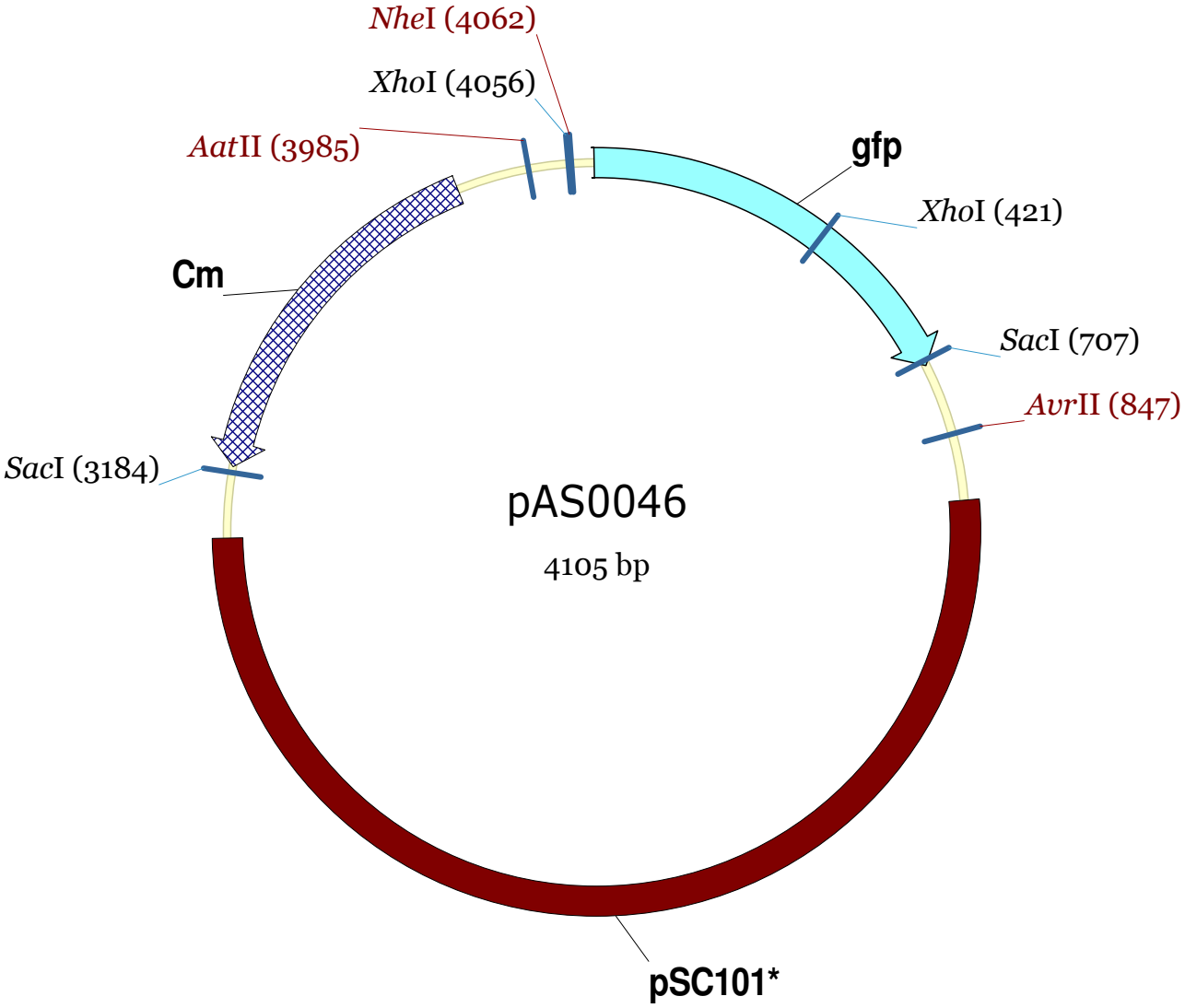
NheI (4062)
XhoI (4056)
AatII (3985)
gfp
XhoI (421)
Cm
SacI (707)
AvrII (847)
SacI (3184)
pAS0046
4105 bp
pSC101*

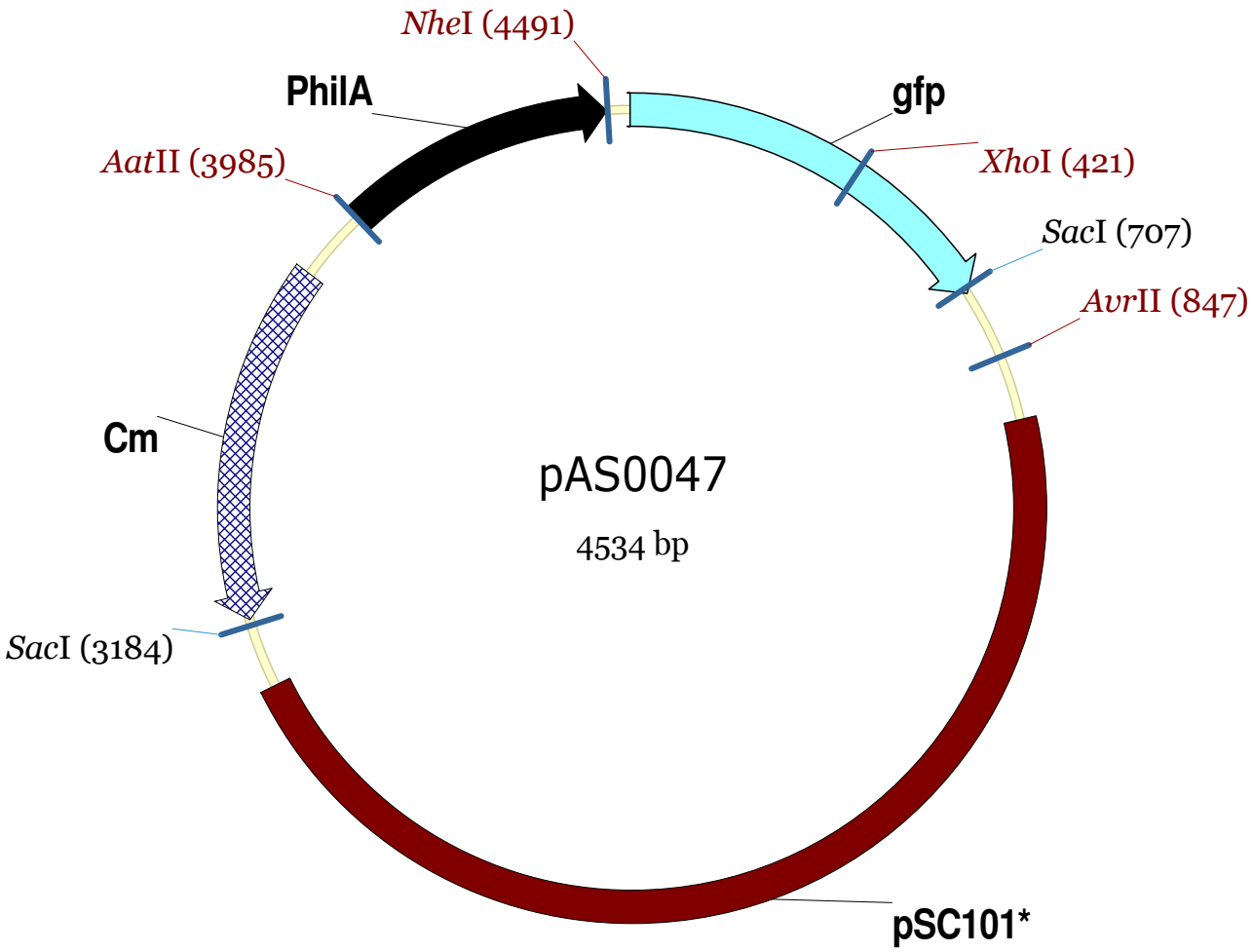
NheI (4491)
PhilA
gfp
AatII (3985)
XhoI (421)
SacI (707)
AvrII (847)
Cm
pAS0047
4534 bp
SacI (3184)
pSC101*

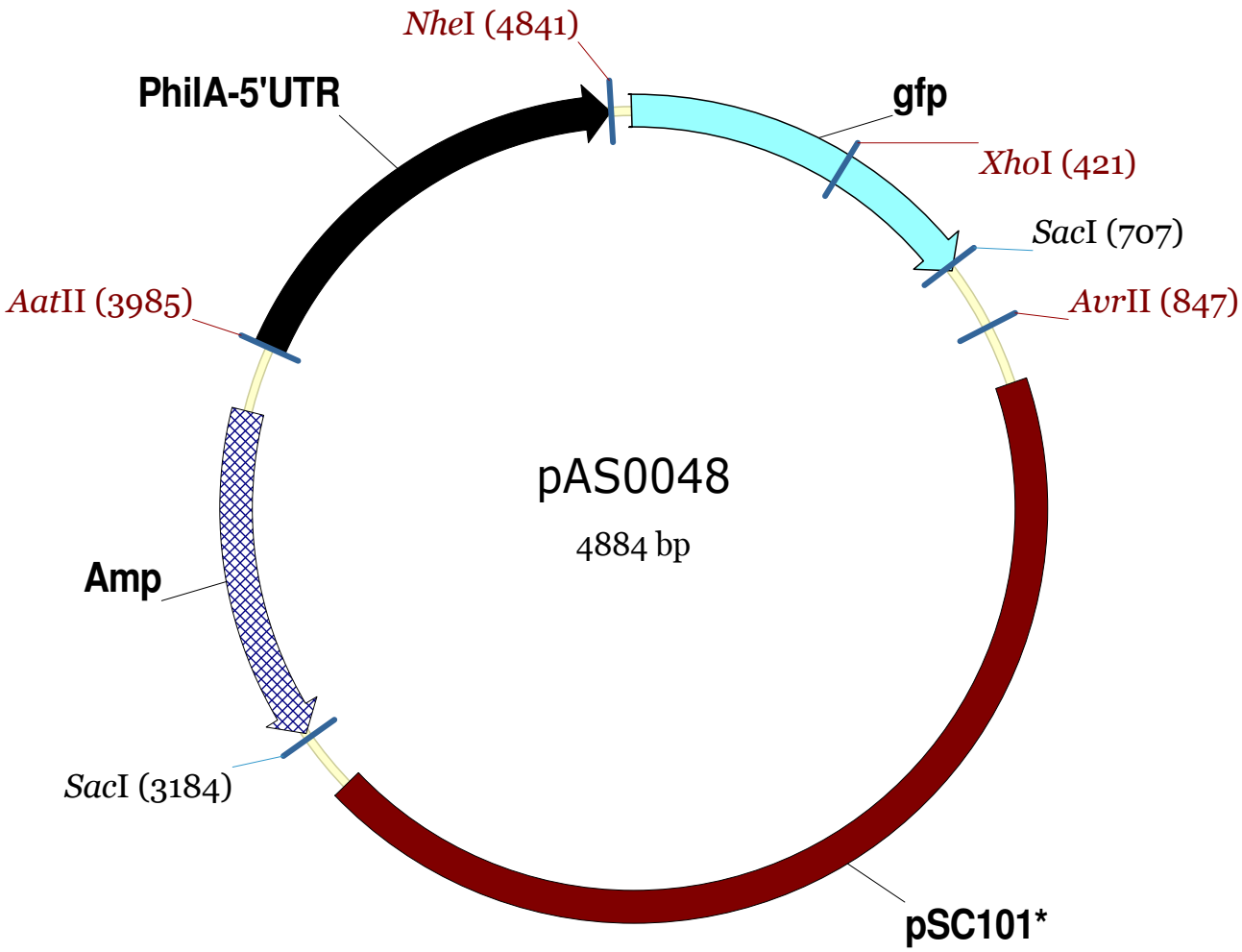
NheI (4841)
PhilA-5'UTR
gfp
XhoI (421)
SacI (707)
AatII (3985)
AvrII (847)
pAS0048
4884 bp
Amp
SacI (3184)
pSC101*

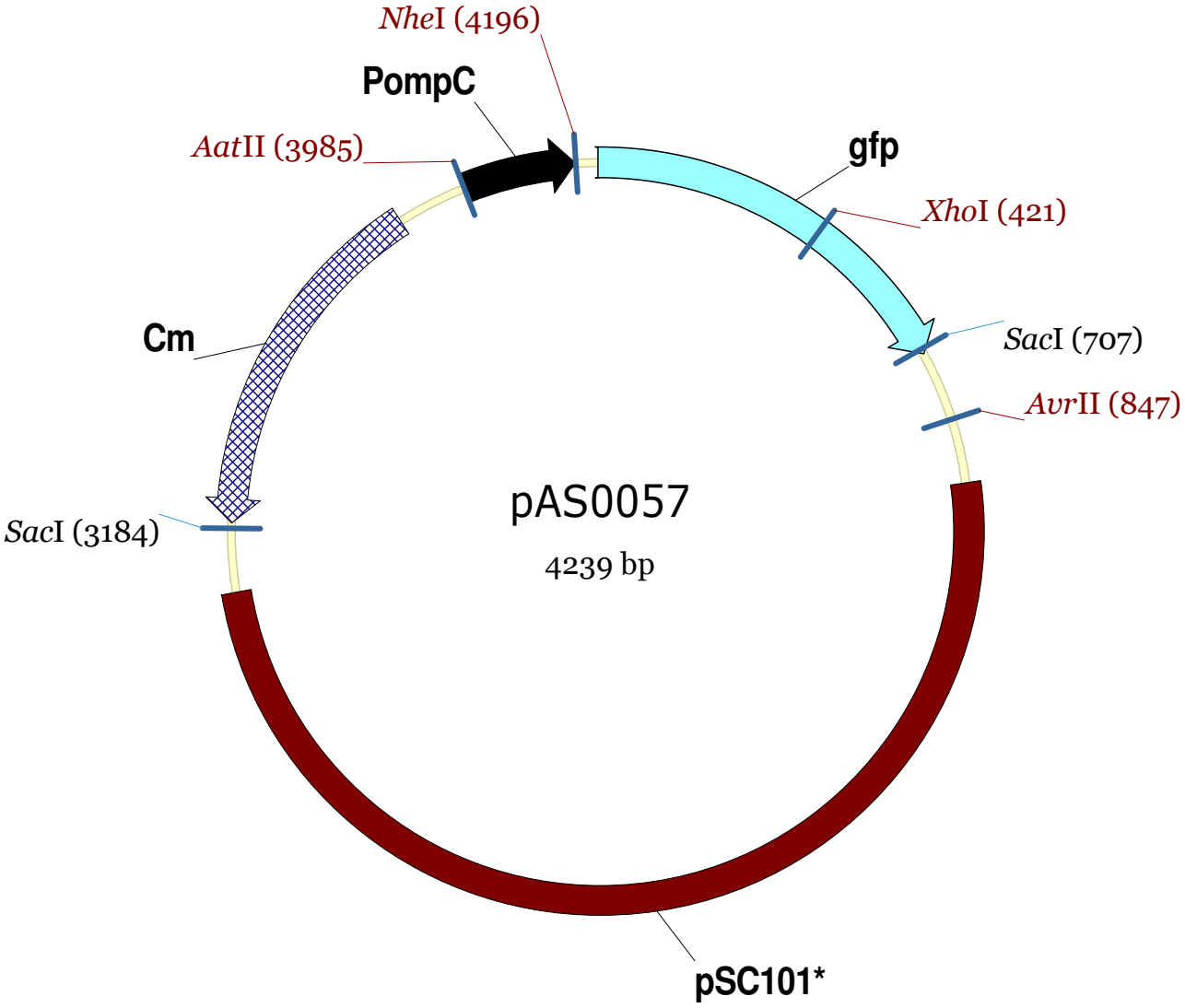
NheI (4196)
PompC
AatII (3985)
gfp
XhoI (421)
Cm
SacI (707)
AvrII (847)
pAS0057
4239 bp
SacI (3184)
pSC101*

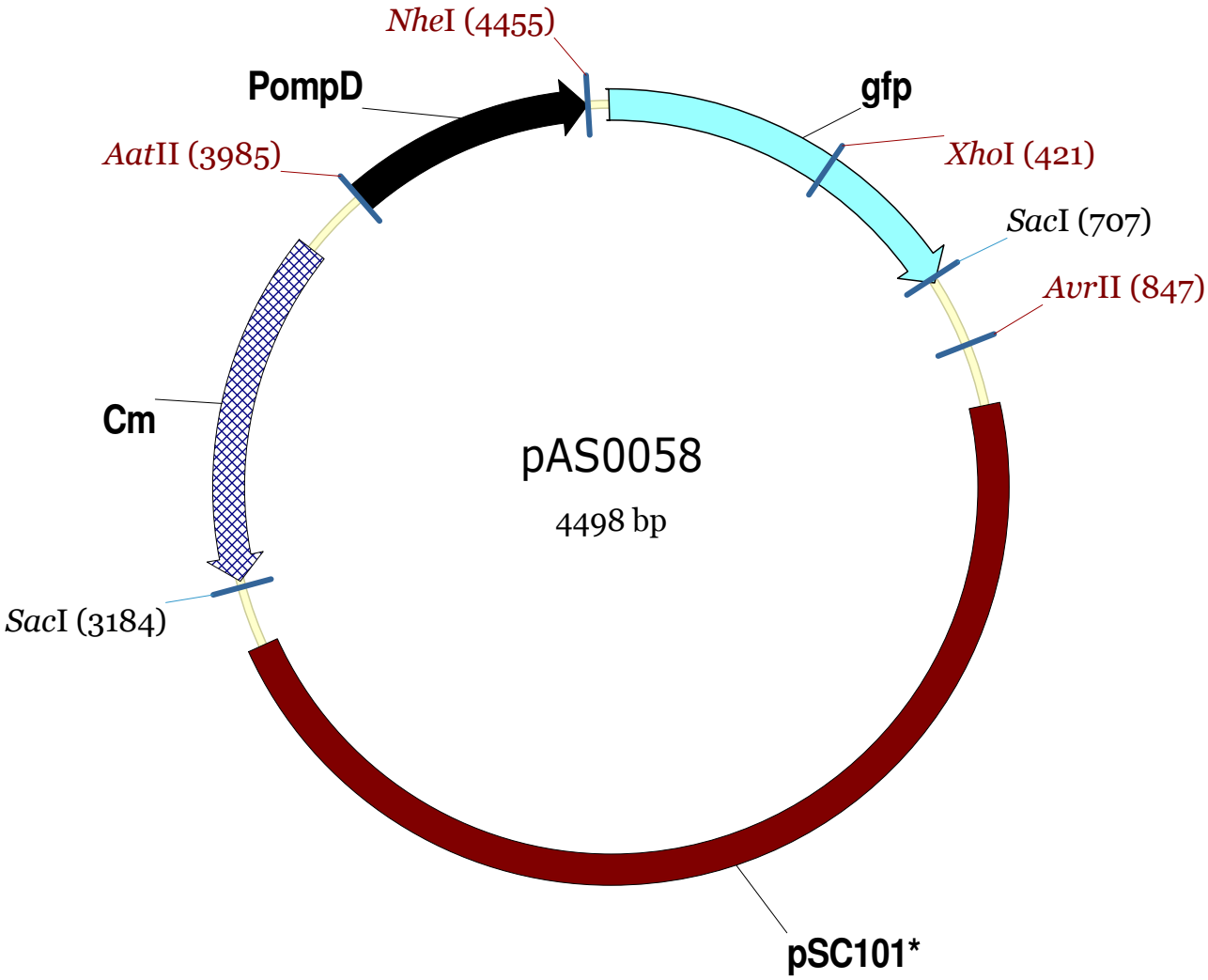
NheI (4455)
PompD
gfp
AatII (3985)
XhoI (421)
SacI (707)
AvrII (847)
Cm
pAS0058
4498 bp
SacI (3184)
pSC101*

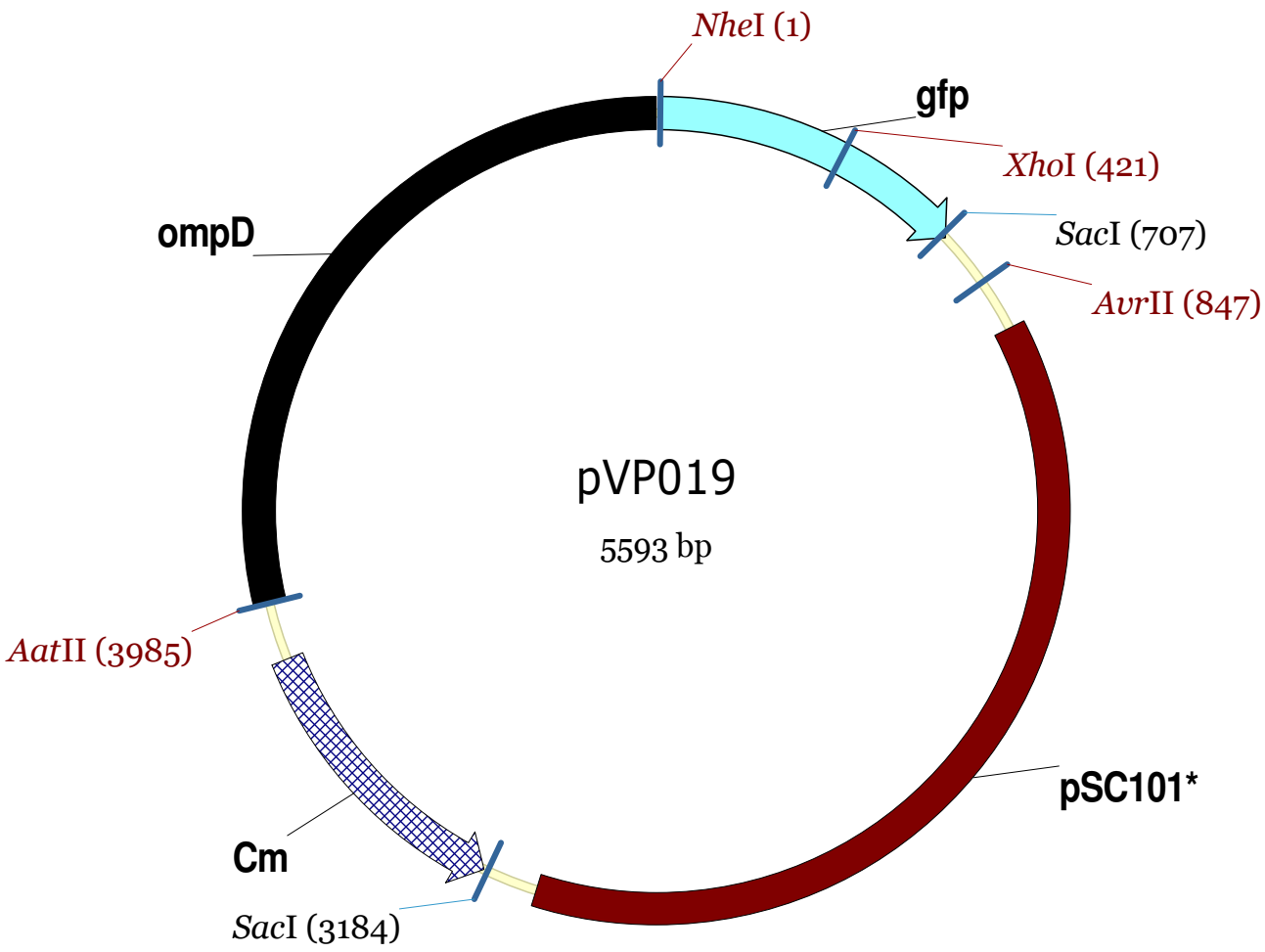
NheI (1)
gfp
XhoI (421)
SacI (707)
AvrII (847)
ompD
pVP019
5593 bp
AatII (3985)
pSC101*
Cm
SacI (3184)

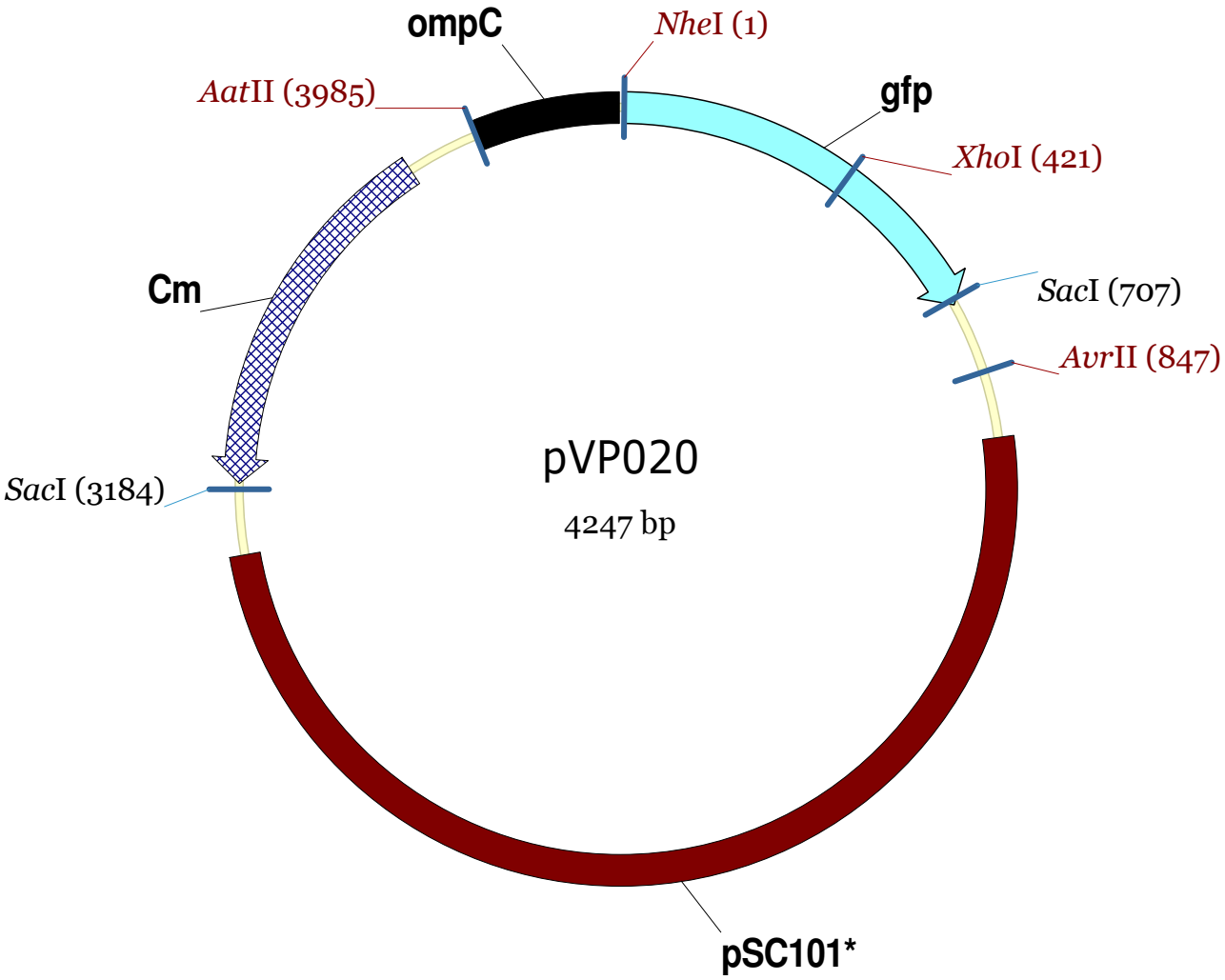
ompC
NheI (1)
AatII (3985)
gfp
XhoI (421)
Cm
SacI (707)
AvrII (847)
pVP020
4247 bp
SacI (3184)
pSC101*

4.2 Deep sequencing analysis of small noncoding RNA and mRNA targets of the global post-transcriptional regulator, Hfq

Alexandra Sittka, Sacha Lucchini, Kai Papenfort, Cynthia M. Sharma, Katarzyna Rolle, Tim T. Binnewies, Jay C. D. Hinton, and Joerg Vogel

PLoS Genetics, 2008

OPEN ACCESS Freely available online

PLoS GENETICS

Deep Sequencing Analysis of Small Noncoding RNA and mRNA Targets of the Global Post-Transcriptional Regulator, Hfq

Alexandra Sittka[1], Sacha Lucchini[2], Kai Papenfort[1], Cynthia M. Sharma[1], Katarzyna Rolle[1], Tim T. Binnewies[3], Jay C. D. Hinton[2]*, Jörg Vogel[1]*

1 Max Planck Institute for Infection Biology, RNA Biology, Berlin, Germany, **2** Institute of Food Research, Norwich Research Park, Norwich, United Kingdom, **3** Center for Biological Sequence Analysis, Technical University of Denmark, Lyngby, Denmark

Abstract

Recent advances in high-throughput pyrosequencing (HTPS) technology now allow a thorough analysis of RNA bound to cellular proteins, and, therefore, of post-transcriptional regulons. We used HTPS to discover the *Salmonella* RNAs that are targeted by the common bacterial Sm-like protein, Hfq. Initial transcriptomic analysis revealed that Hfq controls the expression of almost a fifth of all *Salmonella* genes, including several horizontally acquired pathogenicity islands (SPI-1, -2, -4, -5), two sigma factor regulons, and the flagellar gene cascade. Subsequent HTPS analysis of 350,000 cDNAs, derived from RNA co-immunoprecipitation (coIP) with epitope-tagged Hfq or control coIP, identified 727 mRNAs that are Hfq-bound *in vivo*. The cDNA analysis discovered new, small noncoding RNAs (sRNAs) and more than doubled the number of sRNAs known to be expressed in *Salmonella* to 64; about half of these are associated with Hfq. Our analysis explained aspects of the pleiotropic effects of Hfq loss-of-function. Specifically, we found that the mRNAs of *hilD* (master regulator of the SPI-1 invasion genes) and *flhDC* (flagellar master regulator) were bound by Hfq. We predicted that defective SPI-1 secretion and flagellar phenotypes of the *hfq* mutant would be rescued by overexpression of HilD and FlhDC, and we proved this to be correct. The combination of epitope-tagging and HTPS of immunoprecipitated RNA detected the expression of many intergenic chromosomal regions of *Salmonella*. Our approach overcomes the limited availability of high-density microarrays that have impeded expression-based sRNA discovery in microorganisms. We present a generic strategy that is ideal for the systems-level analysis of the post-transcriptional regulons of RNA-binding proteins and for sRNA discovery in a wide range of bacteria.

Citation: Sittka A, Lucchini S, Papenfort K, Sharma CM, Rolle K, et al. (2008) Deep Sequencing Analysis of Small Noncoding RNA and mRNA Targets of the Global Post-Transcriptional Regulator, Hfq. PLoS Genet 4(8): e1000163. doi:10.1371/journal.pgen.1000163

Editor: William F. Burkholder, Stanford University, United States of America

Received May 8, 2008; **Accepted** July 14, 2008; **Published** August 22, 2008

Funding: This work was supported by the core strategic grant of the BBSRC to the Hinton lab, and funds from the DFG Priority Program SPP1258 *Sensory and Regulatory RNAs in Prokaryotes* to the Vogel lab.

Competing Interests: The authors have declared that no competing interests exist.

* E-mail: jay.hinton@bbsrc.ac.uk (JCDH); vogel@mpiib-berlin.mpg.de (JV)

Introduction

Until now, global gene expression control studies have generally focussed on the transcriptional regulation exerted by the specific action of DNA binding proteins, and on the post-translational regulation governed by specific protein–protein interactions. In comparison, little is known about how RNA binding proteins facilitate the global control of gene expression at the post-transcriptional level. However, the latest discoveries of many small noncoding RNAs (sRNAs) in both pro- and eukaryotes have shown that the interaction of RNA with proteins plays a prominent role in the regulation of cellular processes. In bacteria, the majority of the sRNAs basepair with target mRNAs to regulate their translation and/or decay [1,2,3], and these regulatory events commonly require the bacterial Sm-like protein, Hfq [4,5].

Hfq is one of the most abundant RNA-binding proteins in bacteria [6,7,8]. First identified in *Escherichia coli* as a host factor required for phage Qβ RNA replication ~40 years ago [9], Hfq is now known to have an important physiological role in numerous model bacteria [5]. Almost half of all sequenced Gram-negative and Gram-positive species, and at least one archaeon, encode an Hfq homologue [10,11]. Hfq interacts with regulatory sRNAs and mRNAs, and much of its post-transcriptional function is caused by the facilitation of the generally short and imperfect antisense interactions of sRNAs and their targets [12,13,14,15,16,17]. However, Hfq can also act alone as a translational repressor of mRNA [18,19], and can modulate mRNA decay by stimulating polyadenylation [20,21]. In addition, roles of Hfq in tRNA biogenesis have recently been described [22,23].

The pleiotropy of an *hfq* deletion mutation was first apparent from the multiple stress response-related phenotypes in *E. coli* [24], and partly reflects the reduced efficiency of translation of *rpoS* mRNA, encoding the major stress sigma factor, σS [25,26]. However, Hfq clearly impacts on bacterial physiology in a much broader fashion, including the σS-independent control of virulence factors in pathogenic bacteria (e.g., [27,28,29,30, 31,32,33]). Specifically, deletion of *hfq* attenuates the ability of the model pathogen *Salmonella enterica* serovar Typhimurium (*S.* Typhimurium) to infect mice, to invade epithelial cells, to secrete virulence factors and to survive inside cultured macrophages [32].

Author Summary

The past decade has seen small regulatory RNA become an important new mediator of bacterial mRNA regulation. This study describes a rapid way to identify novel sRNAs that are expressed, and should prove relevant to a variety of bacteria. We purified the epitope-tagged RNA-binding protein, Hfq, and its bound RNA by immunoprecipitation from the model pathogen, *Salmonella enterica* serovar Typhimurium. This new strategy used Next Generation pyrosequencing to identify 727 Hfq-bound mRNAs. The numbers of sRNAs expressed in *Salmonella* was doubled to 64; half are associated with Hfq. We defined the exact coordinates of sRNAs, and confirmed that they are expressed at significant levels. We also determined the Hfq regulon in *Salmonella*, and reported the role of Hfq in controlling transcription of major pathogenicity islands, horizontally acquired regions, and the flagellar cascade. Hfq is reported to be a global regulator that affects the expression of almost a fifth of all *Salmonella* genes. Our new approach will allow sRNAs and mRNAs to be characterized from different genetic backgrounds, or from bacteria grown under particular environmental conditions. It will be valuable to scientists working on genetically tractable bacteria who are interested in the function of RNA-binding proteins and the identification of sRNAs.

Loss of Hfq function also results in a non-motile phenotype for *Salmonella* and the deregulation of >70 abundant proteins, including the accumulation of outer membrane proteins (OMPs); the latter is accompanied by a chronic activation of the σE (σ^{24})-mediated envelope stress response [32,34]. Hfq has also been implicated in the control of *Salmonella* gene expression changes induced by the low gravity condition experienced during spaceflight [35].

Understanding how Hfq controls *Salmonella* gene expression at the post-transcriptional level requires the identification of its sRNA and mRNA ligands. In a pioneering global study in *E. coli*, Zhang *et al.* (2003) used co-immunoprecipitation (coIP) with Hfq-specific antisera and direct detection of the bound RNAs on genomic high-density oligonucleotide microarrays. Although this method proved highly effective for detecting diverse sRNAs and mRNAs in *E. coli*, the requirement for high-density microarrays and specialized antibodies has hampered similar studies in other bacteria. An alternate approach identified individual abundant Hfq-associated RNAs by cDNA cloning or direct sequencing [29,36]; however, these methods are not appropriate for large-scale analyses.

To overcome these limitations for the global identification of Hfq targets in *Salmonella*, we have now used high-throughput pyrosequencing (HTPS, a.k.a. deep sequencing) of RNA associated with an epitope-tagged Hfq protein (Figure 1). We show that this approach recovers Hfq-binding sRNAs with high specificity, and identifies their boundaries with unprecedented resolution. We report the discovery of novel *Salmonella* sRNA genes, detect the expression of many conserved enterobacterial sRNA genes, and provide a set of potential mRNA targets in this model pathogen. Comparison with the transcriptomic profile of an *hfq* mutant showed that Hfq mediates its pleiotropic effects by regulating the master transcription factors of complex regulons, and explained how Hfq is required for *Salmonella* virulence. In microbiology, deep sequencing has been used extensively for genome sequencing, either of individual microbial species [37] or of bacterial communities [38]. This study is the first report that describes the use of deep sequencing to study protein-bound mRNA from bacteria, and to discover bacterial noncoding RNAs.

Results

Transcriptomic Profiling Reveals a Large Hfq Regulon in *Salmonella*

To detect genes that are, directly or indirectly, regulated by Hfq the transcriptomic mRNA profile of the *Salmonella* wild-type and of mutant strain JVS-0255 (Δ*hfq*) was determined. We used two different conditions for the comparison; aerobic growth in L-broth to early stationary phase (ESP; OD_{600} of 2) was chosen because the *hfq* mutation causes drastic protein pattern changes in ESP *Salmonella* [32], and overnight growth in high-salt medium under oxygen limitation (SPI-1-inducing conditions) to specifically activate the *Salmonella* virulence genes required for host cell invasion [39]. Hfq-dependent mRNAs that showed statistically significant changes (≥2-fold) were identified, and we discovered that 734 genes were differentially expressed in the Δ*hfq* strain grown to ESP (279 up-regulated genes, 455 down-regulated genes, Figure 2 and Table S1). Of the 71 proteins known to be Hfq-dependent (as determined by protein levels on 2D gels; [32]), 50% were regulated by Hfq at the transcriptional level (Table S1). Consequently, Hfq controls the expression of 17% of all *Salmonella* genes at ESP (based on the 4425 annotated ORFs; [40]). Growth under SPI-1 inducing conditions revealed 164 differentially expressed genes in Δ*hfq* (91 up-, 73 down-regulated; Table S2). 69% of these genes overlapped with the changes seen in ESP. Taken together, Hfq affects at least 785 genes, or 18% of the *Salmonella* genome.

Classification of the genes deregulated at ESP (Table 1) showed that Hfq impacted upon 26 of the 107 functional groups annotated for *Salmonella* [41]; in seven groups ≥50% of all genes were misregulated. In four of the five major *Salmonella* pathogenicity islands (i.e., SPI-1, -2, -4, -5), and in the flagellar and chemotaxis pathways, >60% of genes were down-regulated, which explains the previously observed invasion and motility phenotypes of Δ*hfq* [32]. Because Hfq affects the mRNAs of σS (RpoS) and σE (RpoE) [25,26,34,42], two major alternative stress σ factors of enterobacteria, we quantified the expression of these sigma factors in *Salmonella* at the mRNA level (ESP) and at the protein level (ESP and SPI-1 inducing conditions). σE mRNA and protein levels were strongly elevated in Δ*hfq* under both conditions tested (Figure S1), confirming the previously observed chronic induction of the envelope stress response. Levels of *rpoS* mRNA were slightly increased, yet RpoS protein levels were strongly decreased. This reflects the poor translation of *rpoS* mRNA in the absence of Hfq (Figure S1 and [25,26]). We used published lists of σE- and σS-dependent genes of *Salmonella* [43,44] to determine how the Hfq-dependent changes we observed were related to the σE and/or σS regulons. We discovered that 55% (41/75) and 73% (54/74) of σE- and σS-dependent genes were also Hfq-dependent. Therefore, a proportion of the Hfq-dependent gene expression changes observed at ESP and under SPI-1 inducing conditions were indirect effects caused by modulation of σS and σE levels by Hfq.

The *S.* Typhimurium genome contains about 444 genes acquired by horizontal gene transfer (HGT; [45]). 122 or 17 of these HGT genes were Hfq-dependent under ESP or SPI-1 inducing conditions, respectively (16 genes being Hfq-dependent under both conditions; Tables S1, S2). In other words, Hfq regulates 28% of the HGT genes, significantly more than the 18% regulated when using the entire *Salmonella* genome for calculation. This may indicate a role of Hfq in the acquisition of DNA from foreign sources, by regulating expression of newly acquired genes at the RNA level.

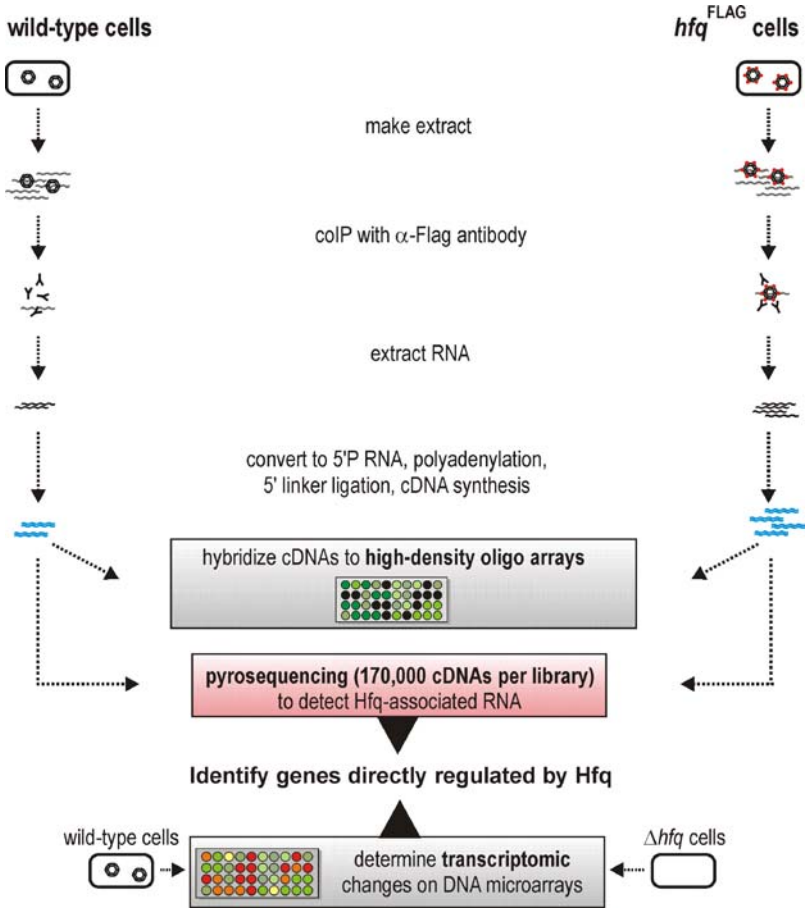

Figure 1. Strategy to identify Hfq targets. RNA was co-immunoprecipitated with Hfq in extracts from ESP-grown *Salmonella* cells (wild-type and chromosomal *hfq*^{FLAG} strain) using an anti-FLAG antibody. The extracted RNA was converted to 5′ monophosphate RNA, and subsequently into cDNA, followed by direct pyrosequencing. Our approach was validated by hybridization of cDNA to high density oligo microarrays. In addition, total RNA of the wild-type strain and its *hfq* deletion mutant was used for transcriptomic analysis using *Salmonella* SALSA microarrays.
doi:10.1371/journal.pgen.1000163.g001

Deep Sequencing of Hfq-Associated RNAs

The variety of transcriptional regulons that showed Hfq-dependent expression patterns could either be mediated by the binding of certain regulatory sRNAs or of specific mRNAs by Hfq. To identify the direct Hfq targets we co-immunoprecipitated RNA with the chromosomally FLAG epitope-tagged Hfq protein expressed by a *Salmonella hfq*^{FLAG} strain [46]. CoIP was performed in extracts prepared from ESP-grown bacteria. The Hfq-associated RNA was converted to cDNA, and a total of 176,907 cDNAs pooled from two independent biological experiments was then characterised by high-throughput pyrosequencing [37]. The resulting sequences, from here on referred to as "Hfq cDNAs", ranged in length from 1 to 145 bp, and 92% were ≥18 bp (Figure 3A). Disregarding small cDNAs (<18 bp), 122,326 sequences were unequivocally mapped to the *Salmonella* genome by WU-BLAST searches (http://blast.wustl.edu/; Figure 2). About half of the mapped cDNAs (57,529) were derived from rRNA, tRNA, and housekeeping RNAs (tmRNA, M1 RNA, and SRP RNA; Figure 3B). Of the remaining 64,797 sequences, the majority corresponded to mRNA regions (53% matched the sense strand of protein-coding regions), followed by known/predicted conserved sRNAs (18%; [47]; for distribution see Figure 3C), predicted *Salmonella*-specific sRNAs (1%; [46]) and sequences that were antisense to ORF regions (3%). The remaining 25% of cDNAs mostly represented intergenic regions (IGRs) and 5′/3′ UTRs, with a few antisense transcripts to tRNAs, rRNAs, and sRNAs (0.1%; Figure 3B).

To confirm that our procedure did effectively enrich Hfq-associated RNAs, we analyzed 175,142 cDNAs from a control coIP using wild-type *Salmonella* (expressing untagged Hfq). Of these "Control cDNAs" which ranged in length from 1 to 290 bp (Figure 3A), 145,873 sequences were ≥18 bp in size and could be correlated to the *Salmonella* chromosome. Most of the inserts (91%) were abundant rRNA, tRNA, and housekeeping RNA transcripts (Fig 3B). The remaining 13,725 sequences were used to calculate the level of enrichment of Hfq-bound RNA (see below).

Visualizing Hfq-Dependent RNAs at the Nucleotide Level

Upon WU-BLAST matching, the number of cDNA hits for each nucleotide position for either strand of the *Salmonella* chromosome was calculated, and visualized using the *Integrated Genome Browser (IGB, Affymetrix)*. This browser allows the visualization of both whole genomes and individual genomic regions. Figure 4 shows the distribution of cDNA sequences over a subsection of the genome, i.e. the ~40 kb SPI-1 virulence region, for which we observed strong enrichment of Hfq cDNAs over the Control cDNAs. As well as the 35 mRNAs of protein-coding genes, SPI-1 encodes the Hfq-dependent InvR sRNA [46]. Enrichment of InvR by coIP with FLAG-tagged Hfq was previously demonstrated by Northern blot analysis [46], and this

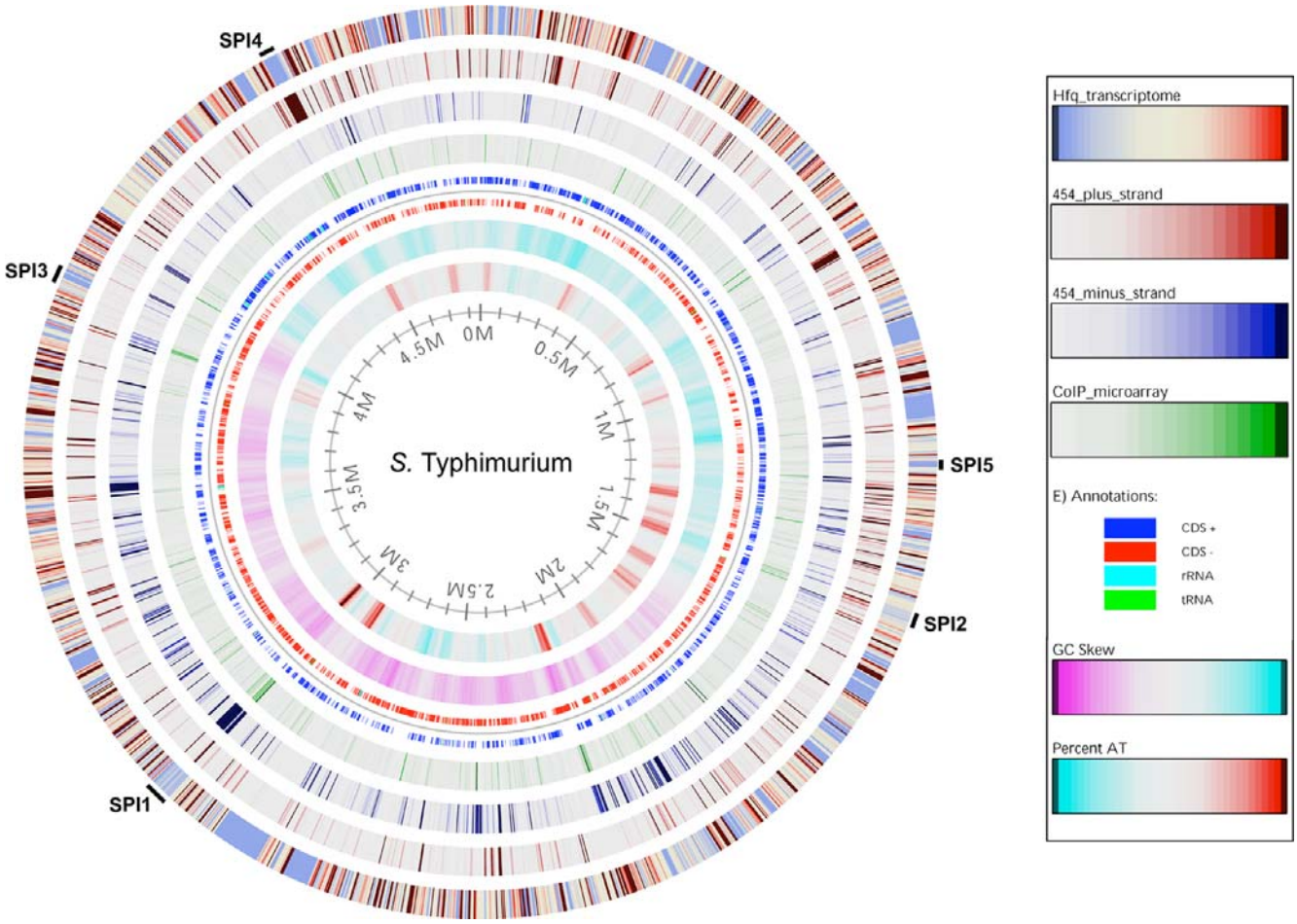

Figure 2. Correlation between HTPS, coIP-on-chip and transcriptomic data upon the *S.* Typhimurium chromosome. The data obtained from transcriptomic, cDNA sequencing and coIP-on-chip analyses of ESP-grown bacteria were mapped onto the *Salmonella* chromosome for direct comparison. The outer (1st) ring displays changes in gene expression in the Δ*hfq* strain compared to the parental SL1344 strain. Genes that are down-regulated in the Δ*hfq* strain are shown as blue; genes that are up-regulated are shown as red. The next three circles show regions coding for Hfq-associated RNA identified by deep sequencing (2nd ring shows positive strand, and 3rd ring shows negative strand) or coIP-on-chip (4th ring). Ring 5 shows the location of coding sequences on the positive strand (CDS+), on the negative strand (CDS−), and the tRNA and rRNA genes. GC-skew [110] is shown in ring 6; purple and blue regions have a GC skew that is below or above the genomic average, respectively. AT-content is shown in ring 7; blue and red regions have an AT-content that is below or above the genomic average, respectively. Numbers on the inside of the innermost circle are the location relative to position zero measured in millions of base-pairs (Mbp) of the *Salmonella* LT2 genome. The location of the SPI-1 to SPI-5 is indicated. An invaluable zoomable version of this atlas is available online at http://www.cbs.dtu.dk/services/GenomeAtlas/suppl/zoomatlas/?zpid = Styphimurium_LT2_Atlas ; click on the region of interest to accurately visualize the data at the level of individual genes.
doi:10.1371/journal.pgen.1000163.g002

result is confirmed by the strong cDNA peak seen at the *invR* locus located at the right-hand SPI-1 border (Figure 4).

Hfq-Dependent sRNAs Are Highly Associated with Hfq

Inspection of the cDNA libraries revealed that a major class were derived from sRNA regions. These sRNAs, as well as their enrichment by Hfq coIP, are listed in Tables 2 and S3. The three most abundant sRNAs, according to the numbers of Hfq cDNA sequences are InvR, SraH (a.k.a. RyhA) and SroB (RybC), and are known to be strongly bound by Hfq [17,46]; coIP of Hfq enriched these three sRNAs by 30- to 57-fold, in comparison to the control reaction. For example, InvR, which binds Hfq with a k_D of 10 nM [46], was represented by 3,236 Hfq cDNAs and 113 Control cDNAs (Table 2). In contrast, other sRNAs not expected to be Hfq-dependent were found in equal numbers in the two samples. For example, the CsrB or CsrC sRNAs which target the conserved RNA-binding protein, CsrA [48], were represented by almost equal numbers in the Hfq and Control cDNAs (CsrB, 67/69; CsrC, 63/64; Table 2). Moreover, cDNAs of the abundant yet Hfq-independent 6S RNA [49] were found in smaller numbers in the Hfq than in the control library (451 versus 836; Table 2).

Figure 5 illustrates the distribution of cDNAs of the three predominant Hfq-bound RNAs and of the Hfq-independent 6S RNA. cDNAs of both the InvR (89 nt; [46]) and SroB (84 nt; [50]) sRNAs mapped along the entire RNA coding sequence from the transcriptional start site to the Rho-independent terminator. SraH, which is transcribed as an unstable 120 nt precursor and processed into an abundant ~58 nt RNA species (3′ part of SraH; [17,51]), was almost exclusively recovered as the processed sRNA. Notably, the borders of the cDNA clusters were in perfect agreement with previous 5′ and/or 3′ end mapping data of the four sRNAs [46,50,51,52]. In other words, our cDNA sequencing approach not only detects association with Hfq, but also identifies the termini of expressed sRNAs at nucleotide-level resolution.

Table 1. Pathway clustering of Hfq-dependent genes at ESP.

pathway[a]	genes in pathway[b]	% up[c]	% down[d]	% genes regulated
Flagellar system	**53**	**0**	**87**	**87**
Chemotaxis	**19**	**0**	**84**	**84**
Fimbrial proteins	24	0	20	20
SPI1	**39**	**0**	**90**	**90**
SPI2	**40**	**0**	**72.5**	**72.5**
SPI3	29	0	14	14
SPI4	**6**	**0**	**100**	**100**
SPI5	**8**	**0**	**62.5**	**62.5**
ABC transporter	188	11	7	**28**
Cyanoamino acid metabolism	10	20	10	**30**
Cystein metabolism	15	20	0	**20**
Fatty acid metabolism & biosynthesis	20	15	15	**30**
Fructose & mannose metabolism	64	2	11	**13**
Glutamate metabolism	29	7	7	**14**
Lipopolysaccharidee biosynthesis	28	3.5	3.5	**7**
Glycerophospholipid metabolism	24	17	12.5	**29.5**
Glycine, serine & threonine metabolism	35	31.5	3	**34.5**
Glycolysis/Gluconeogenesis	28	3	21	**24**
Nitrogen metabolism	33	15	6	**21**
Pentose phosphate pathway	32	12.5	19	**31.5**
Purine metabolism	73	11	4	**15**
Pyrimidine metabolism	49	10	0	**10**
Pyruvate metabolism	49	12	0	**12**
Ribosome	78	35	0	**35**
Selenoamino acid, sulfur metabolism	**18**	**33**	**17**	**50**
Starch & sucrose metabolism	31	3	26	**29**

Hfq-dependent genes in ESP-grown *Salmonella* are shown in Table S1.
[a]Pathway classification according to KEGG (http://www.genome.jp/kegg/; [21]). Pathways in which ≥50% of genes are Hfq-regulated are shadowed.
[b]Number of genes involved in pathway (acc. KEGG).
[c,d]Numbers in percent of genes that were up- or down-regulated in Δ*hfq* compared to wt, (Table S1).
doi:10.1371/journal.pgen.1000163.t001

Identification of Expressed *Salmonella* sRNAs

To evaluate the sRNA expression profile of *Salmonella* more extensively, we analyzed three classes of sRNA candidate loci for coverage by the Hfq and Control cDNAs. First, cDNAs of *E. coli* sRNA candidate loci with predicted conservation in *Salmonella* were inspected [17,47,49,50,51,53,54]. Second, we counted cDNAs of *Salmonella*-specific sRNAs predicted in two recent global screens [46,55]. Third, we manually inspected cDNAs from a third of the *Salmonella* chromosome (first 1.6 Mb) and all major five pathogenicity islands for expression patterns of IGRs indicative of new sRNA genes, and for possible enrichment by Hfq coIP. Using criteria similar to [49], our evaluation of these loci considered orphan promoter/terminator signals, and possible conservation in bacteria other than *E. coli*. Of the latter two classes of candidates (summarized in Table S3), those with an Hfq enrichment factor ≥10 and/or candidates showing strong promoter/terminator predictions were selected for Northern blot analysis. To assess sRNA expression under relevant environmental conditions, we probed RNA from five stages of growth in standard L-broth from exponential to stationary phases, and from two conditions known to strongly induce the expression of the major SPI-1 [39,56] or SPI-2 [57] virulence regions. The results of this analysis are summarized in Table 2 (the whole set of candidates tested is shown in Table S3); including the 26 previously detected *Salmonella* sRNAs [34,46,55,58,59,60,61,62,63], a total of 64 *Salmonella* sRNAs can now be considered to be experimentally validated.

We used Northern blots to detect 10 of the 31 newly identified *Salmonella* sRNAs under the environmental conditions that were tested (Figure 6, Tables 2 and S3). These sRNAs yielded stable transcripts, predominantly in the 50 to 100 nt range (Figure 6A and B). Faint bands of larger transcripts were observed for STnc150 (150 nt), and STnc400 (190 nt), resembling certain *E. coli* sRNAs such as SraH whose precursor is rapidly degraded whilst the processed form accumulates [51]. The STnc150, 400, and 560 sRNAs are almost constitutively expressed, whereas STnc500, 520 and 540 are only expressed in certain environmental conditions. Intriguingly, STnc580 can only be detected under SPI-1 inducing conditions that mimic the environment *Salmonella* encounters in the host intestine. Generally, only candidates represented by ≥20 cDNAs in a cDNA pool yielded a signal on Northern blots (Tables 2 and S3). While this suggests some correlation between intracellular abundance and cDNA frequency, we note the case of STnc150, for which a single cDNA was recovered yet a strong signal was obtained on Northern blots. In contrast, several

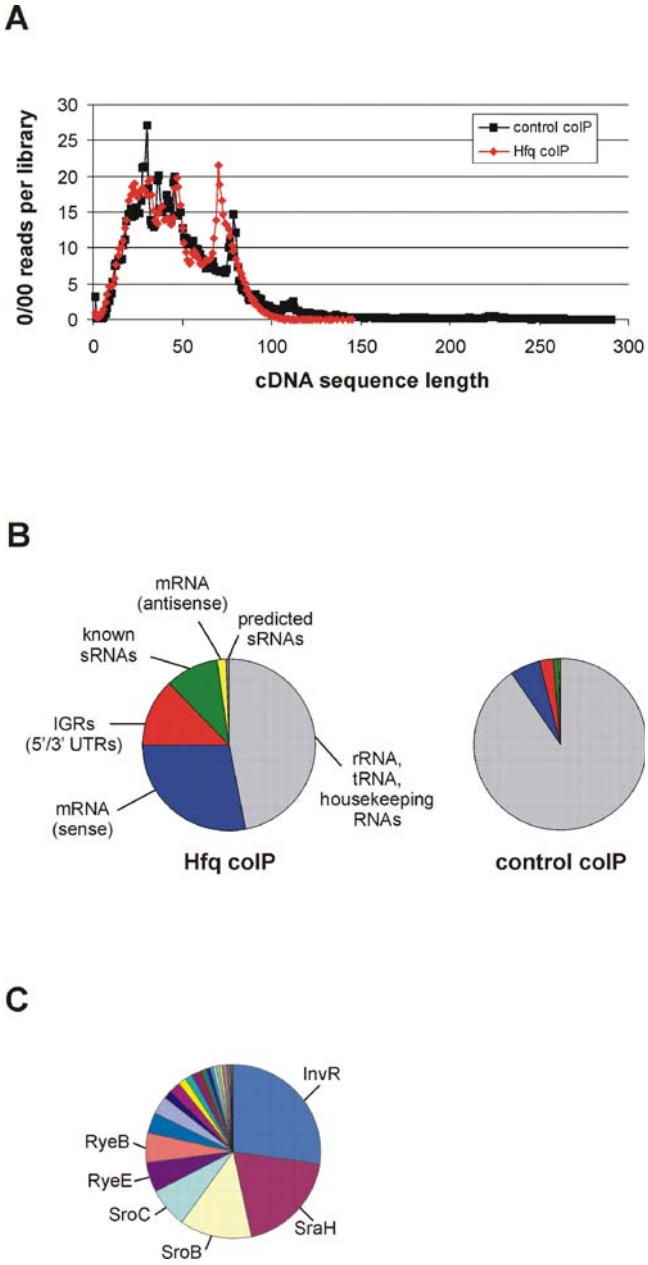

Figure 3. Statistical analysis of the cDNA sequencing results of Hfq-associated RNA. (A) The pyrosequencing results were analyzed by plotting the number of cDNA reads over the read length in bp. The length distribution of all resulting sequences is shown. (B) Pie diagram showing the relative proportions of the different RNA species contained in all sequences that mapped to the *Salmonella* genome. The rRNA, tRNA and housekeeping RNAs are shown in grey. Left panel: Hfq coIP, right panel: control coIP. (C) Pie diagram showing the relative proportions of all Hfq-associated sequences that unequivocally mapped to known sRNA sequences. The names of the six most frequently recovered sRNAs are given.
doi:10.1371/journal.pgen.1000163.g003

candidates with >20 cDNAs failed the Northern blot validation (Table S3). We speculated that the corresponding cDNAs were derived from 5′ or 3′ UTRs of larger mRNA transcripts, and tested this on Northern blots of agarose gels. We tested 14 of such candidates which had the appropriate orientation to flanking mRNA genes to be UTR-derived; six of these showed signals ranging in size from 500 to 2000 nucleotides (STnc180, Stnc190, STnc330, STnc470, STnc610, and STnc640; Figure S2 and Table S3), and are likely to be processed mRNA species.

Three sRNAs expressing stable transcripts of ~85 to 90 nts originate from close to, or within, IS200 transposable elements (Figure 6B). STnc290 and STnc440 are expressed just upstream of *tnpA*_4 and *tnpA*_6, respectively, whereas STnc490 is antisense to the translational start site of the IS200 transposase ORF. IS200 elements generally posses two stem-loop structures, one of which is a Rho-independent transcription terminator that prevents read-through from genes located upstream of the integration site [64]. Given their location, the STnc290 sRNA could originate from processing of the STM3033 transcripts reading into the *tnpA*_4 terminator structure; by analogy, STnc440 would be derived from STM4310 transcripts. If so, this would constitute interesting cases in which transposon insertion has created stable sRNAs. The other IS200 stem-loop functions as a translational repressor by sequestering the start codon of the transposon ORF [64]; STnc490 overlaps with this structure on the opposite strand, and by acting as an antisense RNA may function as an additional repressor of IS200.

We determined whether 8 of the new *Salmonella* sRNAs showed an Hfq-dependent pattern of transcript abundance that correlated with Hfq binding (Figure 6C). The STnc290, 440, 490, 520, 540 and 560 sRNAs were all enriched by Hfq coIP (Table 2), by factors up to 51-fold (STnc440). The expression of the four sRNAs with the highest enrichment factors (STnc290, 440, 520, 560) was strongly reduced in Δ*hfq*, and so classified as Hfq-dependent; in contrast, the accumulation of STnc150, STnc490 and STnc540 (≥1.0-, 5.1-, and 3.3-fold enrichment, respectively) was unaffected in the absence of Hfq. STnc500, which is only detected in samples originating from cultures at OD_{600} of 1, and STnc580, which seems to be specifically expressed under the SPI-1 inducing condition, were not detected on these blots.

In addition to the sRNAs listed above, the cDNAs included two loci predicted to encode small peptides, i.e. shorter than the 34 amino acid cut-off used to define ORFs in the current *Salmonella* genome annotation [40]. These are referred to as STnc250 and STnc570 in Table 2, and correspond to the predicted small *ypfM* and *yneM* mRNA-encoding genes of *E. coli* [49]. Probing of the *Salmonella* loci yielded signals of stable short mRNAs which are expressed in a growth phase-dependent manner (Figure S3).

Hfq-Associated mRNAs

To determine which of the 34,136 cDNAs were derived from Hfq-bound mRNAs and represented genuine mRNA targets, a stringent cutoff was used. An mRNA coding region (CDS) was required to be represented by ≥10 cDNAs to be considered significant, which identified 727 Hfq-bound mRNAs (cistrons) for further analysis. Table 3 lists the top 42 mRNAs with at least 100 cDNAs in the Hfq coIP library (Table S4 lists all 727 mRNAs). In the genome browser, many of these enriched mRNAs were readily visible as a distinct cDNA cluster, e.g., the *ompD* mRNA (encoding the major *Salmonella* outer membrane protein) shown in Figure 7A. A survey of the transcriptomic data revealed that 33% of the Hfq-bound mRNAs showed an Hfq-dependent pattern of gene expression (Table S1). The reciprocal analysis showed that 32% of the Hfq-dependent mRNAs were bound to Hfq (Table S1). We attribute the observed partial overlap of the Hfq coIP and the transcriptomic data (33%) to three major factors. First, Hfq regulates transcription factors, de-regulation of which alters the expression of downstream genes. In other words, not every gene deregulated in the Δ*hfq* strain is necessarily a "direct" Hfq target, i.e. its mRNA bound by Hfq. Second, there may be a considerable

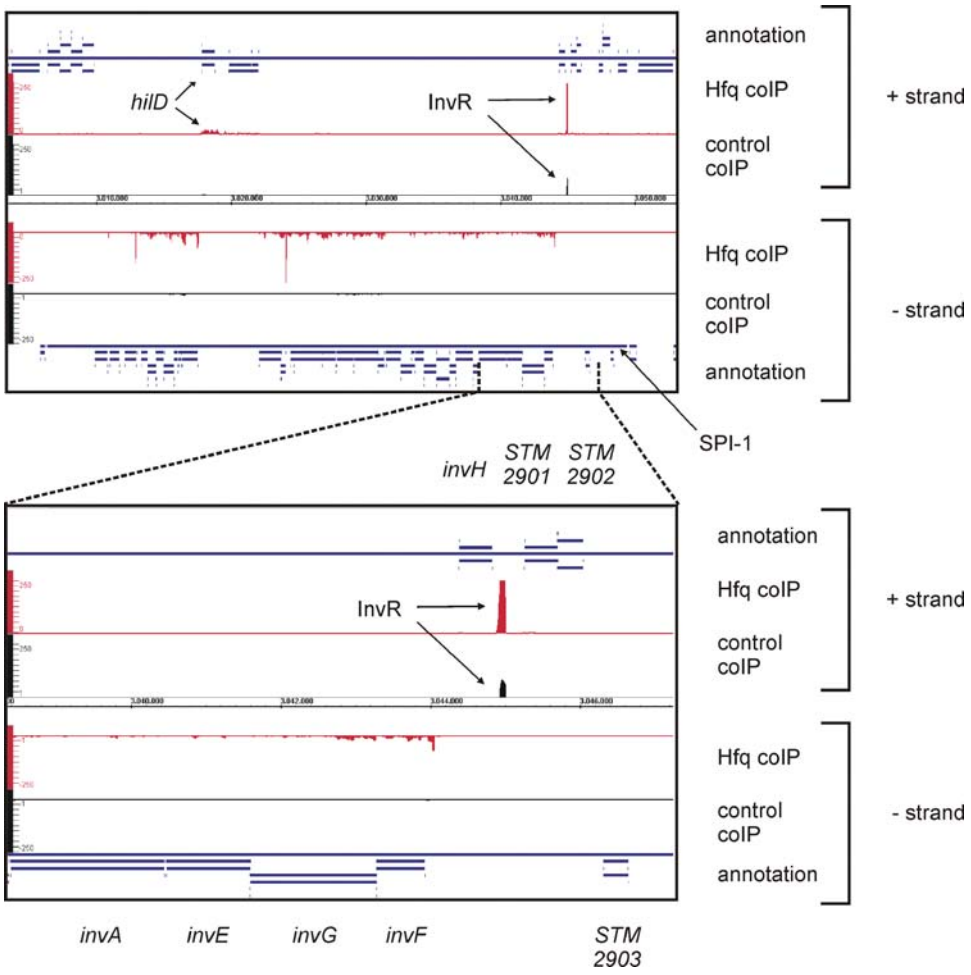

Figure 4. Visualization of pyrosequencing data for the *Salmonella* pathogenicity island 1 (SPI-1) with the Integrated genome Browser (Affymetrix). The upper panel shows an extraction of the screenshot of the Integrated Genome Browser, with the mapped Control and Hfq cDNAs of the SPI-1 region. Shown are the annotations for the "+" and "–" strand (blue), the cDNA sequence distribution from the Hfq coIP for the "+" and "–" strand (red), the cDNA-clone distribution for the control coIP for the "+" and "–" strand (black), and the genome coordinates in the center for the entire SPI-1. The annotation for SPI-1 and the Hfq coIP peaks for *hilD* and the sRNA InvR in the Hfq coIP are indicated. Note, that the clone numbers per nucleotide are scaled to a maximum of 250 for the Hfq and the control coIP, which truncates the high peak for InvR in the Hfq coIP library (>3000 cDNAs). The lower panel shows a close up of the *invR* locus and its adjacent genes.
doi:10.1371/journal.pgen.1000163.g004

number of Hfq-associated mRNAs below our very stringent cut-off for Hfq-association; increasing sequencing depth will overcome this problem. Third, the precise borders of most 5′/3′ UTRs are unknown in *Salmonella* (and any other bacterial genome sequence); consequently, calculations of Hfq enrichment were limited to the CDS of an mRNA. As outlined further below (Figure 7B), this can skew the overall enrichment factor.

To validate our cDNA sequencing approach for the detection of Hfq-bound mRNAs by the conventional approach, we hybridized the RNA obtained from Hfq and control coIP to a *S.* Typhimurium oligonucleotide microarray. Analysis of this coIP-on-Chip experiment with SAM-software (Statistical Analysis of Microarrays; FDR<0.01) identified 365 enriched mRNAs. Nearly half (45%) of these mRNAs corresponded to regions identified by the deep sequencing approach (Table S5; $P<10e-10$). The overlap increased to 67% when genes that showed enrichment values above 5 were taken into consideration. Although coIP-on-Chip displays a lower sensitivity than deep sequencing these two independent methods do generate comparable results for the identification of mRNA-protein interactions.

Genome annotations of protein-coding genes are generally limited to the mRNA coding regions (CDS). Whilst Tables 3 and S4 list absolute hit numbers in annotated CDS, the detailed analysis of cDNA distribution over a given mRNA gene often revealed a more complex picture. For example, the number of *ompA* cDNAs does not drastically differ in the two libraries (Hfq coIP, 102; control coIP, 77), which would question whether *ompA* is an Hfq-bound mRNA. However, up to 12-fold enrichment is seen in some sections of the *ompA* mRNA, e.g., around the AUG and in the central CDS (Figure 7B). Note that the availability of cDNA hit numbers for every single nucleotide of the *Salmonella* chromosome offers the possibility to also analyze 5′ and 3′ UTRs of mRNAs, which are not included in Tables 3 and S4, but could also be targeted by Hfq.

Figure 8A further illustrates the complex enrichment patterns of diverse mRNAs, some of which may be explained by previous data obtained for these transcripts, as discussed below. *i)* cDNAs of Hfq-bound mRNAs of *hilD* (encoding a key transcription factor of the *Salmonella* invasion gene island, SPI-1), *fliC* (which encodes a major flagellin), or *flhDC* (encoding the major transcription factor

Table 2. Compilation of expressed *Salmonella* sRNAs and their enrichment by Hfq coIP.

sRNA[a]	Alternative IDs [b]	Identification [c]	Adjacent genes [d]	Orientation [e]	5′ end [f]	3′ end [f]	cDNA reads control coIP [g]	cDNA reads Hfq coIP [h]	Enrichment [i]	Northern [j]
sgrS	*ryaA*	I	*yabN/leuD*	← → ←	128574	128812	3	61	20.3	
isrA	-	II	STM0294.1n/STM0295	→ → →	339338	339760	0	0		
sroB	*rybC*	I	*ybaK/ybaP*	← → ←	556005	556085	27	1530	56.7	
sroC	-	I	*gltJ/gltI*	← ← ←	728913	728761	26	898	34.5	
rybB	p25	III	STM0869/STM0870	→ ← ←	942632	942554	3	103	34.3	
STnc490[k]	-	IV	*clpA/tnpA_1*	→ ← →	1024975	1025165	75	385	5.1	~85 nt
isrB-1	-	II	*sbcA*/STM1010	← → ←	1104179	1104266	2	4	2.0	
STnc500	-	IV	STM1127/STM1128	← ← ←	1216157	1216440	7	84	12.0	~65 nt
STnc150	-	V	*icdA*/STM1239	→ ← →	1325914	1325649	0	1	≥1.0	~90 nt
isrC	-	II	*envF/msgA*	← → ←	1329145	1329432	0	1	≥1.0	
STnc520	-	IV	STM1248/STM1249	→ ← ←	1332809	1334044	12	100	8.3	~80 nt
isrD	-	II	STM1261/STM1263	→ ← →	1345788	1345738	0	0		
ryhB-2	*isrE*	II	STM1273/*yeaQ*	→ ← →	1352987	1352875	0	0		
STnc540	-	IV	*himA/btuC*	→ → →	1419369	1419570	7	23	3.3	~85 nt
rprA	IS083	I	*ydik/ydiI*	← ← ←	1444938	1444832	37	286	7.7	
rydB	tpe7, IS082	I	*ydiH*/STM1368	→ → ←	1450415	1450519	4	10	2.5	
STnc570[l]	*yneM* ORF	IV	*ydeI/ydeE*	→ ← ←	1593723	1594413	2	21	10.5	~190 nt
STnc560		IV	*ydeI/ydeE*	→ → ←	1593723	1594413	10	290	29.0	~90 nt
isrF	-	II	STM1552/STM1554	→ ← ←	1630160	1629871	1	0		
rydC	IS067	I	STM1638/*cybB*	→ → ←	1729673	1729738	5	245	49.0	
micC	IS063, tke8	III	*nifJ/ynaF*	→ ← →	1745786	1745678	0	15	≥15.0	
STnc580	-	IV	*dbpA*/STM1656	← ← ←	1749662	1750147	11	311	28.3	~100 nt
ryeB	tpke79	I	STM1871/STM1872	→ ← ←	1968155	1968053	24	653	27.2	
dsrA	-	I	*yodD/yedP*	→ ← →	2068736	2068649	6	149	24.8	
rseX	-	I	STM1994/*ompS*	← → →	2077175	2077269	0	3	≥3.0	
ryeC	tp11	I	*yegD*/STM2126	→ → →	2213871	2214016	42	72	1.7	
cyaR	*ryeE*	III	*yegQ*/STM2137	→ → →	2231130	2231216	31	659	21.3	
isrG	-	II	STM2243/STM2244	← → →	2344732	2345013	0	0		
micF	-	III	*ompC/yojN*	← → →	2366913	2367005	0	11	≥11.0	
isrH-2	-	II	*glpC*/STM2287	→ ← →	2394582	2394303	0	0		
isrH-1	-	II	*glpC*/STM2287	→ ← →	2394753	2394303	0	0		
STnc250[l]	*ypfM* ORF	V	*acrD/yffB*	→ ← →	2596882	2596789	6	24	4.0	~220 nt
ryfA	tp1	I	STM2534/*sseB*	→ → ←	2674934	2675228	3	6	2.0	
glmY	tke1, *sroF*	I	*yfhK/purG*	← ← ←	2707847	2707664	20	92	4.6	
isrI	-	II	STM2614/STM2616	→ ← ←	2761576	2761329	0	2	≥2.0	

Table 2. cont.

sRNA[a]	Alternative IDs [b]	Identification [c]	Adjacent genes [d]	Orientation [e]	5′ end [f]	3′ end [f]	cDNA reads control coIP [g]	cDNA reads Hfq coIP [h]	Enrichment [i]	Northern [j]
isrJ	-	II	STM2614/STM2616	→ ← ←	2762031	2761957	1	0		
isrK	-	II	STM2616/STM2617	← ← ←	2762867	2762791	0	0		
isrB-2	-	II	STM2631/sbcA	→ ← →	2770965	2770872	0	0		
isrL	-	II	*smpB*/STM2690	→ ← →	2839399	2839055	0	0		
isrM	-	II	STM2762/STM2763	← → →	2905050	2905378	0	0		
isrN	-	II	STM2764/STM2765	← → ←	2906925	2907067	0	0		
micA	*sraD*	I	*luxS/gshA*	← → ←	2966853	2966926	1	128	128.0	
invR	STnc270	III	*invH*/STM 2901	→ → →	3044924	3045014	113	3236	28.6	
csrB	-	III	*yqcC/syd*	← ← ←	3117059	3116697	69	67		
gcvB	IS145	III	*gcvA/ygdI*	← → ←	3135317	3135522	12	402	33.5	
omrA	*rygB*	III	*aas/galR*	← ← →	3170208	3170122	0	51	≥51.0	
omrB	*t59, rygA, sraE*	III	*aas/galR*	← ← →	3170408	3170322	1	52	52.0	
STnc290	-	V	*tnpA_4*/STM3033	← ← ←	3194996	3194914	2	72	36.0	~85 nt
isrO	-	II	STM3038/STM3039	← → →	3198380	3198580	0	0		
ssrS	-	I	*ygfE/ygfA*	→ → →	3222098	3222280	836	451		
rygC	t27	I	*ygfA/serA*	→ → ←	3222913	3223065	14	17	1.2	
rygD	tp8, C0730	I	*yqiK/rfaE*	→ ← ←	3362474	3362327	17	104	6.1	
sraF	tpk1, IS160	I	*ygjR/ygjT*	→ → →	3392069	3392261	0	25	≥25.0	
sraH	*ryhA*	I	*yhbL/arcB*	← → ←	3490383	3490500	55	2292	41.7	
ryhB-1	*sraI*, IS176	I	*yhhX/yhhY*	← ← →	3715495	3715401	0	2	≥2.0	
istR-1		VI	*ilvB/emrD*	← ← →	3998147	3998018	0	0		~75 nt
istR-2		VI	*ilvB/emrD*	← ← →	3998147	3998018	0	0		~140 nt
STnc400	-	V	STM3844/STM3845	→ → →	4051145	4051340	112	42		~55 nt
glmZ	k19, *ryiA*, *sraJ*	I	*yifK/hemY*	→ → ←	4141650	4141854	20	196	9.8	
Spf	*spf*	I	*polA/yihA*	→ → ←	4209066	4209175	2	33	16.5	
csrC	*sraK, ryiB, tpk2*	III	*yihA/yihI*	← → →	4210157	4210400	63	64		
isrP	-	II	STM4097/STM4098	← → ←	4306719	4306866	0	2	≥2.0	
oxyS	-	I	*argH/oxyR*	→ ← →	4342986	4342866	0	10	≥10.0	
sraL	*ryjA*	III	*soxR*/STM4267	→ ← →	4505010	4504870	0	0		
STnc440	-	V	STM4310/*tnpA_6*	→ → →	4559193	4559277	9	456	50.7	~85 nt
isrQ	-	II	STM4508/STM4509	← → →	4762997	4763158	0	0		

[a]Gene names of *Salmonella* sRNAs that have been experimentally proven here, and in previous studies. Method of identification is given in the third column. sRNA names follow *Salmonella* and/or *E. coli* nomenclature referenced in (Hershberg *et al.*, 2003; Padalon-Brauch *et al.*, 2008; Papenfort *et al.*, 2008), except STnc490, 500, 520, 540, 560, 570, 580, which have been newly predicted in this study (see Supplementary Table S3).
[b]Alternative sRNA IDs. References in (Hershberg *et al.*, 2003; Padalon-Brauch *et al.*, 2008; Papenfort *et al.*, 2008).
[c]Evidence for sRNAs in *Salmonella*.
(I) Conserved sRNA found in *Salmonella* cDNA libraries, and previously shown to be expressed in *E. coli* (relevant ref. in (Papenfort *et al.*, 2008); Table 1).
(II) sRNA previously predicted and validated on Northern blots in *Salmonella* by (Padalon-Brauch *et al.*, 2008).

Table 2. cont.

(III) sRNA previously validated on Northern blots in *Salmonella* (Altier *et al.*, 2000; Figueroa-Bossi *et al.*, 2006; Fortune *et al.*, 2006; Papenfort *et al.*, 2006; Papenfort *et al.*, 2008; Pfeiffer *et al.*, 2007; Sharma *et al.*, 2007; Viegas *et al.*, 2007).
(IV) sRNA predicted through cDNA sequencing and validated by Northern blot analysis in this study.
(V) sRNA previously predicted by (Pfeiffer *et al.*, 2007) is recovered in cDNA sequences and validated by Northern blot analysis in this study.
(VI) IstR sRNAs (Vogel *et al.*, 2004) were not recovered in cDNA sequences but their expression in *Salmonella* validated by Northern blot analysis in this study (Figure S5).
[d]Flanking genes of the intergenic region in which the sRNA candidate is located.
[e]Orientation of sRNA candidate (middle) and flanking genes (→ and ← denote location of a gene on the clockwise or the counterclockwise strand of the *Salmonella* chromosome).
[f]Genomic location of sRNA candidate gene according to the *Salmonella typhimurium* LT2 genome. For STnc470 through STnc640 start and end of the entire intergenic region are given.
[g]Out of 145,873 sequences in total.
[h]Out of 122,326 sequences in total.
[i]Enrichment factor calculated by the number of blastable reads from Hfq coIP over control coIP.
[j]Denotes verification on Northern blot in this study for new RNA transcripts; the estimated size is given in nucleotides.
[k]The cDNA reads map antisense internally of the IS200 element. Based on sequence identity they map to all IS200 elements (*tnpA_1* to *tnpA_6*).
[l]STnc250 and STnc570 contain small ORFs annotated as *ypfM* or *yneM*, respectively, in *E. coli* (Wassarman *et al.*, 2001).
doi:10.1371/journal.pgen.1000163.t002

of the *Salmonella* flagellar genes) were distributed over the entire length of the relevant gene, including the ~300 nt 3′ UTR in the case of *hilD*. Either Hfq does target such a large number of sites on these three mRNAs, or alternatively, given that Hfq is a ribosome-bound protein, these cDNAs may derive from polysome-bound mRNAs. *ii)* cDNAs of *ompD* were also distributed over the entire *ompD* locus, and abruptly ended 50 nt downstream of the *ompD* stop codon, at the predicted Rho-independent terminator; a major cDNA cluster was observed around the *ompD* AUG start codon, i.e. the −70 to +19 region (for separate display of control coIP, Hfq coIP, and enrichment curves see Figure 7A). Intriguingly, this particular region binds Hfq with high affinity *in vitro* ($k_D \leq 1$ nM; [32]). Binding of Hfq to the *ompD* AUG region may control translation initiation analogous to the Hfq-mediated repression of the *E. coli ompA* mRNA [18]. Similarly, cDNAs representing *dppA* clustered at the 5′ end of this mRNA, from the transcriptional +1 site into the N-terminal (signal peptide) coding region. The Hfq-dependent sRNA, GcvB, is known to target the *dppA* 5′ UTR [58], and our data suggest that Hfq-binding to this *dppA* region could enhance GcvB action. *iii)* cDNA clones of the ~10kb *flgBCDEF-GHIJKL* mRNA (flagellar components) were almost exclusively derived from the terminal, 80 nt region downstream of the *flgL* stop codon which includes the terminator. It is possible that Hfq controls flagellar operon mRNA expression through modulation of mRNA decay initiating at the 3′ end. *iv)* Almost all of the 48 cDNAs of the dicistronic *glmUS* mRNA mapped in two clusters to the *glmUS* IGR (188 nt). cDNAs of the upstream cluster start with the adenosine of the *glmU* UGA stop codon and span the first 73 nt of the IGR. In *E. coli*, *glmUS* mRNA undergoes RNaseE-dependent cleavage within the *glmU* UGA to generate a monocistronic *glmS* mRNA [65,66]; the *glmS* mRNA is activated by the GlmZ sRNA, which binds Hfq [49] and the *glmUS* IGR [19]. As mentioned for GcvB/*dppA*, Hfq is likely to aid the binding of GlmZ to the *glmUS* mRNA in the region of the two clusters of cDNAs.

It is worth noting that the extended steps of lysate preparation and antibody incubation involved in the Hfq coIP protocol do cause some mRNA degradation [17]. Our Northern blots did not detect full-length mRNA in the RNA samples from the *Salmonella* Hfq coIP (data not shown). We believe that the sequenced cDNAs were synthesized from a mixture of shorter cDNA fragments, rather than from intact transcripts of several kb in length. The short cDNAs that were prepared from Hfq coIP have the advantage of favoring the primary Hfq binding region.

To confirm that Hfq bound to enriched mRNA regions, corresponding fragments of the *dppA*, *glmUS*, *flhD* and *hilD* mRNAs were *in vitro*-synthesized, and analyzed in gel mobility shift assays (Figure 8B). These RNA fragments were fully shifted by addition of ≤50 nM Hfq hexamer, which suggested significantly stronger binding than to the previously tested, non-specific *metK* mRNA ($k_D \geq 250$ nM; [32]) which is not regulated by Hfq and was not recovered by Hfq coIP (Tables S1 and S4). Thus, the cDNA sequences appear to represent high-affinity, primary binding sites of Hfq on mRNAs.

Mechanisms of Pleiotropic Hfq Effects in Virulence and Flagellar Pathways

Our analyses revealed an intriguing relationship between the transcriptomic and deep sequencing data; the genes belonging to some regulons were consistently down-regulated in the Δ*hfq* mutant, yet Hfq only associated with a few of the relevant mRNAs. For example, the transcriptomic data showed that the entire SPI-1 pathogenicity island was down-regulated in the Δ*hfq* mutant, but the Hfq coIP only showed a strong enrichment for a small subset

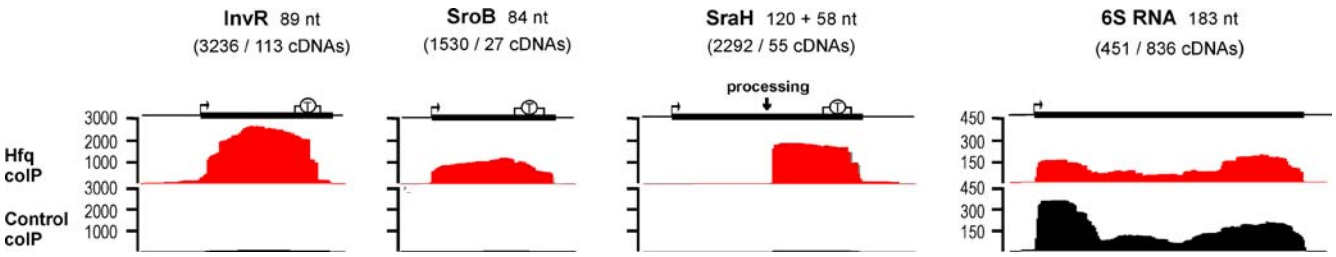

Figure 5. Visualization of the clone distribution of exemplar Hfq dependent and independent sRNAs in *Salmonella*. Clone distribution for sequences mapped to InvR, SroB, SraH, or 6S sRNAs (red: Hfq coIP, black: control coIP). The vertical axis indicates the number of cDNA sequences that were obtained. A bent arrow indicates each sRNA promoter, a circled "T" its transcriptional terminator.
doi:10.1371/journal.pgen.1000163.g005

of SPI-1 genes (*hilC*, *hilD*, *invFGAC*, *sicA*, *sip operon*, *prgHK*, and *orgB*; Tables S1, S4 and Figures 4, S4). Of these, *hilD* encodes the primary transcriptional activator of the SPI-1 region [67]. We hypothesized that loss of Hfq-association with *hilD* mRNA in Δ*hfq* causes loss of HilD protein synthesis, and thereby one of the strongest *hfq* phenotypes, i.e. loss of SPI-1 activation and virulence factor (effector protein) secretion. If so, ectopic HilD overexpression should restore SPI-1 effector secretion to Δ*hfq*. As predicted, overproduction of HilD from a P_{BAD} expression plasmid restored SPI-1 effector secretion to almost wild-type levels in the absence of Hfq (Figure 9A; compare lanes 1 and 4), and also rescued expression of the PrgI needle protein indicative of a functional SPI-1 secretion apparatus (data not shown). In contrast, ectopic production of HilA, the SPI-1 transcription factor that acts downstream of HilD, failed to influence the secretion defect of Δ*hfq*. Preliminary data from gentamicin protection assays that assess epithelial cell invasion of *Salmonella*, suggests that overexpression of HilD increased the invasion rate of the Δ*hfq* strain by a factor of ten (data not shown). Thus, by identifying the *hilD* mRNA as a direct Hfq target, we have revealed the mechanism of part of the pleiotropic virulence defect of the Δ*hfq* strain.

In an analogous situation, 87% of the flagellar genes were down-regulated in the Δ*hfq* mutant, yet Hfq primarily bound to the *flhDC* (class I genes), *flgMN*, *flgKL*, *fliAZ*, *fliD*, *fliI* and *fliP* mRNAs (class II genes) and *fliC* mRNA (class III gene; Tables S1, S4 and Figure S4). *flhDC* encodes the key transcription factor of the flagellar gene cascade, and we predicted that loss of this mRNA would account for much of the flagellar defect of Δ*hfq*, which is associated with strongly reduced levels of the major flagellin, FliC (Figure 9B). Ectopic expression of *flhDC* restored the levels of FliC to almost wild-type levels in the Δ*hfq* strain carrying the pBAD-*flhDC* plasmid (Figure 9B). We note, however, that the previously reported non-motile phenotype of Δ*hfq* on swim agar plates [32] was not rescued by *flhDC* overexpression (data not shown), presumably because the $FlhD_2C_2$-independent chemotaxis genes required for full motility are also down-regulated in the absence of Hfq (Table 1).

Discussion

To understand how bacterial RNA binding proteins such as Hfq mediate the control of global gene expression at the post-transcriptional level, direct targets need to be identified. The first approach that was used to do this in a global fashion involved detection of RNA co-immunoprecipitated with Hfq-specific antibodies on high-density oligonucleotide microarrays, and identified new *E. coli* sRNAs and interesting properties of Hfq [17]. Similarly, microarray-based detection following co-immunoprecipitation of eukaryotic mRNA–protein complexes (mRNPs) identified endogenous organization patterns of mRNAs and cellular proteins [68]. Epitope-tagging of the yeast La homolog was successfully used for global coIP analysis [69]. However, the requirement for custom high-density microarrays and/or species-specific antibodies has impeded similar studies in other organisms. It is now apparent that the ideal sRNA discovery approach would not only detect sRNAs, but would also define their exact sequence. Given the typical genome size of model bacteria (~5 Mb), a high-density oligonucleotide microarray with ~10 million oligonucleotide probes would be required to achieve single basepair resolution. Such arrays do not exist for any organism, and even today's high-density arrays (with 0.5 million features) come with extraordinarily high set-up and printing costs, and are available for very few bacteria. Our strategy remedies these technical and financial limitations.

The identification of Hfq-associated RNAs in *Salmonella* is based upon a powerful chromosomal epitope-tagging approach [70], followed by coIP with a commercially-available antibody, and sequencing of hundreds of thousands cDNAs. The earlier shotgun-cloning studies in bacteria [50,54,71] and many other organisms (reviewed in [72,73]) were limited by costly Sanger-type sequencing of individual cDNA inserts from plasmid vectors. The deep sequencing approach described here avoids a cloning step, and is able to detect small RNAs with unparalleled sensitivity by defining the 5′ and 3′ ends of transcripts at basepair resolution.

Deep sequencing of cDNAs has identified the small RNA component of eukaryotic transcriptomes (e.g., [74,75]), and new classes of noncoding RNAs associated with eukaryotic RNA-binding proteins [76,77]. These studies primarily focussed on the class of 20–30 nucleotide long microRNAs and siRNAs, and typically included size-fractionation steps. Bacterial riboregulators are considerably larger (80-250 nucleotides), and we show that even without prior size fractionation, deep sequencing can capture and define the termini of these large sRNAs.

Our analysis extends the tally of confidently identified sRNAs to 64 in the model pathogen, *S.* Typhimurium (Table 2). Thirty eight of these are conserved sRNAs that were initially identified in *E. coli*, but only a few of their homologues have previously been shown to be expressed in other enteric bacteria [58,59,60,61,62,63,78,79]. A recent study of the widely conserved DsrA and RprA sRNAs [80] failed to validate their expression and/or function in *Salmonella* [81]. Our observation of 149 (DsrA) and 286 (RprA) cDNAs in the Hfq coIP libraries (versus 6/37 in the control library), unequivocally confirmed that these important stress response regulators are both expressed and Hfq-associated. The finding, from this and other studies, that highly-conserved sRNAs are commonly expressed at the transcriptional level should prove useful to researchers working in other bacterial systems.

A significant number of the Hfq-associated cDNAs correspond to sRNA loci that are absent from *E. coli* ([46,55] and Table 2). Of

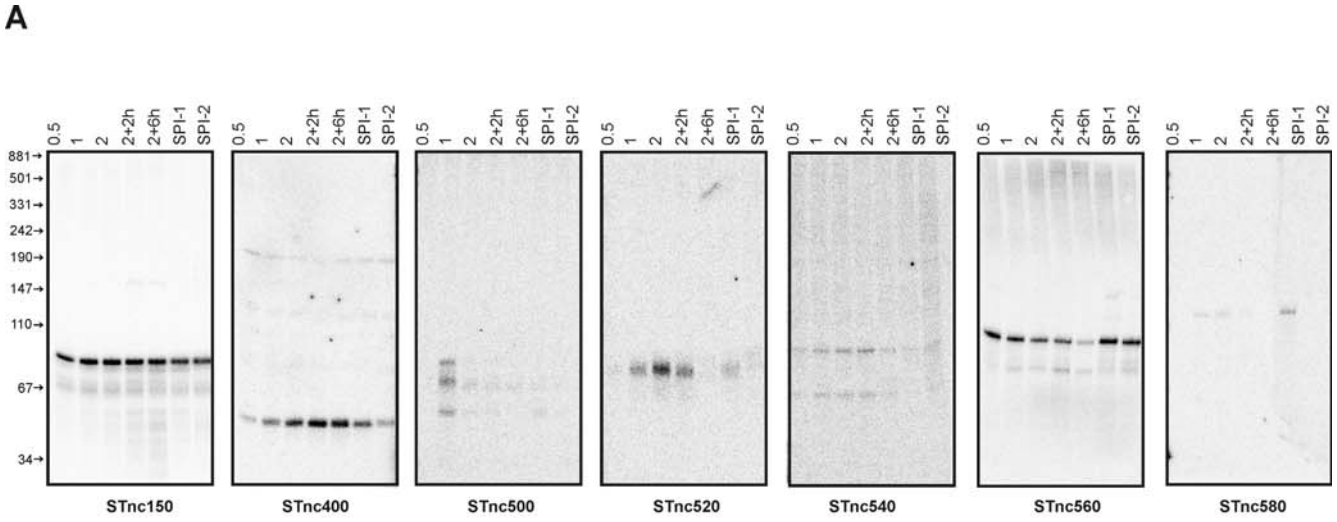
A
0.5
1
2
2+2h
2+6h
SPI-1
SPI-2
881→
501→
331→
242→
190→
147→
110→
67→
34→
STnc150
STnc400
STnc500
STnc520
STnc540
STnc560
STnc580

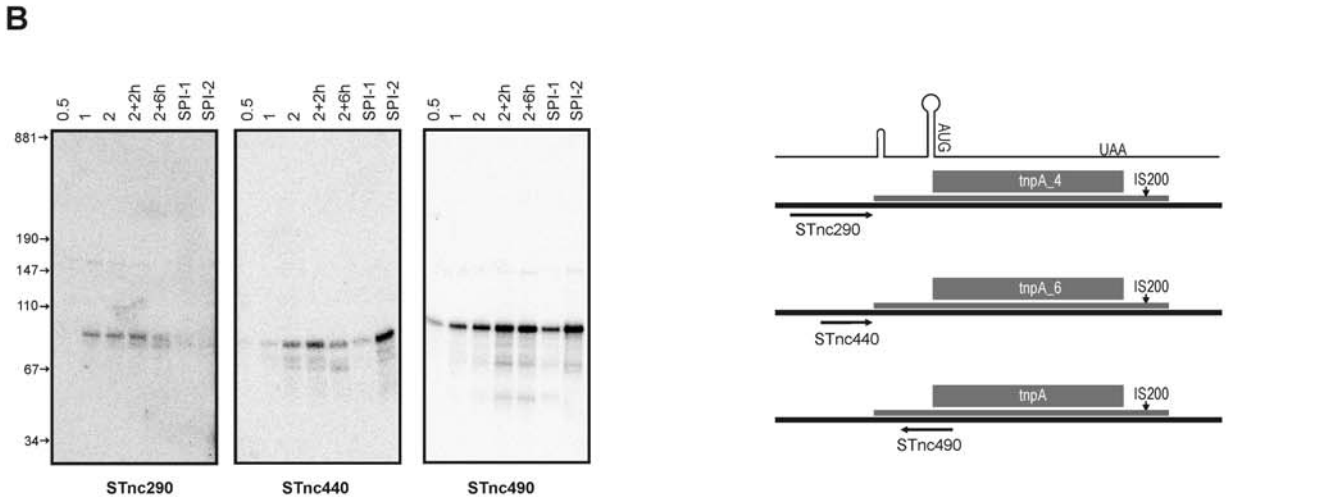
B
0.5
1
2
2+2h
2+6h
SPI-1
SPI-2
881→
190→
147→
110→
67→
34→
STnc290
STnc440
STnc490
AUG
UAA
tnpA_4
IS200
STnc290
tnpA_6
IS200
STnc440
tnpA
IS200
STnc490

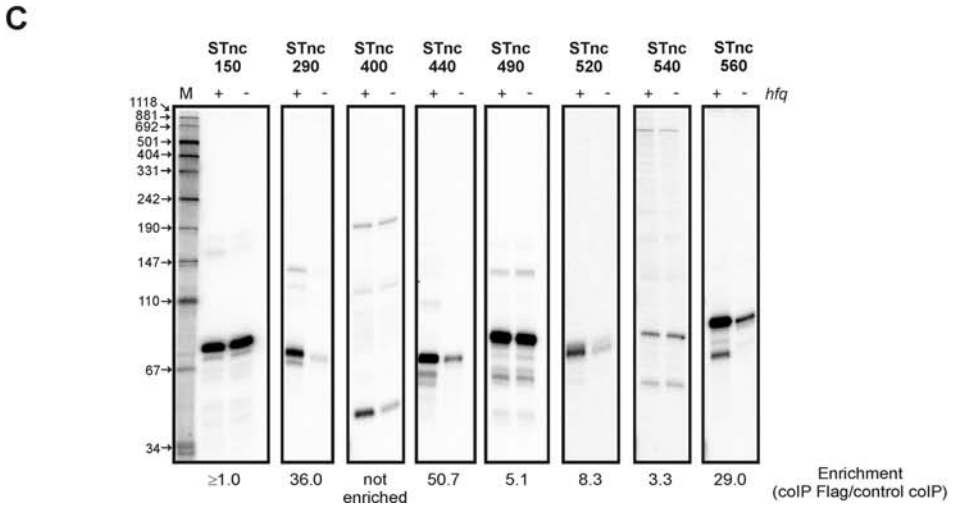
C
STnc 150
STnc 290
STnc 400
STnc 440
STnc 490
STnc 520
STnc 540
STnc 560
M
+
-
hfq
1118
881
692
501
404
331
242
190
147
110
67
34
≥1.0
36.0
not enriched
50.7
5.1
8.3
3.3
29.0
Enrichment (coIP Flag/control coIP)

Figure 6. Expression of 10 new *Salmonella* sRNAs over growth. Total RNA was isolated from *Salmonella* at seven different growth stages and/or conditions and subjected to Northern blot analysis. (A) Blots showing the detection of stable transcripts for seven new sRNAs. The lanes refer to the following samples (from left to right): aerobic growth of the wild-type strain in L-broth to an OD600 of 0.5, 1 or 2; growth continued after the culture reached OD600 of 2 for 2 or 6 hours, respectively; SPI-1 inducing condition; SPI-2 inducing condition. (B) Northern blots of three sRNAs encoded in close proximity (STnc290, STnc440) or antisense (STnc490) to IS200 elements. A schematic presentation of the position of the sRNAs according to the IS200 element is shown to the right. The upper drawing indicates the two stem-loop structures, start codon, and stop codon of the transposase-encoding mRNA of the IS200 elements. The three detected sRNAs are indicated by black arrows. Growth conditions as Panel A. (C) RNA abundance of selected new sRNAs in wild-type (+) versus *hfq* mutant (−) *Salmonella* cells at ESP (OD600 of 2). The enrichment factor of each of these sRNAs in the coIP experiment is given below the blots for comparison.
doi:10.1371/journal.pgen.1000163.g006

these, *invR* exemplifies a sRNA gene that was likely horizontally acquired with the SPI-1 virulence region, early in *Salmonella* evolution [46]. Intriguingly, InvR is the most frequently recovered sRNA (>3,000 cDNAs in the Hfq coIP library), which shows that our approach is not only effective for detecting conserved, but also species-specific sRNAs of recently acquired pathogenicity regions. Horizontal transfer of virulence islands is a driving force in the evolution of bacterial pathogens [82], and knowledge of the functional elements of these islands is key to understanding pathogenesis. Whereas ORF identification in such islands has become routine, island-specific sRNAs are more difficult to recognize by bioinformatic-based approaches.

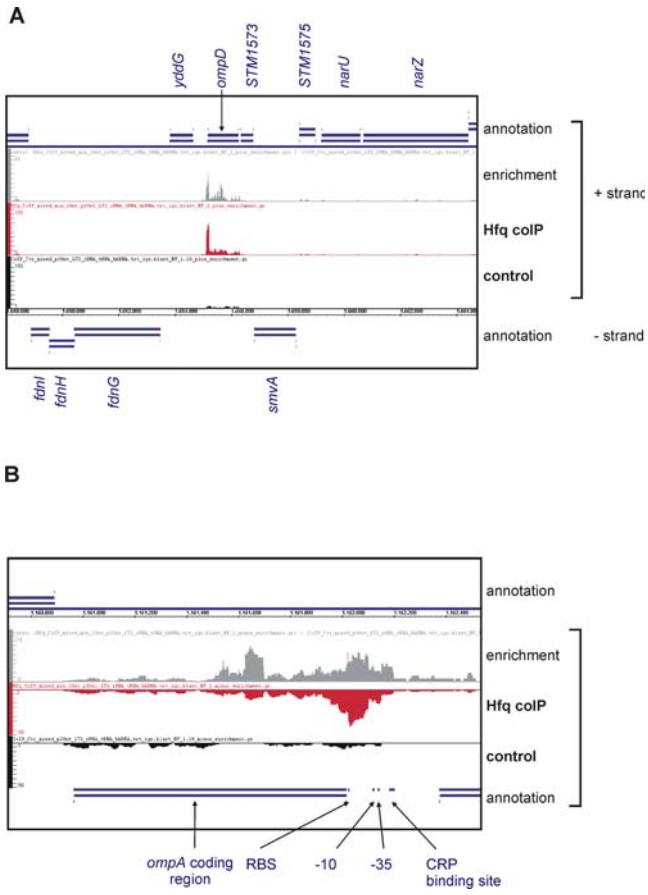

Figure 7. Comparison of Hfq and Control coIP cDNA distributions at the *ompD* and *ompA* loci. Extract of the screenshot of the Integrated Genome Browser, showing the mapped Hfq and Control cDNAs, and the enrichment curve (ratio of reads of Hfq coIP over control coIP) for (A) the *ompD* and (B) *ompA* transcripts. Shown are (from top to bottom) the annotations for the "+" strand (blue), the enrichment curve (grey), the cDNA distributions on the "+" strand for the Hfq coIP (red) and the control coIP (black), the genome coordinates, and the annotations for the "–" strand (blue). In panel A, the annotation of the *ompD* coding region and the flanking genes, *yddG* and STM1573, are indicated. For *ompA*, the CDS, -10 and -35 boxes, as well as the ribosome binding site (RBS) and a CRP binding site are indicated by black arrows.
doi:10.1371/journal.pgen.1000163.g007

Besides confirming InvR, the present study found evidence for the expression of five of the 47 *Salmonella* sRNA candidate loci listed by Pfeiffer *et al.* [46], who predicted orphan promoter/terminator pairs in IGRs (Table S3 and Figure 2). One of these, i.e. STnc250, has turned out as a small mRNA gene (see above). While this study was in progress, others reported the discovery of 18 *Salmonella* expressed sRNA loci [55]. We recovered cDNAs of 8 of these sRNAs (*isrB*-1, *C*, *E*, *I-L*, and *P*; Table 2). The fact that 10 of these sRNAs were not recovered probably reflects their low-level expression under the growth condition used here [55]. This observation suggests an improvement that could be made to our method. RNomics- or microarray-based sRNA discovery methods require sRNAs to be expressed under the chosen assay condition, unlike bioinformatics-aided approaches that score for orphan transcription signals and primary sequence conservation [49,51,83,84] or for conservation of RNA structure [53]. Thus, future studies combining several different growth conditions with increasing sequencing depth are likely to identify even more novel sRNAs.

Regarding the sensitivity of our approach, it is remarkable that RyeB sRNA was found in 653 Hfq cDNAs and 24 Control cDNAs (Table 2); RyeB is late stationary phase-specific [49,50], and barely detectable by probing of *Salmonella* RNA from the coIP assay condition by Northern blot (unpublished results). Moreover, the 24 cDNAs recovered from the control library, i.e. without Hfq coIP, suggest the exciting possibility that deep sequencing of total RNA, without prior enrichment or size-fractionation, will prove to be a successful approach for sRNA discovery. Like any other global method for RNA identification [85,86], our approach is likely to show certain biases, e.g., caused by cross-hybridization in the immunoprecipitation step, or from the limited ability of reverse transcriptase to deal with stable RNA structures in cDNA synthesis, and these will need to be studied in more detail. However, it is clear that deep sequencing resolved the termini of many expressed and/or Hfq-bound sRNAs at basepair resolution (Figure 5), which has not been achieved by other methods.

The combination of HTPS of co-immunoprecipitated sRNAs and mRNAs with transcriptomics partly explains how Hfq acts as a pleiotropic regulator of *Salmonella* gene expression. Transcriptome analysis under two different growth conditions suggests that Hfq regulates the expression of nearly a fifth of all *Salmonella* genes. This proportion of Hfq-dependent genes is similar to *Pseudomonas aeruginosa* (~15% of all genes; [87]), but bigger than for *E. coli* (6.3%; [42]), or *Vibrio cholerae* (5.6%; [30]). However, the different growth conditions and scoring parameters used for these other organisms preclude a direct comparison with our *Salmonella* data. Nonetheless, the strong impact of Hfq on the σS and σE stress regulons that we observed is consistent with the findings in *E. coli* [42] and in part in *V. cholerae* (σE; [30]), and expands the previous work on *Salmonella* σS and σE regulated genes

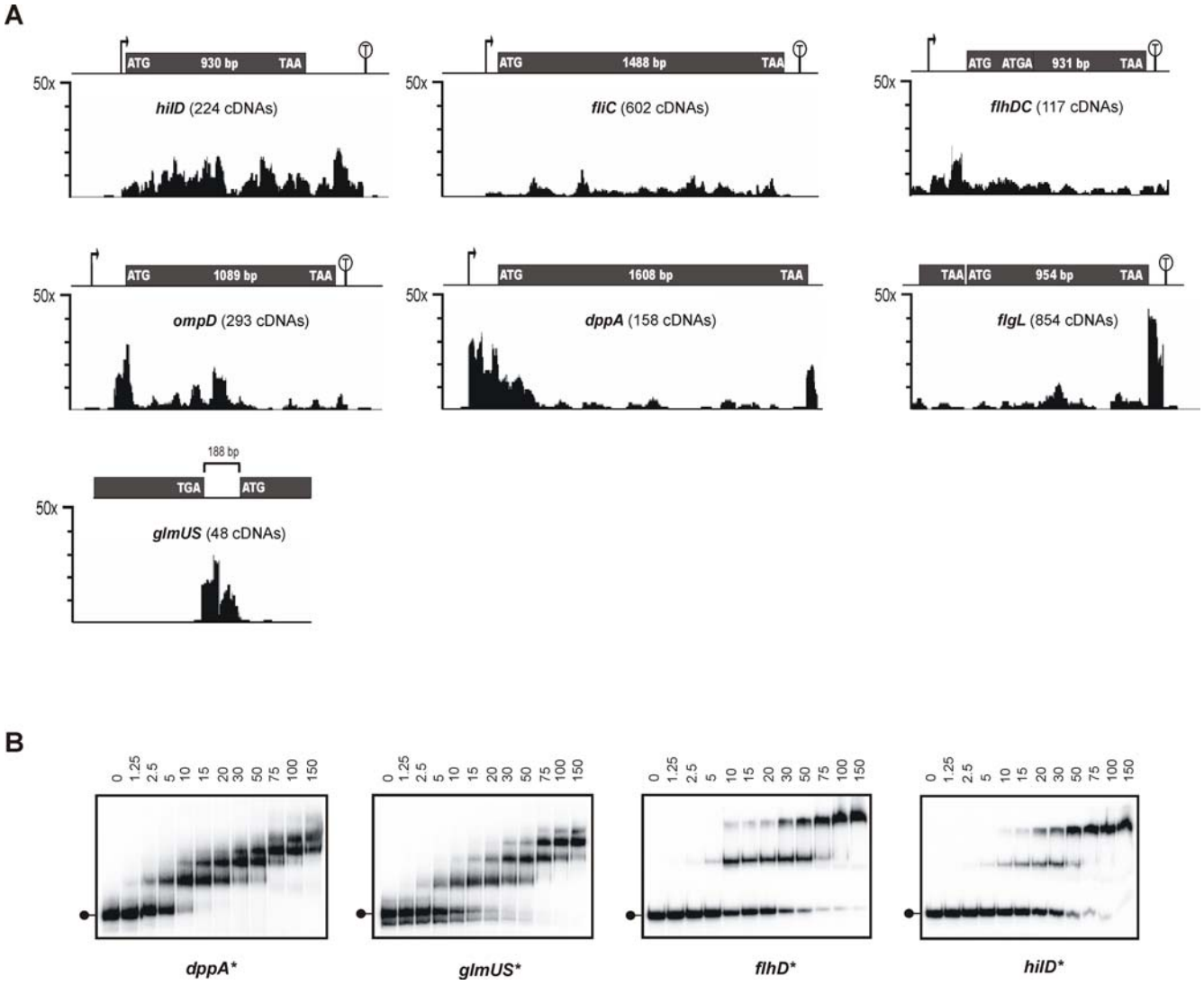

Figure 8. Distribution patterns of cDNAs of Hfq-associated mRNA species and confirmation of binding to Hfq. (A) Different mRNAs are shown with marked open reading frame, promoter and terminator (where known). Start and stop codons are indicated. The clone distribution is represented by a stairstep diagram of fold enrichment in Hfq coIP *vs* control coIP per nucleotide below each mRNA. The vertical axis indicates the enrichment factor in the Hfq coIP calculated over the control coIP. ORF length is given for each gene, for the overlapping ORFs of *flhDC*, or for the intergenic region in the case of *glmUS* mRNA. Numbers in parentheses below each gene name denote number of cDNA sequences obtained from Hfq coIP. Promoters and terminators are indicated as above. (B) The binding of Hfq to four mRNA fragments was confirmed by gel mobility shift assay. ^{32}P-labeled RNA fragments of *dppA*, *glmUS*, *flhD*, or *hilD*, respectively, were incubated with increasing amounts of Hfq protein (concentrations of the hexamer are given in nM above the lanes). The lollipops on the left of the gel panels show the position of the unshifted mRNA fragment. Following 10 minutes incubation at 37°C, samples were resolved on native 6% polyacrylamide gels, autoradiographs of which are shown.
doi:10.1371/journal.pgen.1000163.g008

[34,43,44,88,89,90,91] to a global level. Importantly, our combined transcriptomic and coIP data revealed that Hfq exerts a direct role in gene expression through the control of specific check-points in other well-defined transcriptional regulons, such as HilD in the SPI-1 virulence regulon, and $FlhD_2C_2$ in the flagellar gene expression cascade.

Transcriptomic profiling by itself is clearly unable to differentiate between transcriptional and post-transcriptional effects of Hfq. In contrast, enrichment of a regulated mRNA in the Hfq library has successfully hinted at post-transcriptional regulation by sRNAs. For example, the observation of OmpX overproduction in *Salmonella* Δ*hfq*, combined with *ompX* mRNA enrichment by Hfq coIP in *E. coli* [17], led to the prediction that OmpX synthesis is repressed by an Hfq-dependent antisense sRNA; this sRNA was subsequently identified as CyaR in *Salmonella* [63]. Tables 2 and 3 confirm that both *ompX* mRNA and CyaR strongly associate with *Salmonella* Hfq (22.8-fold and 21.2-fold enrichment, respectively). Our current data set comprises several hundred such candidate mRNAs (Table S4); this catalogue contains many experimentally confirmed targets of *Salmonella* sRNAs, e.g., the *dppA*, *fadL*, *ompD*, or *oppA* mRNAs [34,46,58,59]. Integrating the score for Hfq-association deduced from our experiments, and–where applicable–from the available *E. coli* data [17] into available algorithms such as TargetRNA [92] could significantly improve target predictions for the large class of Hfq-dependent sRNAs.

Such predictions bring new understanding to the pleiotropic phenotypes caused by the absence of Hfq in *Salmonella* [32]. The fact that the *Salmonella hfq* mutant is attenuated for virulence can

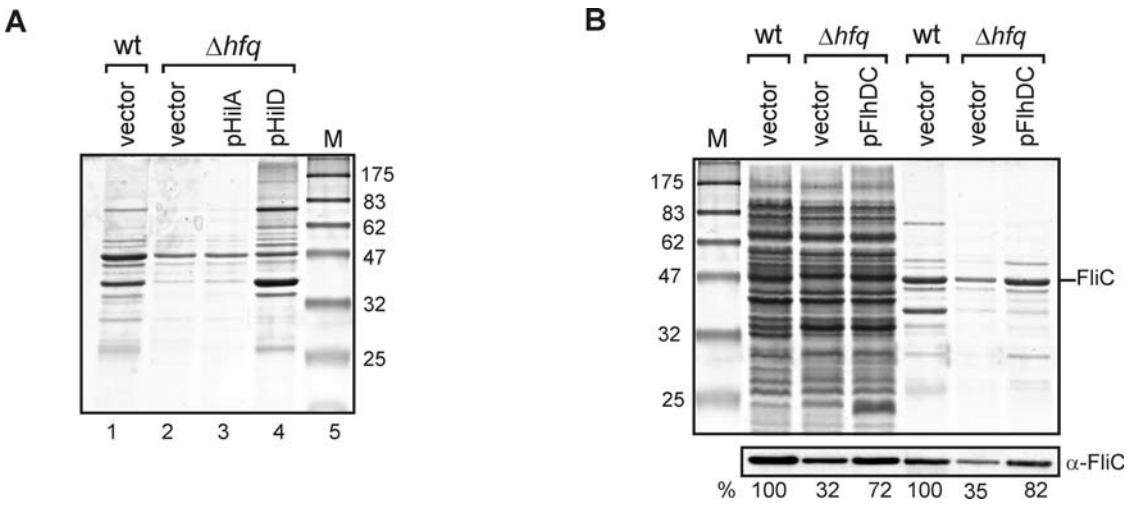

Figure 9. Rescue of complex Δ*hfq* phenotypes by overexpression of identified Hfq target mRNAs. SDS-PAGE analysis (12% gels stained with Coomassie) of (A) secreted proteins upon overexpression of the SPI-1 transcription factors, HilA and HilD from pCH-112 and pAS-0045 (lanes 3 and 4) in *Salmonella* Δ*hfq*. Lanes 1 and 2 show the secreted protein profile of *Salmonella* wild-type and Δ*hfq* bacteria carrying a control vector, pKP8-35. (B) Whole cell and secreted proteins upon overexpression of the flagellar transcription factor, $FlhD_2C_2$. The left hand three lanes show total protein samples, and the right hand three lanes show secreted proteins. Genetic background and plasmids are indicated above the lanes; FlhDC was expressed from plasmid pAS-0081. FliC was also analyzed on a Western blot using a specific antibody (lower panel). FliC protein levels are shown (in %), in comparison to wild-type *Salmonella*, which was set to 100% for either the total protein or secreted protein lanes.
doi:10.1371/journal.pgen.1000163.g009

now be explained by the requirement of Hfq for the expression of all but one key pathogenicity islands of *Salmonella* (SPI-3). In the SPI-1 invasion gene island, HilD acts at the top of a transcription factor cascade to activate SPI-1 genes, and to mediate secretion of effector proteins by the SPI-1 type III secretion system (reviewed in [67,93]). The levels of *hilD* mRNA were sevenfold reduced in Δ*hfq*, but the unchanged activity of a *hilD* promoter fusion in this background (unpublished data) argues against direct transcriptional control by Hfq. Rather, the 7.5-fold enrichment of *hilD* cDNAs by Hfq coIP (Table S4) suggests that *hilD* is post-transcriptionally activated in a Hfq-dependent process, presumably involving an unknown sRNA. Our demonstration that SPI-1 virulence factor secretion is fully restored by HilD overproduction in Δ*hfq* raises the exciting possibility that post-transcriptional *hilD* activation could be key event in *Salmonella* invasion of epithelial cells.

We expect Hfq to have further roles in SPI-1 expression since the protein seems to bind to many mRNAs encoded by this pathogenicity island (Figures 4 and S4). Interestingly, SPI-1 has a significantly higher AT content than the rest of the *S.* Typhimurium chromosome [40], predicting that SPI-1 mRNAs are AU-rich. Coincidently, Hfq primarily recognizes AU-rich single-stranded regions in RNAs [12,94,95,96]. This type of sequence is also recognized by the major endoribonuclease, RNase E, and Hfq has been shown to protect certain RNAs by competitive binding to RNase E sites [97,98]. It is tempting to speculate that Hfq could reduce the impact of DNA from foreign sources by controlling expression of newly acquired AT-rich genes at the RNA level, similar to the role of the H-NS DNA-binding protein in controlling such genes at the DNA level [99,100,101].

Collectively, the present study provides the first picture of the impact of Hfq on *Salmonella* gene expression at both the transcriptional and post-transcriptional level. We believe that more detailed inspection of this freely available data set, in particular of the remaining ~60% of the chromosome that remains to be fully analyzed, as well as sampling under different growth conditions, will expand the gamut of *Salmonella* small mRNA and noncoding RNA genes. In addition, the available data sets should help to discover whether Hfq controls the expression of *cis*-antisense sRNAs that overlap with mRNA coding regions [54], or whether certain *Salmonella* tRNAs are selectively associated with this protein [22,23].

Bacterial genomes encode a large number of RNA binding proteins [102], including globally acting proteins such as the CsrA/RsmA [48] and Csp families [103]. Our generic method will identify the RNA targets of these proteins in any genetically tractable bacterium.

Materials and Methods

Bacterial Strains, Plasmids, and Oligodeoxynucleotides

The *Salmonella enterica* serovar Typhimurium strains used in this study were: JVS-0255 (Δ*hfq*::Cm^R, [32]), JVS-1338 (*hfq*^{FLAG}, [46]), and the isogenic wild-type strain SL1344 [104]. Plasmid pKP8-35 [59] served as a pBAD control plasmid. The SPI-1 transcription factor, HilA, was expressed from pCH-112 [105], and HilD from plasmid pAS-0045 (which carries a *hilD* PCR fragment obtained with primer pair JVO-686/-687 amplified from *Salmonella* DNA, inserted into plasmid pLS-119 [106] by *Nco*I/*EcoR*I cloning). The FlhDC expression plasmid, pAS-0081, was constructed by inserting a PCR fragment obtained with primers JVS-2152/-2153 into plasmid pBAD/*Myc*-His A (Invitrogen) by *Nco*I/*Xho*I cloning. All cloning procedures where carried out in *E. coli* strain Top10 (Invitrogen). Table S6 lists the sequences of oligodeoxynucleotides used in this study for cloning and T7 transcript generation.

Bacterial Growth and L-arabinose Induction

Growth in Lennox (L) broth (220 rpm, 37°C) or on L-plates at 37°C was used throughout this study. Antibiotics (where appropriate) were used at the following concentrations: 50 μg/ml ampicillin, 30 μg/ml chloramphenicol. For early stationary phase (ESP) cultures, 30 ml L-broth in 100 ml flasks were inoculated 1/100 from overnight cultures and incubated at

Table 3. mRNAs represented by ≥100 cDNAs in the pyrosequencing data.

STM number	Gene name[a]	Number of inserts in control coIP[b]	Number of inserts in Hfq coIP[c]	Enrichment[d]	Product[e]
STM4261		254	1042	4.1	putative inner membrane protein
STM2665	*yfiA*	72	648	9.0	ribosome stabilization factor
STM1377	*lpp*	168	608	3.6	murein lipoprotein
STM4087	*glpF*	40	570	14.3	glycerol diffusion
STM1959	*fliC*	248	547	2.2	flagellar biosynthesis protein
STM2874	*prgH*	73	415	5.7	needle complex inner membrane protein
STM2267	*ompC*	63	385	6.1	outer membrane protein C precursor
STM2882	*sipA*	36	354	9.8	secreted effector protein
STM2885	*sipB*	126	335	2.7	translocation machinery component
STM4326	*aspA*	79	328	4.2	aspartate ammonia-lyase
STM2925	*nlpD*	30	300	10.0	lipoprotein
STM4086	*glpK*	115	278	2.4	glycerol kinase
STM2883	*sipD*	34	269	7.9	translocation machinery component
STM0739	*sucD*	14	261	18.6	succinyl-CoA synthetase alpha subunit
STM1572	*ompD*	76	246	3.2	putative outer membrane porin precursor
STM2898	*invG*	16	226	14.1	outer membrane secretin precursor
STM2879	*sicP*	6	224	37.3	secretion chaparone
STM2283	*glpT*	30	221	7.4	sn-glycerol-3-phosphate transport protein
STM1091	*sopB*	23	216	9.4	secreted effector protein
STM1732	*ompW*	28	206	7.4	outer membrane protein W precursor
STM0451	*hupB*	14	198	14.1	DNA-binding protein HU-beta
STM2871	*prgK*	46	198	4.3	needle complex inner membrane lipoprotein
STM2884	*sipC*	96	192	2.0	translocation machinery component
STM4406.S	*ytfK*	6	191	31.8	putative cytoplasmic protein
STM2867	*hilC*	3	187	62.3	invasion regulatory protein
STM2869	*orgB*	8	182	22.8	needle complex export protein
STM2878	*sptP*	20	177	8.9	protein tyrosine phosphatase/GTPase activating protein
STM2894	*invC*	14	175	12.5	type III secretion system ATPase
STM2875	*hilD*	23	174	7.6	invasion protein regulatory protein
STM2284	*glpA*	57	149	2.6	sn-glycerol-3-phosphate dehydrogenase large subunit
STM3526	*glpD*	39	147	3.8	sn-glycerol-3-phosphate dehydrogenase
STM2886	*sicA*	23	146	6.3	secretion chaperone
STM3138		19	143	7.5	putative methyl-accepting chemotaxis protein
STM2896	*invA*	19	142	7.5	needle complex export protein
STM0833	*ompX*	6	137	22.8	outer membrane protein X
STM2899	*invF*	18	129	7.2	invasion regulatory protein
STM2924	*rpoS*	19	129	6.8	RNA polymerase sigma factor
STM0629	*cspE*	9	125	13.9	cold shock protein E
STM2285	*glpB*	33	119	3.6	anaerobic glycerol-3-phosphate dehydrogenase subunit B
STM0736	*sucA*	42	110	2.6	2-oxoglutarate dehydrogenase
STM2445	*ucpA*	5	105	21.0	short chain dehydrogenase
STM1070	*ompA*	77	102	1.3	putative hydrogenase membrane component precurosr

[a]Gene names according to ColiBase (Chaudhuri et al., 2004)
[b]Based on 145,873 sequences
[c]Based on 122,326 sequences
[d]Enrichment factor calculated by the number of blastable reads from Hfq coIP over control coIP.
[e]Product according to KEGG (http://www.genome.jp/kegg/; (Goto et al., 1997)).
doi:10.1371/journal.pgen.1000163.t003

37°C, 220 rpm to an optical density of 2. For SPI-1 induced cultures, 5 ml L-broth containing NaCl (final concentration 0.3 M) was inoculated from single colonies; incubation was carried out for 12 hours at 37°C, 220 rpm in tightly closed 15 ml Falcon tubes. For SPI-2 induced cultures, 70 ml SPI-2 medium [107] in 250 ml flasks were inoculated 1/100 from overnight cultures grown in the same medium. Bacteria were grown at 37°C, 220 rpm until the culture reached an OD of 0.3. For HilA, HilD, and FlhDC expression from pBAD-derived plasmids, growth media were supplemented with 0.1% L-arabinose.

Transcriptomic Experiments

Strain SL1344 and JVS-0255 (Δ*hfq*) were grown in L-broth either to an OD_{600} of 2 (ESP aerobic growth), or for 12 hours under SPI-1 inducing conditions. RNA extraction and data generation were carried out as described with SALSA microarrays [59]. The complete dataset is available at GEO under accession number GSE8985.

SDS PAGE and Western Blot for Protein Quantification

Proteins were resolved by SDS PAGE (12% gels). For Coomassie stain or Western analysis, proteins equivalent to 0.1 OD or 0.05 OD, respectively, were loaded per lane. For FliC detection, strains SL1344 and JVS-0255 carrying the indicated plasmids were grown to an OD of 1, and induced with L-arabinose. Growth continued for one hour, and whole cell and secreted protein fractions were analyzed as described in [32]. FliC was detected using a monoclonal FliC antibody (BioLegend).

RNA Isolation and Northern Blot Analysis

RNA was prepared by hot phenol extraction [108], followed by DNase I treatment. After separation on 5% polyacrylamide (PAA) gels containing 8.3 M Urea, or agarose gels, respectively, RNA was transferred onto Hybond-XL membrane (Amersham). 5 or 10 µg (PAA gels) or 20 µg (agarose gels) RNA was loaded per sample. For detection of new transcripts γ-ATP end-labeled oligodeoxyribonucleotides were used (see Table S7).

Gel Mobility Shift Assay of *In Vitro* RNA

DNA templates carrying a T7 promoter sequence were generated by PCR using genomic DNA and primers as listed in Table S6. For *dppA* oligonucleotides JVO-1034/1035 (the fragment covers the *dppA* region from positions −163 to +73 relative to the start codon) were used. For the PCR of the intergenic region of *glmUS* primer JVO-2471/2472 were used, resulting in a product starting 38 nucleotides upstream of the *glmU* stop codon and extending to nucleotide 113 in the intergenic region. For *flhD*, oligonucleotides JVO-2284/-2285 were used, to yield a fragment that covers *flhD* from position −59 to +38 relative to the start codon. The *hilD* fragment (oligonucleotides JVO-2286/-2287) spans region +400 to +600 relative to the start codon.

In vitro transcription was performed using the MEGAscript High Yield Transcription Kit (Ambion, #1333), followed by DNase I digestion (1 unit, 15 min, 37°C). Following extraction with phenol:chloroform:isopropanol (25:24:1 v/v), the RNA was precipitated overnight at -20°C with 1 vol of isopropanol. RNA integrity was checked on a denaturing polyacrylamide gel. RNA was 5′ end-labeled and purified as described in [59].

Gel mobility shift assays were carried out as described in [32]. In brief, labeled RNA was used in 10 µl reactions at a final concentration of 4 nM. Hfq was added to a final concentration in the range of 1.25 to 150 nM of the hexamer. After incubation for 10 min at 37°C complexes were separated on 6% native PAA gels at 4°C. Signals were detected with a Fuji PhosphorImager.

coIP and Sequence Analysis

Strains SL1344 and JVS-1338 (hfq^{FLAG}) were grown in L-broth under normal aeration at 37°C to ESP. Co-immunoprecipitation was carried out using the protocol published in [46]. For pyrosequencing and coIP-on-Chip experiments, samples of two independent pull down experiments were used. cDNA cloning and pyrosequencing was performed as described for the identification of eukaryotic microRNA [109] but omitting size-fractionation of RNA prior to cDNA synthesis. Microarrays used for the coIP-on-Chip experiments were designed and produced by Oxford Gene Technology (Kidlington, UK). They consist of 21,939 60-mer oligonucleotides tiled throughout the *S.* Typhimurium SL1344 NCTC13347 genome and 636 control oligonucleotides. The SL1344 sequence was obtained from the Sanger Institute (Hinxton, UK) website (http://www.sanger.ac.uk/Projects/Salmonella/). As this genome is not yet fully annotated, the oligonucleotides were associated with corresponding *S.* Typhimurium LT2 genes or intergenic regions, if conserved in both organisms. Full description of the microarray and protocols used for generating and analysing the data are associated with the dataset deposited in the GEO data repository (http://www.ncbi.nlm.nih.gov/geo/) under accession number GSE10149. For detailed description of data analysis using the Integrated Genome Browser see the Supplementary Text S1. In brief, cDNA reads ≥18 nt were mapped to the *Salmonella* chromosome and hits per nucleotide were calculated along the entire genome. To calculate *enrichment factors* for Hfq coIP, the Hfq cDNA number was divided by Control cDNA number at each position of the genome, following normalization to the total number of mapped reads. Upon upload of the *Salmonella* genome sequence and annotation from Genbank (NC_003197.fna and NC_003197.gff), the two graphs for each library were loaded into the Integrated Genome Browser (IGB) of Affymetrix (version IGB-4.56), which can be directly launched by Java Web Start at http://www.affymetrix.com/support/developer/tools/download_igb.affx or downloaded from http://genoviz.sourceforge.net/.

Supporting Information

Figure S1 Expression levels of RpoE and RpoS in wild-type and Δ*hfq* cells. Samples were taken from wild-type and Δ*hfq* strains grown under standard conditions to early stationary phase (OD_{600} of 2) or for 12 hours under SPI-1 inducing conditions, respectively. (A) Analysis of mRNA level by real time PCR for *rpoE*, *degP*, and *rpoS* mRNA. (B) Whole cell proteins were separated by 12% SDS PAGE and sigma factors detected via Western blot. Expression levels of each protein were determined by densitometry and are given as a percentage of the wild-type level of expression below each gel.

Found at: doi:10.1371/journal.pgen.1000163.s001 (0.29 MB TIF)

Figure S2 Northern detection of Hfq bound mRNAs. Total RNA was isolated from *Salmonella* at OD_{600} of 2. Northern blots based on agarose gel for detection of long transcripts showing the detection of six mRNAs.

Found at: doi:10.1371/journal.pgen.1000163.s002 (1.29 MB TIF)

Figure S3 Expression levels of small peptide encoding mRNAs in *Salmonella*. RNA samples were either taken from wild-type or *hfq* mutant *Salmonella* at different growth stages (as in Figure 6 in the main manuscript), and probed for STnc250 and STnc570 over growth (A) or at early stationary phase (B).

Found at: doi:10.1371/journal.pgen.1000163.s003 (0.99 MB TIF)

Figure S4 Hfq binds significantly to a few but not all mRNAs of the SPI-1 and the flagellar regulon. Shown are all genes belonging to the SPI-1 and the flagellar regulon. The level of Hfq-dependent gene regulation is shown as fold-change below each gene (taken from the transcriptomic dataset; Table S1). Representation of cDNAs in pyrosequencing is indicated by different colours (green: 1–10 clones, turquoise: 11–100 clones, orange: 101–500 clones, magenta: ≥501 clones).
Found at: doi:10.1371/journal.pgen.1000163.s004 (0.41 MB TIF)

Figure S5 Expression of IstR-1 and IstR-2 in *Salmonella*. Northern analysis of istR transcripts. Total RNA was extracted from of *E. coli* K12 and *Salmonella* Typhimurium SL1344 cells grown to an OD_{600} of 2, exposed to Mitomycin C (0.5 μg/ml) for 30 min as described by [2]. Length is indicated according to marker sizes in nt. Full-length IstR-1 and IstR-2 are indicated by arrows.
Found at: doi:10.1371/journal.pgen.1000163.s005 (0.28 MB TIF)

Table S1 Deregulated genes in Δ*hfq* at ESP.
Found at: doi:10.1371/journal.pgen.1000163.s006 (0.95 MB DOC)

Table S2 Deregulated genes in Δ*hfq* after 12 hrs SPI-inducing conditions.
Found at: doi:10.1371/journal.pgen.1000163.s007 (0.21 MB DOC)

Table S3 Coverage of known and candidate *Salmonella* sRNA loci in pyrosequencing data.
Found at: doi:10.1371/journal.pgen.1000163.s008 (0.26 MB DOC)

Table S4 mRNAs in Hfq CoIP identified by ≥10 of 170,000 inserts in pyrosequencing data.
Found at: doi:10.1371/journal.pgen.1000163.s009 (0.81 MB DOC)

Table S5 Genes that were significantly enriched in coIP-on-Chip and were identified by pyrosequencing.
Found at: doi:10.1371/journal.pgen.1000163.s010 (0.32 MB DOC)

Table S6 Oligodeoxynucleotides used in this study.
Found at: doi:10.1371/journal.pgen.1000163.s011 (0.06 MB DOC)

Table S7 Oligodeoxynucleotides used for Northern detection.
Found at: doi:10.1371/journal.pgen.1000163.s012 (0.05 MB DOC)

Text S1 Supplementary material and methods.
Found at: doi:10.1371/journal.pgen.1000163.s013 (0.31 MB DOC)

Acknowledgments

We thank R. Reinhart and B. Timmermann for pyrosequencing and *vertis* Biotechnology AG for cDNA construction.

Author Contributions

Conceived and designed the experiments: AS SL JCDH JV. Performed the experiments: AS SL KP KR. Analyzed the data: AS SL KP CMS JCDH JV. Contributed reagents/materials/analysis tools: CMS TTB. Wrote the paper: AS JCDH JV.

References

1. Majdalani N, Vanderpool CK, Gottesman S (2005) Bacterial small RNA regulators. Crit Rev Biochem Mol Biol 40: 93–113.
2. Vogel J, Wagner EG (2007) Target identification of regulatory sRNAs in bacteria. Curr Opin Microbiol 10: 262–270.
3. Storz G, Altuvia S, Wassarman KM (2005) An abundance of RNA regulators. Annu Rev Biochem 74: 199–217.
4. Aiba H (2007) Mechanism of RNA silencing by Hfq-binding small RNAs. Curr Opin Microbiol 10: 134–139.
5. Valentin-Hansen P, Eriksen M, Udesen C (2004) The bacterial Sm-like protein Hfq: a key player in RNA transactions. Mol Microbiol 51: 1525–1533.
6. Ali Azam T, Iwata A, Nishimura A, Ueda S, Ishihama A (1999) Growth phase-dependent variation in protein composition of the Escherichia coli nucleoid. J Bacteriol 181: 6361–6370.
7. Kajitani M, Kato A, Wada A, Inokuchi Y, Ishihama A (1994) Regulation of the Escherichia coli hfq gene encoding the host factor for phage Q beta. J Bacteriol 176: 531–534.
8. Franze de Fernandez MT, Hayward WS, August JT (1972) Bacterial proteins required for replication of phage Q ribonucleic acid. Pruification and properties of host factor I, a ribonucleic acid-binding protein. J Biol Chem 247: 824–831.
9. Franze de Fernandez MT, Eoyang L, August JT (1968) Factor fraction required for the synthesis of bacteriophage Qbeta-RNA. Nature 219: 588–590.
10. Sun X, Zhulin I, Wartell RM (2002) Predicted structure and phyletic distribution of the RNA-binding protein Hfq. Nucleic Acids Res 30: 3662–3671.
11. Nielsen JS, Boggild A, Andersen CB, Nielsen G, Boysen A, et al. (2007) An Hfq-like protein in archaea: Crystal structure and functional characterization of the Sm protein from Methanococcus jannaschii. Rna 13: 2213–2223.
12. Møller T, Franch T, Højrup P, Keene DR, Bachinger HP, et al. (2002) Hfq: a bacterial Sm-like protein that mediates RNA-RNA interaction. Mol Cell 9: 23–30.
13. Kawamoto H, Koide Y, Morita T, Aiba H (2006) Base-pairing requirement for RNA silencing by a bacterial small RNA and acceleration of duplex formation by Hfq. Mol Microbiol 61: 1013–1022.
14. Zhang A, Wassarman KM, Ortega J, Steven AC, Storz G (2002) The Sm-like Hfq protein increases OxyS RNA interaction with target mRNAs. Mol Cell 9: 11–22.
15. Mikulecky PJ, Kaw MK, Brescia CC, Takach JC, Sledjeski DD, et al. (2004) Escherichia coli Hfq has distinct interaction surfaces for DsrA, rpoS and poly(A) RNAs. Nat Struct Mol Biol 11: 1206–1214.
16. Lease RA, Woodson SA (2004) Cycling of the Sm-like protein Hfq on the DsrA small regulatory RNA. J Mol Biol 344: 1211–1223.
17. Zhang A, Wassarman KM, Rosenow C, Tjaden BC, Storz G, et al. (2003) Global analysis of small RNA and mRNA targets of Hfq. Mol Microbiol 50: 1111–1124.
18. Vytvytska O, Moll I, Kaberdin VR, von Gabain A, Bläsi U (2000) Hfq (HF1) stimulates ompA mRNA decay by interfering with ribosome binding. Genes Dev 14: 1109–1118.
19. Urban JH, Vogel J (2008) Two seemingly homologous noncoding RNAs act hierarchically to activate glmS mRNA translation. PLoS Biol 6: e64.
20. Hajnsdorf E, Regnier P (2000) Host factor Hfq of Escherichia coli stimulates elongation of poly(A) tails by poly(A) polymerase I. Proc Natl Acad Sci U S A 97: 1501–1505.
21. Mohanty BK, Maples VF, Kushner SR (2004) The Sm-like protein Hfq regulates polyadenylation dependent mRNA decay in Escherichia coli. Mol Microbiol 54: 905–920.
22. Lee T, Feig AL (2008) The RNA binding protein Hfq interacts specifically with tRNAs. Rna 14: 514–523.
23. Scheibe M, Bonin S, Hajnsdorf E, Betat H, Mörl M (2007) Hfq stimulates the activity of the CCA-adding enzyme. BMC Mol Biol 8: 92.
24. Tsui HC, Leung HC, Winkler ME (1994) Characterization of broadly pleiotropic phenotypes caused by an hfq insertion mutation in Escherichia coli K-12. Mol Microbiol 13: 35–49.
25. Muffler A, Fischer D, Hengge-Aronis R (1996) The RNA-binding protein HF-I, known as a host factor for phage Qbeta RNA replication, is essential for rpoS translation in Escherichia coli. Genes Dev 10: 1143–1151.
26. Brown L, Elliott T (1996) Efficient translation of the RpoS sigma factor in Salmonella typhimurium requires host factor I, an RNA-binding protein encoded by the hfq gene. J Bacteriol 178: 3763–3770.
27. Sharma AK, Payne SM (2006) Induction of expression of hfq by DksA is essential for Shigella flexneri virulence. Mol Microbiol 62: 469–479.
28. Sonnleitner E, Hagens S, Rosenau F, Wilhelm S, Habel A, et al. (2003) Reduced virulence of a hfq mutant of Pseudomonas aeruginosa O1. Microb Pathog 35: 217–228.
29. Christiansen JK, Nielsen JS, Ebersbach T, Valentin-Hansen P, Sogaard-Andersen L, et al. (2006) Identification of small Hfq-binding RNAs in Listeria monocytogenes. Rna 12: 1383–1396.
30. Ding Y, Davis BM, Waldor MK (2004) Hfq is essential for Vibrio cholerae virulence and downregulates sigma expression. Mol Microbiol 53: 345–354.

31. Nakao H, Watanabe H, Nakayama S, Takeda T (1995) yst gene expression in Yersinia enterocolitica is positively regulated by a chromosomal region that is highly homologous to Escherichia coli host factor 1 gene (hfq). Mol Microbiol 18: 859–865.
32. Sittka A, Pfeiffer V, Tedin K, Vogel J (2007) The RNA chaperone Hfq is essential for the virulence of Salmonella typhimurium. Mol Microbiol 63: 193–217.
33. Robertson GT, Roop RM Jr (1999) The Brucella abortus host factor I (HF-I) protein contributes to stress resistance during stationary phase and is a major determinant of virulence in mice. Mol Microbiol 34: 690–700.
34. Figueroa-Bossi N, Lemire S, Maloriol D, Balbontin R, Casadesus J, et al. (2006) Loss of Hfq activates the sigma-dependent envelope stress response in Salmonella enterica. Mol Microbiol 62: 838–852.
35. Wilson JW, Ott CM, Zu Bentrup KH, Ramamurthy R, Quick L, et al. (2007) Space flight alters bacterial gene expression and virulence and reveals a role for global regulator Hfq. Proc Natl Acad Sci U S A 104: 16299–16304.
36. Antal M, Bordeau V, Douchin V, Felden B (2005) A small bacterial RNA regulates a putative ABC transporter. J Biol Chem 280: 7901–7908.
37. Margulies M, Egholm M, Altman WE, Attiya S, Bader JS, et al. (2005) Genome sequencing in microfabricated high-density picolitre reactors. Nature 437: 376–380.
38. Yooseph S, Sutton G, Rusch DB, Halpern AL, Williamson SJ, et al. (2007) The Sorcerer II Global Ocean Sampling expedition: expanding the universe of protein families. PLoS Biol 5: e16.
39. Lee CA, Falkow S (1990) The ability of Salmonella to enter mammalian cells is affected by bacterial growth state. Proc Natl Acad Sci U S A 87: 4304–4308.
40. McClelland M, Sanderson KE, Spieth J, Clifton SW, Latreille P, et al. (2001) Complete genome sequence of Salmonella enterica serovar Typhimurium LT2. Nature 413: 852–856.
41. Goto S, Bono H, Ogata H, Fujibuchi W, Nishioka T, et al. (1997) Organizing and computing metabolic pathway data in terms of binary relations. Pac Symp Biocomput. pp 175–186.
42. Guisbert E, Rhodius VA, Ahuja N, Witkin E, Gross CA (2007) Hfq modulates the sigmaE-mediated envelope stress response and the sigma32-mediated cytoplasmic stress response in Escherichia coli. J Bacteriol 189: 1963–1973.
43. Skovierova H, Rowley G, Rezuchova B, Homerova D, Lewis C, et al. (2006) Identification of the sigmaE regulon of Salmonella enterica serovar Typhimurium. Microbiology 152: 1347–1359.
44. Bang IS, Frye JG, McClelland M, Velayudhan J, Fang FC (2005) Alternative sigma factor interactions in Salmonella: sigma and sigma promote antioxidant defences by enhancing sigma levels. Mol Microbiol 56: 811–823.
45. Garcia-Vallve S, Guzman E, Montero MA, Romeu A (2003) HGT-DB: a database of putative horizontally transferred genes in prokaryotic complete genomes. Nucleic Acids Res 31: 187–189.
46. Pfeiffer V, Sittka A, Tomer R, Tedin K, Brinkmann V, et al. (2007) A small non-coding RNA of the invasion gene island (SPI-1) represses outer membrane protein synthesis from the Salmonella core genome. Mol Microbiol 66: 1174–1191.
47. Hershberg R, Altuvia S, Margalit H (2003) A survey of small RNA-encoding genes in Escherichia coli. Nucleic Acids Res 31: 1813–1820.
48. Babitzke P, Romeo T (2007) CsrB sRNA family: sequestration of RNA-binding regulatory proteins. Curr Opin Microbiol 10: 156–163.
49. Wassarman KM, Repoila F, Rosenow C, Storz G, Gottesman S (2001) Identification of novel small RNAs using comparative genomics and microarrays. Genes Dev 15: 1637–1651.
50. Vogel J, Bartels V, Tang TH, Churakov G, Slagter-Jager JG, et al. (2003) RNomics in Escherichia coli detects new sRNA species and indicates parallel transcriptional output in bacteria. Nucleic Acids Res 31: 6435–6443.
51. Argaman L, Hershberg R, Vogel J, Bejerano G, Wagner EG, et al. (2001) Novel small RNA-encoding genes in the intergenic regions of Escherichia coli. Curr Biol 11: 941–950.
52. Brownlee GG (1971) Sequence of 6S RNA of E. coli. Nat New Biol 229: 147–149.
53. Rivas E, Klein RJ, Jones TA, Eddy SR (2001) Computational identification of noncoding RNAs in E. coli by comparative genomics. Curr Biol 11: 1369–1373.
54. Kawano M, Reynolds AA, Miranda-Rios J, Storz G (2005) Detection of 5′- and 3′-UTR-derived small RNAs and cis-encoded antisense RNAs in Escherichia coli. Nucleic Acids Res 33: 1040–1050.
55. Padalon-Brauch G, Hershberg R, Elgrably-Weiss M, Baruch K, Rosenshine I, et al. (2008) Small RNAs encoded within genetic islands of Salmonella typhimurium show host-induced expression and role in virulence. Nucleic Acids Res.
56. Song M, Kim HJ, Kim EY, Shin M, Lee HC, et al. (2004) ppGpp-dependent stationary phase induction of genes on Salmonella pathogenicity island 1. J Biol Chem 279: 34183–34190.
57. Deiwick J, Nikolaus T, Erdogan S, Hensel M (1999) Environmental regulation of Salmonella pathogenicity island 2 gene expression. Mol Microbiol 31: 1759–1773.
58. Sharma CM, Darfeuille F, Plantinga TH, Vogel J (2007) A small RNA regulates multiple ABC transporter mRNAs by targeting C/A-rich elements inside and upstream of ribosome-binding sites. Genes Dev 21: 2804–2817.
59. Papenfort K, Pfeiffer V, Mika F, Lucchini S, Hinton JC, et al. (2006) sigma(E)-dependent small RNAs of Salmonella respond to membrane stress by accelerating global omp mRNA decay. Mol Microbiol 62: 1674–1688.
60. Fortune DR, Suyemoto M, Altier C (2006) Identification of CsrC and characterization of its role in epithelial cell invasion in Salmonella enterica serovar Typhimurium. Infect Immun 74: 331–339.
61. Viegas SC, Pfeiffer V, Sittka A, Silva IJ, Vogel J, et al. (2007) Characterization of the role of ribonucleases in Salmonella small RNA decay. Nucleic Acids Res 35: 7651–7664.
62. Altier C, Suyemoto M, Ruiz AI, Burnham KD, Maurer R (2000) Characterization of two novel regulatory genes affecting Salmonella invasion gene expression. Mol Microbiol 35: 635–646.
63. Papenfort K, Pfeiffer V, Lucchini S, Sonawane A, Hinton JC, et al. (2008) Systematic deletion of Salmonella small RNA genes identifies CyaR, a conserved CRP-dependent riboregulator of OmpX synthesis. Mol Microbiol in press.
64. Beuzon CR, Marques S, Casadesus J (1999) Repression of IS200 transposase synthesis by RNA secondary structures. Nucleic Acids Res 27: 3690–3695.
65. Kalamorz F, Reichenbach B, Marz W, Rak B, Görke B (2007) Feedback control of glucosamine-6-phosphate synthase GlmS expression depends on the small RNA GlmZ and involves the novel protein YhbJ in Escherichia coli. Mol Microbiol 65: 1518–1533.
66. Joanny G, Le Derout J, Brechemier-Baey D, Labas V, Vinh J, et al. (2007) Polyadenylation of a functional mRNA controls gene expression in Escherichia coli. Nucleic Acids Res 35: 2494–2502.
67. Ellermeier JR, Slauch JM (2007) Adaptation to the host environment: regulation of the SPI1 type III secretion system in Salmonella enterica serovar Typhimurium. Curr Opin Microbiol 10: 24–29.
68. Tenenbaum SA, Lager PJ, Carson CC, Keene JD (2002) Ribonomics: identifying mRNA subsets in mRNP complexes using antibodies to RNA-binding proteins and genomic arrays. Methods 26: 191–198.
69. Inada M, Guthrie C (2004) Identification of Lhp1p-associated RNAs by microarray analysis in Saccharomyces cerevisiae reveals association with coding and noncoding RNAs. Proc Natl Acad Sci U S A 101: 434–439.
70. Uzzau S, Figueroa-Bossi N, Rubino S, Bossi L (2001) Epitope tagging of chromosomal genes in Salmonella. Proc Natl Acad Sci U S A 98: 15264–15269.
71. Willkomm DK, Minnerup J, Huttenhofer A, Hartmann RK (2005) Experimental RNomics in Aquifex aeolicus: identification of small non-coding RNAs and the putative 6S RNA homolog. Nucleic Acids Res 33: 1949–1960.
72. Hüttenhofer A, Brosius J, Bachellerie JP (2002) RNomics: identification and function of small, non-messenger RNAs. Curr Opin Chem Biol 6: 835–843.
73. Hüttenhofer A (2005) Experimental RNomics: A Global Approach to Identify Non-coding RNAs in Model Organisms. In: Hartmann R, Bindereif A, Schön A, Westhof E, eds (2005) Handbook of RNA Biochemistry. Weinheim, Germany: WILEY-VCH Verlag GmbH. pp 643–654.
74. Lu C, Tej SS, Luo S, Haudenschild CD, Meyers BC, et al. (2005) Elucidation of the small RNA component of the transcriptome. Science 309: 1567–1569.
75. Ruby JG, Jan C, Player C, Axtell MJ, Lee W, et al. (2006) Large-scale sequencing reveals 21U-RNAs and additional microRNAs and endogenous siRNAs in C. elegans. Cell 127: 1193–1207.
76. Aravin A, Gaidatzis D, Pfeffer S, Lagos-Quintana M, Landgraf P, et al. (2006) A novel class of small RNAs bind to MILI protein in mouse testes. Nature 442: 203–207.
77. Girard A, Sachidanandam R, Hannon GJ, Carmell MA (2006) A germline-specific class of small RNAs binds mammalian Piwi proteins. Nature 442: 199–202.
78. Bossi L, Figueroa-Bossi N (2007) A small RNA downregulates LamB maltoporin in Salmonella. Mol Microbiol 65: 799–810.
79. Julio SM, Heithoff DM, Mahan MJ (2000) ssrA (tmRNA) plays a role in Salmonella enterica serovar Typhimurium pathogenesis. J Bacteriol 182: 1558–1563.
80. Repoila F, Majdalani N, Gottesman S (2003) Small non-coding RNAs, co-ordinators of adaptation processes in Escherichia coli: the RpoS paradigm. Mol Microbiol 48: 855–861.
81. Jones AM, Goodwill A, Elliott T (2006) Limited role for the DsrA and RprA regulatory RNAs in rpoS regulation in Salmonella enterica. J Bacteriol 188: 5077–5088.
82. Dobrindt U, Hochhut B, Hentschel U, Hacker J (2004) Genomic islands in pathogenic and environmental microorganisms. Nat Rev Microbiol 2: 414–424.
83. Chen S, Lesnik EA, Hall TA, Sampath R, Griffey RH, et al. (2002) A bioinformatics based approach to discover small RNA genes in the Escherichia coli genome. Biosystems 65: 157–177.
84. Livny J, Brencic A, Lory S, Waldor MK (2006) Identification of 17 Pseudomonas aeruginosa sRNAs and prediction of sRNA-encoding genes in 10 diverse pathogens using the bioinformatic tool sRNAPredict2. Nucleic Acids Res 34: 3484–3493.
85. Hüttenhofer A, Vogel J (2006) Experimental approaches to identify non-coding RNAs. Nucleic Acids Res 34: 635–646.
86. Altuvia S (2007) Identification of bacterial small non-coding RNAs: experimental approaches. Curr Opin Microbiol 10: 257–261.

87. Sonnleitner E, Schuster M, Sorger-Domenigg T, Greenberg EP, Blasi U (2006) Hfq-dependent alterations of the transcriptome profile and effects on quorum sensing in Pseudomonas aeruginosa. Mol Microbiol 59: 1542–1558.
88. Rhodius VA, Suh WC, Nonaka G, West J, Gross CA (2006) Conserved and variable functions of the sigmaE stress response in related genomes. PLoS Biol 4: e2.
89. Fang FC, Chen CY, Guiney DG, Xu Y (1996) Identification of sigma S-regulated genes in Salmonella typhimurium: complementary regulatory interactions between sigma S and cyclic AMP receptor protein. J Bacteriol 178: 5112–5120.
90. Robbe-Saule V, Coynault C, Ibanez-Ruiz M, Hermant D, Norel F (2001) Identification of a non-haem catalase in Salmonella and its regulation by RpoS (sigmaS). Mol Microbiol 39: 1533–1545.
91. Ibanez-Ruiz M, Robbe-Saule V, Hermant D, Labrude S, Norel F (2000) Identification of RpoS (sigma(S))-regulated genes in Salmonella enterica serovar typhimurium. J Bacteriol 182: 5749–5756.
92. Tjaden B, Goodwin SS, Opdyke JA, Guillier M, Fu DX, et al. (2006) Target prediction for small, noncoding RNAs in bacteria. Nucleic Acids Res 34: 2791–2802.
93. Jones BD (2005) Salmonella invasion gene regulation: a story of environmental awareness. J Microbiol 43 Spec No. pp 110–117.
94. Sledjeski DD, Whitman C, Zhang A (2001) Hfq is necessary for regulation by the untranslated RNA DsrA. J Bacteriol 183: 1997–2005.
95. Senear AW, Steitz JA (1976) Site-specific interaction of Qbeta host factor and ribosomal protein S1 with Qbeta and R17 bacteriophage RNAs. J Biol Chem 251: 1902–1912.
96. Zhang A, Altuvia S, Tiwari A, Argaman L, Hengge-Aronis R, et al. (1998) The OxyS regulatory RNA represses rpoS translation and binds the Hfq (HF-I) protein. Embo J 17: 6061–6068.
97. Folichon M, Arluison V, Pellegrini O, Huntzinger E, Regnier P, et al. (2003) The poly(A) binding protein Hfq protects RNA from RNase E and exoribonucleolytic degradation. Nucleic Acids Res 31: 7302–7310.
98. Moll I, Afonyushkin T, Vytvytska O, Kaberdin VR, Blasi U (2003) Coincident Hfq binding and RNase E cleavage sites on mRNA and small regulatory RNAs. Rna 9: 1308–1314.
99. Lucchini S, Rowley G, Goldberg MD, Hurd D, Harrison M, et al. (2006) H-NS mediates the silencing of laterally acquired genes in bacteria. PLoS Pathog 2: e81.
100. Navarre WW, Porwollik S, Wang Y, McClelland M, Rosen H, et al. (2006) Selective silencing of foreign DNA with low GC content by the H-NS protein in Salmonella. Science 313: 236–238.
101. Doyle M, Fookes M, Ivens A, Mangan MW, Wain J, et al. (2007) An H-NS-like stealth protein aids horizontal DNA transmission in bacteria. Science 315: 251–252.
102. Anantharaman V, Koonin EV, Aravind L (2002) Comparative genomics and evolution of proteins involved in RNA metabolism. Nucleic Acids Res 30: 1427–1464.
103. Yamanaka K, Fang L, Inouye M (1998) The CspA family in Escherichia coli: multiple gene duplication for stress adaptation. Mol Microbiol 27: 247–255.
104. Hoiseth SK, Stocker BA (1981) Aromatic-dependent Salmonella typhimurium are non-virulent and effective as live vaccines. Nature 291: 238–239.
105. Lostroh CP, Bajaj V, Lee CA (2000) The cis requirements for transcriptional activation by HilA, a virulence determinant encoded on SPI-1. Mol Microbiol 37: 300–315.
106. Schechter LM, Lee CA (2001) AraC/XylS family members, HilC and HilD, directly bind and derepress the Salmonella typhimurium hilA promoter. Mol Microbiol 40: 1289–1299.
107. Lober S, Jackel D, Kaiser N, Hensel M (2006) Regulation of Salmonella pathogenicity island 2 genes by independent environmental signals. Int J Med Microbiol 296: 435–447.
108. Mattatall NR, Sanderson KE (1996) Salmonella typhimurium LT2 possesses three distinct 23S rRNA intervening sequences. J Bacteriol 178: 2272–2278.
109. Berezikov E, Thuemmler F, van Laake LW, Kondova I, Bontrop R, et al. (2006) Diversity of microRNAs in human and chimpanzee brain. Nat Genet 38: 1375–1377.
110. Lobry JR (1996) Asymmetric substitution patterns in the two DNA strands of bacteria. Mol Biol Evol 13: 660–665.

4.2.1 Supplementary information

to the paper

Deep sequencing analysis of small noncoding RNA and mRNA targets of the global post-transcriptional regulator, Hfq

Alexandra Sittka, Sacha Lucchini, Kai Papenfort, Cynthia M. Sharma, Katarzyna Rolle, Tim T. Binnewies, Jay C. D. Hinton, and Joerg Vogel

SUPPLEMENTARY MATERIAL

Deep sequencing analysis of small noncoding RNA and mRNA targets of the global post-transcriptional regulator, Hfq

Alexandra Sittka, Sacha Lucchini, Kai Papenfort, Cynthia Sharma, Katarzyna Rolle,

Tim T. Binnewies, Jay C.D. Hinton and Jörg Vogel

SUPPLEMENTARY MATERIALS AND METHODS

Analysis and visualization of pyrosequencing results

After 5'end linker and polyA-tail clipping from the initial pyrosequencing results, all inserts ≥ 18 nt of the Hfq coIP and control coIP libraries were separately mapped to the *Salmonella* LT2 genome (NC_003197.fna) using WU-BLAST (http://blast.wustl.edu/). From the resulting blast positions one graph for each strand of the *Salmonella* chromosome was calculated, where the number of cDNA hits for each nucleotide position was plotted. To compare the graphs of the Hfq coIP and control coIP, the graphs were normalized to number of blastable reads. Following upload of the *Salmonella* genome sequence and annotation (NC_003197.fna and NC_003197.gff), the two graphs for each library were loaded into the Integrated Genome Browser (IGB) of Affymetrix (http://www.affymetrix.com/support/developer/tools/download_igb.aff, version IGB-4.56). Different panels show the annotations for the "+" and "–" strand (blue), the graphs for the "+" and "-" strand of the Hfq coIP (red) and the control coIP (black), and the genome coordinates in the center. A specific genomic region can be selected for further analysis (*e.g.* SPI-1, Fig. 4).

SPI-1 represents an example of an entire genomic region highly enriched in the Hfq coIP library. In contrast, very few cDNA sequences mapping to SPI-1 are contained in the control coIP library. The flanking genes of *invR* (i.e. the border of SPI-1) nicely give an example of the specificity of the method (Fig. 4). While cDNAs mapping to the InvR sRNA gene represent the most abundant cluster in the Hfq coIP library, the genes in the closest proximity are barely represented in this library. In addition, the example of InvR underlines the reliability of the method to identify Hfq-dependent sRNAs.

The numbers of cDNA clones that overlap *Salmonella* sRNA genes or annotated ORFs are listed in Table S3 (sRNAs) and S4 (mRNAs). Comparing the numbers of cDNAs obtained for the Hfq coIP *vs.* control coIP, false positive sequences in the list of cDNAs of Hfq-bound RNAs were easily detected (see CsrB and CsrC, Table S3), based on the number of sequences received from the control coIP. In those cases the number of sequences was almost identical in the Hfq coIP and the control coIP libraries (note that the numbers are not normalized to the number of blastable reads.) While Table S3 and S4 only present absolute numbers of sequences, which map along an entire RNA transcript, it is necessary to analyze a gene of interest in detail. The ratio of hits per nucleotide of the Hfq coIP to hits from the control coIP provides a measure of enrichment, which can be visualized for every single nucleotide in a stepstair diagram. In the case of *ompD*, the number of cDNAs obtained in the Hfq coIP library (246) compared to those of control coIP library (76) lead to an overall enrichment factor of 3.3. Analysis of the single cDNA sequences over the entire transcript

length reveals single “hot spots” in the transcript bound by Hfq, leading to enrichment factors up to 30 (for the region spanning the ATG start codon; Fig. 7A). However, the number of *ompA* cDNA sequences received in Hfq coIP (102) *vs.* control coIP (77) only lead to an overall enrichment factor of 1.3. At first glance, this would lead one to assume that *ompA* is not an Hfq-bound mRNA. However, closer inspection of the clone distribution along the entire mRNA, and of the enrichment of certain parts of the mRNA, reveals that the 5’ region (around ATG start codon) and a central region are highly enriched in the Hfq coIP (up to 12-fold; Fig. 7B)). Such detailed inspection offers the advantage of being able to analyze the 5’/3’ UTRs of mRNAs, which are not included in Table S4, but are known to be often bound by Hfq.

Quantitative RT-PCR

The wild-type strain SL1344 and JVS-0255 (□*hfq*) were grown in liquid culture from single colonies to an OD_{600} of 2 or for 12 hours under SPI-1 inducing conditions, respectively. Experiments were carried out as described previously [1]. Briefly, RNA was isolated using the SV40 Total RNA Isolation kit (Promega) according to manufacturer’s instructions. Expression of *rpoE*, *degP*, and *rpoS* mRNA was quantitatively assessed by qRT-PCR in a 7900HT (Applied Biosystems), with the *rfaH* gene as reference. For each reaction (25µL final vol.) 1µl of RNA sample (100 ng/ reaction) were mixed with 0.25µl of primer pairs (0.5 µM final) and 12.5 µL of SYBR Green mix (Qiagen). For coupled cDNA synthesis and target gene amplification 0.25µl of Quantitect RT mix was added. Each sample was assayed in triplicate for each run. Control RNA from wild-type cells was used to construct a standard curve for all inspected genes. Reaction conditions were: 30 min 50°C, 15 min 95°C, and 45 cycles at 94°C for 20 sec, 60°C for 40 sec, and 72°C for 40 sec. Oligodeoxynucleotides used in this experiment (JVO-1234/1235 (*degP*), JVO-1117/1118 (*rfaH*), JVO-1236/1237 (*rpoE*), JVO-1342/1343 (*rpoS*)) are listed in Table S6.

Western blot

Cultures were inoculated into fresh medium 1/100 from o/n cultures. Incubation was carried out under standard conditions to early stationary phase (OD_{600} of 2) or for 12 hours under SPI-1 inducing condition, respectively. Whole cell proteins were resolved by 12 % SDS PAGE and transferred to a PVDF membrane. Sigma proteins were detected using monoclonal antibodies against RpoE or RpoS, respectively (Neoclone).

Northern analysis

Cultures were inoculated into fresh medium 1/100 from o/n cultures. Incubation was carried out under standard conditions to logarithmic phase. RNA was extracted using TRIzol

Reagent. For detailed protocol see [2].

Figure S1

Expression levels of RpoE and RpoS in wild-type and Δ*hfq* cells. Samples were taken from wild-type and Δ*hfq* strains grown under standard conditions to early stationary phase (OD_{600} of 2) or for 12 hours under SPI-1 inducing condition, respectively. (A) Analysis of mRNA level by real time PCR for *rpoE*, *degP*, and *rpoS* mRNA. (B) Whole cell proteins were separated by 12% SDS PAGE and sigma factors detected via Western blot. Expression levels of each protein were determined by densitometry and are given as a percentage of the wild-type level of expression below each gel.

Figure S2

Hfq binds significantly to a few but not all mRNAs of the SPI-1 and the flagellar regulon. Shown are all genes belonging to the SPI-1 and the flagellar regulon. The level of Hfq-dependent gene regulation is shown as fold change below each gene (taken from the transcriptomic dataset; Table S1). Representation of cDNAs in pyrosequencing is indicated by different colours (green: 1-10 clones, turquoise: 11-100 clones, orange: 101-500 clones, magenta: ≥501 clones).

Figure S3

Northern detection of Hfq bound mRNAs. Total RNA was isolated from *Salmonella* at OD_{600} of 2. Northern blots based on agarose gel for detection of long transcripts showing the detection of six mRNAs.

Figure S4

Expression levels of small peptide encoding mRNAs in *Salmonella*. RNA samples were either taken from wild-type or *hfq* mutant *Salmonella* at different growth stages (as in Fig. 6 in the main manuscript), and probed for STnc250 and STnc570 over growth **(A)** or at early staionary phase **(B)**.

Figure S5

Expression of IstR-1 and IstR-2 in *Salmonella*. Northern analysis of *istR* transcripts. Total RNA was extracted from of *E. coli* K12 and *Salmonella* Typhimurium SL1344 cells grown to an OD600 of 2, exposed to Mitomycin C (0.5 μg/ml) for 30 min as described by [2]. Length is indicated according to marker sizes in nt. Full-length IstR-1 and IstR-2 are indicated by arrows.

References

1. Papenfort K, Pfeiffer V, Mika F, Lucchini S, Hinton JC, et al. (2006) sigma(E)-dependent small RNAs of Salmonella respond to membrane stress by accelerating global omp mRNA decay. Mol Microbiol 62: 1674-1688.
2. Vogel J, Argaman L, Wagner EG, Altuvia S (2004) The small RNA IstR inhibits synthesis of an SOS-induced toxic peptide. Curr Biol 14: 2271-2276.
3. Chaudhuri RR, Khan AM, Pallen MJ (2004) coliBASE: an online database for Escherichia coli, Shigella and Salmonella comparative genomics. Nucleic Acids Res 32: D296-299.
4. Goto S, Bono H, Ogata H, Fujibuchi W, Nishioka T, et al. (1997) Organizing and computing metabolic pathway data in terms of binary relations. Pac Symp Biocomput: 175-186.
5. Sittka A, Pfeiffer V, Tedin K, Vogel J (2007) The RNA chaperone Hfq is essential for the virulence of Salmonella typhimurium. Mol Microbiol 63: 193-217.
6. Garcia-Vallve S, Guzman E, Montero MA, Romeu A (2003) HGT-DB: a database of putative horizontally transferred genes in prokaryotic complete genomes. Nucleic Acids Res 31: 187-189.
7. Papenfort K, Pfeiffer V, Lucchini S, Sonawane A, Hinton JC, et al. (2008) Systematic deletion of Salmonella small RNA genes identifies CyaR, a conserved CRP-dependent riboregulator of OmpX synthesis. Mol Microbiol in press.
8. Hershberg R, Altuvia S, Margalit H (2003) A survey of small RNA-encoding genes in Escherichia coli. Nucleic Acids Res 31: 1813-1820.
9. Padalon-Brauch G, Hershberg R, Elgrably-Weiss M, Baruch K, Rosenshine I, et al. (2008) Small RNAs encoded within genetic islands of Salmonella typhimurium show host-induced expression and role in virulence. Nucleic Acids Res.
10. Sharma CM, Darfeuille F, Plantinga TH, Vogel J (2007) A small RNA regulates multiple ABC transporter mRNAs by targeting C/A-rich elements inside and upstream of ribosome-binding sites. Genes Dev 21: 2804-2817.
11. Pfeiffer V, Sittka A, Tomer R, Tedin K, Brinkmann V, et al. (2007) A small non-coding RNA of the invasion gene island (SPI-1) represses outer membrane protein synthesis from the Salmonella core genome. Mol Microbiol 66: 1174-1191.
12. Figueroa-Bossi N, Lemire S, Maloriol D, Balbontin R, Casadesus J, et al. (2006) Loss of Hfq activates the sigma-dependent envelope stress response in Salmonella enterica. Mol Microbiol 62: 838-852.
13. Fortune DR, Suyemoto M, Altier C (2006) Identification of CsrC and characterization of its role in epithelial cell invasion in Salmonella enterica serovar Typhimurium. Infect Immun 74: 331-339.
14. Viegas SC, Pfeiffer V, Sittka A, Silva IJ, Vogel J, et al. (2007) Characterization of the role of ribonucleases in Salmonella small RNA decay. Nucleic Acids Res 35: 7651-7664.
15. Altier C, Suyemoto M, Ruiz AI, Burnham KD, Maurer R (2000) Characterization of two novel regulatory genes affecting Salmonella invasion gene expression. Mol Microbiol 35: 635-646.
16. Wassarman KM, Repoila F, Rosenow C, Storz G, Gottesman S (2001) Identification of novel small RNAs using comparative genomics and microarrays. Genes Dev 15: 1637-1651.

Figure S1

Sittka *et al.*, 2008

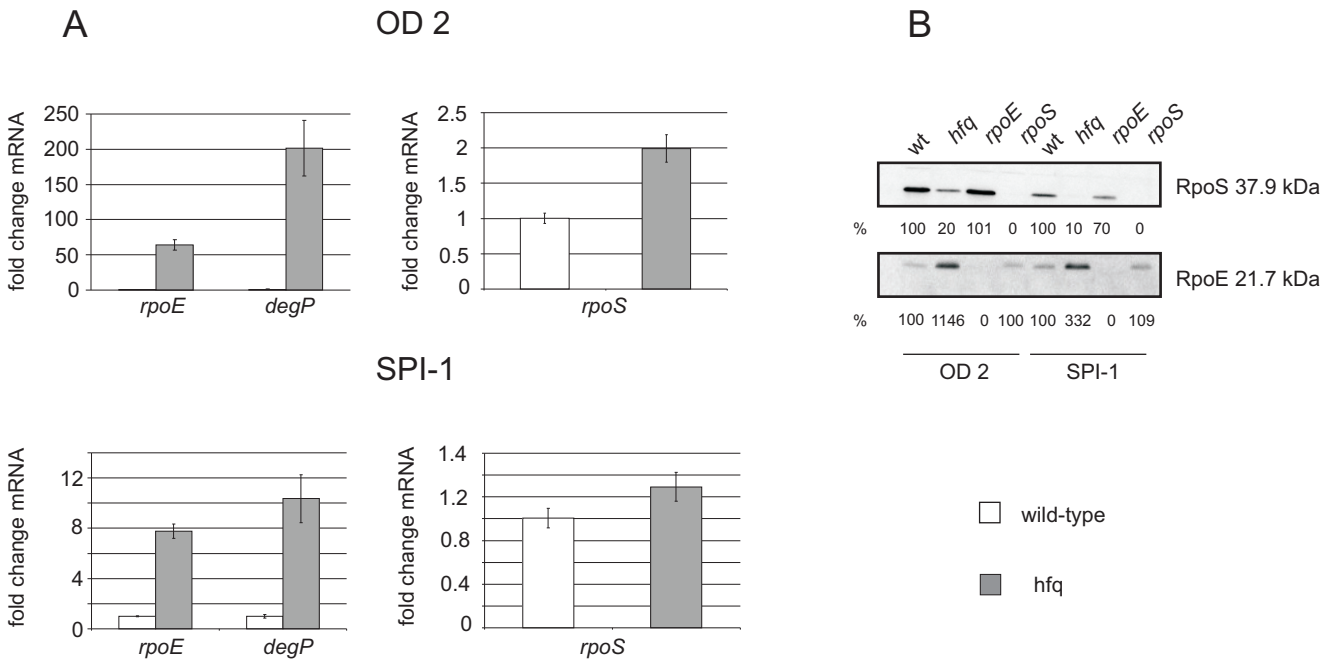

Figure S2

Sittka *et al.*, 2008

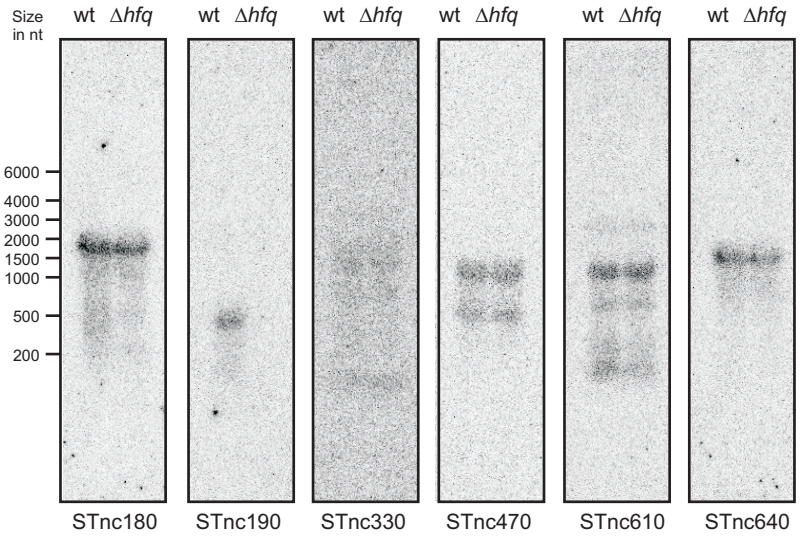

Figure S3

Sittka *et al.*, 2008

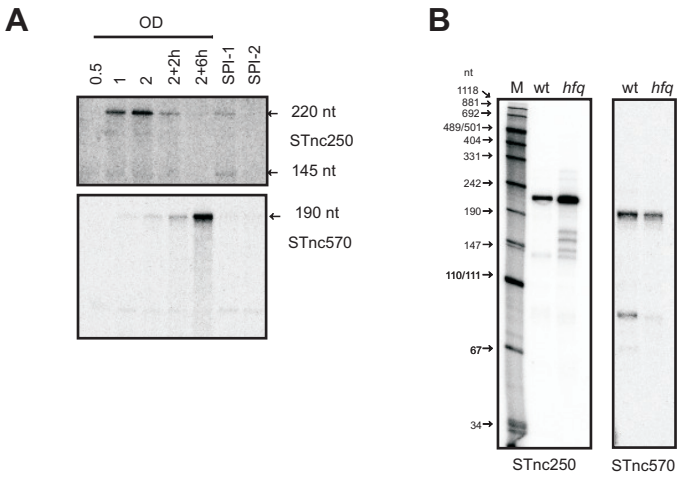

Figure S4

Sittka *et al.*, 2008

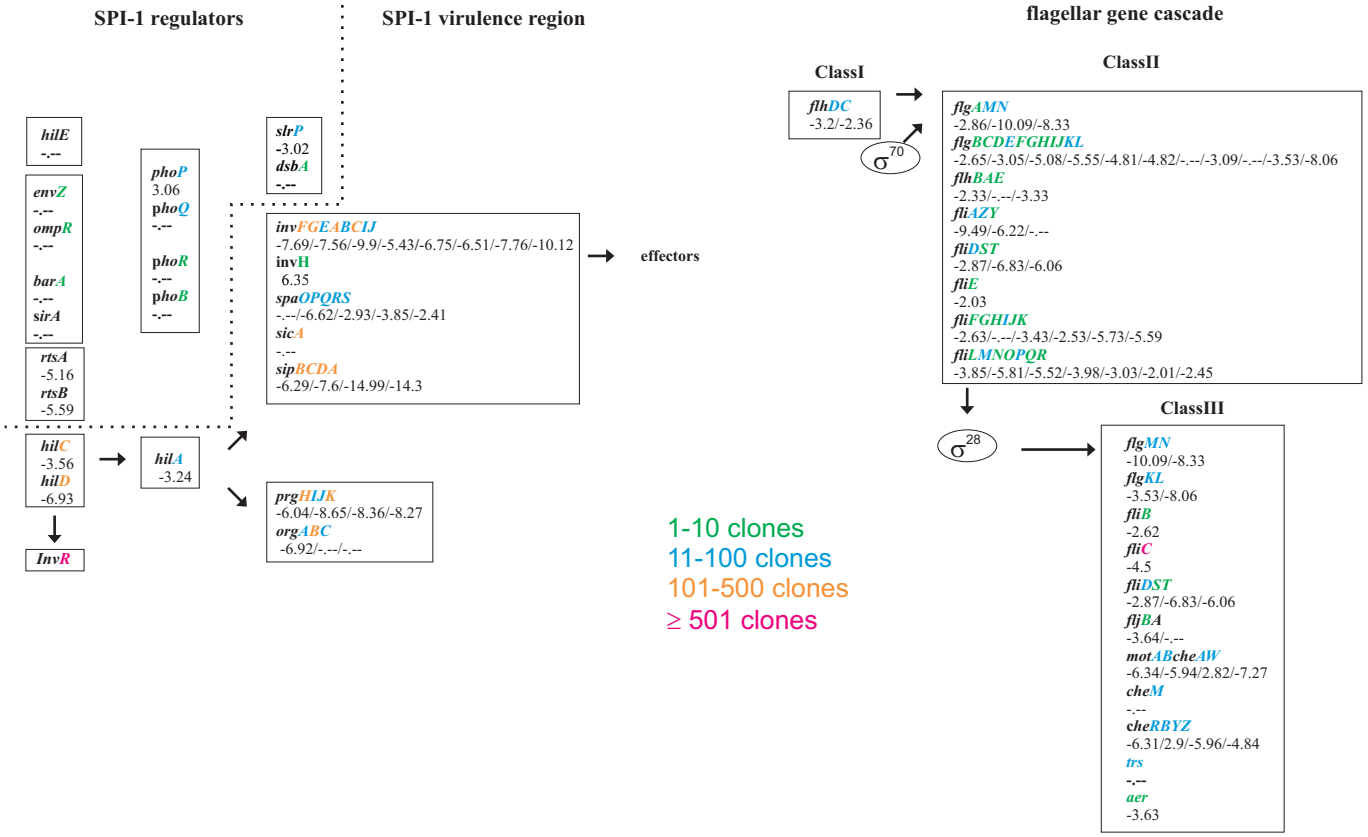

Figure S5

Sittka *et al.*, 2008

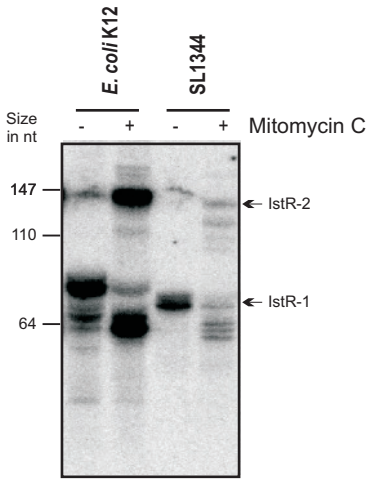

Table S1: Deregulated genes in Δ*hfq* at ESP

Gene name[a]	Fold change	Product[b]	2D-analysis[c]	HGT[d]	coIP on Chip	cDNA coverage
ybfM	231.48	putative outer membrane protein	X		X	X
ybfN	179.86	putative lipoprotein				X
napC	48.08	periplasmic nitrate reductase, cytochrome c-type protein				
htrA	41.15	periplasmic serine protease Do, heat shock protein	X			
napG	39.68	ferredoxin-type protein: electron transfer				
napH	35.84	ferredoxin-type protein: electron transfer				
napF	29.5	ferredoxin-type protein: electron transfer				X
rseA	27.32	anti sigma E (sigma 24) factor, negative regulator				
yraP	24.75	paral putative periplasmic protein	X			
napB	19.12	periplasmic nitrate reductase, small subunit, cytochrome C550, in complex with NapA				
aphA	18.55	non-specific acid phosphatase/phosphotransferase, class B	X		X	X
narP	18.42	response regulator in two-component regulatory system with NarQ (or NarX)			X	X
yfaZ	17.7	putative inner membrane protein			X	
yhjW	17.18	putative membrane-associated, metal-dependent hydrolase			X	
napD	17.04	periplasmic nitrate reductase				
cysA	15.48	ABC superfamily (atp_bind), sulfate permease A protein; chromate resistance				
STM1253	15.41	putative inner membrane protein		X		
ycbK	14.22	putative outer membrane protein				
nrfA	13.64	nitrite reductase periplasmic cytochrome c(552)				
rpoE	12.76	sigma E (sigma 24) factor of RNA polymerase, response to periplasmic stress				X
tpx	12.41	thiol peroxidase	X			X
ygiM	11.93	putative SH3 domain protein				
yraO	11.78	putative phosphoheptose isomerase				
nrfD	11.55	putative nitrate reductase, formate dependent				
yfiO	10.88	putative lipoprotein				
cysD	10.65	ATP-sulfurylase, subunit 1 (ATP:sulfate adenylyltransferase)				
yiaD	10.55	putative outer membrane lipoprotein	X			
glnH	10.27	ABC superfamily (bind_prot), glutamine high-affinity transporter	X		X	
rseB	9.9	anti sigma E (sigma 24) factor, negative regulator				X
nrfB	9.26	formate-dependent nitrite reductase; a penta-haeme cytochrome c				
phnA	8.93	putative alkylphosphonate uptake protein in phosphonate metabolism			X	
yggN	8.93	putative periplasmic protein			X	X
cysW	8	ABC superfamily (membrane), thiosulfate permease W protein				
citA	7.87	citrate-proton symporter				
cysP	7.69	ABC superfamily (bind_prot), thiosulfate transport protein	X			
ydjN	7.63	part of a kinase, putative domain shared with transporter				
ccmG	7.58	heme lyase disulfide oxidoreductase, cytocyhrome c-type biogenesis		X		
ygjU	7.58	putative dicarboxylate permease			X	X
yaeT	7.25	putative outer membrane antigen	X			X
ansB	7.09	periplasmic L-asparaginase II			X	X
rfaK	7.04	putative hexose transferase, lipopolysaccharide core biosynthesis		X	X	
dctA	6.76	DAACS family, C4-dicarboxylic acids transport protein				X
dppA	6.49	ABC superfamily (peri_perm), dipeptide transport protein	X		X	X
oppA	6.45	ABC superfamily (periplasm), oligopeptide transport protein with chaperone properties	X		X	X
STM2447	6.37	putative outer membrane lipoprotein				
lrhA	6.33	NADH dehydrogenase transcriptional repressor (LysR family)			X	X
ccmF	6.21	cytochrome c-type biogenesis protein		X		
cysI	6.21	sulfite reductase, alpha subunit, NADPH dependent				
gcvH	6.06	glycine cleavage complex protein H, carrier of aminomethyl moiety via covalently bound lipoyl cofactor				X
ycbL	5.85	putative Metallo-beta-lactamase				
yhjG	5.81	putative inner membrane protein				
stdA	5.78	putative fimbrial-like protein		X	X	
STM1539	5.75	putative hydrogenase-1 small subunit				
rplD	5.68	50S ribosomal subunit protein L4, regulates expression of S10 operon				X
sdaC	5.65	putative HAAAP family, serine transport protein			X	
nlpB	5.59	lipoprotein-34	X			
hlpA	5.52	histone-like protein, located in outer membrane				
STM1255	5.38	putative ABC transporter periplasmic binding protein				
rpsG	5.35	30S ribosomal subunit protein S7, initiates assembly				
yhjJ	5.35	putative Zn-dependent peptidase				
rplW	5.05	50S ribosomal subunit protein L23				

STM4351	5.05	putative arginine-binding periplasmic protein				
nrfC	5	putative nitrite reductase; formate-dependent, Fe-S centers				
rplB	4.83	50S ribosomal subunit protein L2				
STM4466	4.76	putative carbamate kinase				
cysK	4.69	subunit of cysteine synthase A and O-acetylserine sulfhydrolase A				
yfgD	4.61	putative arsenate reductase				
mglB	4.52	ABC superfamily (peri_perm), galactose transport protein	X			X
nrfE	4.52	formate-dependent nitrite reductase; involved in attachment of haem c to cytochrome c552				
STM4195	4.52	putative Na+-dependent transporter				
ushA	4.52	UDP-sugar hydrolase 5'-nucleotidase			X	X
yijD	4.41	putative inner membrane protein				
rseC	4.39	regulator of sigma E (sigma 24) factor				
STM4465	4.31	putative ornithine carbamoyltransferase				
cspD	4.27	similar to CspA but not cold shock induced	X			X
cutC	4.24	copper homeostasis protein			X	X
STM0509	4.24	putative outer membrane protein				
STM0719	4.18	putative UDP-galactopyranose mutase		X		
rbsB	4.17	ABC superfamily (peri_perm), D-ribose transport protein	X		X	X
gdhA	4.1	glutamate dehydrogenase, NADP-specific				
yabJ	4.07	putative ABC-transport protein			X	
gcvT	4.03	glycine cleavage complex protein T, aminomethyltransferase, tetrahydrofolate-dependent				X
cysN	4	ATP-sulfurylase, subunit 1 (ATP:sulfate adenylyltransferase)				
hflK	3.94	with HflC, part of modulator for protease specific for FtsH phage lambda cII repressor				
STM1747	3.94	putative inner membrane protein			X	
cycA	3.89	APC family, D-alanine/D-serine/glycine transport protein				
pal	3.88	tol protein required for outer membrane integrity, uptake of group A colicins, and translocation of phage DNA to cytoplasm	X			X
ybhQ	3.77	putative inner membrane protein				X
glpT	3.76	MFS family, sn-glycerol-3-phosphate transport protein				X
purC	3.75	phosphoribosylaminoimidazole-succinocarboxamide synthetase (SAICAR synthetase)				
STM1538	3.73	putative hydrogenase-1 large subunit				
rpsC	3.72	30S ribosomal subunit protein S3				X
rplV	3.7	50S ribosomal subunit protein L22				
STM4276	3.65	putative cytoplasmic protein				
ddg	3.64	cold shock-induced palmitoleoyl transferase				
glpQ	3.64	glycerophosphodiester phosphodiesterase, periplasmic	X			X
livK	3.62	ABC superfamily (bind_prot), branched-chain amino acid transporter, high-affinity				
tsx	3.62	nucleoside channel; receptor of phage T6 and colicin K				
rplC	3.6	50S ribosomal subunit protein L3	X			X
ndk	3.58	nucleoside diphosphate kinase				X
PSLT103	3.58					
gcvP	3.57	glycine cleavage complex protein P, glycine decarboxylase				X
hflC	3.55	with HflK, part of modulator for protease specific for FtsH phage lambda cII repressor				
STM2494	3.55	putative inner membrane or exported	X			X
rplP	3.52	50S ribosomal subunit protein L16				
STM3169	3.5	putative dicarboxylate-binding periplasmic protein				
tig	3.5	peptidyl-prolyl cis/trans isomerase, trigger factor; a molecular chaperone involved in cell division				
cysC	3.48	adenosine 5'-phosphosulfate kinase				
cpxP	3.45	periplasmic repressor of cpx regulon by interaction with CpxA, rescue from transitory stresses			X	X
cca	3.42	tRNA nucleotidyl transferase				
yfgL	3.4	putative serine/threonine protein kinase				X
rpsS	3.39	30S ribosomal subunit protein S19				X
STM2238	3.39	putative phage protein			X	
rfbP	3.36	LPS side chain defect: bifunctional enzyme: undecaprenol-phosphate galactosephosphotransferase, and O-antigen transfer		X	X	X
ibpB	3.33	small heat shock protein				X
ptr	3.32	protease III	X			
ytfJ	3.32	putative transcriptional regulator			X	
PSLT066	3.31					
ompF	3.29	outer membrane protein 1a (ia;b;f), porin	X			X
STM3170	3.28	putative inner membrane protein				
STM4467	3.26	putative arginine deiminase				
ycfS	3.26	putative periplasmic protein				
mreB	3.23	rod shape-determining protein; HSP70 class molecular chaperones involved in cell morphogenesis				
mod	3.18	DNA methylase; restriction system				
mgtA	3.16	P-type ATPase, Mg2+ ATPase transporter				
mglA	3.15	ABC superfamily (atp_bind), galactose (methyl-galactoside) transport			X	X

		protein				
slp	3.14	putative outer membrane protein				
rplN	3.12	50S ribosomal subunit protein L14				X
oppB	3.05	ABC superfamily (membrane), oligopeptide transport protein				X
sixA	3.04	phosphohistidine phosphatase				
fadD	2.94	acyl-CoA synthetase (long-chain-fatty-acid--CoA ligase)			X	
pyrI	2.94	aspartate carbamoyltransferase, regulatory subunit (allosteric regulation)				
ycfR	2.94	putative outer membrane protein				
lrp	2.92	regulator for lrp regulon and high-affinity branched-chain amino acid transport system; mediator of of leucine response (AsnC family)			X	X
rplF	2.87	50S ribosomal subunit protein L6				
STM2747	2.87	putative cytoplasmic protein		X	X	
mglC	2.86	ABC superfamily (membrane), methyl-galactoside transport protein			X	
ydgH	2.86	putative periplasmic protein				
STM2746	2.85	putative Excinuclease ATPase subunit		X	X	
rplX	2.83	50S ribosomal subunit protein L24				
cysM	2.82	cysteine synthase B (O-acetylserine sulfhydrolase B)				
rpmC	2.82	50S ribosomal subunit protein L29				
STM0906	2.82	Fels-1 prophage		X		
glpF	2.81	MIP channel, glycerol diffusion			X	X
STM4305	2.79	putative anaerobic dimethyl sulfoxide reductase, subunit A				X
STM1368	2.78	putative Na+-dicarboxylate symporter				
yfgM	2.76	putative inner membrane protein				
agp	2.69	glucose-1-phosphatase				
priB	2.69	primosomal replication protein N				X
pyrB	2.68	aspartate carbamoyltransferase, catalytic subunit				
yaeL	2.67	putative membrane-associated Zn-dependent protease				
STM1256	2.65	putative ABC transporter				
hflX	2.64	putative GTP-ase, together with HflCK possibly involved in phage lambda cII repressor stability			X	X
STM1250	2.64	putative cytoplasmic protein		X		
fabI	2.62	enoyl-[acyl-carrier-protein] reductase (NADH)				
stdB	2.62	putative outer membrane usher protein				
ytgA	2.62	putative inner membrane protein			X	
rplE	2.61	50S ribosomal subunit protein L5				X
rpsA	2.6	30S ribosomal subunit protein S1				
ybhC	2.6	putative pectinesterase				
greA	2.59	transcription elongation factor, cleaves 3' nucleotide of paused mRNA	X			
nhaB	2.59	NhaB family of transport protein, Na+/H+ antiporter, regulator of intracellular pH				
lpxD	2.58	UDP-3-O-(3-hydroxymyristoyl)-glucosamine n-acyltransferase				X
potD	2.56	ABC superfamily (peri_perm), spermidine/putrescine transporter				
tktA	2.54	transketolase 1 isozyme				
fumA	2.53	fumarase A (fumarate hydratase class I), aerobic isozyme				X
serA	2.52	D-3-phosphoglycerate dehydrogenase				
mdoH	2.51	membrane glycosyltransferase; synthesis of membrane-derived oligosaccharide (MDO)/synthesis of OPGs (osmoregulated periplasmic glucans)				
hmpA	2.48	dihydropteridine reductase 2 and nitric oxide dioxygenase activity				
tsf	2.48	protein chain elongation factor EF-Ts	X			X
serC	2.46	3-phosphoserine aminotransferase / phosphohydroxythreonine transaminase				X
tolB	2.46	tol protein required for outer membrane integrity, uptake of group A colicins, and translocation of phage DNA to cytoplasm, may be part of multiprotein peptidoglycan recycling complex (Two domains)				X
rpmG	2.44	50S ribosomal subunit protein L33				
sbp	2.44	ABC superfamily (bind_prot), sulfate transport protein				
STM3127	2.44	putative cytoplasmic protein				
surA	2.44	peptidyl-prolyl cis-trans isomerase, survival protein	X			
hemN	2.43	O2-independent coproporphyrinogen III oxidase				
rpsB	2.43	30S ribosomal subunit protein S2				X
rpsH	2.43	30S ribosomal subunit protein S8, and regulator				X
yfcB	2.43	putative methylase				
STM4423	2.42	putative AraC-type DNA-binding domain-containing protein				
STM4424	2.42	putative endonuclease				
bacA	2.4	bacitracin resistance; possibly phosphorylates undecaprenol				
fabB	2.4	3-oxoacyl-[acyl-carrier-protein] synthase I				X
oppD	2.4	ABC superfamily (atp-binding), oligopeptide transport protein				X
ybhR	2.4	putative ABC superfamily (membrane) transport protein				
btuB	2.39	outer membrane receptor for transport of vitamin B12, E colicins, and bacteriophage BF23				
kdgK	2.39	ketodeoxygluconokinase				
rpsN	2.39	30S ribosomal subunit protein S14				
htpX	2.38	heat shock protein, integral membrane protein				
PSLT102	2.38				X	
plsB	2.37	glycerolphosphate acyltransferase activity				
fusA	2.36	protein chain elongation factor EF-G, GTP-binding				X

engA	2.35	putative GTP-binding protein				
pyrL	2.34	pyrBI operon leader peptide				
rpoH	2.33	sigma H (sigma 32) factor of RNA polymerase; transcription of heat shock proteins induced by cytoplasmic stress				X
rpsL	2.33	30S ribosomal subunit protein S12				
rpsD	2.31	30S ribosomal subunit protein S4	X			X
sbmA	2.31	putative ABC superfamily transporter			X	X
ttk	2.3	putative transcriptional regulator (TetR/ArcR family)			X	
fepE	2.29	ferric enterobactin (enterochelin) transporter			X	
STM2706	2.28	Fels-2 prophage: similar to tail fiber protein in phage P2				
oafA	2.26	O-antigen five: acetylation of the O-antigen (LPS)			X	
rpsQ	2.26	30S ribosomal subunit protein S17				
sdaB	2.26	L-serine dehydratase (L-threonine deaminase 2)				
rfbK	2.25	LPS side chain defect: phosphomannomutase		X	X	X
yijC	2.25	putative transcriptional repressor (TetR/AcrR family)				X
glyQ	2.24	glycine tRNA synthetase, alpha subunit				
prsA	2.24	phosphoribosylpyrophosphate synthetase	X			
psd	2.24	phosphatidylserine decarboxylase				
dinI	2.23	DNA damage-inducible protein I, inhibits UmuD processing				
rplR	2.23	50S ribosomal subunit protein L18				
STM0908	2.23	Fels-1 prophage				
tgt	2.23	tRNA-guanine transglycosylase				
trmA	2.23	tRNA (uracil-5-)-methyltransferase				
yiiD	2.23	putative acetyltransferase				
ydgR	2.22	putative POT family, peptide transport protein				
res	2.21	DNA restriction (DNA helicase				
tolQ	2.21	tol protein, membrane-spanning inner membrane proteins, required for outer membrane integrity, uptake of group A colicins, and translocation of phage DNA to cytoplasm				
PSLT068	2.2					
STM2705	2.2	Fels-2 prophage			X	
rpsE	2.19	30S ribosomal subunit protein S5				X
STM1131	2.19	putative outer membrane protein		X		
yceH	2.19	putative cytoplasmic protein				
yhgG	2.19	putative cytoplasmic protein				
STM1530	2.18	putative outer membrane protein			X	
ushB	2.17	CDP-diacylglycerol phosphotidylhydrolase				
glyA	2.16	serine hydroxymethyltransferase				
glyS	2.16	glycine tRNA synthetase, beta subunit				
mopB	2.16	chaperone Hsp10, affects cell division				
rpmD	2.16	50S ribosomal subunit protein L30				
trmD	2.16	tRNA (guanine-7-)-methyltransferase				X
STM4306	2.15	putative anaerobic dimethyl sulfoxide reductase, subunit B				
feoB	2.14	FeoB family, ferrous iron transport protein B				
pyrE	2.14	orotate phosphoribosyltransferase				
yidC	2.14	putative Preprotein translocase subunit YidC				
hybC	2.13	hydrogenase-2, large subunit				X
STM1607	2.13	putative outer membrane lipoprotein				
cadB	2.12	APC family, lysine/cadaverine transport protein				
gnd	2.12	gluconate-6-phosphate dehydrogenase, decarboxylating			X	X
rfbU	2.12	LPS side chain defect: mannosyl transferase		X	X	X
STM4307	2.12	putative anaerobic dimethyl sulfoxide reductase, subunit C				
nirC	2.11	FNT family, nitrite transport protein				
yggT	2.11	putative integral membran resistance protein				
yhcB	2.11	putative periplasmic protein				X
PSLT069	2.1					
STM1252	2.1	putative cytoplasmic protein		X		
STM2237	2.1	putative inner membrane protein				
STM2754	2.1	putative hexulose 6 phosphate synthase			X	
ydcG	2.1	paral putative periplasmic glucans biosynthesis protein				
rplO	2.09	50S ribosomal subunit protein L15				X
yaiW	2.09	putative outer membrane lipoprotein				
aroP	2.08	APC family, aromatic amino acid transporter				
STM3604	2.08	putative inner membrane protein				X
STM4464	2.07	putative arginine repressor				
yhcG	2.07	putative cytoplasmic protein				
prpC	2.06	putative citrate synthase				
rpmF	2.06	50S ribosomal subunit protein L32				
yheO	2.06	putative regulator				
asd	2.05	aspartate-semialdehyde dehydrogenase				
kbl	2.05	2-amino-3-ketobutyrate CoA ligase (glycine acetyltransferase)	X			
STM0149	2.05	putative permease of the Na+:galactoside symporter family				
STM3259	2.05	PTS family galactitol-specific enzyme IIB				
STM4418	2.05	sugar (and other) transporter				
agsA	2.04	Molecular chaperone (small heat shock protein) Tomoyasu, T (2003) J.		X		

		Bact. 185: 6331-9				
PSLT003	2.04					
STM1485	2.04	acid shock protein				
STM1540	2.04	putative hydrolase				
STM2236	2.04	putative phage protein				
STM2636	2.04	Gifsy-1 prophage: similar to integrase in phage				
STM2767	2.04	putative Superfamily I DNA and RNA helicase		X	X	X
uraA	2.04	NCS2 family, uracil transport protein				
sfbA	2.03	putative ABC-type transport system ATPase component/cell division protein			X	
crp	2.02	catabolite activator protein (CAP), cyclic AMP receptor protein (CRP family)			X	X
maeB	2.02	paral putative transferase	X			X
ompD	2.02	new outer membrane protein; predicted bacterial porin				X
nirD	2.01	nitrite reductase, small subunit			X	
mpl	2	UDP-N-acetylmuramate:L-alanyl-gamma-D-glutamyl- meso-diaminopimelate ligase				X
STM3633	2	putative bacterial regulatory proteins, lacI family				
rfaD	-2	ADP-L-glycero-D-mannoheptose-6-epimerase				X
STM1324	-2	putative cytoplasmic protein				X
STM2905	-2	putative acetyltransferase		X		
fhlA	-2.01	formate hydrogen-lyase transcriptional activator for fdhF, hyc and hyp operons (EBP family)				
fliQ	-2.01	flagellar biosynthesis				
gcd	-2.01	glucose dehydrogenase				
proW	-2.01	ABC superfamily (membrane), glycine/betaine/proline transport protein				
ptsG	-2.02	Sugar Specific PTS family, glucose-specific IIBCcomponent			X	X
fliE	-2.03	putative Flagellar hook-basal body protein				
STM0856	-2.03	putative electron transfer flavoprotein alpha subunit		X		
yneC	-2.03	putative inner membrane protein		X		
yjjV	-2.04	putative hydrolase				
PSLT023	-2.05					
yhjD	-2.05	putative tRNA-processing ribonuclease				
yncD	-2.05	paral putative outer membrane receptor				
celA	-2.06	PTS family, sugar specific enzyme IIB for cellobiose, arbutin, and salicin		X	X	X
ybhL	-2.06	putative permease				X
celD	-2.07	transcriptional repressor of cel operon (AraC/XylS family)				
ddlB	-2.07	D-alanine-D-alanine ligase B, affects cell division				X
pagD	-2.08	PhoP regulated		X		
rfaF	-2.08	ADP-heptose; LPS heptosyltransferase 1				X
STM1630	-2.08	putative inner membrane protein		X		
STM2614	-2.08	Gifsy-1 prophage				
ynbE	-2.08	putative outer membrane lipoprotein				
ynfD	-2.08	putative outer membrane protein				
ldhA	-2.09	fermentative D-lactate dehydrogenase, NAD-dependent				
ydfZ	-2.09	putative cytoplasmic protein				
yjjU	-2.09	putative phosphoesterase				X
ynhG	-2.09	putative LysM domain				
qor	-2.1	quinone oxidoreductase, NADPH dependent				
csgA	-2.11	curlin major subunit, coiled surface structures; cryptic		X		
STM1859	-2.11	putative cytoplasmic protein				
STM1939	-2.11	putative glucose-6-phosphate dehydrogenase		X	X	X
ugpC	-2.11	ABC superfamily (atp_bind), sn-glycerol 3-phosphate transport protein				
ycfH	-2.11	putative metal-dependent hydrolase				
yegH	-2.11	putative inner membrane protein				
ygdP	-2.11	putative invasion protein; NTP pyrophosphohydrolase				X
deoC	-2.13	2-deoxyribose-5-phosphate aldolase				
STM0081	-2.13	putative secreted protein				
pfkB	-2.14	6-phosphofructokinase II				
soxR	-2.14	redox-sensing transcriptional activator SoxR, contains iron-sulfur center for redox-sensing (MerR family)				
ugpA	-2.14	ABC superfamily (membrane), sn-glycerol 3-phosphate transport protein				
STM1123	-2.15	putative periplasmic protein				
STM1809	-2.15	putative cytoplasmic protein				
rhaS	-2.16	positive regulator for rhaBAD operon (AraC/XylS family)			X	
dmsA	-2.17	anaerobic dimethyl sulfoxide reductase, subunit A				X
mscL	-2.17	mechanosensitive channel				X
pgpB	-2.18	phosphatidylglycerophosphate phosphatase B				X
ssaV	-2.19	Secretion system apparatus: homology with the LcrD family of proteins		X		
fidL	-2.2	putative inner membrane protein		X		X
ybeL	-2.2	putative cytoplasmic protein				X
yohI	-2.2	putative nitrogen regulation protein				
ssaT	-2.21	Secretion system apparatus: homology with YscT of the secretion system of Yersinia		X	X	
STM2208	-2.21	putative inner membrane protein				
yohD	-2.21	putative DedA family, membrane protein				

modB	-2.22	ABC superfamily (membrane), molybdate transporter				
STM1562	-2.22	putative periplasmic transport protein		X		
yhjQ	-2.22	putative ATPase involved in chromosome partitioning				
erfK	-2.23	putative periplasmic protein				
modC	-2.23	ABC superfamily (atp_bind), molybdate transporter				
STM1672	-2.23	putative cytoplasmic protein		X		
pfkA	-2.24	6-phosphofructokinase I				X
ssaS	-2.24	Secretion system apparatus: homology with YscS of the secretion system of Yersinia		X	X	
ycgR	-2.24	putative inner membrane protein				
bcfA	-2.25	fimbrial subunit				
STM2126	-2.25	putative HlyD family secretion protein				
caiF	-2.27	transcriptional regulator of cai and fix operon				X
STM1858	-2.27	putative cytoplasmic protein		X		
hopD	-2.28	leader peptidase HopD				
STM1633	-2.28	putative periplasmic binding protein		X		
STM1988	-2.28	putative cytoplasmic protein				
STM4310	-2.28	putative inner membrane protein		X	X	
glgX	-2.29	glycosyl hydrolase				X
STM1624	-2.29	putative cytoplasmic protein				
ynhA	-2.29	putative SufE protein probably involved in Fe-S center assembly				
glgB	-2.3	1,4-alpha-glucan branching enzyme			X	X
STM1054	-2.31	Gifsy-2 prophage				
ygiW	-2.31	putative outer membrane protein				
marT	-2.32	putative transcriptional regulatory protein				
pgtE	-2.32	Phosphoglycerate transport: outer membrane protein E				
yehV	-2.32	putative transcriptional repressor (MerR family)				
ymgE	-2.32	putative transglycosylase-associated protein				
flhB	-2.33	putative part of export apparatus for flagellar proteins				
yadI	-2.33	putative PTS enzyme				
astE	-2.35	succinylglutamate desuccinylase				
STM0810	-2.35	putative inner membrane protein				
flhC	-2.36	regulator of flagellar biosynthesis, acts on class 2 operons			X	X
yhjL	-2.36	putative TPR-repeat-containing protein				X
ymdC	-2.36	putative phospholipase				X
STM0381	-2.37	putative inner membrane protein				
STM4206	-2.37	putative phage glucose translocase				
glgC	-2.38	glucose-1-phosphate adenylyltransferase				X
phnB	-2.38	putative cytoplasmic protein				
ycdC	-2.38	putative transcriptional repressor (TetR/AcrR family)				
acrR	-2.39	acrAB operon repressor (TetR/AcrR family)			X	
STM0053	-2.39	putative transcription regulator, histidine kinase for citrate			X	
yaiA	-2.39	putative cytoplasmic protein				
pflA	-2.4	pyruvate formate lyase activating enzyme 1				
srfA	-2.4	ssrAB activated gene				
STM0033	-2.4	putative 5'-nucleotidase		X		
STM4257	-2.4	putative inner membrane or exported		X	X	X
gppA	-2.41	guanosine pentaphosphatase and exopolyphosphatase				
spaS	-2.41	surface presentation of antigens; secretory proteins		X		X
STM2245	-2.42	putative outer membrane protein				
tdcC	-2.43	HAAAP family, L-threonine/ L-serine permease, anaerobically inducible				
STM3681	-2.44	putative transcriptional regulator				
STM4071	-2.44	putative Mannose-6-phosphate isomerase				
fliR	-2.45	putative flagellar biosynthetic protein				
pykF	-2.45	pyruvate kinase I (formerly F), fructose stimulated				
ssaQ	-2.46	Secretion system apparatus		X	X	
STM2803	-2.46	putative regulatory protein, gntR family				
PSLT040	-2.47					
yeeY	-2.47	putative transcriptional regulator, LysR family				
ssaP	-2.5	Secretion system apparatus		X		
STM1055	-2.51	Gifsy-2 prophage				
STM1147	-2.51	putative ACR related to the C-terminal domain of histone macroH2A1				X
STM2585A	-2.51	Gifsy-1 prophage: Homolog of pagK				
sseF	-2.52	Secretion system effector				
ychM	-2.52	putative SulP family transport protein				
fliI	-2.53	flagellum-specific ATP synthase				X
STM2137	-2.54	putative cytoplasmic protein				
yhjO	-2.54	glycosyltransferase, probably involved in cell wall biogenesis				
ydeV	-2.56	putative sugar kinase				
STM0082	-2.57	putative secreted protein			X	
STM1491	-2.57	ABC-type proline/glycine betaine transport systems, ATPase component				
STM2904	-2.57	putative ABC-type transport system		X		
glgA	-2.58	glycogen synthase				
otsB	-2.59	trehalose-6-phosphate phophatase, biosynthetic				
uspB	-2.61	universal stress protein B, involved in stationary-phase resistance to ethanol				X

fliB	-2.62	N-methylation of lysine residues in flagellin				
fliF	-2.63	flagellar biosynthesis; basal-body MS(membrane and supramembrane)-ring and collar protein				
sscB	-2.63	Secretion system chaparone		X		
ydcX	-2.63	putative inner membrane protein				
ydiU	-2.63	putative cytoplasmic protein				X
sanA	-2.64	vancomycin sensitivity			X	X
sinR	-2.64	transcriptional regulator			X	
yeeZ	-2.64	putative dehydratase				
flgB	-2.65	flagellar biosynthesis, cell-proximal portion of basal-body rod				
yneB	-2.65	putative fructose-1,6-bisphosphate aldolase				X
yjcC	-2.67	putative diguanylate cyclase/phosphodiesterase				
STM4575	-2.68	putative outer membrane protein				
adiY	-2.7	transcriptional activator of adiA (AraC/XylS family)			X	
mtlR	-2.7	repressor for mtl				
STM0860	-2.7	putative inner membrane protein		X		
mug	-2.72	DNA glycosylase, G/U mismatch specific				
suhB	-2.72	inositol monophosphatase				
yjfO	-2.72	putative lipoprotein				X
ftnB	-2.73	ferritin-like protein				X
STM1484	-2.73	putative protease				
STM2475	-2.73	putative cytoplasmic protein				
yqjG	-2.73	putative glutathione S-transferase				X
malT	-2.74	transcriptional activator of the mal genes, binds inducer (maltotriose) and ATP (LysR familiy)				X
orf319	-2.75	putative inner membrane protein				X
STM3152	-2.75	putative methyl-accepting chemotaxis protein				
rnc	-2.76	RNase III, ds RNA				
ssaD	-2.78	Secretion system apparatus		X		
yhbP	-2.78	putative cytoplasmic protein				
zur	-2.78	transcriptional repressor of znuABC operon (Fur family)				X
STM4219	-2.79	putative cytoplasmic protein				
yneA	-2.79	putative ABC superfamily (peri_perm), sugar transport protein				
pagK	-2.8	PhoPQ-activated gene		X		X
ybeQ	-2.8	putative TPR repeat protein				
yhhT	-2.8	putative PerM family permease				
aidB	-2.81	putative acyl-CoA dehydrogenase; adaptive response (transcription activated by Ada)				
exbD	-2.81	uptake of enterochelin; tonB-dependent uptake of B colicins				
cheA	-2.82	sensory histitine protein kinase, transduces signal between chemo- signal receptors and CheB and CheY				X
pagC	-2.82	PhoP regulated: reduced macrophage survival	X	X		X
proP	-2.83	MFS family, low-affinity proline transporter (proline permease II)			X	X
yajO	-2.83	putative oxidoreductase / K + channel protein				
soxS	-2.84	transcriptional activator of superoxide response regulon (AraC/XylS family)				
ydcW	-2.84	putative aldehyde dehydrogenase				
bcsC	-2.85	endo-1,4-D-glucanase				
flgA	-2.86	flagellar biosynthesis; assembly of basal-body periplasmic P ring				
PSLT039	-2.86					
dbpA	-2.87	ATP-dependent RNA helicase, stimulated by 23S rRNA				
fliD	-2.87	flagellar biosynthesis; filament capping protein; enables filament assembly				X
sifB	-2.87	Salmonella translocated effector: translocated by SPI-2		X		X
gabT	-2.88	4-aminobutyrate aminotransferase				
yehX	-2.88	putative ABC-type proline/glycine betaine transport system, ATPase component				
modA	-2.89	ABC superfamily (peri_perm), molybdate transporter				X
STM1987	-2.89	putative inner membrane protein				
ybaJ	-2.89	putative cytoplasmic protein		X		X
yhjR	-2.89	putative cytoplasmic protein				
cheB	-2.9	methyl esterase, response regulator for chemotaxis (cheA sensor)				X
srfC	-2.9	ssrAB activated gene: predicted coiled-coil structure				
ssaO	-2.9	Secretion system apparatus		X		
fruA	-2.91	Sugar Specific PTS system, fructose-specific transport protein				
phsA	-2.91	Hydrogen sulfide production: membrane anchoring protein				X
yhjN	-2.91	putative cellulose synthase				
STM1330	-2.92	putative DNA/RNA non-specific endonuclease				
astB	-2.93	succinylarginine dihydrolase				
spaQ	-2.93	surface presentation of antigens; secretory proteins		X		
galP	-2.96	MFS family, galactose:proton symporter				
STM0948	-2.96	putative cytoplasmic protein				
cfa	-3	cyclopropane fatty acyl phospholipid synthase				
cigR	-3.02	putative inner membrane protein				
slrP	-3.02	leucine-rich repeat protein			X	X
STM1698	-3.02	putative inner membrane protein				
STM3155	-3.02	putative cytoplasmic protein			X	
yjcB	-3.02	putative inner membrane protein			X	

fliP	-3.03	flagellar biosynthesis				X
ycgB	-3.03	putative cytoplasmic protein				X
yhjS	-3.03	putative cytoplasmic protein				
yjgB	-3.03	putative alcohol dehydrogenase				
STM1934	-3.04	putative outer membrane lipoprotein				
flgC	-3.05	flagellar biosynthesis, cell-proximal portion of basal-body rod				
sufS	-3.05	selenocysteine lyase				
ssaC	-3.06	Secretion system apparatus		X		
STM2715	-3.07	Fels-2 prophage: probable prophage lysozyme		X		
ychH	-3.08	putative inner membrane protein				X
flgI	-3.09	putative flagella basal body protein				
yhjT	-3.09	putative inner membrane protein				
phsB	-3.12	Hydrogen sulfide production: iron- sulfur subunit; electron transfer				
ssaN	-3.12	Secretion system apparatus: homology with the YscN family of proteins				X
fic	-3.14	putative cell filamentation protein, stationary phase induced gene, affects cell division				
ssaB	-3.14	Secretion system apparatus		X		
STM1056	-3.15	Gifsy-2 prophage; Homolog of msgA				
yohC	-3.16	paral putative transport protein				
manY	-3.19	Sugar Specific PTS family, mannose-specific enzyme IIC				X
STM1026	-3.19	Gifsy-2 prophage				
flhD	-3.2	regulator of flagellar biosynthesis, acts on class 2 operons			X	X
ybhK	-3.21	putative cytoplasmic protein				
yjfN	-3.22	putative inner membrane protein				X
hilA	-3.24	invasion genes transcription activator		X	X	X
ompA	-3.27	putative hydrogenase, membrane component				X
STM4258	-3.28	putative methyl-accepting chemotaxis protein		X	X	X
manX	-3.31	Sugar Specific PTS family, mannose-specific enzyme IIAB				X
STM4316	-3.31	putative cytoplasmic protein		X	X	
grxB	-3.32	glutaredoxin 2				X
flhE	-3.33	flagellar protein				
blc	-3.34	outer membrane lipoprotein (lipocalin)				
pipB2	-3.34	Pathogenicity island encoded protein: SPI3		X		X
yqhE	-3.37	2,5-diketo-D-gluconate reductase A				
ratA	-3.41	putative outer membrane protein				
trg	-3.42	methyl-accepting chemotaxis protein III, ribose and galactose sensor receptor				X
ydeJ	-3.42	putative Competence-damaged protein				
fliH	-3.43	flagellar biosynthesis; possible export of flagellar proteins				
sseJ	-3.44	Salmonella translocated effector: regulated by SPI-2		X		
yhcN	-3.44	putative outer membrane protein				
ycfQ	-3.45	putative transcriptional repressor (TetR/AcrR family)				
yebW	-3.46	putative inner membrane lipoprotein				
sseG	-3.47	Secretion system effector		X		
ugpQ	-3.47	glycerophosphodiester phosphodiesterase, cytosolic				
csgC	-3.49	putative curli production protein		X		
narY	-3.49	nitrate reductase 2, beta subunit				
yobG	-3.5	putative inner membrane protein				X
ssrA	-3.52	Secretion system regulator:Sensor component		X		
flgK	-3.53	flagellar biosynthesis, hook-filament junction protein 1				X
otsA	-3.54	trehalose-6-phosphate synthase				
STM1561	-3.54	putative outer membrane or secreted lipoprotein				
celG	-3.55	putative glucosidase			X	X
sscA	-3.55	Secretion system chaparone				X
ybiI	-3.55	putative DnaK suppressor protein				
hilC	-3.56	bacterial regulatory helix-turn-helix proteins, araC family		X	X	X
STM1851	-3.57	putative cytoplasmic protein				
talA	-3.58	transaldolase A				
acnA	-3.61	aconitate hydratase 1				X
STM1398	-3.61			X		
sptP	-3.62	protein tyrosine phosphate		X	X	X
ssaR	-3.62	Secretion system apparatus: homology with YscR of the secretion system of Yersinia		X		
ugpB	-3.62	ABC superfamily (peri_perm), sn-glycerol 3-phosphate transport protein				
aer	-3.63	aerotaxis sensor receptor, senses cellular redox state or proton motive force				
STM1967	-3.63	putative 50S ribosomal protein				
fljB	-3.64	Flagellar synthesis: phase 2 flagellin (filament structural protein)		X		
yedP	-3.65	putative hydrolase of the HAD superfamily				
STM4574	-3.67	putative outer membrane protein				
ybhO	-3.67	cardiolipin (CL) synthase				
STM2405	-3.69	putative thiamine pyrophosphate enzymes				
yibF	-3.69	putative glutathione S-transferase				
STM1261	-3.7	putative cytoplasmic protein				
tsr	-3.71	methyl-accepting chemotaxis protein I, serine sensor receptor				X
osmC	-3.74	putative resistance protein, osmotically inducible				

STM0972	-3.74	homologous to secreted protein sopD				
yhfG	-3.74	putative cytoplasmic protein				
sufC	-3.75	putative ABC superfamily (atp_bind) transport protein				
ydiY	-3.76	putative salt-induced outer membrane protein				
narW	-3.8	nitrate reductase 2, delta subunit, assembly function				
fliL	-3.85	flagellar biosynthesis				
spaR	-3.85	surface presentation of antigens; secretory proteins		X		X
STM3154	-3.86	putative ATP-dependent RNA helicase-like protein				X
STM1329	-3.89	putative inner membrane protein				
sufD	-3.89	required for stability of iron-sulfur component of FhuF				
manZ	-3.91	Sugar Specific PTS family, mannose-specific enzyme IID				X
sugE	-3.93	putative DMT superfamily transport protein				
rpsV	-3.95	30S ribosomal subunit protein S22				
yebF	-3.95	putative periplasmic protein				X
STM1239	-3.96	putative cytoplasmic protein		X	X	X
fliO	-3.98	flagellar biosynthesis		X		
yncB	-3.98	putative NADP-dependent oxidoreductase				X
yceK	-4.02	putative outer membrane lipoprotein				
yqjK	-4.04	putative inner membrane protein				
STM3774	-4.05	putative inner membrane protein				
yehY	-4.11	putative ABC-type proline/glycine betaine transport systems, permease component				X
yhjE	-4.12	putative MFS family transport protein				
sitD	-4.15	Salmonella iron transporter: fur regulated				
yahO	-4.16	putative periplasmic protein				X
aldB	-4.25	aldehyde dehydrogenase B (lactaldehyde dehydrogenase)				X
STM4259	-4.25	putative ABC exporter outer membrane component homolog		X		X
yhjH	-4.27	putative Diguanylate cyclase/phosphodiesterase domain 3				X
sicP	-4.29	chaparone, related to virulence		X	X	X
chaB	-4.31	cation transport regulator				
sseD	-4.35	Secretion system effector		X		
yfdC	-4.35	putative transport				
sufA	-4.41	putative HesB-like domain				
ggt	-4.49	gamma-glutamyltranspeptidase				
ssaK	-4.49	Secretion system apparatus		X		
fliC	-4.5	flagellar biosynthesis; flagellin, filament structural protein	X			X
sseE	-4.5	Secretion system effector		X		
phsC	-4.52	Hydrogen sulfide production: membrane anchoring protein				
STM1267	-4.62	putative cytoplasmic protein		X		
STM3156	-4.67	putative cytoplasmic protein				
yhhA	-4.69	putative outer membrane protein				
STM4262	-4.7	putative ABC-type bacteriocin/lantibiotic exporter, contain an N-terminal double-glycine peptidase domain		X		X
yeaH	-4.72	putative cytoplasmic protein				X
tktB	-4.75	transketolase 2, isozyme				
sufB	-4.79	putative ABC transporter				
flgF	-4.81	flagellar biosynthesis, cell-proximal portion of basal-body rod				X
flgG	-4.82	flagellar biosynthesis, cell-distal portion of basal-body rod				
cheZ	-4.84	chemotactic response; CheY protein phophatase				X
STM3362	-4.92	putative periplasmic protein			X	X
STM1731	-5.03	putative catalase				X
STM3688	-5.05	putative cytoplasmic protein				
flgD	-5.08	flagellar biosynthesis, initiation of hook assembly				X
yohF	-5.09	putative oxidoreductase				
sopB	-5.11	Salmonella outer protein: homologous to ipgD of Shigella		X		X
rtsA	-5.16	putative AraC-type DNA-binding domain-containing protein		X	X	
iagB	-5.2	cell invasion protein		X		X
ssrB	-5.24	Secretion system regulator: transcriptonal activator, homologous with degU/uvrY/bvgA		X		X
STM0080	-5.25	putative outer membrane lipoprotein				
STM1397	-5.26			X		
bfr	-5.29	bacterioferrin, an iron storage homoprotein		X		
STM4312	-5.31	putative phage protein		X	X	
ugtL	-5.34	putative membrane protein: homology with chitinase from Schizosaccharomyces				X
yegS	-5.36	putative diacylglycerol kinase catalytic domain				
STM1558	-5.37	putative glycosyl hydrolase				X
STM4313	-5.42	putative cytoplasmic protein		X	X	
invA	-5.43	invasion protein		X	X	X
adhE	-5.44	iron-dependent alcohol dehydrogenase of the multifunctional alcohol dehydrogenase AdhE				X
yfbK	-5.46	putative von Willebrand factor, vWF type A domain				
STM4260	-5.47	membrane permease, predicted cation efflux pump		X	X	X
STM1301	-5.5	putative mutator MutT protein				
fliN	-5.52	flagellar biosynthesis, component of motor switch and energizing				
flgE	-5.55	flagellar biosynthesis, hook protein				X

fliK	-5.59	flagellar hook-length control protein				
rtsB	-5.59	putative bacterial regulatory proteins, luxR family		X		
sseC	-5.66	Secretion system effector		X		X
sdiA	-5.69	transcriptional regulator of ftsQAZ gene cluster (LuxR/UhpA family)				X
STM3132	-5.72	putative xylanase/chitin deacetylase				X
treA	-5.72	trehalase, periplasmic				X
fliJ	-5.73	flagellar fliJ protein				
fliM	-5.81	flagellar biosynthesis, component of motor switch and energizing				X
spy	-5.85	periplasmic protein related to spheroblast formation				
ssaL	-5.89	Secretion system apparatus		X		
yodD	-5.9	putative cytoplasmic protein				
motB	-5.94	enables flagellar motor rotation, linking torque machinery to cell wall				X
cheY	-5.96	chemotaxis regulator, transmits chemoreceptor signals to flagelllar motor components				X
prgH	-6.04	cell invasion protein		X		X
STM2780	-6.04	Homolog of pipB, putative pentapeptide repeats (8 copies)		X		
yehZ	-6.05	putative ABC superfamily (bind_prot) transport protein (possibly glycine betaine choline transport for osmoprotection)				X
fliT	-6.06	flagellar biosynthesis; possible export chaperone for FliD				
STM0362	-6.13	putative cytoplasmic protein				
psiF	-6.14	induced by phosphate starvation				
STM2404	-6.14	putative chloride channel permease				
sprB	-6.2	transcriptional regulator		X		X
ygaE	-6.2	putative transcriptional repressor (GntR familiy)				
fliZ	-6.22	putative regulator of FliA				X
avrA	-6.28	putative inner membrane protein		X	X	X
sipB	-6.29	cell invasion protein				X
cheR	-6.31	glutamate methyltransferase, response regulator for chemotaxis				X
motA	-6.34	proton conductor component of motor, torque generator				X
invH	-6.35	invasion protein		X	X	
ssaI	-6.36	Secretion system apparatus		X		
STM1328	-6.4	putative outer membrane protein	X		X	X
poxB	-6.42	pyruvate dehydrogenase/oxidase FAD and thiamine PPi cofactors, cytoplasmic in absence of cofactors				
invC	-6.51	surface presentation of antigens; secretory proteins			X	X
STM3133	-6.52	putative amidohydrolase				X
yhbO	-6.54	putative intracellular proteinase				
invB	-6.57	surface presentation of antigens; secretory proteins		X		X
osmE	-6.58	transcriptional activator of ntrL gene				X
yccJ	-6.6	putative cytoplasmic protein				
spaP	-6.62	surface presentation of antigens; secretory proteins		X	X	X
ssaG	-6.73	Secretion system apparatus		X		
fliS	-6.83	flagellar biosynthesis; repressor of class 3a and 3b operons (RflA activity)				X
ssaH	-6.86	Secretion system apparatus		X		
STM1089	-6.91	putative inner membrane protein		X		
orgA	-6.92	putative flagellar biosynthesis/type III secretory pathway protein		X	X	X
hilD	-6.93	regulatory helix-turn-helix proteins, araC family		X	X	X
ecnR	-7.26	putative bacterial regulatory protein, luxR family				
cheW	-7.27	purine-binding chemotaxis protein; regulation				X
msyB	-7.28	acidic protein suppresses mutants lacking function of protein export				
ssaJ	-7.28	Secretion system apparatus: homology with the yscJ/mxiJ/prgK family of lipoproteins		X		X
yeaQ	-7.43	putative inner membrane protein		X		X
invG	-7.56	invasion protein; outer membrane		X	X	X
sipC	-7.6	cell invasion protein	X	X		X
yqjE	-7.62	putative inner membrane protein				
invF	-7.69	invasion protein		X	X	X
STM2870	-7.75	putative inner membrane protein		X	X	
invI	-7.76	surface presentation of antigens; secretory proteins		X		
tcp	-7.91	methyl-accepting transmembrane citrate/phenol chemoreceptor				X
sopA	-7.93	Secreted effector protein of Salmonella dublin				X
iacP	-7.94	putative acyl carrier protein		X	X	X
flgL	-8.06	flagellar biosynthesis; hook-filament junction protein			X	X
prgK	-8.27	cell invasion protein; lipoprotein, may link inner and outer membranes		X		X
sodC	-8.3	copper/zinc superoxide dismutase				
flgN	-8.33	flagellar biosynthesis: belived to be export chaperone for FlgK and FlgL				X
prgJ	-8.36	cell invasion protein; cytoplasmic		X		X
sopE2	-8.64	TypeIII-secreted protein effector: invasion-associated protein		X	X	X
prgI	-8.65	cell invasion protein; cytoplasmic		X		
adhP	-8.66	alcohol dehydrogenase, propanol preferring				
STM4261	-8.67	putative inner membrane protein		X	X	X
STM4519	-8.71	putative NAD-dependent aldehyde dehydrogenase				
wraB	-8.77	trp-repressor binding protein				X
STM1300	-8.79	putative periplasmic protein				X
STM2585	-8.91	Gifsy-1 prophage: similar to transpose				

STM2139	-9.13	putative inner membrane protein		X		
osmB	-9.36	osmotically inducible lipoprotein				
fliA	-9.49	sigma F (sigma 28) factor of RNA polymerase, transcription of late flagellar genes (class 3a and 3b operons)				X
STM1560	-9.54	putative alpha amylase				
invE	-9.9	invasion protein		X		X
flgM	-10.09	anti-FliA (anti-sigma) factor; also known as RflB protein				X
invJ	-10.12	surface presentation of antigens; secretory proteins		X		X
yiaG	-10.17	putative transcriptional regulator			X	
yqjC	-10.17	putative periplasmic protein				X
STM0359	-10.31	putative cytoplasmic protein				
ybaY	-10.35	glycoprotein/polysaccharide metabolism				X
STM2868	-10.64	putative cytoplasmic protein		X	X	
sopD	-10.73	secreted protein in the Sop family; transferred to eukaryotic cells				X
cheM	-10.78	methyl accepting chemotaxis protein II, aspartate sensor-receptor				X
dps	-10.99	stress response DNA-binding protein; starvation induced resistance to H2O2	X			X
STM1629	-11.31	putative dipicolinate reductase		X	X	
phoH	-11.78	PhoB-dependent, ATP-binding pho regulon component				
yeaG	-11.81	putative Ser protein kinase				X
ecnB	-12.19	putative entericidin B precursor				X
ygaU	-12.72	putative LysM domain				
fbaB	-13.2	3-oxoacyl-[acyl-carrier-protein] synthase I				
STM1841	-13.44	putative outer membrane or exported			X	X
ampH	-14.03	penicillin- binding protein				
sipA	-14.3	cell invasion protein	X	X		X
elaB	-14.43	putative inner membrane protein				
sipD	-14.99	cell invasion protein		X	X	X
ydeI	-15.37	putative periplasmic protein				
ygdI	-16.14	putative lipoprotein				X
pipC	-16.34	Pathogenicity island encoded protein: homologous to ipgE of Shigella		X		X
yciE	-16.68	putative cytoplasmic protein				
katE	-16.7	catalase; hydroperoxidase HPII(III), RpoS dependent				X
ygaM	-17.53	putative inner membrane protein				
ybgS	-17.94	putative homeobox protein				
STM1513	-18.8	putative cytoplasmic protein				
ymdF	-20.76	putative cytoplasmic protein				
hfq	-21.66	host factor I for bacteriophage Q beta replication, a growth-related protein			X	X
yghA	-24.47	putative oxidoreductase				X
yciF	-24.49	putative cytoplasmic protein				
yjbJ	-28.92	putative cytoplasmic protein				X
yciG	-33.88	putative cytoplasmic protein				
osmY	-34.13	hyperosmotically inducible periplasmic protein, RpoS-dependent stationary phase gene	X			X

[a]Gene names according to ColiBase [3]

[b] Product according to KEGG (http://www.genome.jp/kegg/; [4])

[c] Assignment according to [5]

[d] Assignment according to HGT-GB (http://www.tinet.org/~debb/HGT/; [6]

Table S2: Deregulated genes in Δ*hfq* after 12 hrs SPI-inducing conditions

Gene name[a]	Fold change	Product[b]	2D-analysis[c]	HGT[d]
ybfM	62.11	putative outer membrane protein	X	
pagC	45.66	PhoP regulated: reduced macrophage survival	X	X
ybfN	34.36	putative lipoprotein		
virK	16.31	virulence gene; homologous sequence to virK in Shigella		
yggN	8.70	putative periplasmic protein		
ugtL	8.70	putative membrane protein: homology with chitinase from Schizosaccharomyces		X
rseA	8.20	anti sigma E (sigma 24) factor, negative regulator		
ddg	7.04	cold shock-induced palmitoleoyl transferase		
ygiM	6.85	putative SH3 domain protein		
STM1044	6.45			
STM1253	6.33	putative inner membrane protein		X
STM1583	6.21	putative cytoplasmic protein		
rseB	6.17	anti sigma E (sigma 24) factor, negative regulator		
STM2585A	6.10	Gifsy-1 prophage: Homolog of pagK		
yhjW	6.06	putative membrane-associated, metal-dependent hydrolase		
STM4257	5.68	putative inner membrane or exported		X
STM4260	5.21	membrane permease, predicted cation efflux pump		X
STM1698	5.18	putative inner membrane protein		
STM4259	5.18	putative ABC exporter outer membrane component homolog		X
yraP	4.85	paral putative periplasmic protein	X	
phoN	4.78	non-specific acid phosphatase		
sscB	4.69	Secretion system chaperone		X
sixA	4.65	phosphohistidine phosphatase		
pmrD	4.55	polymyxin resistance protein B		
mig-14	4.46	putative transcription activator		
sseI	4.46	Gifsy-2 prophage; putative type III secreted protein		
yobG	4.44	putative inner membrane protein		
STM1330	4.44	putative DNA/RNA non-specific endonuclease		
sseJ	4.39	Salmonella translocated effector: regulated by SPI-2		X
yraO	4.29	putative phosphoheptose isomerase		
gcvH	4.26	glycine cleavage complex protein H, carrier of aminomethyl moiety via covalently bound lipoyl cofactor		
rpoE	4.18	sigma E (sigma 24) factor of RNA polymerase, response to periplasmic stress		
gcvP	4.17	glycine cleavage complex protein P, glycine decarboxylase		
STM1854	3.94	putative inner membrane protein		
ompC	3.91	outer membrane protein 1b (ib;c), porin		
htrA	3.91	periplasmic serine protease Do, heat shock protein	X	
pagK	3.91	PhoPQ-activated gene		X
ybhQ	3.88	putative inner membrane protein		
rna	3.82	RNase I, cleaves phosphodiester bond between any two nucleotides		

hflK	3.77	with HflC, part of modulator for protease specific for FtsH phage lambda cII repressor		
pgtE	3.65	Phosphoglycerate transport: outer membrane protein E		
ydgR	3.64	putative POT family, peptide transport protein		
cutC	3.57	copper homeostasis protein		
rseC	3.56	regulator of sigma E (sigma 24) factor		
STM2303	3.56	putative inner membrane protein		
pdgL	3.38	Periplasmic dipeptidase for D-ala-D-ala digestion in peptidoglycan		
hflC	3.36	with HflK, part of modulator for protease specific for FtsH phage lambda cII repressor		
sseD	3.24	Secretion system effector		X
pagD	3.23	PhoP regulated		X
STM4504	3.13	putative cytoplasmic protein		
yaeT	3.13	putative outer membrane antigen	X	
hflX	3.11	putative GTP-ase, together with HflCK possibly involved in phage lambda cII repressor stability		
yhjJ	3.08	putative Zn-dependent peptidase		
phoP	3.06	response regulator in two-component regulatory system with PhoQ, transcribes genes expressed under low Mg+ concentration (OmpR family)		
STM1052	3.06			
ycbK	3.03	putative outer membrane protein		
STM1697	2.99	putative Diguanylate cyclase/phosphodiesterase domain 2		
sspH2	2.96	Leucine-rich repeat protein, induced by the SPI-2 regulator ssrA/B		
hlpA	2.91	histone-like protein, located in outer membrane		
gst	2.89	glutathionine S-transferase		
STM1839	2.88	putative periplasmic or exported protein		
STM2447	2.83	putative outer membrane lipoprotein		
gcvT	2.82	glycine cleavage complex protein T, aminomethyltransferase, tetrahydrofolate-dependent		
STM3036	2.72	putative inner membrane protein		
yfcN	2.67	putative Smr domain		
cca	2.62	tRNA nucleotidyl transferase		
surA	2.62	peptidyl-prolyl cis-trans isomerase, survival protein	X	
mreB	2.57	rod shape-determining protein; HSP70 class molecular chaperones involved in cell morphogenesis		
ycbL	2.56	putative Metallo-beta-lactamase		
citA	2.55	citrate-proton symporter		
STM0081	2.53	putative secreted protein		
ybhR	2.50	putative ABC superfamily (membrane) transport protein		
lpxD	2.49	UDP-3-O-(3-hydroxymyristoyl)-glucosamine n-acyltransferase		
STM2585	2.49	Gifsy-1 prophage: similar to transpose		
STM4261	2.46	putative inner membrane protein		X
ydiV	2.44	putative Diguanylate cyclase/phosphodiesterase domain 1		
kdgK	2.44	ketodeoxygluconokinase		
yraR	2.43	putative nucleoside-diphosphate-sugar epimerase		
pdxA	2.38	NAD-dependent dehydrogenase/carboxylase; pyridoxine phosphate biosynthetic protein PdxJ-PdxA subunit		
yfiD	2.33	putative formate acetyltransferase		
STM0082	2.22	putative secreted protein		
yfeK	2.21	putative periplasmic protein		
yidY	2.19	putative MFS family tranport protein (1st mdule)		
STM1940	2.16	putative cell wall-associated hydrolase		

bacA	2.15	bacitracin resistance; possibly phosphorylates undecaprenol		
yiiD	2.14	putative acetyltransferase		
aphA	2.13	non-specific acid phosphatase/phosphotransferase, class B	X	
yijD	2.07	putative inner membrane protein		
ygcA	2.05	putative RNA methyltransferase		
thrC	2.03	threonine synthase		
yheO	2.02	putative regulator		
yciE	-2.04	putative cytoplasmic protein		
yhjH	-2.05	putative Diguanylate cyclase/phosphodiesterase domain 3		
wraB	-2.07	trp-repressor binding protein		
ygaM	-2.10	putative inner membrane protein		
nrdA	-2.13	ribonucleoside diphosphate reductase 1, alpha subunit		
STM3362	-2.16	putative periplasmic protein		
glmS	-2.18	L-glutamine:D-fructose-6-phosphate aminotransferase		
mtlR	-2.23	repressor for mtl		
ybgS	-2.23	putative homeobox protein		
cheZ	-2.27	chemotactic response; CheY protein phophatase		
yjfN	-2.29	putative inner membrane protein		
ecnR	-2.29	putative bacterial regulatory protein, luxR family		
fbaB	-2.30	3-oxoacyl-[acyl-carrier-protein] synthase I		
flgK	-2.33	flagellar biosynthesis, hook-filament junction protein 1		
fimD	-2.35	outer membrane usher protein		
ydeZ	-2.38	putative ABC superfamily (membrane), sugar transport protein		
STM3156	-2.39	putative cytoplasmic protein		
osmB	-2.43	osmotically inducible lipoprotein		
katE	-2.46	catalase; hydroperoxidase HPII(III), RpoS dependent		
potE	-2.46	APC family, putrescine/ornithine antiporter		
yciF	-2.50	putative cytoplasmic protein		
cheB	-2.52	methyl esterase, response regulator for chemotaxis (cheA sensor)		
STM0699	-2.52	putative cytoplasmic protein		
gapA	-2.60	glyceraldehyde-3-phosphate dehydrogenase A		
STM3155	-2.60	putative cytoplasmic protein		
cfa	-2.63	cyclopropane fatty acyl phospholipid synthase		
STM2281	-2.64	putative transcriptional regulator, LysR family		
STM3154	-2.65	putative ATP-dependent RNA helicase-like protein		
cyoC	-2.67	cytochrome o ubiquinol oxidase subunit III		
hha	-2.74	hemolysin expression modulating protein (involved in environmental regulation of virulence factors)		
cyoD	-2.74	cytochrome o ubiquinol oxidase subunit IV		
fliT	-2.82	flagellar biosynthesis; possible export chaperone for FliD		
fliZ	-2.82	putative regulator of FliA		
nuoA	-2.83	NADH dehydrogenase I chain A		
cheW	-2.88	purine-binding chemotaxis protein; regulation		
yccJ	-2.97	putative cytoplasmic protein		
ybaJ	-2.98	putative cytoplasmic protein		X
agsA	-2.99	Molecular chaperone (small heat shock protein)		X

flgL	-2.99	Flagellar biosynthesis; hook-filament junction protein		
STM1093	-3.07	putative cytoplasmic protein		
fimC	-3.08	periplasmic chaperone, required for type 1 fimbriae		X
ygaU	-3.16	putative LysM domain		
cyoB	-3.17	cytochrome o ubiquinol oxidase subunit I		
sodC	-3.19	copper/zinc superoxide dismutase		
osmE	-3.20	transcriptional activator of ntrL gene		
yqjC	-3.25	putative periplasmic protein		
STM0731	-3.29	putative inner membrane protein		
tcp	-3.39	methyl-accepting transmembrane citrate/phenol chemoreceptor		X
cheR	-3.44	glutamate methyltransferase, response regulator for chemotaxis		
flgN	-3.56	flagellar biosynthesis: belived to be export chaperone for FlgK and FlgL		
yeaG	-3.60	putative Ser protein kinase		
mopA	-3.65	chaperone Hsp60 with peptide-dependent ATPase activity, affects cell division		
cheY	-3.88	chemotaxis regulator, transmits chemoreceptor signals to flagelllar motor components		
fliS	-3.94	flagellar biosynthesis; repressor of class 3a and 3b operons (RflA activity)		
cyoA	-4.09	cytochrome o ubiquinol oxidase subunit II	X	
cheM	-4.29	methyl accepting chemotaxis protein II, aspartate sensor-receptor		
motB	-4.31	enables flagellar motor rotation, linking torque machinery to cell wall		
speF	-4.40	ornithine decarboxylase isozyme, inducible		
motA	-4.44	proton conductor component of motor, torque generator		
mopB	-4.63	chaperone Hsp10, affects cell division		
ygdI	-4.69	putative lipoprotein		
fimA	-4.76	major type 1 subunit fimbrin (pilin)		
ecnB	-6.04	putative entericidin B precursor		
orfX	-6.20	putative cytoplasmic protein		
osmY	-6.39	hyperosmotically inducible periplasmic protein, RpoS-dependent stationary phase gene	X	X
dps	-6.62	stress response DNA-binding protein; starvation induced resistance to H2O2	X	
STM1851	-6.68	putative cytoplasmic protein		
yciG	-7.37	putative cytoplasmic protein		
flgM	-10.31	anti-FliA (anti-sigma) factor; also known as RflB protein		
STM1513	-15.52	putative cytoplasmic protein		
fliC	-15.65	flagellar biosynthesis; flagellin, filament structural protein	X	
ymdF	-19.63	putative cytoplasmic protein		
hfq	-32.55	host factor I for bacteriophage Q beta replication, a growth-related protein		

[a]Gene names according to ColiBase [3]

[b] Product according to KEGG (http://www.genome.jp/kegg/; [4])

[c] Assignment according to [5]

[d] Assignment according to HGT-GB (http://www.tinet.org/~debb/HGT/; [6])

Table S3: Coverage of known and candidate *Salmonella* sRNA loci in pyrosequencing data

sRNA[a]	Alternative IDs[b]	Identification[c]	Adjacent genes[d]	Orientation[e]	5' end[f]	3' end[f]	454 control coIP[g]	454 Hfq coIP[h]	Enrichment[i]	Northern[j]
STnc10	-	V	STM0038/*nhaA*	→ ← →	46114	46050	0	0		np
STnc20	-	V	STM0042/*rpsT*	← → ←	51926	52260	1	2	2.0	np
STnc30	-	V	*lytB*/STM005	→ → →	58792	58923	1	0		np
STnc470	-	IV	STM0081/STM0082	→ ← ←	94548	94770	0	70	≥70.0	~1250nt
sgrS	*ryaA*	I	*yabN/leuD*	← → ←	128574	128812	3	61	20.3	
STnc40	-	V	*secA/mutT*	→ → →	161464	161537	0	0		np
STnc50	-	V	*lpdA*/STM0155	→ ← →	182539	182458	0	0		np
STnc60	-	V	*fhuB/stfA*	→ ← →	230277	230063	0	0		np
isrA	-	II	STM0294.1n/STM0295	→ → →	339338	339760	0	0		
sroB	*rybC*	I	*ybaK/ybaP*	← → ←	556005	556085	27	1530	56.7	
STnc480	-	IV	*glxK/ylbA*	→ ← ←	587848	587926	4	74	18.5	nd
STnc70	-	V	*dsbG/ahpC*	← → →	670157	670305	5	7	1.4	np
sroC	-	I	*gltJ/gltI*	← ← ←	728913	728761	26	898	34.5	
rybB	p25	III	STM0869/STM0870	→ ← ←	942632	942554	3	103	34.3	
STnc80	-	V	STM0897/STM0898	← → ←	967580	967900	0	0		np
STnc90	-	V	STM0903/STM0904	→ → ←	974284	974363	0	0		np
STnc100	-	V	STM0904/STM0905	← → →	975011	975224	0	0		np
STnc110	-	V	STM0905/STM0906	→ → →	976578	976765	0	0		np
STnc120	-	V	STM0929/*orfB*	← ← →	1004777	1004432	0	0		np
STnc490[k]	-	IV	*clpA/tnpA_1*	→ ← →	1024975	1025165	75	385	5.1	~85nt
STnc130	-	V	*serS/dmsA*	→ ← →	1045232	1045098	0	0		nd
isrB-1	-	II	*sbcA*/STM1010	← → ←	1104179	1104266	2	4	2.0	
STnc140	-	V	STM1025/STM1026	← → ←	1113681	1113750	0	0		np
STnc500	-	IV	STM1127/STM1128	← ← ←	1216157	1216440	7	84	12.0	~65nt
sraB	*pke2*	I	*yceF/yceD*	← → →	1275071	1275236	0	0		
STnc640	-	IV	*icdA*/STM1239	→ → →	1325636	1326082	0	10	≥10.0	~1500nt
STnc150	-	V	*icdA*/STM1239	→ ← →	1325914	1325649	0	1	≥1.0	~90nt
isrC	-	II	*envF/msgA*	← → ←	1329145	1329432	0	1	≥1.0	
STnc510	-	IV	STM1245/*pagC*	→ → →	1331440	1332250	4	28	7.0	nd
STnc520	-	IV	STM1248/STM1249	→ ← ←	1332809	1334044	12	100	8.3	~80nt
STnc160	-	V	STM1262/STM1263	→ ← →	1345782	1345732	0	0		np
isrD	-	II	STM1261/STM1263	→ ← →	1345788	1345738	0	0		
ryhB-2	*isrE*	II	STM1273/*yeaQ*	→ ← →	1352987	1352875	0	0		
STnc530	-	IV	*yeaJ/yeaH*	→ ← →	1359779	1360418	2	15	7.5	nd
STnc540	-	IV	*himA/btuC*	→ → →	1419369	1419570	7	23	3.3	~85nt
rprA	IS083	I	*ydik/ydil*	← ← ←	1444938	1444832	37	286	7.7	
rydB	tpe7, IS082	I	*ydiH*/STM1368	→ → ←	1450415	1450519	4	10	2.5	
STnc550	-	IV	*purR/sodB*	← → ←	1508946	1509412	6	10	1.7	nd
STnc570[l]	*yneM*, small ORF	IV	*ydeI/ydeE*	→ ← ←	1593723	1594413	2	21	10.5	~190nt
STnc560	*hbrC*	IV	*ydeI/ydeE*	→ → ←	1593723	1594413	10	290	29.0	~90nt
STnc170	-	V	STM1528/STM1530	← ← →	1606116	1605784	0	0		np
isrF	-	II	STM1552/STM1554	→ ← ←	1630160	1629871	1	0		
rydC	IS067	I	STM1638/*cybB*	→ → ←	1729673	1729738	5	245	49.0	
micC	IS063, tke8	III	*nifJ/ynaF*	→ ← →	1745786	1745678	0	15	≥15.0	
STnc580	-	IV	*dbpA*/STM1656	← ← ←	1749662	1750147	11	311	28.3	~100nt
STnc180	-	V	*acnA/cysB*	← ← ←	1807776	1807565	1	5	5.0	~2000nt
STnc190	-	V	STM1841/*kdgR*	→ → ←	1937518	1937652	1	12	12.0	~500nt
ryeB	tpke79	I	STM1871/STM1872	→ ← ←	1968155	1968053	24	653	27.2	
STnc200	-	V	*edd/zwf*	← ← ←	1979598	1979550	0	3	≥3.0	nd
STnc210	-	V	*yecA*/STM1939	← → ←	2032404	2032580	0	0		np
dsrA	-	I	*yodD/yedP*	→ ← →	2068736	2068649	6	149	24.8	
rseX	-	I	STM1994/*ompS*	← → →	2077175	2077269	0	3	≥3.0	
STnc220	-	V	*ompS/cspB*	→ ← ←	2079068	2078990	0	8	≥8.0	nd
STnc230	-	V	*pocR/pduF*	← → ←	2115370	2115452	0	0		np
STnc240	-	V	*yeeF/yeeY*	← ← ←	2147409	2147333	0	1	≥1.0	np
ryeC	tp11	I	*yegD*/STM2126	→ → →	2213871	2214016	42	72	1.7	
cyaR	*ryeE*	III	*yegQ*/STM2137	→ → →	2231130	2231216	31	659	21.3	
isrG	-	II	STM2243/STM2244	← → →	2344732	2345013	0	0		
micF	-	III	*ompC/yojN*	← → →	2366913	2367005	0	11	≥11.0	
isrH-2	-	II	*glpC*/STM2287	→ ← →	2394582	2394303	0	0		
isrH-1	-	II	*glpC*/STM2287	→ ← →	2394753	2394303	0	0		
STnc250[l]	*ypfM*, small ORF	V	*acrD/yffB*	→ ← →	2596882	2596789	6	24	4.0	~220nt

ryfA	tp1	I	STM2534/*sseB*	→ → ←	2674934	2675228	3	6	2.0	
glmY	tke1, *sroF*	I	*yfhK/purG*	← ← ←	2707847	2707664	20	92	4.6	
isrI	-	II	STM2614/STM2616	→ ← ←	2761576	2761329	0	2	≥2.0	
isrJ	-	II	STM2614/STM2616	→ ← ←	2762031	2761957	1	0		
isrK	-	II	STM2616/STM2617	← ← ←	2762867	2762791	0	0		
isrB-2	-	II	STM2631/*sbcA*	→ ← →	2770965	2770872	0	0		
isrL	-	II	*smpB*/STM2690	→ ← →	2839399	2839055	0	0		
isrM	-	II	STM2762/STM2763	← → →	2905050	2905378	0	0		
isrN	-	II	STM2764/STM2765	← → ←	2906925	2907067	0	0		
STnc260	-	V	STM2816/*luxS*	← → ←	2966073	2966247	0	0		np
micA	*sraD*	I	*luxS/gshA*	← → ←	2966853	2966926	1	128	128.0	
STnc590	-	IV	*avrA/sprB*	← ← ←	3010807	3010966	3	27	9.0	nd
STnc600	-	IV	*hilD/hilA*	→ → →	3018766	3019855	3	68	22.7	nd
invR	STnc270	III	*invH*/STM 2901	→ → →	3044924	3045014	113	3236	28.6	
csrB	-	III	*yqcC/syd*	← ← ←	3117059	3116697	69	67		
gcvB	IS145	III	*gcvA/ygdI*	← → ←	3135317	3135522	12	402	33.5	
omrA	*rygB*	III	*aas/galR*	← ← →	3170208	3170122	0	51	≥51.0	
omrB	*t59, rygA, sraE*	III	*aas/galR*	← ← →	3170408	3170322	1	52	52.0	
STnc280	-	V	*kduI/yqeF*	← → ←	3179540	3179622	0	1	≥1.0	np
STnc290	-	V	*tnpA_4*/STM3033	← ← ←	3194996	3194914	2	72	36.0	~85nt
isrO	-	II	STM3038/STM3039	← → →	3198380	3198580	0	0		
ssrS	-	I	*ygfE/ygfA*	→ → →	3222098	3222280	836	451		
rygC	t27	I	*ygfA/serA*	→ → ←	3222913	3223065	14	17	1.2	
STnc300	-	V	STM3123/STM3124	← ← →	3283965	3283807	0	0		np
rygD	tp8, C0730	I	*yqiK/rfaE*	→ ← ←	3362474	3362327	17	104	6.1	
sraF	tpk1, IS160	I	*ygjR/ygjT*	→ → →	3392069	3392261	0	25	≥25.0	
STnc310	-	V	*ygjT/ygjU*	→ ← →	3393327	3393267	0	0		np
STnc320	-	V	*yhaO/tdcG*	← → ←	3404895	3404949	0	1	≥1.0	np
STnc610	-	IV	*yhbC/metY*	← ← ←	3458296	3458578	1	19	19.0	~1250nt
STnc330	-	V	*greA/dacB*	← ← →	3468553	3468497	1	12	12.0	~1500nt
sraH	*ryhA*	I	*yhbL/arcB*	← → ←	3490383	3490500	55	2292	41.7	
STnc340	-	V	*tnpA_5/yhfL*	← ← →	3635884	3635756	0	0		nd
ryhB-1	*sraI*, IS176	I	*yhhX/yhhY*	← ← →	3715495	3715401	0	2	≥2.0	
STnc350	-	V	*uspA/yhiP*	→ ← →	3761440	3761373	0	0		nd
STnc360	-	V	*yhjB/yhjC*	← → →	3780254	3780402	0	0		np
STnc370	-	V	STM3654/*glyS*	← → ←	3839688	3839758	0	0		np
STnc380	-	V	STM3691/*lldP*	→ ← →	3885736	3885629	0	0		np
STnc390	-	V	*yibD/tdh*	← ← ←	3902653	3902594	0	0		nd
istR-1	-	VI	*ilvB/emrD*	← ← →	3998147	3998018	0	0		~75nt
istR-2	-	VI	*ilvB/emrD*	← ← →	3998147	3998018	0	0		~140nt
STnc400	-	V	STM3844/STM3845	→ → →	4051145	4051340	112	42		~55nt
STnc410	-	V	*glmU*/STM3863	← → ←	4072507	4072730	0	0		np
glmZ	k19, *ryiA*, *sraJ*	I	*yifK/hemY*	→ → ←	4141650	4141854	20	196	9.8	
spf	-	I	*polA/yihA*	→ → ←	4209066	4209175	2	33	16.5	
csrC	*sraK*, *ryiB*, *tpk2*	III	*yihA/yihI*	← → →	4210157	4210400	63	64		
STnc420	-	V	*yiiG*/STM4041	→ ← ←	4251539	4251480	0	0		np
isrP	-	II	STM4097/STM4098	← → ←	4306719	4306866	0	2	≥2.0	
oxyS	-		*argH/oxyR*	→ ← →	4342986	4342866	0	10	10.0	
STnc430	-	V	*pgi/yjbE*	→ ← →	4442059	4441898	0	0		np
STnc620	-	IV	*ssb*/STM4257	→ → →	4476817	4477856	4	41	10.3	nd
sraL	*ryjA*	III	*soxR*/STM4267	→ ← →	4505010	4504870	0	0		
STnc630	-	IV	*proP/basS*	→ → ←	4532473	4532638	1	27	27.0	nd
STnc440	-	V	STM4310/*tnpA_6*	→ → →	4559193	4559277	9	456	50.7	~85nt
STnc450	-	V	*ytfL/msrA*	← ← ←	4645134	4645079	0	0		np
STnc460	-	V	STM4503/STM4504	→ ← →	4758332	4758187	0	0		np
isrQ	-	II	STM4508/STM4509	← → →	4762997	4763158	0	0		

[a] Gene names of *Salmonella* sRNAs that have been experimentally proven here, and in previous studies. Method of identification is given in the third column. sRNA names follow *Salmonella* and/or *E. coli* nomenclature referenced in [7,8,9], except STnc470 to STnc630, which have been newly predicted in this study.

[b] Alternative sRNA IDs. References in [7,8,9].

[c] Evidence for sRNAs in *Salmonella*.

(I) Conserved sRNA found in *Salmonella* cDNA libraries, and previously shown to be expressed in *E. coli* (relevant ref. in [7]; Table 1).

(II) sRNA previously predicted and validated on Northern blots in *Salmonella* by [9].

(III) sRNA previously validated on Northern blots in *Salmonella* [1,7,10,11,12,13,14,15].

(IV) sRNA predicted through cDNA sequencing and validated by Northern blot analysis in this study.

(V) sRNA previously predicted by [11].

(VI) IstR sRNAs [2] were not recoverd in cDNA sequences but their expression in *Salmonella* validated by northern blot analysis in this study (Fig. S5).

[d] Flanking genes of the intergenic region in which the sRNA candidate is located.

[e] Orientation of sRNA candidate (middle) and flanking genes (→ and ← denote location of a gene on the clockwise or the counterclockwise strand of the *Salmonella* chromosome).

[f] Genomic location of sRNA candidate gene according to the *Salmonella typhimurium* LT2 genome. For STnc470 through STnc640 start and end of the entire intergenic region are given.

[g] Out of 145,873 sequences in total.

[h] Out of 122,326 sequences in total.

[i] Enrichment factor calculated by the number of blastable reads from Hfq coIP over control coIP.

[j] Denotes verification on Northern blot in this study for new RNA transcripts; the estimated size is given in nucleotides (np = not probed; nd = no detectable transcript).

[k] The cDNA reads map antisense internally of the IS200 element. Based on sequence identity they map to all IS200 elements (*tnpA_1* to *tnpA_6*).

[l] STnc250 and STnc570 contain small ORFs annotated as *ypfM* or *yneM*, respectively, in *E. coli* [16].

Table S4: mRNAs in Hfq CoIP identified by ≥10 of 170,000 inserts in pyrosequencing data

STM number	Gene name[a]	Number of inserts in control coIP[b]	Number of inserts in Hfq coIP[c]	Product[d]
STM4261		254	1042	putative inner membrane protein
STM2665	yfiA	72	648	ribosome stabilization factor
STM1377	lpp	168	608	murein lipoprotein
STM4087	glpF	40	570	glycerol diffusion
STM1959	fliC	248	547	flagellar biosynthesis protein
STM2874	prgH	73	415	needle complex inner membrane protein
STM2267	ompC	63	385	outer membrane protein C precursor
STM2882	sipA	36	354	secreted effector protein
STM2885	sipB	126	335	translocation machinery component
STM4326	aspA	79	328	aspartate ammonia-lyase
STM2925	nlpD	30	300	lipoprotein
STM4086	glpK	115	278	glycerol kinase
STM2883	sipD	34	269	translocation machinery component
STM0739	sucD	14	261	succinyl-CoA synthetase alpha subunit
STM1572	ompD	76	246	putative outer membrane porin precursor
STM2898	invG	16	226	outer membrane secretin precursor
STM2879	sicP	6	224	secretion chaparone
STM2283	glpT	30	221	sn-glycerol-3-phosphate transport protein
STM1091	sopB	23	216	secreted effector protein
STM1732	ompW	28	206	outer membrane protein W precursor
STM0451	hupB	14	198	DNA-binding protein HU-beta
STM2871	prgK	46	198	needle complex inner membrane lipoprotein
STM2884	sipC	96	192	translocation machinery component
STM4406.S	ytfK	6	191	putative cytoplasmic protein
STM2867	hilC	3	187	invasion regulatory protein
STM2869	orgB	8	182	needle complex export protein
STM2878	sptP	20	177	protein tyrosine phosphatase/GTPase activating protein
STM2894	invC	14	175	type III secretion system ATPase
STM2875	hilD	23	174	invasion protein regulatory protein
STM2284	glpA	57	149	sn-glycerol-3-phosphate dehydrogenase large subunit
STM3526	glpD	39	147	sn-glycerol-3-phosphate dehydrogenase
STM2886	sicA	23	146	secretion chaperone
STM3138		19	143	putative methyl-accepting chemotaxis protein
STM2896	invA	19	142	needle complex export protein
STM0833	ompX	6	137	outer membrane protein X
STM2899	invF	18	129	invasion regulatory protein
STM2924	rpoS	19	129	RNA polymerase sigma factor
STM0629	cspE	9	125	cold shock protein E
STM2285	glpB	33	119	anaerobic glycerol-3-phosphate dehydrogenase subunit B
STM0736	sucA	42	110	2-oxoglutarate dehydrogenase
STM2445	ucpA	5	105	short chain dehydrogenase
STM1070	ompA	77	102	putative hydrogenase membrane component precurosr
STM2282	glpQ	31	98	periplasmic glycerophosphodiester phosphodiesterase

STM3500	pckA	33	96	phosphoenolpyruvate carboxykinase
STM3649	cspA	7	94	major cold shock protein
STM0748	tolB	7	90	translocation protein TolB precursor
STM1782	ychH	10	90	putative inner membrane protein
STM3420	secY	30	87	preprotein translocase SecY
STM1171	flgN	8	80	putative FlgK/FlgL export chaperone
STM0737	sucB	12	79	dihydrolipoamide acetyltransferase
STM2891	spaO	8	77	type III secretion protein
STM2892	invJ	10	75	needle length control protein
STM3281	nlpI	19	75	lipoprotein
STM1887	yebK	0	74	putative transcriptional regulator
STM4360	miaA	5	74	tRNA delta(2)-isopentenylpyrophosphate transferase
STM4260		16	71	predicted cation efflux pump
STM0738	sucC	19	70	succinyl-CoA synthetase subunit beta
STM1919	cheM	12	70	methyl accepting chemotaxis protein II
STM0740	cydA	21	69	cytochrome d terminal oxidase polypeptide subunit I
STM2870	orgA	16	69	needle complex assembly protein
STM3150	hypO	2	68	putative Ni/Fe hydrogenase small subunit
STM3630	dppA	6	68	dipeptide transport protein
STM2328	nuoA	3	66	NADH dehydrogenase alpha subunit
STM0945	clpA	13	65	ATP-binding subunit of serine protease
STM1923	motA	9	65	flagellar motor protein
STM2897	invE	14	65	invasion protein
STM1921	cheA	16	62	chemotaxis sensory histidine protein kinase
STM2314		20	61	putative chemotaxis signal transduction protein
STM2895	invB	11	60	secretion chaperone
STM1230	phoQ	8	58	sensor kinase protein
STM4262		8	58	putative ABC-type bacteriocin/lantibiotic exporter
STM1751	hns	13	57	DNA-binding protein HLP-II
STM4336	ecnB	3	57	putative entericidin B precursor
STM1090	pipC	10	55	pathogenicity island-encoded protein C
STM2957	rumA	4	55	23S rRNA (uracil-5-)-methyltransferase
STM1922	motB	10	54	flagellar motor protein
STM2868	orgC	7	54	putative cytoplasmic protein
STM2872	prgJ	8	54	needle complex minor subunit
STM4232	malM	7	54	periplasmic protein precursor
STM1184	flgL	8	53	flagellar hook-associated protein
STM4258		10	53	putative methyl-accepting chemotaxis protein
STM4362	hflX	7	53	putative GTP-ase
STM1066	rmf	4	52	ribosome modulation factor
STM1431	sodB	21	52	superoxide dismutase
STM3604		8	52	putative inner membrane protein
STM1765	narK	11	50	nitrite extrusion protein
STM2261	napF	13	50	electron transfer protein
STM3053	gcvP	30	50	glycine dehydrogenase
STM3466	crp	4	50	catabolite activator protein
STM0600	cstA	19	49	carbon starvation protein
STM1285	yeaG	16	49	putative serine protein kinase

STM1311	osmE	11	49	transcriptional activator
STM3515	malT	14	49	transcriptional regulator MalT
STM0960	ftsK	8	47	cell division protein
STM1203	ptsG	8	47	glucose-specific IIBC component
STM3711	rfaF	3	47	ADP-heptose-LPS heptosyltransferase 1
STM4361	hfq	5	47	RNA-binding protein Hfq
STM0943	cspD	5	46	stress response protein
STM1183	flgK	5	46	flagellar hook-associated protein
STM2065	phsA	3	46	thiosulfate reductase precursor
STM2088	rfbX	1	46	putative O-antigen transferase
STM2873	prgI	15	46	needle complex major subunit
STM4151	rplJ	6	46	50S ribosomal protein L10
STM4325	dcuA	19	45	anaerobic C4-dicarboxylate transporter
STM0617	rna	3	44	RNase I
STM1231	phoP	3	44	response regulator
STM2889	spaQ	2	44	needle complex export protein
STM3803	yidF	5	44	putative cytoplasmic protein
STM4152	rplL	2	44	50S ribosomal protein L7/L12
STM0439	cyoE	16	43	protoheme IX farnesyltransferase
STM2001	yeeI	6	43	putative inner membrane protein
STM2893	invI	10	43	needle complex assembly protein
STM2876	hilA	4	42	invasion protein transcriptional activator
STM2881	iacP	6	42	acyl carrier protein
STM3197	glgS	2	42	glycogen synthesis protein GlgS
STM0158	acnB	21	41	aconitate hydratase
STM0741	cydB	20	41	cytochrome d terminal oxidase polypeptide subunit II
STM2286	glpC	27	41	sn-glycerol-3-phosphate dehydrogenase K-small subunit
STM0039	nhaA	2	40	Na+/H antiporter
STM1336	rplT	10	40	50S ribosomal protein L20
STM1917	cheB	16	40	chemotaxis-specific methylesterase
STM2081	gnd	3	40	6-phosphogluconate dehydrogenase
STM2082	rfbP	3	40	undecaprenol-phosphate galactosephosphotransferase/O-antigen transferase
STM2326	nuoC	7	40	NADH dehydrogenase I chain C/D
STM2827	alaS	3	40	alanyl-tRNA synthetase
STM3106	ansB	3	40	periplasmic L-asparaginase II
STM3807	yidE	1	40	hypothetical protein
STM0457	cof	2	39	putative hydrolase
STM1960	fliD	14	39	flagellar hook-associated protein
STM3404	smg	9	39	hypothetical protein
STM4060	cpxP	1	39	periplasmic repressor
STM0831	dps	9	38	DNA protection during starvation conditions
STM1057	pepN	5	37	aminopeptidase N
STM1838	yobF	7	37	putative cytoplasmic protein
STM3359	mdh	14	37	malate dehydrogenase
STM4315		0	37	putative DNA-binding protein
STM0994	mukB	4	36	condesin subunit B
STM1746.S	oppA	5	36	oligopeptide transport protein
STM1841		0	36	hypothetical protein

STM2660	clpB	46	36	ATP-dependent protease
STM3884	rbsB	6	36	D-ribose transport protein
STM4305.S		3	36	putative anaerobic dimethylsulfoxide reductase subunit A
STM0129	murC	4	35	UDP-N-acetylmuramate--L-alanine ligase
STM1165	grxB	5	35	glutaredoxin 2
STM1386	ttrS	6	35	sensory histidine kinase
STM1742	oppF	3	35	oligopeptide transport protein
STM1855	sopE2	4	35	type III-secreted effector protein
STM3162	yghB	2	35	hypothetical protein
STM1238	icdA	17	34	isocitrate dehydrogenase
STM1333	thrS	10	34	threonyl-tRNA synthetase
STM1918	cheR	8	34	glutamate methyltransferase
STM2323.S	nuoG	15	34	NADH dehydrogenase gamma subunit
STM3419	rpmJ	9	34	50S ribosomal protein L36
STM3430	rplN	10	34	50S ribosomal protein L14
STM3445	tuf	37	34	elongation factor Tu
STM4259		7	34	putative ABC exporter outer membrane component
STM0013	dnaJ	2	33	heat shock protein
STM1925	flhD	1	33	transcriptional activator FlhD
STM1956	fliA	11	33	flagellar biosynthesis sigma factor FliA
STM2956	relA	5	33	(p)ppGpp synthetase I
STM3700	gpsA	1	33	NAD(P)H-dependent glycerol-3-phosphate dehydrogenase
STM4154	rpoC	37	33	DNA-directed RNA polymerase beta' subunit
STM4237	lexA	6	33	LexA repressor
STM0964	dmsA	7	32	anaerobic dimethyl sulfoxide reductase subunit A
STM1085	yccA	4	32	putative transport protein
STM1164	yceB	3	32	putative outer membrane lipoprotein
STM3592	yhiP	4	32	putative peptide transport protein
STM4562		3	32	putative inner membrane protein
STM0614	ybdQ	9	31	putative universal stress protein
STM1837	cspC	11	31	cold shock protein
STM3183	icc	4	31	cyclic 3',5'-adenosine monophosphate phosphodiesterase
STM3577	tcp	11	31	methyl-accepting transmembrane citrate/phenol chemoreceptor
STM0749	pal	7	30	peptidoglycan-associated lipoprotein precursor
STM1583		1	30	putative cytoplasmic protein
STM1955	fliZ	3	30	putative FliA-regulator
STM2432	ptsI	7	30	PEP-protein phosphotransferase
STM3006	ygdQ	3	30	putative transport protein
STM4582	slt	0	30	soluble lytic murein transglycosylase
STM0093	imp	2	29	organic solvent tolerance protein precursor
STM0224	yaeT	5	29	putative outer membrane protein precursor
STM0687	ybfM	2	29	putative outer membrane protein
STM0688	ybfN	1	29	putative lipoprotein
STM1888	pykA	6	29	pyruvate kinase
STM3705	yibP	2	29	hypothetical protein
STM0120	mraW	4	28	S-adenosyl-methyltransferase
STM1172	flgM	10	28	anti-FliA factor
STM1334.c	infC	11	28	translation initiation factor IF-3

STM1996	cspB	0	28	putative cold-shock protein
STM3918	rfe	2	28	undecaprenyl-phosphate N-acetylglucosaminyltransferase
STM4153	rpoB	11	28	DNA-directed RNA polymerase beta subunit
STM0472	maa	4	27	maltose O-acetyltransferase
STM0800	slrP	9	27	leucine-rich repeat protein
STM2301	pqaB	4	27	putative melittin resistance protein
STM2532		3	27	putative inner membrane lipoprotein
STM3004	ygdP	3	27	dinucleoside polyphosphate hydrolase
STM3055	gcvT	7	27	aminomethyltransferase
STM3865	atpD	17	27	ATP synthase subunit B
STM4243	yjbN	1	27	hypothetical protein
STM4561	osmY	7	27	hyperosmotically-inducible periplasmic protein
STM0130	ddl	6	26	D-alanylalanine synthetase
STM0226	lpxD	3	26	UDP-3-O-[3-hydroxymyristoyl] glucosamine N-acyltransferase
STM0366	yahO	5	26	putative periplasmic protein
STM0734	sdhA	25	26	succinate dehydrogenase catalytic subunit
STM1290	gapA	11	26	glyceraldehyde-3-phosphate dehydrogenase
STM1924.S	flhC	3	26	flagellar transcriptional activator
STM2368	truA	0	26	tRNA pseudouridine synthase A
STM3070	epd	3	26	D-erythrose 4-phosphate dehydrogenase
STM3216		6	26	putative methyl-accepting chemotaxis protein
STM4037	fdoG	26	26	formate dehydrogenase alpha subunit
STM4076	ydeZ	6	26	putative sugar transport protein
STM0122	ftsI	7	25	division specific transpeptidase
STM0125	mraY	1	25	phospho-N-acetylmuramoyl-pentapeptide-transferase
STM1196	acpP	10	25	acyl carrier protein
STM1317	celG	0	25	hypothetical protein
STM1318	katE	4	25	hydroperoxidase HPII
STM1324		5	25	putative cytoplasmic protein
STM1338	pheT	13	25	phenylalanyl-tRNA synthetase beta subunit
STM1661	ydaA	18	25	putative universal stress protein
STM1801	ycgO	2	25	cell volume regulation protein CvrA
STM1938	yecA	7	25	putative metal-binding protein
STM1947	uvrY	2	25	response regulator
STM2318	nuoL	6	25	NADH dehydrogenase subunit L
STM2983	ygdI	6	25	putative lipoprotein
STM3003	ptsP	8	25	transcriptional regulator
STM3403	yrdD	4	25	putative DNA topoisomerase
STM3616	yhjL	5	25	tetratricopeptide repeat protein
STM3701	secB	5	25	export protein SecB
STM3968	udp	8	25	uridine phosphorylase
STM4343	frdA	15	25	fumarate reductase
STM1349	pps	9	24	phosphoenolpyruvate synthase
STM1601	ugtL	1	24	hypothetical protein
STM2530		3	24	putative anaerobic dimethylsulfoxide reductase
STM2888	spaR	2	24	needle complex export protein
STM4170	hupA	12	24	DNA-binding protein HU-alpha
STM4368	vacB	4	24	putative exoribonuclease

STM0735	sdhB	8	23	succinate dehydrogenase catalytic subunit
STM0863	dacC	2	23	D-alanyl-D-alanine carboxypeptidase
STM1000	asnS	3	23	asparaginyl-tRNA synthetase
STM1749	adhE	9	23	iron-dependent alcohol dehydrogenase
STM1920	cheW	6	23	chemotaxis docking protein
STM2083	rfbK	1	23	phosphomannomutase
STM2327	nuoB	3	23	NADH dehydrogenase beta subunit
STM2526	ndk	2	23	nucleoside diphosphate kinase
STM2651	yfiQ	11	23	putative acetyl-CoA synthetase
STM3591	uspA	14	23	universal stress protein A
STM3702	grxC	2	23	glutaredoxin 3
STM3808.S	ibpB	1	23	small heat shock protein
STM3972	aarF	8	23	putative ubiquinone biosynthesis protein UbiB
STM4257		5	23	hypothetical protein
STM0186	dksA	12	22	dnaK suppressor protein
STM0452	cypD	3	22	peptidyl-prolyl isomerase
STM0730	gltA	16	22	citrate synthase
STM1094	pipD	2	22	pathogenicity island-encoded protein D
STM1249		5	22	utative periplasmic protein
STM2091	rfbG	3	22	CDP glucose 4,6-dehydratase
STM2296	ais	0	22	aluminum-inducible protein
STM2780	pipB2	3	22	secreted effector protein
STM2890	spaP	2	22	needle complex export protein
STM4410	ytfN	6	22	putative periplasmic protein
STM1161.S	yceP	1	21	putative cytoplasmic protein
STM1190	yceD	9	21	putative metal-binding protein
STM1283	yeaJ	2	21	putative methyl-accepting chemotaxis protein
STM1286	mipA	6	21	MltA-interacting protein A
STM1291	yeaA	1	21	methionine sulfoxide reductase B
STM1683	tyrR	1	21	transcriptional regulator
STM1795		9	21	putative glutamic dehyrogenase-like protein
STM1916	cheY	3	21	chemotaxis regulator
STM1941		0	21	putative inner membrane protein
STM1945	pgsA	2	21	phosphatidylglycerophosphate synthetase
STM2391	fadL	1	21	outer membrane-bound fatty acid transporter
STM3147	hybC	3	21	hydrogenase-2 large subunit
STM3282	pnp	4	21	polynucleotide phosphorylase
STM3415	rpoA	11	21	DNA-directed RNA polymerase alpha subunit
STM3417	rpsK	8	21	30S ribosomal protein S11
STM4240	yjbJ	13	21	putative cytoplasmic protein
STM4330	groEL	43	21	chaperonin GroEL
STM0653	ybeL	3	20	putative cytoplasmic protein
STM0732	sdhC	4	20	succinate dehydrogenase cytochrome b556 large membrane subunit
STM1713	cysB	3	20	transcriptional regulator for cysteine regulon
STM2035	cbiA	4	20	cobyrinic acid a,c-diamide synthase
STM2322	nuoH	6	20	NADH dehydrogenase subunit H
STM2533	sseA	4	20	putative sulfurtransferase
STM3187	ygiB	0	20	putative inner membrane protein

STM3538	glgB	10	20	glycogen branching enzyme
STM3708	tdh	5	20	L-threonine 3-dehydrogenase
STM3710	rfaD	9	20	ADP-L-glycero-D-mannoheptose-6-epimerase
STM3900	ilvL	2	20	ilvGEDA operon leader peptide
STM3996	yihE	1	20	putative type II homoserine kinase
STM0088	apaH	2	19	diadenosinetetraphosphatase
STM0124	murF	6	19	D-alanine-D-alanine ligase
STM0128	murG	4	19	N-acetylglucosaminyl transferase
STM0133	ftsZ	7	19	cell division protein FtsZ
STM0449	clpX	10	19	ATP-dependent protease ATP-binding subunit
STM1398	sseB	2	19	translocation machinery component
STM1660.S	fnr	4	19	transcriptional regulator
STM1754	ychK	0	19	putative phosphoesterase
STM1796	treA	6	19	trehalase
STM1875	yobA	0	19	putative copper resistance protein
STM2059	yeeX	1	19	hypothetical protein
STM2184	sanA	3	19	vancomycin sensitivity
STM2270	rcsB	0	19	response regulator
STM2280		1	19	putative permease
STM2433	crr	7	19	glucose-specific PTS system enzyme IIA component
STM2681	grpE	1	19	heat shock protein
STM2782	mig-14	1	19	putative transcriptional activator
STM3113	nupG	2	19	nucleoside transport
STM3426	rpsH	6	19	30S ribosomal protein S8
STM3986	trkH	3	19	potassium transport protein
STM4331	yjeI	6	19	putative outer membrane lipoprotein
STM4391	rpsF	1	19	30S ribosomal protein S6
STM0132	ftsA	6	18	cell division protein
STM0474	ybaJ	4	18	putative cytoplasmic protein
STM0508	ybbP	2	18	putative inner membrane protein
STM0750	ybgF	4	18	putative periplasmic protein
STM0959	lrp	1	18	leucine-responsive regulatory protein
STM1148.S	ymdC	6	18	putative phospholipase
STM1335	rpmI	5	18	50S ribosomal protein L35
STM1602	sifB	0	18	secreted effector protein
STM1745	oppB	1	18	oligopeptide permease ABC transporter membrane component
STM1804.S	ycgB	4	18	putative cytoplasmic protein
STM1840	yobG	2	18	putative inner membrane protein
STM1867	pagK	0	18	PagK
STM1950	sdiA	3	18	transcriptional regulator
STM2214	spr	2	18	putative lipoprotein
STM2333	yfbS	1	18	putative response regulator
STM2486		1	18	putative inner membrane protein
STM2640	rpoE	2	18	RNA polymerase sigma-70 factor
STM2675	rimM	3	18	16S rRNA-processing protein
STM2945	sopD	3	18	secreted effector protein
STM3186	tolC	10	18	outer membrane channel precursor protein
STM3229	yqjD	3	18	putative inner membrane protein

STM3272	yhbS	4	18	putative transport protein
STM3286	infB	4	18	translation initiation factor IF-2
STM3373	mreC	0	18	rod shape-determining protein
STM3434	rpsC	20	18	30S ribosomal protein S3
STM3611	yhjH	1	18	hypothetical protein
STM3680	aldB	3	18	aldehyde dehydrogenase B
STM3867	atpA	27	18	ATP synthase subunit A
STM4078	yneB	9	18	hypothetical protein
STM0134	lpxC	15	17	UDP-3-O-[3-hydroxymyristoyl] N-acetylglucosamine deacetylase
STM0160	yacL	1	17	hypothetical protein
STM0211	yaeH	13	17	putative cytoplasmic protein
STM0311	yafJ	0	17	putative glutamine amidotransferase
STM0327		6	17	putative cytoplasmic protein
STM0440	cyoD	6	17	cytochrome o ubiquinol oxidase subunit IV
STM0465	ybaY	11	17	hypothetical protein
STM0733	sdhD	6	17	succinate dehydrogenase cytochrome b556 small membrane subunit
STM0772	gpmA	12	17	phosphoglyceromutase
STM0962	ycaJ	3	17	hypothetical protein
STM0971		0	17	putative cytoplasmic protein
STM1177	flgE	13	17	flagellar hook protein
STM1444	slyA	2	17	transcriptional regulator SlyA
STM1626	trg	1	17	methyl-accepting chemotaxis protein III
STM1638		1	17	putative SAM-dependent methyltransferase
STM1830	manX	12	17	mannose-specific enzyme IIAB
STM1972	fliI	3	17	flagellum-specific ATP synthase
STM2061	sbmC	8	17	DNA gyrase inhibitor
STM2767		1	17	putative DNA/RNA helicase
STM2796	yqaE	0	17	putative transport protein
STM2800		1	17	putative inner membrane protein
STM2865	avrA	2	17	secreted effector protein
STM3056	visC	3	17	hypothetical protein
STM3069	pgk	17	17	phosphoglycerate kinase
STM3154		0	17	putative ATP-dependent RNA helicase-like protein
STM3184	yqiB	3	17	putative cytoplasmic protein
STM3188	ygiC	6	17	putative glutathionylspermidine synthase
STM3228	yqjC	5	17	putative periplasmic protein
STM3407	fmt	3	17	methionyl-tRNA formyltransferase
STM3436	rpsS	8	17	30S ribosomal protein S19
STM3440	rplC	3	17	50S ribosomal protein L3
STM3715	rfaZ	0	17	lipopolysaccharide core biosynthetic protein
STM3879	yieN	0	17	putative regulatory protein
STM3885	rbsK	1	17	ribokinase
STM4411	ytfP	2	17	putative cytoplasmic protein
STM0068	caiF	0	16	of cai/fix operon transcriptional regulator
STM0222	cdsA	4	16	CDP-diglyceride synthase
STM0228	lpxA	1	16	UDP-N-acetylglucosamine acyltransferase
STM0446	bolA	1	16	putative regulatory protein
STM0448	clpP	2	16	ATP-dependent Clp protease proteolytic subunit

STM1227	pepT	4	16	peptidase T
STM1313	celB	0	16	sugar-specific enzyme II
STM1328		2	16	putative outer membrane protein
STM1389	orf319	4	16	putative inner membrane protein
STM1682	tpx	1	16	thiol peroxidase
STM1839		1	16	hypothetical protein
STM1915	cheZ	2	16	chemotactic response protein
STM2060	yeeA	1	16	putative inner membrane protein
STM2259	napA	23	16	periplasmic nitrate reductase
STM2299	yfbG	9	16	hypothetical protein
STM2300		3	16	putative cytoplasmic protein
STM2316.S	nuoN	2	16	NADH dehydrogenase subunit N
STM2325	nuoE	5	16	ATP synthase subunit E
STM2337	ackA	5	16	acetate/propionate kinase
STM2390	yfcZ	4	16	putative cytoplasmic protein
STM2652	pssA	2	16	phosphatidylserine synthase
STM3068	fba	9	16	fructose-bisphosphate aldolase
STM3320	rpoN	9	16	DNA-directed RNA polymerase subunit N
STM3321	yhbH	7	16	putative sigma N modulation factor
STM3728	rpmB	1	16	50S ribosomal protein L28
STM3917	rho	2	16	transcription termination factor Rho
STM4495		5	16	putative type II restriction enzyme methylase subunit
STM4512	iadA	1	16	isoaspartyl dipeptidase
STM4541	mdoB	3	16	phosphoglycerol transferase I
STM0012	dnaK	8	15	molecular chaperone DnaK
STM0126	murD	4	15	UDP-N-acetylmuramoyl-L-alanyl-D-glutamate synthetase
STM0127	ftsW	3	15	essential cell division gene
STM0666	lnt	4	15	apolipoprotein N-acyltransferase
STM0667	ybeX	3	15	putative transport protein
STM1071	sulA	3	15	cell division inhibitor
STM1400	sseC	2	15	translocation machinery component
STM1445	slyB	6	15	putative outer membrane lipoprotein
STM1463	add	2	15	adenosine deaminase
STM1480	pntB	1	15	pyridine nucleotide transhydrogenase
STM1533		1	15	putative hydrogenase
STM1641	hrpA	3	15	ATP-dependent helicase
STM1651	nifJ	3	15	putative pyruvate-flavodoxin oxidoreductase
STM1805	fadR	1	15	fatty acid metabolism regulator
STM2084	rfbM	1	15	mannose-1-phosphate guanylyltransferase
STM2089	rfbJ	1	15	CDP-abequose synthase
STM2309	menD	4	15	2-oxoglutarate decarboxylase
STM2346		0	15	putative NTP pyrophosphohydrolase
STM2472	maeB	5	15	phosphate acetyltransferase
STM2646	yfiD	9	15	putative formate acetyltransferase
STM2952	eno	5	15	phosphopyruvate hydratase
STM3002	lgt	0	15	prolipoprotein diacylglyceryl transferase
STM3054	gcvH	3	15	glycine cleavage system protein H
STM3209	rpsU	2	15	30S ribosomal protein S21

STM3402	yrdC	1	15	putative dsRNA-binding protein
STM3416	rpsD	7	15	30S ribosomal protein S4
STM3418	rpsM	4	15	30S ribosomal protein S13
STM3446	fusA	19	15	elongation factor EF-2
STM3537	glgX	3	15	glycogen debranching enzyme
STM3586.S	yhiH	5	15	putative ABC-type multidrug transport system ATPase component
STM3864	atpC	13	15	ATP synthase subunit epsilon
STM3958	recQ	0	15	ATP-dependent DNA helicase
STM3999	polA	4	15	DNA polymerase I
STM4073	ydeW	1	15	putative transcriptional repressor
STM4241	zur	0	15	transcriptional repressor
STM4290	proP	2	15	low-affinity proline transporter
STM4297	melR	1	15	melibiose operon regulator
STM4359	mutL	4	15	DNA mismatch repair protein
STM0064	dapB	1	14	dihydrodipicolinate reductase
STM0365	yahN	0	14	putative transport protein
STM0417	ribH	0	14	riboflavin synthase subunit beta
STM0665	gltI	5	14	glutamate/aspartate transporter
STM0694	fldA	0	14	flavodoxin
STM0743	ybgE	3	14	putative inner membrane lipoprotein
STM0963	serS	5	14	seryl-tRNA synthetase
STM1234.S	trmU	4	14	tRNA (5-methylaminomethyl-2-thiouridylate)-methyltransferase
STM1239		1	14	putative cytoplasmic protein
STM1284	yeaH	4	14	hypothetical protein
STM1409	ssaJ	0	14	needle complex inner membrane lipoprotein
STM1589	yncB	9	14	putative NADP-dependent oxidoreductase
STM1712	acnA	8	14	aconitate hydratase
STM1731		3	14	putative catalase
STM1845	prc	2	14	carboxy-terminal protease
STM1846	proQ	0	14	putative solute/DNA competence effector
STM2033	cbiC	1	14	precorrin-8X methylmutase
STM2090	rfbH	6	14	CDP-6-deoxy-D-xylo-4-hexulose-3-dehydrase
STM2297	yfbE	2	14	4-amino-4-deoxy-L-arabinose lipopolysaccharide-modifying enzyme
STM2298	pmrF	3	14	putative glycosyl transferase
STM2320	nuoJ	3	14	NADH dehydrogenase subunit J
STM2489	dapA	2	14	dihydrodipicolinate synthase
STM2674	trmD	3	14	tRNA (guanine-N(1)-)-methyltransferase
STM2829	recA	3	14	recombinase A
STM2866	sprB	2	14	transcriptional regulator
STM2877	iagB	4	14	invasion protein precursor
STM3058	pepP	4	14	proline aminopeptidase P II
STM3061	ygfA	0	14	putative ligase
STM3149	hybA	0	14	putative hydrogenase-2 component
STM3223	ygjR	4	14	putative dehydrogenase
STM3225	ygjU	3	14	putative dicarboxylate permease
STM3342	sspA	2	14	stringent starvation protein A
STM3369	yhdP	2	14	putative protease
STM3534	glgP	4	14	glycogen phosphorylase

STM3919	wzzE	0	14	enterobacterial common antigen chain length regulator
STM3939	cyaA	3	14	adenylate cyclase
STM3947	dapF	2	14	diaminopimelate epimerase
STM4089	menG	5	14	ribonuclease activity regulator protein RraA
STM4409	ytfM	2	14	putative outer membrane protein
STM4517	yjiO	0	14	putative transport protein
STM4586	rob	1	14	transcriptional regulator
STM0123	murE	5	13	UDP-N-acetylmuramoylalanyl-D-glutamate--2,6-diaminopimelate ligase
STM0212		1	13	putative inner membrane protein
STM0537	cysS	2	13	cysteinyl-tRNA synthetase
STM0543	fimA	1	13	fimbrin
STM0791	hutH	7	13	histidine ammonia-lyase
STM0865	ybjG	1	13	putative permease
STM0940	ybjX	1	13	VirK-like protein
STM0944	clpS	2	13	ATP-dependent Clp protease adaptor protein ClpS
STM0961	lolA	4	13	outer-membrane lipoprotein carrier protein precursor
STM1112	cbpA	0	13	DNA-binding protein
STM1221	cobB	1	13	NAD-dependent deacetylase
STM1488	mlc	4	13	pts operon transcriptional repressor
STM1679	mppA	4	13	periplasmic murein tripeptide transport protein
STM1777	hemA	3	13	glutamyl-tRNA reductase
STM1848	yebS	1	13	putative inner membrane protein
STM1881	yebF	4	13	putative periplasmic protein
STM1886	zwf	3	13	glucose-6-phosphate 1-dehydrogenase
STM1935	ftn	3	13	cytoplasmic ferritin
STM1946	uvrC	5	13	excinuclease ABC subunit C
STM1979	fliP	3	13	flagellar biosynthesis protein
STM2080	udg	1	13	UDP-glucose/GDP-mannose dehydrogenase
STM2086	rfbU	2	13	mannosyl transferase
STM2093	rfbI	6	13	CDP-6-deoxy-delta-3,4-glucoseen reductase
STM2215	rtn	1	13	hypothetical protein
STM2226	yejK	0	13	nucleoid-associated protein NdpA
STM2317	nuoM	5	13	NADH dehydrogenase subunit M
STM2321	nuoI	3	13	NADH dehydrogenase subunit I
STM2324	nuoF	8	13	NADH dehydrogenase I chain F
STM2336		0	13	hypothetical protein
STM2638	rseB	0	13	periplasmic negative regulator of sigmaE
STM2662	rluD	3	13	ribosomal large subunit pseudouridine synthase D
STM2677	ffh	5	13	4.5S-RNP protein
STM2887	spaS	2	13	type III secretion protein
STM3157	yghA	6	13	oxidoreductase
STM3226	yqjA	1	13	hypothetical protein
STM3296	hflB	9	13	ATP-dependent zinc-metallo protease
STM3368	tldD	4	13	microcin B17-processing protein
STM3410	mscL	4	13	large-conductance mechanosensitive channel
STM3536	glgC	7	13	glucose-1-phosphate adenylyltransferase
STM3569	ftsX	2	13	putative cell division protein
STM3704	pmgI	5	13	phosphoglyceromutase

STM3719	rfaB	0	13	lipopolysaccharide-1,6-D-galactosyltransferase
STM3871	atpB	6	13	ATP synthase subunit A
STM3973	tatA	2	13	twin argininte translocase protein A
STM4275	acs	1	13	acetyl-coenzyme A synthetase
STM4367	yjeB	3	13	putative negative regulator
STM4404	cysQ	2	13	sulfite biosynthetic protein
STM4580.S	nadR	0	13	nicotinamide-nucleotide adenylyltransferase
STM0131	ftsQ	2	12	cell division protein
STM0216	rpsB	5	12	30S ribosomal protein S2
STM0217	tsf	6	12	elongation factor Ts
STM0408	secF	1	12	protein export protein SecF
STM0442	cyoB	11	12	cytochrome o ubiquinol oxidase subunit I
STM0450	lon	5	12	ATP-dependent protease Lon
STM0542	folD	0	12	5,10-methylene-tetrahydrofolate dehydrogenase/5,10-methylene-tetrahydrofolate cyclohydrolase
STM0669	phoL	3	12	putative phosphate starvation-inducible protein
STM0683	nagA	5	12	N-acetylglucosamine-6-phosphate deacetylase
STM0802	moaA	2	12	molybdenum cofactor biosynthesis protein A
STM0807	ybhL	3	12	putative permease
STM0888	artM	0	12	arginine transport system component
STM0934	ltaA	1	12	L-allo-threonine aldolase
STM1119	wraB	8	12	TrpR binding protein WrbA
STM1246	pagC	14	12	virulence membrane protein PAGC precursor
STM1486	ynfM	0	12	putative transport protein
STM1511	ydfG	0	12	putative oxidoreductase
STM1558		2	12	putative glycosyl hydrolase
STM1582	nhoA	0	12	putative arylamine N-acetyltransferase
STM1710	pgpB	0	12	phosphatidylglycerophosphate phosphatase B
STM1743	oppD	3	12	oligopeptide transporter ATP-binding component
STM1752	galU	1	12	glucose-1-phosphate uridylyltransferase
STM1807	dsbB	0	12	disulfide bond formation protein B
STM1976	fliM	9	12	flagellar motor switch protein
STM2067	sbcB	2	12	exonuclease I
STM2217	yejB	1	12	putative ABC-type dipeptide/oligopeptide/nickel transport system permease
STM2246	narP	0	12	response regulator
STM2378	fabB	10	12	3-oxoacyl-(acyl carrier protein) synthase
STM2388	yfcX	1	12	putative dehydrogenase
STM2520	yfgL	3	12	putative serine/threonine protein kinase
STM2688	smpB	1	12	SsrA-binding protein
STM2781	virK	1	12	virulence protein
STM2814	emrA	0	12	multidrug resistance secretion protein
STM2950		2	12	putative metal-dependent hydrolase
STM3040	lysS	5	12	lysyl-tRNA synthetase
STM3107	yggN	1	12	putative periplasmic protein
STM3153	yqhA	3	12	hypothetical protein
STM3189	ygiD	0	12	putative cytoplasmic protein
STM3201	glnE	2	12	adenylyl transferase for glutamine synthetase
STM3297	ftsJ	2	12	23S rRNA methyltransferase
STM3441	rpsJ	2	12	30S ribosomal protein S10

STM3453	fkpA	3	12	FKBP-type peptidyl-prolyl cis-trans isomerase
STM3589	pitA	0	12	low-affinity phosphate transporter
STM3602		1	12	putative regulatory protein
STM3758	fidL	0	12	putative inner membrane protein
STM3872	atpI	2	12	ATP synthase subunit I
STM3970	ubiE	0	12	ubiquinone/menaquinone biosynthesis methyltransferase
STM4127	yijC	1	12	putative transcriptional repressor
STM4249	aphA	3	12	non-specific acid phosphatase/phosphotransferase
STM4390		1	12	putative cytoplasmic protein
STM4392	priB	1	12	primosomal replication protein N
STM0046	ileS	4	11	isoleucyl-tRNA synthetase
STM0047	lspA	3	11	signal peptidase II
STM0121	ftsL	0	11	cell division protein
STM0221	uppS	0	11	undecaprenyl pyrophosphate synthetase
STM0475	acrB	12	11	acridine efflux pump
STM0476	acrA	2	11	acridine efflux pump
STM0484	dnaX	2	11	DNA polymerase III subunits gamma and tau
STM0648	leuS	7	11	leucyl-tRNA synthetase
STM0685	nagE	2	11	N-acetylglucosamine-specific enzyme IIABC
STM0781	modA	4	11	molybdate transporter
STM0814	ybhQ	5	11	putative inner membrane protein
STM0819	ybiH	1	11	putative transcriptional repressor
STM0870		0	11	hypothetical protein
STM0941	ybjY	1	11	hypothetical protein
STM0977	serC	3	11	phosphoserine aminotransferase
STM1147		0	11	hypothetical protein
STM1167	rimJ	0	11	acetylatase
STM1185	rne	0	11	RNase E
STM1195	fabG	4	11	3-ketoacyl-(acyl-carrier-protein) reductase
STM1300		1	11	putative periplasmic protein
STM1415	ssaN	0	11	type III secretion system ATPase
STM1468	fumA	5	11	fumarase A
STM1594	srfB	5	11	putative virulence protein
STM1744	oppC	3	11	oligopeptide transport protein
STM1847	yebR	0	11	putative nucleotide-binding protein
STM1900	ntpA	0	11	dATP pyrophosphohydrolase
STM1939		0	11	putative glucose-6-phosphate dehydrogenase
STM2028	cbiG	2	11	cobalamin biosynthesis protein CbiG
STM2066	sopA	0	11	secreted effector protein
STM2165	yehZ	0	11	putative transport protein
STM2186		4	11	putative NADPH-dependent glutamate synthase beta chain
STM2362	purF	6	11	amidophosphoribosyltransferase
STM2446		0	11	putative iron-dependent peroxidase
STM2494		3	11	hypothetical protein
STM2536	pepB	1	11	aminopeptidase B
STM2819	yqaA	0	11	putative inner membrane protein
STM3132		4	11	putative xylanase/chitin deacetylase
STM3133		2	11	putative amidohydrolase

STM3144	hypA	0	11	hydrogenase nickel incorporation protein
STM3207	ygiH	2	11	hypothetical protein
STM3230	yqjE	6	11	putative inner membrane protein
STM3362		0	11	putative periplasmic protein
STM3421	rplO	11	11	50S ribosomal protein L15
STM3428	rplE	4	11	50S ribosomal protein L5
STM3465	yhfA	3	11	putative inner membrane protein
STM3467	yhfK	1	11	putative inner membrane protein
STM3481	trpS	3	11	tryptophanyl-tRNA synthetase
STM3568	rpoH	7	11	RNA polymerase sigma factor
STM3590	uspB	0	11	universal stress protein UspB
STM3614	dctA	0	11	C4-dicarboxylate transport protein
STM3617		1	11	endo-1,4-D-glucanase
STM3718	rfaI	4	11	lipopolysaccharide-alpha-1,3-D-galactosyltransferase
STM3773		2	11	putative transcriptional regulator
STM3797	ivbL	3	11	ilvB operon leader peptide
STM3915	trxA	5	11	thioredoxin
STM3938	hemC	4	11	porphobilinogen deaminase
STM3961	pldB	2	11	lysophospholipase L2
STM3975	tatC	0	11	Sec-independent protein secretion pathway component
STM3978	yigC	1	11	putative oxidoreductase
STM4062	pfkA	4	11	6-phosphofructokinase
STM4221	pgi	3	11	glucose-6-phosphate isomerase
STM4239		5	11	putative cytoplasmic protein
STM4334	efp	1	11	elongation factor P
STM4378	yjfN	8	11	putative inner membrane protein
STM4379	yjfO	14	11	putative lipoprotein
STM4416	mpl	0	11	UDP-N-acetylmuramate/L-alanyl-gamma-D-glutamyl-meso-diaminopimelate ligase
STM4470	yjgD	1	11	putative cytoplasmic protein
STM4514.S	yjiH	0	11	putative inner membrane protein
STM4533	tsr	3	11	methyl-accepting chemotaxis protein I
STM4563	yjjU	0	11	putative phosphoesterase
STM0003	thrB	2	10	homoserine kinase
STM0159		1	10	putative restriction endonuclease
STM0318	yafA	3	10	hypothetical protein
STM0376	sbmA	0	10	putative ABC transporter membrane protein
STM0407	secD	1	10	protein export protein SecD
STM0494	ushA	3	10	UDP-sugar hydrolase/5'-nucleotidase
STM0652		6	10	putative sigma-54 dependent transcriptional regulator
STM0872	grxA	0	10	glutaredoxin 1
STM0890	artI	1	10	arginine transport system
STM0999	ompF	3	10	outer membrane protein F precursor
STM1018		0	10	hypothetical protein
STM1176	flgD	6	10	flagellar basal body rod modification protein
STM1178	flgF	4	10	cell-proximal portion of basal-body rod
STM1269		0	10	chorismate mutase
STM1270	yeaS	0	10	putative transport protein
STM1274	yeaQ	1	10	putative inner membrane protein

STM1297	selD	1	10	selenophosphate synthetase
STM1312	celA	0	10	sugar-specific enzyme IIB
STM1345	ydiU	2	10	hypothetical protein
STM1391	ssrB	3	10	transcriptional activator
STM1399	sscA	0	10	secretion system chaparone
STM1410		0	10	putative cytoplasmic protein
STM1433	ydhD	3	10	putative glutaredoxin protein
STM1536		0	10	putative hydrogenase maturation protease
STM1685	ycjX	0	10	putative ATPase
STM1714	topA	2	10	DNA topoisomerase I
STM1815	minD	5	10	cell division inhibitor protein
STM1831	manY	8	10	mannose-specific enzyme IIC
STM1832	manZ	5	10	mannose-specific enzyme IID
STM1907	cutC	0	10	copper homeostasis protein
STM1961	fliS	5	10	flagellar protein FliS
STM2026	cbiJ	2	10	precorrin-6x reductase
STM2032	cbiD	3	10	cobalt-precorrin-6A synthase
STM2034	cobD	1	10	cobalamin biosynthesis protein
STM2036	pocR	2	10	transcriptional regulator
STM2039	pudB	7	10	polyhedral body protein
STM2087	rfbV	1	10	abequosyltransferase
STM2154	mrp	0	10	putative ATP-binding protein
STM2164	yehY	2	10	putative ABC-type proline/glycine betaine transport system permease component
STM2189	mglA	0	10	methyl-galactoside transport protein
STM2190	mglB	1	10	galactose transport protein
STM2201	yeiE	1	10	putative transcriptional regulator
STM2306	menC	1	10	O-succinylbenzoate synthase
STM2330	lrhA	0	10	NADH dehydrogenase transcriptional repressor
STM2361		3	10	putative regulatory protein
STM2483	dapE	2	10	succinyl-diaminopimelate desuccinylase
STM2523	gcpE	1	10	4-hydroxy-3-methylbut-2-en-1-yl diphosphate synthase
STM2524	yfgA	9	10	hypothetical protein
STM2557	cadC	0	10	transcriptional activator
STM2679	yfjD	1	10	hypothetical protein
STM2858	hypE	2	10	putative hydrogenase formation protein
STM3043	dsbC	0	10	protein disulfide isomerase II
STM3122		1	10	putative arylsulfatase
STM3195	ribB	3	10	3,4-dihydroxy-2-butanone 4-phosphate synthase
STM3266	yraO	1	10	putative phosphoheptose isomerase
STM3338	nanT	0	10	putative sialic acid transporter
STM3341	sspB	1	10	stringent starvation protein B
STM3347	yhcB	0	10	putative periplasmic protein
STM3363	yhcO	1	10	putative cytoplasmic protein
STM3423	rpsE	6	10	30S ribosomal protein S5
STM3439	rplD	1	10	50S ribosomal protein L4
STM3570	ftsE	0	10	putative cell division ATPase
STM3594	prlC	2	10	oligopeptidase A
STM3624	yhjU	4	10	putative inner membrane protein

STM3703	yibN	3	10	putative rhodanese-like sulfurtransferase
STM3845		0	10	putative inner membrane protein
STM3926	wzxE	0	10	O-antigen translocase
STM4091	hslU	2	10	ATP-dependent protease ATP-binding subunit
STM4093	ftsN	0	10	essential cell division protein
STM4147	secE	0	10	translocase
STM4314		0	10	putative regulatory protein
STM4403	cpdB	1	10	2',3'-cyclic nucleotide 2'-phosphodiesterase/3'-nucleotidase bifunctional periplasmic precursor protein
STM4438	pmbA	0	10	putative antibiotic maturation protein
STM4503		3	10	putative inner membrane protein
STM4513	yjiG	0	10	putative permease
STM4524	hsdS	0	10	type I restriction enzyme specificity protein

[a]Gene names according to ColiBase [3]

[b]Based on 145,873 sequences

[c]Based on 122,326 sequences

[d]Product according to KEGG (http://www.genome.jp/kegg/; [4])

Table S5: Genes that were significantly enriched in coIP-on-Chip and were identified by pyrosequencing

Gene name[a]	Enrichment overr wt[b]	454
STM2506	21.12	
ybfM	19.29	X
STM1747	17.10	
aphA	15.51	X
ytfK	14.23	X
cpxP	11.67	X
cof	10.15	X
yqjA	10.15	X
STM1841	8.92	X
oppA	8.66	X
STM2880	8.53	
STM1939	8.40	X
ygdQ	8.22	X
cutC	8.09	X
glpF	7.95	X
yceB	7.87	X
cspE	7.50	X
sicP	7.47	X
yihO	7.42	
dppA	7.42	X
STM0159	7.37	X
STM2281	7.35	
hfq	7.31	X
yceP	7.30	X
truA	7.05	X
gltI	7.03	X
rfbP	7.03	X
yejG	7.02	
yafJ	7.01	X
orgA	6.89	X
miaA	6.89	X
yidF	6.86	X
zwf	6.72	X
acrR	6.71	
rfbX	6.62	X
nuoA	6.57	X
STM1128	6.51	
rfbU	6.41	X
ychK	6.38	X
lrhA	6.26	X
yeaJ	6.21	X
STM2507	6.16	
rfaB	6.11	X
yabI	6.08	
pykA	6.07	X
hilA	6.04	X
ssaS	6.00	
ssaT	6.00	
ytfL	5.92	
STM3845	5.87	X
pepN	5.85	X
fmt	5.83	X
ucpA	5.83	X
yqiB	5.79	X
pitA	5.71	X
icc	5.68	X
rpoS	5.64	X
STM0082	5.62	
ybaP	5.62	
hilC	5.62	X
hsdS	5.59	X
ddlA	5.56	
STM0571	5.49	
ycbW	5.46	
celA	5.43	X

pocR	5.39	X
rfbJ	5.37	X
STM1530	5.35	
maa	5.33	X
sucD	5.31	X
yafK	5.27	
ygjU	5.24	X
STM1093	5.22	
STM4312	5.19	
yeeI	5.13	X
STM2901	5.09	
STM4313	5.07	
marA	5.07	
STM2870	5.06	
narP	5.06	X
STM2742	5.06	
sptP	5.00	X
yrdC	4.96	X
dedA	4.95	
STM2747	4.95	
yjbN	4.94	X
STM2690	4.94	
nlpC	4.92	
ylbA	4.90	
STM2705	4.87	
STM3461	4.82	
marR	4.80	
ygcA	4.80	
invH	4.80	
rfaZ	4.79	X
solA	4.79	
yebK	4.78	X
sanA	4.76	X
sdhC	4.75	X
glmS	4.74	
imp	4.72	X
iacP	4.72	X
STM2986	4.71	
argR	4.70	
ytfJ	4.70	
nirD	4.70	
relA	4.70	X
STM4257	4.69	X
mglA	4.68	X
phnA	4.66	
mltC	4.65	
rfaI	4.63	X
rfaC	4.63	
STM3846	4.62	
yidG	4.60	
rtsA	4.58	
ycfJ	4.57	
STM0497	4.56	
glnH	4.55	
rbsB	4.54	X
cspA	4.49	X
rfaJ	4.49	
yecA	4.47	X
mglC	4.45	
STM4493	4.42	
STM4497	4.41	
yhjW	4.41	
thyA	4.39	
hilD	4.39	X
ompX	4.39	X
STM1018	4.38	X
hha	4.36	
ptsG	4.33	X
ytfM	4.32	X
STM1839	4.32	X
ais	4.30	X
STM4316	4.30	
oppF	4.29	X
celG	4.27	X
ydeD	4.26	

yiaG	4.25	
flgL	4.25	X
yejK	4.24	X
STM3528	4.24	
STM2280	4.22	X
rfbV	4.20	X
STM2238	4.19	
STM4261	4.19	X
ydiV	4.18	
STM1554	4.17	
ychJ	4.16	
STM1023	4.12	
STM4260	4.11	X
STM4310	4.10	
STM2530	4.10	X
ubiB	4.08	
STM2746	4.07	
foxA	4.06	
nlpD	4.06	X
adiY	4.06	
STM1629	4.05	
STM1656	4.02	
STM2767	4.02	X
polA	4.02	X
kdpE	4.01	
aefA	4.01	
STM2868	4.00	
nirB	3.99	
def	3.97	
STM2610	3.97	
flhD	3.94	X
malM	3.94	X
rfaK	3.94	
slt	3.93	X
STM3251	3.93	
oafA	3.92	
STM4258	3.92	X
hybG	3.91	
baeR	3.90	
yidQ	3.90	
yeiU	3.88	
glpK	3.88	X
araC	3.88	
cobB	3.87	X
sdhD	3.87	X
STM2314	3.86	X
gnd	3.86	X
STM3773	3.86	X
lnt	3.85	X
acrD	3.84	
STM1874	3.82	
uvrY	3.81	X
ssaQ	3.79	
ytgA	3.78	
crp	3.77	X
STM2135	3.76	
STM1785	3.76	
yihG	3.76	
STM2329	3.74	
tdh	3.73	X
rfaQ	3.72	
STM1239	3.72	X
spaO	3.72	X
rbsK	3.70	X
marB	3.70	
invG	3.69	X
sdaC	3.69	
aroE	3.67	
sucC	3.66	X
rfc	3.66	
rfbI	3.65	X
avrA	3.64	X
ymbA	3.63	
STM4534	3.62	
STM2225	3.62	

dsbB	3.61	X
STM3362	3.61	X
ybeX	3.61	X
STM4495	3.61	X
alkB	3.61	
STM1328	3.59	X
STM1014	3.59	
lgt	3.57	X
nuoB	3.57	X
smpB	3.54	X
STM1130	3.54	
apaG	3.53	
apaH	3.53	X
ybjE	3.53	
dlhH	3.53	
ttk	3.52	
stdA	3.51	
invF	3.51	X
STM0053	3.50	
yahN	3.50	X
STM2950	3.50	X
STM0341	3.50	
sbmA	3.50	X
clpB	3.49	X
STM3155	3.49	
rfbM	3.48	X
yibR	3.48	
hnr	3.48	
STM4494	3.47	
STM1254	3.46	
yfeA	3.46	
STM2186	3.45	X
STM3651	3.44	
invC	3.44	X
STM3533	3.44	
hpaR	3.43	
ydeZ	3.43	X
STM0307	3.43	
ygaC	3.42	
yfaZ	3.42	
orf245	3.42	
STM2754	3.42	
rfaL	3.41	
ftn	3.40	X
pldB	3.39	X
hupB	3.38	X
yajD	3.38	
STM3291	3.38	
dacC	3.38	X
STM4597	3.38	
yobA	3.37	X
yffH	3.36	
ybjT	3.36	
lpxO	3.35	
invA	3.35	X
gltJ	3.34	
mdoC	3.34	
STM1673	3.34	
fepE	3.34	
STM2766	3.34	
sfbA	3.34	
STM4420	3.34	
mukB	3.33	X
STM2449	3.33	
yfeZ	3.33	
yhfK	3.32	X
gltB	3.32	
msbB	3.31	
yecH	3.31	
STM3084	3.31	
STM4308	3.31	
ubiX	3.30	
flk	3.30	
dfp	3.30	
hflX	3.30	X

glnA	3.29	
ydiJ	3.29	
ygiH	3.29	X
lasT	3.29	
STM1041	3.28	
STM0344	3.27	
yjgG	3.27	
STM3906	3.26	
STM3907	3.26	
lrp	3.26	X
yciT	3.25	
yeaL	3.25	
fadD	3.24	
ydeW	3.23	X
STM3698	3.23	
proP	3.23	X
yigZ	3.22	
yicL	3.22	
STM2011	3.22	
ybfE	3.22	
rfbK	3.21	X
hemF	3.21	
flhC	3.20	X
STM1532	3.19	
perM	3.19	
yfgB	3.19	
rfbC	3.19	
ytfN	3.18	X
orfX	3.18	
aroM	3.17	
yabJ	3.17	
yggN	3.17	X
proQ	3.15	X
STM3516	3.15	
yadQ	3.14	
glgB	3.14	X
sopE2	3.12	X
STM3138	3.12	X
pagP	3.12	
STM1697	3.11	
sipD	3.11	X
pqiA	3.11	
sinR	3.11	
STM0672	3.11	
yeaS	3.11	X
dapB	3.10	X
STM3785	3.09	
rplL	3.09	X
STM0870	3.09	X
STM1550	3.08	
nhaA	3.08	X
STM0652	3.07	X
ushA	3.07	X
STM3517	3.07	
ydgT	3.06	
hscA	3.06	
hscB	3.06	
spaP	3.06	X
yjcB	3.06	
STM2377	3.05	
yeaA	3.05	X
STM0835	3.05	
yfeL	3.05	
araJ	3.05	
cysS	3.04	X
yjfL	3.04	
yfcH	3.04	
ytfP	3.04	X
leuZ	3.04	
allC	3.03	
tatB	3.03	
tatC	3.03	X
ssaU	3.02	
ansB	3.01	X

[a]Gene names according to ColiBase [3]

[b]When several oligonucleotides displaying significant enrichment corresponded to a single gene, the average enrichment over those oligonucleotides is shown.

Table S6: Oligodeoxynucleotides used in this study

Name	Sequence
JVO-0686	GGCCATGGAAAATGTAACCTTTGTAAG
JVO-0687	GTTTTGAATTCATGGTTCGCCATTTTTATGA
JVO-1034	GTTTTTTTTAATACGACTCACTATAGGATGAGGGGCATTTTATG
JVO-1035	TTGCTGCAACGGTCAT
JVO-1117	TCAGCCATTTTGTGCGCTT
JVO-1118	TTCAGGATCGACAACGCCTT
JVO-1234	AGGTTTGGCATTGTCGCCT
JVO-1235	CTTTTTCGAGCATCGGTGC
JVO-1236	ACTATTGAGTCCCTCCCGGAAG
JVO-1237	ACCGGACAATCCATGATAGCC
JVO-1342	TCGCTTGCCGATTCACATT
JVO-1343	CAATTTCTTCCGCACTCGGT
JVO-2152	GTTTTCCATGGGAACAATGCATAC
JVO-2153	GTTTTCTCGAGAACAGCCTGTTCGATC
JVO-2284	GTTTTTAATACGACTCACTATAGGTTCCCGGCGACATCA
JVO-2285	ATGTGTTTTAGCAACTCGGATG
JVO-2286	GTTTTTAATACGACTCACTATAGGTCTATACGCCTGACTTTCCT
JVO-2287	TTACAGTTACTGCAACCTTTG
JVO-2405	CCTATGGGAGCGCGGTG
JVO-2406	GTCAGAATACGACATTTTGGTACTC
JVO-2446	GATAACCTGAGACCCCCCTG
JVO-2447	AATACCCCCAAAAGCATTCG
JVO-2448	ATATAAACGCGCCAGTCCAT
JVO-2471	GTTTTTAATACGACTCACTATAGGATAAGCAAGGCTGGCAG
JVO-2472	GCCTTGTAGAGAGTGGGG
JVO-3140	CGGGTGGGATGAAATCGTAA
JVO-3141	TTAGTGTCTGGCGAAACGCT
JVO-3142	GTTGCTGCGGTGTAATAAGACA
JVO-3143	TACGTTTGAGCTCAGGGTCG
JVO-3249	AGAGAGTCAGCGCCGGG
JVO-3250	AATTAAAACCACCCGCCG
JVO-3251	CAGGCTACCAACCACCTCC
JVO-3252	TATGGAGCGCAACGCC
JVO-3253	GCGGTCTGGTGTACCTTCC
JVO-3254	CGGGTCATCTTTCAGGCTG
JVO-3255	TGCTTATACGCTACCGGGC
JVO-3256	CTGCCTAACATCTCGTTTCTCC
JVO-3257	GCCACGGTTCTCACCG
JVO-3258	CAGCACACTACACAGGGTCG
JVO-3259	ACCTTGCTGGCGCTCTC
JVO-3260	CATCTTGCGGTCTGGCA
JVO-3261	CATCGCGTTGCCAACTT
JVO-3262	AAGACCCTGGCGCGGTT
JVO-3263	CTTAGCAGCCTTGTAGAAGAGC
JVO-3264	AAACTTGACACCGTTCGGC
JVO-3265	GTGCCTCCGAACGGAAG
JVO-3266	GCGACAATCACGCCCAG

Table S7: Oligodeoxynucleotides used for Northern detection

Name	Sequence	Target region
JVO-2405	CCTATGGGAGCGCGGTG	STnc250
JVO-2406	GTCAGAATACGACATTTTGGTACTC	STnc290
JVO-2407	TTATTTGGACTACCTGGATG	STnc340
JVO-2408	TATGAGGAGGACAATTACCG	STnc440
JVO-2445	TACCGGACAATAATCCCTAC	STnc130
JVO-2446	GATAACCTGAGACCCCCCTG	STnc150
JVO-2448	ATATAAACGCGCCAGTCCAT	STnc180
JVO-2466	TCTGGCGGAACCTGCC	STnc220
JVO-2468	CACACCTGTCGGGCGTT	STnc310
JVO-2469	CGCAGTCCCAGGTCAGC	STnc330
JVO-2498	CTTATGTGGGCGTTTTGTTT	STnc350
JVO-2499	AATGACACCAACCTTTTACG	STnc390
JVO-2500	CTAGAGGAGGCGCTAGAAAG	STnc400
JVO-3140	CGGGTGGGATGAAATCGTAA	STnc190
JVO-3141	TTAGTGTCTGGCGAAACGCT	STnc400
JVO-3142	GTTGCTGCGGTGTAATAAGACA	STnc180
JVO-3143	TACGTTTGAGCTCAGGGTCG	STnc180
JVO-3144	TCATGTTACCGGTAAAATACCACC	STnc200
JVO-3249	AGAGAGTCAGCGCCGGG	STnc600
JVO-3250	AATTAAAACCACCCGCCG	STnc620
JVO-3251	CAGGCTACCAACCACCTCC	STnc590
JVO-3252	TATGGAGCGCAACGCC	STnc580
JVO-3253	GCGGTCTGGTGTACCTTCC	STnc610
JVO-3254	CGGGTCATCTTTCAGGCTG	STnc540
JVO-3255	TGCTTATACGCTACCGGGC	STnc560
JVO-3256	CTGCCTAACATCTCGTTTCTCC	STnc570
JVO-3257	GCCACGGTTCTCACCG	STnc480
JVO-3258	CAGCACACTACACAGGGTCG	STnc630
JVO-3259	ACCTTGCTGGCGCTCTC	STnc470
JVO-3260	CATCTTGCGGTCTGGCA	STnc490
JVO-3261	CATCGCGTTGCCAACTT	STnc500
JVO-3262	AAGACCCTGGCGCGGTT	STnc520
JVO-3263	CTTAGCAGCCTTGTAGAAGAGC	STnc640
JVO-3264	AAACTTGACACCGTTCGGC	STnc510
JVO-3265	GTGCCTCCGAACGGAAG	STnc530
JVO-3266	GCGACAATCACGCCCAG	STnc550

5. Summary

Hfq is a RNA-binding protein which exists in homohexamers *in vivo*. Based on its folding, containing the highly conserved Sm1 and Sm2 motifs, it belongs to the growing family of Sm and Sm-like (Lsm) proteins. It has been shown, that Hfq is a pleiotropic regulator in bacteria which is involved in a broad variety of functions.

The RNA chaperone Hfq is essential for the virulence of *Salmonella typhimurium*

Even though *hfq* has turned out to have no severe influence on the growth or the viability of the pathogenic bacterium *Salmonella* Typhimurium under laboratory conditions, we could show that it is strongly involved in the regulation of pathogenicity. A Δ*hfq* mutant leads to loss of effector protein expression and secretion and thereby to reduced invasion of non-phagocytic cells and to reduced ability of intracellular replication in macrophages. Based on these observations, loss of infectivity in a mouse-model of infection could be proven. Further studies revealed not only lack of secreted proteins in the Δ*hfq* mutant, but showed severe changes in the overall protein pattern when compared to its isogenic wild type strain, with an overrepresentation of membrane and membrane-associated proteins. Concerning the virulence phenotype, we have been able to restore effector protein expression (even if not their secretion) by overexpression of one of the major transcription factors involved in expression of virulence genes encoded in *Salmonella* pathogenicity island 1 (SPI1), namely HilA. Additionally, we could show that alteration in mRNA stability is causing for example the increase of the major outer membrane protein, OmpD or the decrease in the flagellar protein, FliC.

Deep sequencing analysis of small noncoding RNA and mRNA targets of the global post-transcriptional regulator, Hfq

Our analysis represents a demonstration for usage of high throughput pyrosequencing (HTPS) in bacteria to determine the large regulon of the pleiotropic regulator, Hfq. The combination of transcriptomics with co-immunoprecipitation (coIP) of direct binding partners of Hfq and subsequent cDNA library synthesis and its sequencing allowed the

dissection of genes directly influenced by Hfq and downstream effects based on deregulation of transcription factors. By analysis of RNA co-immunoprecipitated with Hfq compared to control coIPs in *Salmonella* Typhimurium lysates we were able to determine specific enrichment factors for a large set of mRNAs as well as sRNAs. Comparison with the transcriptomic data showed that Hfq regulates multiple major transcription factors, like a transcription factor of SPI1, HilD, and the major transcription factor, $FlhD_2C_2$, regulating the large class of flagellar genes in *Salmonella* and other bacterial species. By overexpression of these transcription factors we could restore phenotypes of a Δ*hfq* mutant, e.g. loss of effector protein expression and secretion and reduced expression of the class III flagellar gene, FliC. Concerning sRNA expression in *Salmonella*, we found 10 new sRNAs in this pathogen and were able to verify the expression of a large set of sRNAs that have been known to be conserved in the model organism, *Escherichia coli*. Aside noncoding RNAs also two mRNAs encoding for small open reading frames (ORFs) in *E. coli* could be detected in the coIP RNA sample from *Salmonella* Typhimurium.

6. Zusammenfassung

Hfq ist ein RNA-bindendes Protein, welches *in vivo* als Homohexamer vorliegt. Basierend auf seiner Struktur, die die hoch konservierten Sm1 and Sm2 Motive aufweist, wird es in die wachsende Familie der Sm und Sm-ähnlichen (Lsm) Proteine eingeordnet. Wir konnten zeigen, dass Hfq ein pleiotroper Regulator in Bakterien ist, der eine Vielzahl von Funktionen aufweist und in multiple Prozesse involviert ist.

Das RNA Chaperon Hfq ist essentiell fuer die Virulenz von *Salmonella* Typhimurium

Wir konnten zeigen, dass Hfq keinen grossen Einfluss auf das Wachstum oder die Vitalität des pathogenen Bakteriums *Salmonella* Typhimurium unter Laborbedingungen hat. Allerdings ist Hfq ein wichtiger Regulator der Pathogenizität dieses Bakteriums. Die Deletion von *hfq* in *Salmonella* führt sowohl zum Verlust der Expression als auch der Sekretion von Effektorproteinen, wodurch die Invasion in nicht-phagozytierende Zellen und die intrazelluläre Replikation in Makrophagen (phagozytierende Zellen) reduziert ist. Die verminderte Infektiosität der Δ*hfq* Mutante konnte auch im Infektionsmodel der Maus gezeigt werden. Weiterführende Studien zeigten massive Änderungen im gesamten Proteinprofil. Die am häufigsten misregulierten Proteine gehörten zu der Klasse der Membran- und membranassoziierten Proteine. Durch Überexpression des Haupttranskriptionsfaktors von SPI1, HilA, konnte die Expression der Effektorproteine, aber nicht deren Sekretion wieder hergestellt werden. Zusätzlich konnte gezeigt werden, dass Veränderungen der mRNA-Stabilitäten den starken Anstieg des Hauptmembranproteins, OmpD und die Abnahme des Flagellarproteins FliC bewirkten.

Hochdurchsatzsequenzierung von kleinen nichtkodierenden RNA und mRNA Bindungspartnern des globalen posttranskriptionalen Regulators Hfq

Mit der Methode der Hochdurchsatzsequenzierung [“high throughput pyrosequencing“ (HTPS)] konnten wir das weitreichende Regulon des pleiotropen Regulators Hfq

analysieren. Durch den Vergleich von Transkriptom-Daten mit Sequenzen aus der Coimmunopräzipitation (CoIP) von direkten Bindungspartnern von Hfq konnten Gene unterschieden werden, die direkt von Hfq beeinflusst sind, von Genen, die als Folge deregulierter Transkriptionsfaktoren in der Δ*hfq* Mutante misreguliert sind. Durch die Gegenüberstellung der Hfq-CoIP und der Kontroll-CoIP konnten Hfq-spezifische Anreicherungsfaktoren für eine grosse Anzahl von verschiedenen mRNAs und von sRNAs in *Salmonella* Typhimurium ermittelt werden. Hfq reguliert diverse Transkriptionsfaktoren, wie z.B. einen der Transkriptionsfaktor von SPI1, HilD und den Haupttranskriptionsfaktor $FlhD_2C_2$, der Flagellargene in *Salmonella* und anderen Bakterienspezies, reguliert. Durch Überexpression dieser Transkriptionsfaktoren konnten Phänotypen einer Δ*hfq* Mutante, wie der Verlust der Expression und Sekretion von Effektorproteinen, sowie die reduzierte Expression des in Klasse III der Flagellargene kodierten Flagellingens, FliC, komplementiert werden. Des weiteren wurde die Expression von 10 neuen sRNAs in diesem Pathogen nachgewiesen und die Expression von im Modellorganismus *E. coli* konservierten sRNAs in *Salmonella* bestätigt. Neben nichtkodierenden RNAs konnten auch zwei mRNAs, welche für kleine Protein in *E. coli* kodieren in den CoIP RNA Proben von *Salmonella* Typhimurium detektiert werden.

7. Outlook

The construction of a set of mutants in the *Salmonella hfq* locus provides a useful tool for the precise analysis of this deletion of a global RNA-binding protein. The here defined *hfq* phenotypes that relate to virulence and global gene expression, which are largely independent of σS and σE, need further analysis to dissect secondary effects, based on deregulation of genes that are exclusively due to Hfq binding. In light of the variability and diversity of Hfq function(s) in virulence among different pathogens, the clear loss of SPI1 expression and the secretion phenotype shown here for *Salmonella* provide an excellent basis to dissect the mechanisms of Hfq functions in a well-characterized model pathogen.

Analysis of protein patterns on one- and two-dimensional gels showed that the expression of a large number of *Salmonella* genes is affected by Hfq. Those could be classified to diverse functional categories. The protein expression data serves as a tool to search for putative direct Hfq target genes. Given that Hfq has recently been in the spotlight as a small RNA-binding protein, the altered periplasm of Δ*hfq* cells is of particular interest. The ~200 nt GcvB RNA of *E. coli* as well as its *Salmonella* homologue were shown to negatively regulate periplasmic proteins, which all accumulate to higher levels in the Δ*hfq* strain. Clearly, also for other small regulatory RNAs, regulating a broad range of mRNAs, the data will allow the search for putative targets.

This study implicates Hfq as a major post-transcriptional regulator of *Salmonella* gene expression. Interestingly, similar to H-NS that recognizes AT-rich sequences in DNA, Hfq binds to AU-rich RNA species. It is worth looking more closely into Hfq regulated gene classes to investigate if Hfq plays a similar role by specifically acting on AU-rich mRNAs of newly acquired genes (genetic islands acquired via horizontal gene transfer vary significantly in their AT content from the *Salmonella* core genome). If so, Hfq may again turn out to be the ‘host factor’ as which it was originally described.

To understand how bacterial RNA-binding proteins such as Hfq mediate the control of global gene expression at the post-transcriptional level, direct targets need to be identified. The approach used here overcomes the requirement for custom high-density microarrays and/or species-specific antibodies. Additionally, it could be shown that our sRNA discovery approach not only detects sRNAs, but also defines their exact sequences.

We show that even without prior size fractionation, HTPS can capture and define the termini of these sRNAs. These findings should prove useful to researchers working in other bacterial systems. The detection of the InvR sRNA, located in SPI1 in *Salmonella* shows that our approach is not only effective for detecting conserved, but also species-specific sRNAs of recently acquired pathogenicity regions. Future studies combining several different growth conditions with increasing sequencing depth are likely to identify even more novel sRNAs. The present study provides the first picture of the impact of Hfq on *Salmonella* gene expression at both the transcriptional and post-transcriptional level. More detailed inspection of our freely available data set, as well as sampling under different growth conditions, will expand the gamut of *Salmonella* small mRNA and noncoding RNA genes. In addition, the available data sets could help to discover whether Hfq controls the expression of *cis*-antisense sRNAs that overlap with mRNA coding regions, or whether *Salmonella* tRNAs are selectively associated with this protein. Bacterial genomes encode a large number of RNA binding proteins and our generic method will identify the RNA targets of these proteins in any genetically tractable bacterium.

8. Appendix

All chemicals used throughout this study were purchased from Merck (Darmstadt), Roth (Karlsruhe), and Sigma (Munich).

8.1 Equipment

Horizontal Electrophoresis Systems	
PerfectBlue Mini S, M, L	Peqlab, Erlangen
Hybon-XL Membrane for Nucleic Acid Transfer	GE Healthcare, München
Imaging Plates BAS-IP MS 2325, 2340	Fujifilm, Düsseldorf
Imaging Plates Cassettes BAS 2325, 2340	Fujifilm, Düsseldorf
Inoculation Loops 10 µl	VWR, Darmstadt
L-shape Bacteriology Loops	VWR, Darmstadt
MicroSpin G-25, G-50 Columns	GE Healthcare, München
Microtiter Plates (96-well)	Nunc, Wiesbaden
Pipetman P10, P20, P200, P1000	Gilson, Bad Camberg
Pipetboy acu	Integra Biosciences, Fernwald
PolyScreen PVDF Transfer Membrane	PerkinElmer, Waltham, Massachusetts, USA
Reagent and Centrifuge Tubes 15, 50 ml	Sarstedt, Nümbrecht
Safe-Lock Tubes 1.5 ml, 2.0 ml	Eppendorf, Wesseling-Berzdorf
Semi-dry Electroblotter SEDEC M	Peqlab, Erlangen
Semi-micro Cuvettes	Sarstedt, Nümbrecht
Serological Pipets 5 ml, 10 ml, 25 ml	Corning, Wiesbaden
Tank Electroblotter PerfectBlue Web S, M	Peqlab, Erlangen
Thermo-Tubes 0.2 ml	Abigene, Hamburg
Ventilation Cap Tubes 13 ml	Sarstedt, Nümbrecht
Vertical Electrophoresis Systems	
PerfectBlue Twin S, L	Peqlab, Erlangen
Sterile fiters (0.2 µm pore size)	Whatman, Dassel

8.2 Instruments

Analytical Balances TE64, TE601	Sartorius, Göttingen
Centrifuge 5415R, 5810R	Eppendorf, Wesseling-Berzdorf
Centrifuge RC5C Plus (Rotor: SS-34)	Thermo Scientific, Langenselbold
DNA Engine Thermal Cycler	Bio-Rad, München
E. coli Pulser	Bio-Rad, München
Electrophoresis Power Supplies	
EV 232, EV202, E802	Consort, Turnhout, Belgium
Eraser for Imaging Plates	Raytest, Straubenhardt
Gel Documentation System Gel Doc 2000	Biorad, München
Gel Dryer Model 583	Biorad, München
GenePix 4000A scanner	Axon Instruments, Inc., Concord, Ontario, Canada
Hybridization Oven Compact-Line OV4	Biometra, Göttingen
Imaging System LAS-3000	Fujifilm, Düsseldorf
Incubator Innovens Category 1	Jouan, Unterhaching
Incubator Shaker Innova 44	New Brunswick Scientific, Nürtingen
MultiTempIII Thermostatic Circulator	Amersham Biosciences, Freiburg
Refrigerated Incubator Shaker C24KC	New Brunswick Scientific, Nürtingen
Spectrophotometer NanoDrop ND-1000	Peqlab, Erlangen
Thermomixer comfort	Eppendorf, Wesseling-Berzdorf
Phosphoimager FLA-3000	Fujifilm, Düsseldorf
qRT-PCR 7900HT	Applied Biosystems, Foster City, California, USA
Ultrospec 10 photometer	Amersham Biosciences
Victor^3 1420 Multilabel Counter	PerkinElmer, Waltham, Massachusetts USA
Vortex-Genie 2	Scientific Industries, Bohemia, New York, USA

8.3 Enzymes, proteins, and size markers

Albumin Fraktion V	Roth, Karlsruhe

Calf Intestine Alkaline Phosphatase	Fermentas, St. Leon-Rot
Deoxyribonuclease I	Fermentas, St. Leon-Rot
GeneRuler 1kb DNA Ladder	Fermentas, St. Leon-Rot
Lysozyme	Roth, Karlsruhe
pUC Mix Marker, 8	Fermentas, St. Leon-Rot
pUC19 DNA/*MspI* (HpaII) Marker, 23	Fermentas, St. Leon-Rot
Phusion High-Fidelity DNA Polymerase	New England Biolabs, Frankfurt a.M.
Prestained Protein Marker Broad Range	New England Biolabs, Frankfurt a.M.
RNA ladder Low Range, High Range	Fermentas, St. Leon-Rot
Stratascript reverse transcriptase	Stratagene, Cedar Creek, Texas, USA
Superase-In RNase Inhibitor	Ambion, Austin, Texas, USA
T4 DNA Ligase	Fermentas, St. Leon-Rot
T4 Polynucleotide Kinase	Fermentas, St. Leon-Rot
Taq DNA polymerase	New England Biolabs, Frankfurt a.M.

8.4 Antibodies and antisera

ECL Anti-Mouse IgG (sheep), HPR-conjugated	GE Healthcare, München
ECL Anti-Rabbit IgG (donkey), HPR-conjugated	GE Healthcare, München
Monoclonal Anti-FLAG M2 Antibody (mouse)	Sigma-Aldrich, Taufkirchen
Monoclonal Anti-GFP antibodies (mouse)	Roche, Mannheim
Monoclonal Anti-Myc (mouse)	Santa Cruz Biotechnology, Santa Cruz, California, USA
Monoclonal Anti-FliC (mouse)	BioLegend, San Diego, California, USA
Monoclonal Anti-RpoE (mouse)	Neoclone, Madison, Wisconsin, USA
α-SipC antiserum (rabbit)	MPI-IB Berlin, Michael Kolbe
α-SipD antiserum (rabbit)	MPI-IB Berlin, Michael Kolbe
α-SopB antiserum (rabbit)	MPI-IB Berlin, Michael Kolbe
α-SopE antiserum (rabbit)	MPI-IB Berlin, Michael Kolbe
α-PrgI antiserum (rabbit)	MPI-IB Berlin, Michael Kolbe
α-RpoS antiserum (rabbit)	FU Berlin, Regine Hengge

8.5 Commercially available systems

MAXIscript T7 Kit	Ambion, Austin Texas, USA
MEGAscript T7 Kit	Ambion, Austin Texas, USA
NucleoSpin Extract II	Macherey-Nagel, Düren
NucleoSpin Plasmid QuickPure	Macherey-Nagel, Düren
PageBlue Protein Staining Solution	Fermentas, St. Leon-Rot
Rediprime II DNA Labeling System	GE Healthcare, München
Roti-Hybriquick	Roth, Karlsruhe
Sample Loading Buffer	Fermentas, St. Leon-Rot
SV40 Total RNA Isolation System	Promega, Madison, Wisconsin, USA
TRIzol Reagent	Invitrogen, Karlsruhe
Western Lightning Chemiluminescence Reagent	Perkin Elmer, Weiterstadt

8.6 Synthetic DNA oligonucleotides

DNA oligonucleotides were obtained from Sigma. The sequence is given in 5' to 3' direction.

Number	Use	Sequence
JVO-0076	*Salmonella hfq* verification sense primer	GAAGTATTACAGGTTGTTGGTG
JVO-0077	*Salmonella hfq* verification antisense primer	GCATCATAACGGTCAAACA
JVO-0078	Sense primer for cloning of *Salmonella hfq* into pTYB11 (INTEIN-CN)	GGTGGTTGCTCTTCCAACATGGCTAAGGGGCAATCTTT
JVO-0084	Antisense primer for cloning of *Salmonella hfq* into pTYB11 (INTEIN-CN)	TTATTCAGTCTCTTCGCTGTCCT
JVO-0182	Antisense primer for *Salmonella hfq* His-tagging with XbaI site	GTTTTTTCTAGATTAATGATGATGATGATGATGTTCAGT CTCTTCGCTGTCC
JVO-0222	Antisense oligo for probing for InvR RNA	GATAAATGCAACGTAAGAGACAAATG
JVO-	Sense primer for *Salmonella*	GAAAGACGCGCATTTGT

0236	MicA riboprobe template	
JVO-0252	Primer downstream of *Salmonella hfq* with P1 site of plasmid pKD3 for *hfq* control strain	GCGATTATCCGACGCCCCCGACATGGATAAACAGCGC GTGAAGTGTAGGCTGGAGCTGCTTC
JVO-0253	Primer in *Salmonella hfq* 3' part with P2 site of plasmid pKD3 for *hfq* control strain	ACGCGCAGGGGTCTACTGCGCAACAGGACAGCGAAGA GACTGAATAAGGTCCATATGAATATCCTCCTTAG
JVO-0266	Antisense primer in *Salmonella* MicA with T7 promoter sequence for riboprobe template	GTTTTTTTTTAATACGACTCACTATAGGGAGGCACGGAG TGGCCAAA
JVO-0318	Primer upstream of *Salmonella hfq* with P2 site of plasmid pKD3 for *hfq* deletion mutant	CAGAATCGAAAGGTTCAAAGTACAAATAAGCATATAAGG AAAAGAGGTCCATATGAATATCCTCCTTAG
JVO-0319	Sense primer for chromosomal His-tagging of *Salmonella hfq* with P2 site of plasmid pKD3	ACGCGCAGGGGTCTACTGCGCAACAGGACAGCGAAGA GACTGAACATCATCATCATCATTAAGGTCCATATGA ATATCCTCCTTAG
JVO-0321	Antisense oligo for probing for GcvB RNA	CAATTGCAAACACAACAACACAACATC
JVO-0322	Antisense oligo for probing for 5S RNA	CTACGGCGTTTCACTTCTGAGTTC
JVO-0370	Sense primer for cloning of *Salmonella hfq* with its own promoter with XhoI site	GTTTTTCTCGAGCCTGCCTAAGGC
JVO-0397	Sense primer for *Salmonella ompA* riboprobe template	CGGTAGAGTAACTATTGAGCAGAT
JVO-0398	Antisense primer in *Salmonella ompA* with T7 promoter sequence for riboprobe template	GTTTTTTTTTTAATACGACTCACTATAGGGAGGCCTAAC CAGTCGTAGC
JVO-0686	Sense primer for *hilD* cloning in pBAD-Myc/His vector with NcoI site	GGCCATGGAAAATGTAACCTTTGTAAG
JVO-0687	Antisense primer for *hilD* cloning in pBAD-Myc/His vector with EcoRI site	GTTTTGAATTCATGGTTCGCCATTTTTATGA
JVO-0717	Antisense primer for translational fusion to 12^{th} aa and generation of PCR probe	GTTTTTGCTAGCTGGTACCAGGAGGG

	of *Salmonella* OmpC with NheI site	
JVO-0719	Sense primer for generation of PCR probe of *Salmonella* OmpC with BfrBI site	GTTTTATGCATGCCGACTGGTTAATGAG
JVO-0726	Antisense primer for translational fusion to 15th aa of *Salmonella* OmpD with NheI site	GTTTTTGCTAGCCAACAGGGAAGTCAC
JVO-0751	Sense primer for *Salmonella* OmpD riboprobe template with BfrBI site	GTTTTATGCATAGTCTGCCATTGACAAAC
JVO-0801	Sense primer for transcriptional GFP fusion of *Salmonella ompC* with AatII site	GTTTTGACGTCTATTTGTGCTTATTTTTACTTG
JVO-0802	Sense primer for transcriptional GFP fusion of *Salmonella ompD* with AatII site	GTTTTGACGTCAAATCAATATTGAAACGG
JVO-0805	Antisense primer for transcriptional GFP fusion of *Salmonella ompC* with NheI site	GTTTTGCTAGCATGCCTTTATTGCTTTTTTATG
JVO-0806	Sense primer for transcriptional GFP fusion of *Salmonella ompD* with AatII site	GTTTTGACGTCTCGACCCGCTGTACCT
JVO-0807	Antisense primer for transcriptional GFP fusion of *Salmonella ompD* with NheI site	GTTTTGCTAGCGCGTGTTTCCTCAACCA
JVO-0811	Primer upstream of *Salmonella ompD* with P1 site of pKD3 for *ompD* deletion mutant	GGAGATCTCGATCACACAAATTAAAATAATTTGTAATCG TGTAGGCTGGAGCTGCTTC
JVO-0812	Primer downstream of *Salmonella ompD* with P2 site of pKD3 for *ompD* deletion mutant	CCAGCCCTGAAAGGACTGGCTTTGTATTCAGACTACAA CAAAAGGTCCATATGAATATCCTCCTTAG
JVO-0817	*Salmonella ompD* verification sense primer	GTTTTTCTCGAGCCAATAGTCCCCTCCGA

JVO-0818	*Salmonella ompD* verification antisense primer	GTTTTTTCTAGACTGCACGGCATACTCCT
JVO-0837	Sense primer for FLAG-tagging of *Salmonella* HilA with binding site in pSUB11	CAAAAGATGGAAACAGGATCCCCGCTTGATTAAATTAC GGGACTACAAAGACCATGACGG
JVO-0838	Antisense primer for FLAG-tagging of *Salmonella* HilA with binding site in pSUB11	ATGATAAAAAAATAATGCATATCTCCTCTCTCAGATTTTA CCATATGAATATCCTCCTTAG
JVO-0839	*Salmonella hilA* verification sense primer	CCACGGCGAAGCTATT
JVO-0840	*Salmonella hilA* verification antisense primer	GCCCATGCCGTATTTAT
JVO-0888	Sense primer for construction of transcriptional GFP fusion plasmid (pAS0046)	GTTTTCTCGAGGCTAGCTAAGTAGTACTTAGATTTAAGA AGGAGATATACATATGGCCAGCAAAGGAGAA
JVO-0889	Sense primer for transcriptional GFP fusion of *Salmonella hilA* with AatII site	GTTTTTGACGTCAGCGTAAGAATTCGTCC
JVO-0890	Sense primer for transcriptional GFP fusion of *Salmonella hilA* with NheI site	GTTTTTGCTAGCTATCTTACTGCATTTTTTT
JVO-0906	Sense primer for *Salmonella* RybB riboprobe template	5'P-GCCACTGCTTTTCTTTGA (sense RybB template)
JVO-0934	Antisense primer in *Salmonella ompD* with T7 promoter sequence for riboprobe template	GTTTTTTTTTTAATACGACTCACTATAGGGAGGTTAACT GATCGTTGATCTG
JVO-0984	Antisense primer in *Salmonella rybB* with T7 promoter sequence for riboprobe template	gttttttttTAATACGACTCACTATAGGGAggGTTGATGGGCT CC
JVO-1034	Sense primer for *Salmonella dppA* with T7 promoter sequence for *in vitro* transcription	GTTTTTTTTAATACGACTCACTATAGGATGAGGGGCATT TTATG
JVO-1035	Antisense primer for *Salmonella dppA* T7 template	TTGCTGCAACGGTCAT
JVO-1058	Antisense primer in *Salmonella ompD* for probing for *ompD* mRNA	CGTGAACTTTACCGTACA

JVO-1117	Sense primer for *Salmonella rfaH* realtime PCR	TCAGCCATTTTGTGCGCTT
JVO-1118	Antisense primer for *Salmonella rfaH* realtime PCR	TTCAGGATCGACAACGCCTT
JVO-1186	Sense primer for *Salmonella ompD* with T7 promoter sequence for *in vitro* transcription	TTTTCTCGAGTTAATACGACTCACTATAGGCCATTGACAAACG
JVO-1234	Sense primer for *Salmonella degP* realtime PCR	AGGTTTGGCATTGTCGCCT
JVO-1235	Antisense primer for *Salmonella degP* realtime PCR	CTTTTTCGAGCATCGGTGC
JVO-1236	Sense primer for *Salmonella rpoE* realtime PCR	ACTATTGAGTCCCTCCCGGAAG
JVO-1237	Antisense primer for *Salmonella rpoE* realtime PCR	ACCGGACAATCCATGATAGCC
JVO-1298	Sense primer for *Salmonella hilA* riboprobe template	CGAGCCCGTAGAATATGA
JVO-1299	Antisense primer in *Salmonella hilA* with T7 promoter sequence for riboprobe template	GTTTTTTTTTTAATACGACTCACTATAGGGAGGCTTCGAGCAGGATG
JVO-1342	Sense primer for *Salmonella rpoS* realtime PCR	TCGCTTGCCGATTCACATT
JVO-1343	Antisense primer for *Salmonella rpoS* realtime PCR	CAATTTCTTCCGCACTCGGT
JVO-1592	Antisense primer in *Salmonella fliC* for probing for *fliC* mRNA	GCGTATCCAGACCCAGGGTCTGAGAG
JVO-1595	Antisense primer in *Salmonella fljB* for probing for *fljB* mRNA	GCGCCAGCCGCAAGGGT
JVO-1701	Sense primer for *Salmonella metK* with T7 promoter sequence for *in vitro* transcription	GTTTTTTTTAATACGACTCACTATAGGATCCATCCATACTGATTAACACT
JVO-1702	Antisense primer in *Salmonella metK* for *in vitro* transcription	GCAGGATAGCGTCCAAC
JVO-2152	Sense primer for *flhDC* cloning in pBAD-Myc/His vector with NcoI site	GTTTTCCATGGGAACAATGCATAC

JVO-2153	Antisense primer for *flhDC* cloning in pBAD-Myc/His vector with XhoI site	GTTTTCTCGAGAACAGCCTGTTCGATC
JVO-2284	Sense primer for *Salmonella flhD* with T7 promoter sequence for *in vitro* transcription	GTTTTTAATACGACTCACTATAGGTTCCCGGCGACATCA
JVO-2285	Antisense primer in *Salmonella flhD* for *in vitro* transcription	ATGTGTTTTAGCAACTCGGATG
JVO-2286	Sense primer for *Salmonella hilD* with T7 promoter sequence for *in vitro* transcription	GTTTTTAATACGACTCACTATAGGTCTATACGCCTGACTTTCCT
JVO-2287	Antisense primer in *Salmonella hilD* for *in vitro* transcription	TTACAGTTACTGCAACCTTTG
JVO-2405	Antisense oligo for probing for STnc270 RNA	CCTATGGGAGCGCGGTG
JVO-2406	Antisense oligo for probing for STnc290 RNA	GTCAGAATACGACATTTTGGTACTC
JVO-2407	Antisense oligo for probing for STnc340 RNA	TTATTTGGACTACCTGGATG
JVO-2408	Antisense oligo for probing for STnc440 RNA	TATGAGGAGGACAATTACCG
JVO-2445	Antisense oligo for probing for STnc130 RNA	TACCGGACAATAATCCCTAC
JVO-2446	Antisense oligo for probing for STnc150 RNA	GATAACCTGAGACCCCCCTG
JVO-2447	Antisense oligo for probing for STnc180 RNA	AATACCCCCAAAAGCATTCG
JVO-2448	Antisense oligo for probing for STnc190 RNA	ATATAAACGCGCCAGTCCAT
JVO-2466	Antisense oligo for probing for STnc220 RNA	TCTGGCGGAACCTGCC
JVO-2468	Antisense oligo for probing for STnc310 RNA	CACACCTGTCGGGCGTT
JVO-2469	Antisense oligo for probing for STnc330 RNA	CGCAGTCCCAGGTCAGC
JVO-2471	Sense primer for *Salmonella glmUS* IGR with T7 promoter	GTTTTTAATACGACTCACTATAGGATAAGCAAGGCTGGCAG

	sequence for *in vitro* transcription	
JVO-2472	Antisense primer in *Salmonella glmUS* IGR for *in vitro* transcription	GCCTTGTAGAGAGTGGGG
JVO-2498	Antisense oligo for probing for STnc350 RNA	CTTATGTGGGCGTTTTGTTT
JVO-2499	Antisense oligo for probing for STnc390 RNA	AATGACACCAACCTTTTACG
JVO-2500	Antisense oligo for probing for STnc400 RNA	CTAGAGGAGGCGCTAGAAAG
JVO-3140	Antisense oligo for probing for STnc190 RNA	CGGGTGGGATGAAATCGTAA
JVO-3141	Antisense oligo for probing for STnc400 RNA	TTAGTGTCTGGCGAAACGCT
JVO-3142	Antisense oligo for probing for STnc180 RNA	GTTGCTGCGGTGTAATAAGACA
JVO-3143	Antisense oligo for probing for STnc180 RNA	TACGTTTGAGCTCAGGGTCG
JVO-3144	Antisense oligo for probing for STnc200 RNA	TCATGTTACCGGTAAAATACCACC
JVO-3249	Antisense oligo for probing for STnc600 RNA	AGAGAGTCAGCGCCGGG
JVO-3250	Antisense oligo for probing for STnc620 RNA	AATTAAAACCACCCGCCG
JVO-3251	Antisense oligo for probing for STnc590 RNA	CAGGCTACCAACCACCTCC
JVO-3252	Antisense oligo for probing for STnc580 RNA	TATGGAGCGCAACGCC
JVO-3253	Antisense oligo for probing for STnc610 RNA	GCGGTCTGGTGTACCTTCC
JVO-3254	Antisense oligo for probing for STnc540 RNA	CGGGTCATCTTTCAGGCTG
JVO-3255	Antisense oligo for probing for STnc560 RNA	TGCTTATACGCTACCGGGC
JVO-3256	Antisense oligo for probing for STnc570 RNA	CTGCCTAACATCTCGTTTCTCC
JVO-	Antisense oligo for probing for STnc480 RNA	GCCACGGTTCTCACCG

3257		
JVO-3258	Antisense oligo for probing for STnc630 RNA	CAGCACACTACACAGGGTCG
JVO-3259	Antisense oligo for probing for STnc470 RNA	ACCTTGCTGGCGCTCTC
JVO-3260	Antisense oligo for probing for STnc490 RNA	CATCTTGCGGTCTGGCA
JVO-3261	Antisense oligo for probing for STnc500 RNA	CATCGCGTTGCCAACTT
JVO-3262	Antisense oligo for probing for STnc520 RNA	AAGACCCTGGCGCGGTT
JVO-3263	Antisense oligo for probing for STnc640 RNA	CTTAGCAGCCTTGTAGAAGAGC
JVO-3264	Antisense oligo for probing for STnc510 RNA	AAACTTGACACCGTTCGGC
JVO-3265	Antisense oligo for probing for STnc530 RNA	GTGCCTCCGAACGGAAG
JVO-3266	Antisense oligo for probing for STnc550 RNA	GCGACAATCACGCCCAG
pZE-Xba	Sense primer for construction of *transcriptional* GFP-fusion plasmid (pAS-0046)	TCGTTTTATTTGATGCCTCTAGA

8.7 Plasmids

name	**fragment**	**Comment**	**origin / marker**	**reference**
pJV300		ColE1 control plasmid, based on pZE12-luc, P_{LlacO} promoter transcribes a ~ 50 nt nonsense transcript (*rrnB* terminator)	ColE1 / Amp^R	this study
pJV859-8	P_{LtetO}- *gfp*	GFP control plasmid (constitutive GFP exprssion)	pSC101* / Cm^R	Urban and Vogel, 2007
pJV968-1	*'lacZ'*	ColE control plasmid, carries 1.5 kb internal *lacZ* fragment	ColE1 / Amp^R	(Vogel *et al.*, 2004)
pVP003	*luc*	control plasmid; low copy version of pZE12-luc	pSC101* / Amp^R	this study
pVP004-1	*Hfq*-6HIS	pStHfq-6H, expresses a HIS-tagged Hfq under control of its own promoter; includes	pSC101* / Amp^R	this study

		1014 bp upstream of *hfq* reading frame		
pVP009		low copy version of control plasmid pJV300	pSC101* / Amp^R	this study
pVP010	*Hfq*-6xHIS	6xHIS-tagged *hfq* ORF of *Salmonella* Typhimurium under control of the constitutive P_{LlacO} promoter; based on pVP003	pSC101* / Amp^R	this study
pVP0012	*'lacZ'*	Low-copy version of control plasmid pJV968-1 (Sittka et al., 2007)	pSC101* / Amp^R	this study
pVP019	*ompD::gfp*	*ompD* translational GFP fusion plasmid	pSC101* / Cm^R	this study
pVP020	*ompC::gfp*	*ompC* translational GFP fusion plasmid	pSC101* / Cm^R	this study
pAS009	*hfq*	Overexpression plasmid of *Salmonella hfq* (cloned in N-terminal fusion vector pTYB 11)	M13 / AmpR	this study
pAS0045	P_{BAD}-*hilD-Myc-His*	pHilD; *hilD* ORF in pBAD/*Myc*-His	pBR322 / Amp^R	this study
pAS0046	*gfp*	transcriptional fusions plasmid, based on pJV859-8	pSC101* / Cm^R	this study
pAS0047-2	P_{hilA}-*gfp*	*hilA* transcriptional GFP fusion plasmid	pSC101* / Cm^R	this study
pAS0057-1	P_{ompC}-*gfp*	*ompC* transcriptional GFP fusion plasmid	pSC101* / Cm^R	this study
pAS0058-1	P_{ompD}-*gfp*	*ompD* transcriptional GFP fusion plasmid	pSC101* / Cm^R	this study
pAS0081	P_{BAD}-*flhDC-Myc-His*	pFlhDC; *flhDC* operon in pBAD/*Myc*-His vector	pBR322 / Amp^R	this study
pAS0090	*gfp*	Transcriptional fusion positive control plasmid; based on pXG-1 (Urban & Vogel, 2007)	p15A / Cm^R	this study
pJU004		GFP negative control plasmid	pSC101* / Cm^R	Urban and Vogel, 2007
pBAD/*Myc*-His A		pBAD control plasmid	pBR322 / Amp^R	Invitrogen
pZS*24-MCS1	*luc*	General expression vector	pSC101* / Km^R	(Lutz and Bujard, 1997)
pBAD 18-Kn		pBAD control plasmid	pBR322 / Km^R	(Guzman *et al.*,

				1995)
pCH112	P_{BAD}-*hilA*-*Myc*-*His*	pHilA; *hilA* ORF in pBAD/*Myc*-His	pBR322 / Amp^R	(Lostroh *et al.*, 2000)
pKD3		Template for mutant construction; carries chloramphenicol cassette	oriRγ $\tilde{I}$ Amp^R	(Datsenko and Wanner, 2000)
pKD4		Template for mutant construction; carries kanamycin cassette	oriRγ $\tilde{I}$ Amp^R	(Datsenko and Wanner, 2000)
pKD46	P_{araB}-γ-*β*-*exo*	Temperature sensitive *red* recombinase expression plasmid	oriR101 / Amp^R	(Datsenko and Wanner, 2000)
pCP20		Temperature sensitive FLP recombinase expression plasmid	oriR101 / Amp^R, Cm^R	(Datsenko and Wanner, 2000)
pSUB11		Template for mutant construction; 3xFLAG linked to a Km^R cassette	R6KoriV, Amp^R	(Uzzau *et al.*, 2001)
pZA31-luc	*luc*	general expression plasmid	p15A / Cm^R	(Lutz and Bujard, 1997)
pZE12-luc	*luc*	general expression plasmid	ColE1 / Amp^R	(Lutz and Bujard, 1997)
pTYB-11		Protein overexpression plasmid (IMPACT-CN system)	M13 / AmpR	NEB

8.8 Strains

Strain	**Relevant markers/ genotype**	**Reference/ source**
***S.* Typhimurium**		
SL1344	Str^R *hisG rpsL xyl*	(Hoiseth & Stocker, 1981)
JVS-00177	SL1344 *hfq*-6His-Cm^R	this study
JVS-00179	SL1344 *hfq*-Cm^R	this study

JVS-00255	SL1344 Δ*hfq*::Cm^R	this study
JVS-00405	SL1344 Δ*spi1*	S. Pätzold, MPIIB-Berlin (unpublished)
JVS-00584	SL1344 Δ*hfq*	this study
JVS-00735	SL1344 Δ*ompD*::Km^R	this study
JVS-00748	SL1344 Δ*rpoS*	(Kowarz *et al.*, 1994)
JVS-00756	SL1344 *hilA*-3xFLAG-Km^R	this study
JVS-00822	SL1344 Δ*hfq*::Cm^R/Δ*ompD*::Km^R	this study
JVS-01338	SL1344 *hfq*-3xFLAG	(Pfeiffer et al., 2007)
E. coli		
TOP10	*mcr*A Δ(*mrr-hsd*RMS-*mcr*BC) Φ80*lac*ZΔM15 Δ*lac*X74 *deo*R *rec*A1 *ara*D139 Δ(*ara-leu*)7697 *gal*U *gal*K *rps*L *end*A1 *nup*G	Invitrogen
TOP10F'	F´{*lacI*^{q} Tn*10* (Tet^R)} *mcr*A Δ(*mrr-hsd*RMS-*mcr*BC) Φ80*lac*ZΔM15 Δ*lac*X74 *deo*R *rec*A1 *ara*D139 Δ(*ara-leu*)7697 *gal*U *gal*K *rps*L *end*A1 *nup*G	Invitrogen
ER 2566	F$^-$ Δ$^-$ *fhuA*2 [*lon*] *ompT lacZ ::T7 gene*1 *gal sulA*11 Δ(*mcrC-mrr*) 114 *::IS10 R*(*mcr*-73 *:: miniTn*10)2 *R*(*zgb*-210 *::Tn*10) (*Tet^S*) *end*A1 [*dcm*]	New England Biolabs

8.9 Abbreviation Index

% (v/v)	% (volume / volume)
% (w/v)	% (weight / volume)
A	Adenosine
Aa	Amino acid
Amp	Ampicillin
APS	Ammonium persulfate
ATP	Adenosine triphosphate
ATPase	ATP hydrolyzing enzyme
Bp	Base pair
C	Cytidine
cDNA	Complementary DNA
Cfu	Colony forming unit
CI	Competitive Index
Cm	Chloramphenicol
CsrA	Carbon storage regulator A
CTP	Cytidine triphosphate
DMSO	Dimethyl sulfoxide
DNA	Deoxyribonucleic acid

dNTPs	Deoxyribonucleotide
DTT	Dithiothreitol
E. coli	*Escherichia coli*
EDTA	Ethylendiamine tetraacetate
Fig.	Figure
FRET	Fluorescence resonance energy transfer
G	Guanosine
GFP	Green fluorescent protein
GTP	Guanosine triphosphate
Hfq	Host factor for phage Qβ replication
HGT	Horizontal gene transfer
IGR	Intergenic region
Kan	Kanamycin
L-broth	Lennox broth
Lsm	Sm-like
mRNA	Messenger RNA
Nt	Nucleotide
o/n	Overnight
ORF	Open reading frame
PAA	Polyacrylamide
P-bodies	Processing bodies
PBS	Phosphat buffered saline
PCR	Polymerase chain reaction
PNK	Polynucleotide kinase
PNPase	Polynucleotide phosphorylase
RBS	Ribosome binding site
RNA	Ribonucleic acid
RNP	Ribonucleoprotein complex
rRNA	Ribosomal RNA
RNase	Ribonuclease
RNase P	ribonuclease P
rNTP	Ribonucleotide
SCV	*Salmonella* containing vacuole
SD	Shine Dalgarno sequence
SDS	Sodiumdodecylsulfate
SPI	*Salmonella* pathogenicity island
sRNA	Small noncoding RNAs

SRP	signal recognition particle
snRNA	small nuclear RNA
snoRNA	small nucleolar RNA
snRNP	small nuclear ribonucleoprotein particle
TEMED	Tetramethylethylendiamin
Tris	Tris-(hydroxymethyl)-aminomethan
tRNA	Transfer RNA
TTSS	Type three secretion system
Tyr	Tyrosin
U	Uridine
UTP	Uridine triphosphate
UTR	Untranslated region

Units

°C	Degree Celsius
Da	Dalton
G	Gram
H	Hour
L	Litre
M	Meter
M	Molar
Min	Minute
OD_{600}	Optical density at 600nm
Rpm	rotations per minute
S	Second

Dimension

K	kilo (10^{3})
M	milli (10^{-3})
M	mikro (10^{-6})
N	nano (10^{-9})
P	piko (10^{-12})

Acknowledgements

I would like to thank …

… Dr. Joerg Vogel for the opportunity of the PhD thesis, for encouraging me to present my data over the last years on many conferences, and for the supervision of my work.

… Prof. Dr. R. K. Hartmann for being the first referee of my work.

… Prof. Dr. A. Wilde for being the second referee of my work.

… Prof. Dr. Beatrix Suess, PD Dr. K. Reuter, and Prof. Dr. Michael Keusgen for participation in the commission.

… Dr. Michael Weber for writing the protocol during the exam.

… all members of Vogel lab for the time we had together.

… my familiy and friends for their support and for putting up with me during the sometimes stressfull time.

… Norman for encouraging and supporting me, especially during the final ‘hot’ phase.

Publications arising from this work and co-operations

Articles

Manuscript “Deep sequencing analysis provides evidence for the conserved small RNA-binding property of diverse eubacterial and archaeal Hfq proteins” in preparation.

Sittka A, Lucchini S, Papenfort K, Sharma C, Rolle K, Binnewies TT, Hinton JC, Vogel J (2008) *Deep sequencing analysis of small noncoding RNA and mRNA targets of the global post-transcriptional regulator, Hfq.* **PLoS Genetics**

Pfeiffer V, **Sittka A**, Tomer R, Tedin K, Brinkmann V, Vogel J (2007) *A small noncoding RNA of the invasion gene island (SPI-1) represses outer membrane protein synthesis from the Salmonella core genome.* **Molecular Microbiology,** 66(5):1174-1191

Viegas S, Pfeiffer V, **Sittka A**, Silva IJ, Vogel J, Arraiano CM (2007) *Characterization of the role of Ribonucleases in Salmonella small RNA decay.* **Nucleic Acids Research,** 35(22):7651-7664

Sittka A, Pfeiffer V, Tedin K, Vogel J (2007) *The RNA chaperone Hfq is essential for the virulence of Salmonella typhimurium.* **Molecular Microbiology,** 63(1), 193-217.

Posters

Vereinigung fuer allgemeine und angewandte Mikrobiologie (VAAM) 2008, Frankfurt/Main, Germany
Sittka A, Lucchini S, Papenfort K, Sharma CM, Rolle K, Hinton JCD, Vogel J; *High throughput sequencing identifies the mRNAs and sRNAs bound to Hfq, the Sm-like protein of Salmonella*

RNA conference 2007, Madison, USA

Sittka A, Lucchini S, Papenfort K, Rolle K, Hinton JCD, Vogel J; *Functions of Hfq and other Sm-like proteins in a bacterial pathogen*

European initiative for basic research in microbiology and infectious diseases (EIMID) 2006, Siena, Italy
Poster
Sittka A, Pfeiffer V, Vogel J; *The RNA chaperone, Hfq is required for Salmonella virulence*

Vereinigung fuer allgemeine und angewandte Mikrobiologie (VAAM) 2006, Jena, Germany
Sittka A, Pfeiffer V, Vogel J; *The RNA chaperone, Hfq is required for Salmonella virulence*

Host-Pathogen Interaction and Human Diseases 2005, Cambridge, UK
Sittka A, Pfeiffer V, Vogel J; *The RNA chaperone, Hfq is required for Salmonella virulence*

RNA conference 2005, Banff, Canada
Sittka A, Sharma CM, Vogel J, *Identification of Small Regulatory RNAs in Helicobacter pylori*

Lebenslauf

Alexandra Sittka

Date of Birth:	December 22nd 1975
Place of Birth:	Berlin / Germany
Nationality:	German

Education and Research

August 1982-July 1988	Elementary School, Berlin
Agust 1988-July 1995	High School, Berlin (July 1995 school-leaving examination)
October 1995-September 2001	Study, Dept. Biology, Freie Universtität Berlin, Berlin, Germany Main subject: Microbiology 2. Subject: Genetics 3. Subject: Molecular Biology 4. Subject: Medical Microbiology
09/1999 – 03/2002	Teaching Assistant, Dept. Biology, Microbiology, Freie Universität Berlin, Berlin, Germany
10/1999 – 11/1999	Short-term practical study, Dept. Bacteriology P12 Horizontaler Gentransfer, Robert Koch-Institut, Berlin, Germany
02/2000 – 03/2000	Short-term practical study, Dept.Biology, Insect Immunology, Freie Universität Berlin, Berlin, Germany
04/2000 – 09/2001	Undergraduate research assistant, AG Ribosomen, Max Planck Institute for Molecular Genetics, Berlin, Germany
September 2001 - June 2002	Diploma thesis, AG Ribosomen, Max Planck Institute for Molecular Genetics, Berlin, Germany Subject: Influence of antibiotics on the *in vitro* and *in vivo* assembly of ribosomal subunits from E*scherichia coli D10*.

September 2002 - June 2004	Senior Research Associate, Ribosome Biochemistry and Microbiology group, Rib-X Pharmaceuticals, New Haven, CT 06511, USA
August 2004-present	Graduate student, RNA Biology, Max Planck Institute for Infection Biology, Berlin, Germany

Selbständigkeitserklärung

Ich versichere, dass ich meine Dissertation

„Role of the RNA-binding protein, Hfq in the model pathogen *Salmonella* Typhimurium“

selbständig, ohne unerlaubte Hilfe angefertigt und mich dabei keiner anderen als der von mir ausdrücklich bezeichneten Quellen bedient habe.

Die Dissertation wurde in der jetzigen oder einer ähnlichen Form noch an keiner anderen Hochschule eingereicht und hat noch keinen sonstigen Prüfungszwecken gedient.

_____ _____

(Ort/Datum) (Unterschrift mit Vor- und Zuname)